

# Distributional records of Ross Sea (Antarctica) planktic Copepoda from bibliographic data and samples curated at the Italian National Antarctic Museum (MNA): checklist of species collected in the Ross Sea sector from 1987 to 1995

Guido Bonello<sup>1</sup>, Marco Grillo<sup>1</sup>, Matteo Cecchetto<sup>1,2</sup>, Marina Giallain<sup>2</sup>,  
Antonia Granata<sup>3</sup>, Letterio Guglielmo<sup>4</sup>, Luigi Pane<sup>2</sup>, Stefano Schiaparelli<sup>1,2</sup>

**1** Italian National Antarctic Museum (MNA, Section of Genoa), University of Genoa, Genoa, Italy **2** Department of Earth, Environmental and Life Science (DISTAV), University of Genoa, Genoa, Italy **3** Department of Chemical, Biological, Pharmaceutical and Environmental Sciences (ChiBioFarAm), University of Messina, Messina, Italy **4** Stazione Zoologica Anton Dohrn (SZN), Villa Pace, Messina, Italy

Corresponding author: Stefano Schiaparelli ([stefano.schiaparelli@unige.it](mailto:stefano.schiaparelli@unige.it))

---

Academic editor: Kai Horst George | Received 23 March 2020 | Accepted 9 July 2020 | Published 17 September 2020

---

<http://zoobank.org/AE10EA51-998A-43D5-9F5B-62AE23B31C14>

---

**Citation:** Bonello G, Grillo M, Cecchetto M, Giallain M, Granata A, Guglielmo L, Pane L, Schiaparelli S (2020) Distributional records of Ross Sea (Antarctica) planktic Copepoda from bibliographic data and samples curated at the Italian National Antarctic Museum (MNA): checklist of species collected in the Ross Sea sector from 1987 to 1995. ZooKeys 969: 1–22. <https://doi.org/10.3897/zookeys.969.52334>

---

## Abstract

Distributional data on planktic copepods (Crustacea, Copepoda) collected in the framework of the III<sup>rd</sup>, V<sup>th</sup>, and X<sup>th</sup> Expeditions of the Italian National Antarctic Program (PNRA) to the Ross Sea sector from 1987 to 1995 are here provided. Sampling was performed with BIONESS and WP2 nets at 94 sampling stations at depths of 0–1,000 m, with a special focus on the Terra Nova Bay area. Altogether, this dataset comprises 6,027 distributional records, out of which 5,306 were obtained by digitizing original data reports and 721 are based on physical museum vouchers curated by the Italian National Antarctic Museum (MNA, Section of Genoa). The MNA samples include 8,224 individual specimens that were identified to the lowest possible taxonomic level. They belong to four orders, 25 families, 52 genera, and 82 morphological units (out of which 17 could be determined at the genus level only). A variety of environmental data were also recorded at each of the sampling stations, and we report original abundances (ind/m<sup>3</sup>) to enable future species distribution modelling. From a biogeographic point of view, the distributional data here reported represented new records for the Global Biogeographic Information Facility (GBIF) registry. In particular, 62% of the total number of species are new records for the Ross Sea sector and another 28% new records for the Antarctic region.

**Keywords**

abundance, biogeography, BIONESS, distribution, museum collection, Terra Nova Bay

**Introduction**

The study of planktic copepods in the Ross Sea represented one of the earliest scientific efforts and targets of the first oceanographic expeditions of the Italian National Antarctic Research Program (PNRA), which started in 1985. One of the underlying reasons for this dedication was the fact that, at the time of sampling, there was a general lack of exhaustive and accessible literature about Copepoda for the Ross Sea region. Therefore, specific sampling activities were planned to define the copepod community structure and establish a reference baseline for comparisons with future research findings (Amato 1990).

Copepods are one of the key groups in marine trophic chains, representing up to 70% of the mesozooplanktic biomass, a condition typically found in all Antarctic seas (Carli et al. 2002). Besides their dominance, Antarctic planktic copepods are also important because of their degree of adaptation to the exacerbated seasonality of food availability, which is determined by the polar light regime and sea ice dynamics, both affecting the primary production (Hagen and Schnack-Schiel 1996). This led to a variety of specific physiological and developmental strategies. For example, some pelagic herbivorous copepods synchronize their gonadal and life-stage with phytoplankton blooms to gain the best from the extremely short Antarctic summer months (Hagen and Schnack-Schiel 1996; Minutoli et al. 2017). Other species are intimately linked to the sea ice, which provides an important habitat for small grazers in general but especially copepods (Loots et al. 2009; Pusceddu et al. 2009). Many Antarctic copepods represent a numerically dominant fraction of sea-ice communities and may have annual life cycles which take place completely in, partially within, or underneath the sea ice (Schnack-Schiel et al. 1995, 2001; Tanimura et al. 1996; Swadling 2001, Guglielmo et al. 2007). Other species, such as *Calanoides acutus* (Giesbrecht, 1902), *Calanus propinquus* (Brady, 1883), and *Metridia gerlachei* (Giesbrecht, 1902), are known to accumulate wax esters and triacylglycerols to overcome winter conditions (Schnack-Schiel and Hagen 1994; Hagen et al. 1993; Reinhardt and Van Vleet 1986). Other meso- to bathypelagic carnivorous species such as *Paraeuchaeta antarctica* (Giesbrecht, 1902) (Zmijewska 1993; Mazzocchi et al. 1995) exert an essential ecological and trophic role, being at the same time predators of smaller species belonging to the genera *Oithona*, *Oncaea*, and *Metridia* (Oresland 1991, 1995; Oresland and Ward 1993) and prey for larger macrozooplanktic organisms such as amphipods and mysids (Hopkins 1985), chaetognaths (Oresland 1995), midwater fishes (Williams 1985; Kellermann 1987), and even for benthic organisms such as brittle stars (Dearborn et al. 2011).

During the first Italian oceanographic expeditions in the Ross Sea, it was therefore natural to focus on copepods, and specifically on their distribution (Carli et al. 2000,

2002; Zunini Sertorio et al. 2000) and diversity (Carli et al. 1990, 1992; Zunini Sertorio et al. 1990, 1992).

The present copepod dataset from the Ross Sea is the eighth MNA contribution to the Antarctic Biodiversity Portal, the thematic Antarctic node for both the Ocean Biogeographic Information System (AntOBIS) and the Global Biodiversity Information Facility (ANTABIF) (<http://www.biodiversity.aq>). Previous MNA contributions focused on Mollusca, Tanaidacea, Fungi, Ophiuroidea, Porifera, Bryozoa, and Rotifera (Ghiglione et al. 2013, 2018; Piazza et al. 2014; Selbmann et al. 2015; Cecchetto et al. 2017, 2019; Garlasché et al. 2020).

This dataset also represents an Italian contribution to the CCAMLR CONSERVATION MEASURE 91-05 (2016) for the Ross Sea region Marine Protected Area, specifically, addressing Annex 91-05/C (“long-term monitoring of benthic ecosystem functions”).

## Project description

**Project title:** Distributional records of Ross Sea (Antarctica) planktic Copepoda from bibliographic data and samples curated at the Italian National Antarctic Museum (MNA): checklist of species collected in the Ross Sea sector from 1987 to 1995.

**Curator and promoter:** Stefano Schiaparelli.

**Personnel:** Bonello Guido, Marco Grillo, Matteo Cecchetto, Marina Giallain, Antonia Granata, Letterio Guglielmo, Luigi Pane, Stefano Schiaparelli.

**Funding:** Data originated in the framework of the first three Italian Antarctic Oceanographic expeditions carried out from 1988 to 1995 within 3 different research projects funded by the PNRA:

- III<sup>rd</sup> Italian Antarctic expedition (1987/1988), Project: “*Zooplankton – distribuzione spaziale e verticale delle comunità zooplanctoniche nella Baia di Terra Nova (Mare di Ross) con particolare riferimento al Krill*”; Project code 2.1.4.2.; R/V “*Polar Queen*”; Scientific coordinator: Prof. Letterio Guglielmo.
- V<sup>th</sup> Italian Antarctic expedition (1989/1990), Project: “*Campagna oceanografica nel mare di Ross*”; R/V “*Cariboo*”; Scientific coordinator: Prof. Letterio Guglielmo.
- X<sup>th</sup> Italian Antarctic expedition (1994–1995), Project: “*Ecologia zooplankton e micronecton*”; Project code (6.9); R/V “*Malippo*”; Scientific coordinator: Dr. Riccardo Cattaneo-Vietti

The Italian National Antarctic Museum (MNA) hired two experts, G. Bonello and M. Grillo, with the research contracts #2993 and #2992, respectively, issued on June 25<sup>th</sup> 2019, to revise plankton collections dating back to the first Italian Expeditions.

## Design description

As the dataset here presented was assembled from data and vouchers collected in the framework of different oceanographic expeditions, which had multiple scientific targets and deployed a variety of sampling gears to investigate the water column physi-

cal features and plankton diversity, we briefly introduce the general motivations and scopes of each one of these PNRA expeditions.

The oldest records of the dataset correspond to samples collected during the III<sup>rd</sup> Italian Antarctic expedition in 1987–1988, only two years after the opening of the Italian research station “Mario Zucchelli” (called “Terra Nova” at that time). This was also the first Italian Antarctic oceanographic expedition, and since there was practically no previous information on the study site (Terra Nova Bay, Ross Sea), the objective of this expedition was to define the spatial and temporal variability of physical, chemical and biological characteristics in this area (Faranda et al. 2000). The line of research on zooplankton developed for this peculiar expedition engaged multiple researchers and pursued the development of a first characterization of the community structure, on the taxonomic, spatial and ecological aspects for the region (Carli et al. 1990; Guglielmo et al. 1990; McKenzie et al. 1990; Zunini Sertorio et al. 1990).

The second oceanographic expedition (V<sup>th</sup> Italian Antarctic Expedition) took place two years later and investigated a larger geographic area in the Pacific sector of the Southern Ocean. The larger scale of the geographic study site reflected the more ambitious (compared to the first expedition) objectives of the expedition, aiming at achieving a better understanding of the functioning of the Antarctic pelagic ecosystems, through the study of hydrodynamic features (Faranda et al. 2000) in an area characterized by water mass distribution associated with frontal systems. Within this framework, the study of zooplanktic communities would have allowed a better characterization of the effects of these abiotic features on the trophic structure (Benassi et al. 1992; Carli et al. 1992; Guglielmo et al. 1992; Zunini Sertorio et al. 1992).

Finally, the third oceanographic expedition (X<sup>th</sup> Italian Antarctic Expedition) was carried out during the austral summer of 1994–1995. Most of the sampling was conducted along the 175° meridian, from the northern continental slope to the Ross Sea Ice Shelf. The main purpose of the expedition was to further investigate the effects of the ice-edge retreat on primary production (Faranda et al. 2000). As part of the project, the coastal zooplankton community structure, as well as an evaluation of the biomass and lipid content of the total zooplankton, was examined (Carli et al. 2002; Pane et al. 2004).

This dataset is not only important for the history of Italian research in Antarctica, but, as it dates back to 1987, it also provides a source of historical data, hence representing a useful baseline to measure possible changes and shifts in copepod abundance and diversity in the Ross Sea area that may have occurred in the meantime. At the same time, as the highly ambitious scopes of those expeditions also lead to the production, for the same sampling stations, of an extensive amount of biological and chemical-physical information, as well as about other taxa (Table 1), this copepod dataset can also be used to model and understand species distributions occurring in an environmental setting of more than 30 years ago to be compared with present-day situation.

**Table 1.** Type of sampling and main bibliographic references about the the III<sup>rd</sup>, V<sup>th</sup>, and X<sup>th</sup> Expeditions of the Italian National Antarctic Program (PNRA).

Type of data	References
<b>Water column communities</b>	
Bacterioplankton and heterotrophic bacteria	Bruni et al. 1990
Picoplankton	La Ferla et al. 1992
Phytoplankton	Goffart et al. 1992; Innamorati et al. 1992; Nuccio et al. 1992
Zooplankton	Guglielmo et al. 1990, 1992; Hecq and Guglielmo 1992
Microzooplankton	(Fonda Umani and Monti 1990; Maugeri 1992)
<b>Physical variables</b>	
Temperature	Innamorati et al. 1990; Magazzù and Decembrini 1990; Fabiano et al. 1991a
Practical salinity, density excess, and potential temperature	Boldrin and Stocchino 1990
Salinity	Innamorati et al. 1990
Nutrients, dissolved oxygen, pH, total alkalinity, and total inorganic carbon	Catalano and Benedetti 1990; Catalano et al. 1991a, 1991b; Catalano 1992
<b>Biological variables</b>	
Particulate organic matter	Fabiano et al. 1991b, 1991c, 1992
Total suspended matter, particulate carbohydrates, proteins, and lipids	Fabiano et al. 1992
Total and fractioned photosynthetic pigments concentration and primary production	Innamorati et al. 1990, 1991; Magazzù and Decembrini 1991, 1992; Saggiomo et al. 1992

## Methods

### Study extent and sampling description

As the distributional information provided in this data paper (Fig. 1) originates from three different PNRA expeditions that had a variety of scientific targets and research teams involved, the sampling stations included are only those where quantitative sampling methods were used and copepods were found.

For the III<sup>rd</sup> PNRA Expedition (first Italian Antarctic Expedition), 32 sampling stations located mainly in Terra Nova Bay between 72°S and 75°S of latitude and 163°E and 173°E of longitude (from 05/01/1988 to 21/02/1988) were investigated (Guglielmo et al. 1990). The V<sup>th</sup> PNRA Expedition (second Italian Antarctic Expedition) investigated a larger geographic area in the Pacific sector of the Southern Ocean, starting from 50°S to the Balleny Islands and finally reaching Terra Nova bay. The data included in this dataset correspond to 23 sampling stations surveyed between 62°S and 75°S and 161°E and 177°W (from 25/11/1989 to 12/1/1990) (Guglielmo et al. 1992). During this expedition, each station was sampled twice, and the duplicates were indicated as “bis” (e.g., Station 18/18bis). For the X<sup>th</sup> PNRA Expedition (third Italian Antarctic Expedition), five stations surveyed in the area surrounding “Mario Zucchelli” station (from 02/11/94 to 03/01/95) were included.

The majority of mesozooplankton samples from this dataset (i.e., those from the III<sup>rd</sup> and the V<sup>th</sup> PNRA Expeditions) were collected using an Eznet-BIONESS multi-

net (Fig. 2) (Sameoto et al. 1980), a very efficient zooplankton sampler consisting of multiple (usually ten) nets, stacked horizontally, opened and closed at desired depths by an on-board operator while the instrument is towed from a vessel (ICES 2000). Due to the exceptional filtration to mouth area ratio (10:1), a 90% filtration efficiency can be reached for a clean net towed at 1.5 m/s.

The Eznet-BIONESS was equipped with a KMS II (ME Meerestechnik Elektronik GmbH) multiparametric probe (that recorded temperature, salinity, depth, light attenuation, and oxygen concentration) and two acoustic doppler flowmeters (SM 21H-ME Meerestechnik Elektronik GmbH), put inside and outside the filtering apparatus, that recorded speed, in- and out-flow through the net, filtration efficiency, and net number. Different mesh sizes were used during the sampling activity but, regarding Copepoda, only 500  $\mu\text{m}$  and 250  $\mu\text{m}$  sizes were considered.

Another sampling device employed during these PNRA activities (X<sup>th</sup> PNRA Expedition) was a Working Party II (WP2 – UNEP FAO) standardized net (Fraser 1966; ICES 2000). This net had a 57 cm (0.25 m<sup>2</sup>) opening, a length of 2.6 m, and a 200  $\mu\text{m}$  mesh size. The WP2 was equipped with inner and outer General Oceanic flowmeter to the evaluation of the filtration efficacy. Sampling depths ranged from 200 m to the surface, depending on the sea-bottom depth of the sampling points (Carli et al. 2002).

More details about the sampling methodologies and procedures adopted during the III<sup>rd</sup> and V<sup>th</sup> PNRA Expeditions can be found in Guglielmo et al. (1990, 1992).

All samples collected during the three campaigns were preserved on board in a 4% buffered formaldehyde seawater solution and later dispatched to various experts (see below) for determination. Specimens now present in the collections of the Italian National Antarctic Museum are stored in 96% Ethanol.

## Spatial coverage

**General geographic description:** The study area covers a large portion of the north-western Ross Sea, spanning from the Drygalski Ice Tongue in Terra Nova Bay to the continental slope surrounding the Central Basin. Some sampling stations were located at the Balleny Islands and other northern areas (Fig. 1).

**Coordinates:** Latitude bounding coordinates: -61.99067 and -75.40556; Longitude bounding coordinates: 161.82867 and -177.74167

## Temporal coverage

05 January 1988 to 11 February 1995.

## Dataset description and quality control

**Title:** Distributional records of Ross Sea (Antarctica) planktic Copepoda from bibliographic data and samples curated at the Italian National Antarctic Museum (MNA).

**Character encoding:** UTF-8;

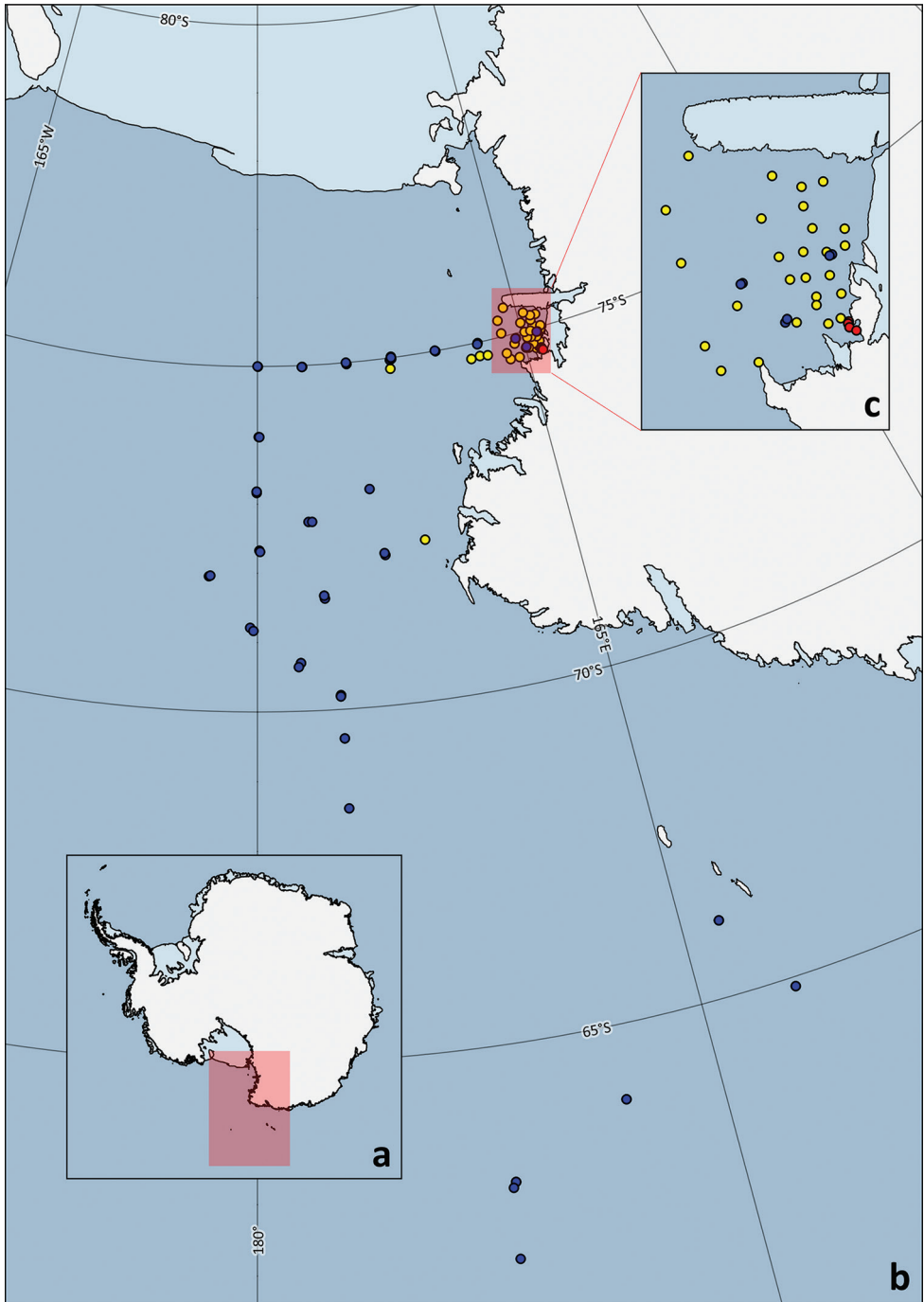


**Figure 1.** Sampling stations for III<sup>rd</sup> (yellow), V<sup>th</sup> (blue), and X<sup>th</sup> (red) expedition **a** overview of spatial extent in Antarctica **b** sampling stations in the Western Ross Sea **c** focus on Terra Nova Bay sampling stations. This map was produced using the collection of datasets “Quantarctica” (Matsuoka et al. 2017) and QGIS (QGIS Development Team 2020).

**Format name:** Darwin Core Archive format;

**Distribution:** <https://doi.org/10.15468/zndaaw>

**Language:** English;

**Metadata language:** English;

**License of use:** This dataset [Distributional records of Ross Sea (Antarctica) planktic Copepoda from bibliographic data and samples curated at the Italian National Antarctic Museum (MNA)] is made available under the Creative Commons Attribution License (CC-BY) 4.0: <http://www.creativecommons.org/licenses/by/4.0/legalcode>

**Date of metadata creation:** 10 Feb. 2020;

This dataset comprises a total of 6,027 distributional records, out of which 5,306 were obtained by digitizing original data reports (hereafter “literature records”) and 721 are based on physical museum vouchers (hereafter “MNA collection records”) curated by the MNA (Section of Genoa).

All literature records (defined by the term ‘HumanObservation’ under the column ‘BasisOfRecord’) were manually extracted from five different data reports published in 1990, 1992, and 2002 (Carli et al. 1990, 1992, 2002; Zunini Sertorio et al. 1990, 1992). The information regarding the sampling events for the III<sup>rd</sup> and V Italian Antarctic expeditions (e.g. sampling station coordinates, depth, volume filtered, etc.) was manually extracted from two other data reports (Guglielmo et al. 1990, 1992). The general characteristics of the sampling events are reported in the “Event” dataset with starting and ending coordinates (‘footprintWKT’ term) along with information on the subsequent samples handling (e.g., the examined aliquot) listed under the Darwin Core term ‘dynamicProperties’. All the MNA collection records (defined by the term ‘PreservedSpecimen’ under the column ‘BasisOfRecord’) correspond to a section of the entire batch of samples collected during the III<sup>rd</sup> and V<sup>th</sup> expeditions that were not previously sorted at the species level.

As the two different types of distributional data, i.e., MNA collection records and literature records, originated from the same sampling events, an apparent conflict might derive from multiple records sharing the same taxonomy, sampling event (i.e., sampling station, depth) and organism quantity information in the dataset. However, all the MNA collection records originated from plankton aliquots not previously studied and published, thus representing additional data that were not included by the original authors. Most of the literature records are reported with their original abundance values (number of individuals per volume unit, e.g. m<sup>3</sup>), whereas all the MNA collection records are reported in terms of number of individuals per museum vial. Some literature records from the V<sup>th</sup> expedition were originally reported with the number of individuals (Zunini Sertorio et al. 1992), instead of an abundance measure. However, the number of individuals reported for these bibliographic records can indeed be converted in abundance measures, as the authors of the original bibliographic reference provided the volumetric information on the aliquot examined.

All data were then gathered in a single dataset formatted to fulfil the Darwin Core standard protocol (Wieczorek et al. 2012) required by the OBIS scheme (<http://www.iobis.org/manual/lifewatchqc/>) and according to the SCAR-MarBIN Data Toolkit (<http://www.scarmarbin.be/documents/SM-FATv1.zip>). The dataset was uploaded

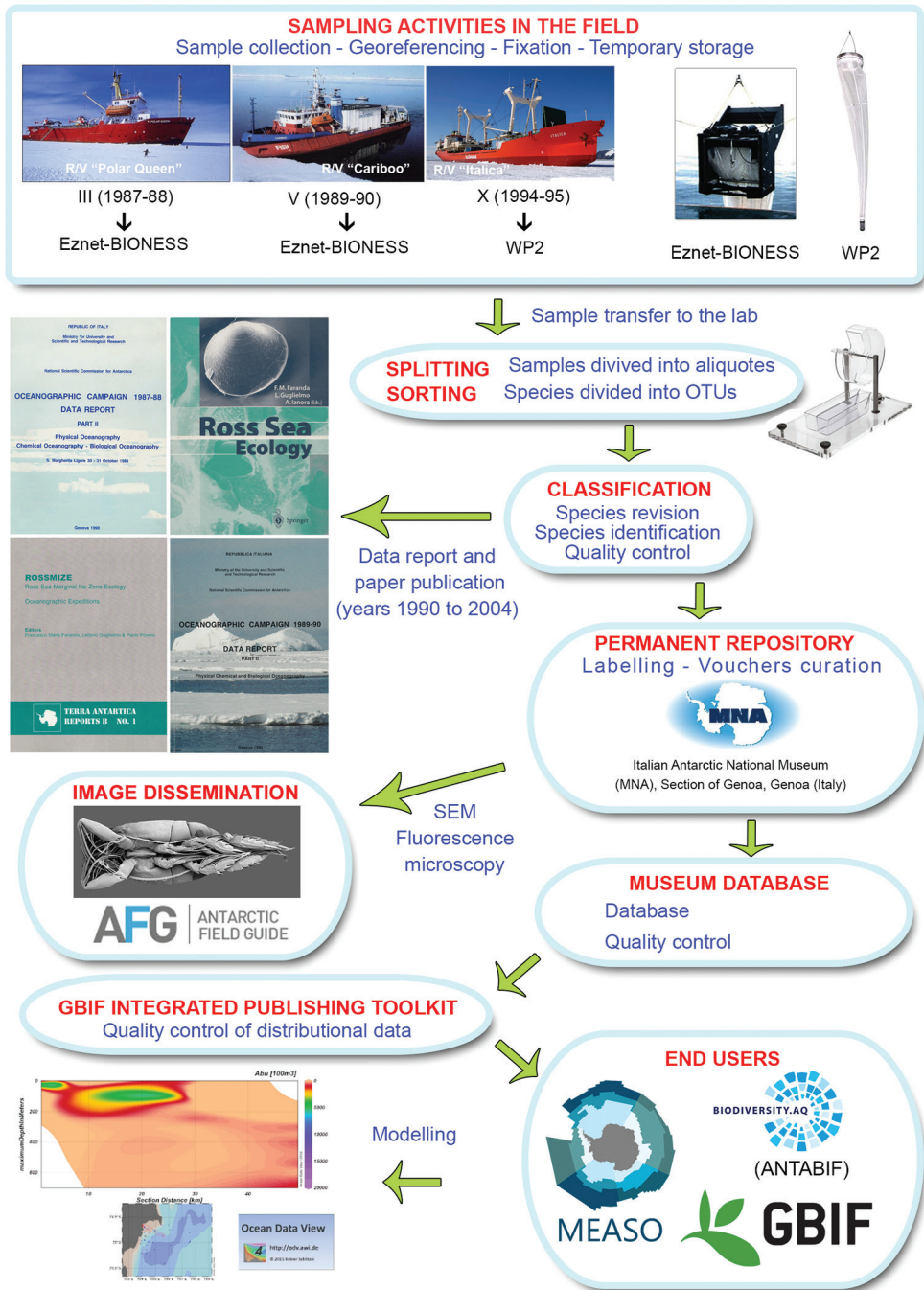


**Figure 2.** Flowchart representing all stages in dataset development and publishing.

and integrated with the ANTOBIS database (the geospatial component of SCAR-MarBIN). The taxonomy was checked and updated using WoRMS (Horton et al. 2019, World Register of Marine Species; <http://www.marinespecies.org>; last accessed

02 December 2019). Different control and data-cleaning steps (e.g., scientific name check and spelling) were undertaken to increase data quality (Fig. 2).

The Darwin Core elements included in the dataset are: occurrenceID, BasisOfRecord (HumanObservation for the bibliographic records and PreservedSpecimen for the museum specimen records), type (identifying the nature of the resource), scientificName (the name in the lowest taxonomic rank identified and updated according to WoRMS with authorship and date for the records identified at the species level), order, family, genus, specificEpithet, scientificNameAuthorship (corresponding to the updated taxonomy according to WoRMS, together with the previous four elements), originalNameUsage (the original identification as reported in the bibliographic resource), identificationQualifier (the qualifier for the uncertainty of identification, following Sigovini et al. 2016), scientificNameID (the globally unique identifier for the taxonomic information related to the scientificName and stored in WoRMS), taxonRemarks (notes and considerations regarding the taxonomy of the record), organismQuantity, organismQuantityType (the type of quantification system used, such as the number of individuals or abundance per 100 or one cubic metre), sex, lifeStage (following the controlled vocabulary ‘BODC parameter semantic model biological entity development stage terms’ at <https://github.com/nvs-vocabs/S11>), occurrenceRemarks (name of the PNRA research expedition), fieldNumber (name of the sampling station and net number, separated by an underscore), eventDate (date of the sampling event), decimalLatitude, decimalLongitude, minimumDepthInMeters, maximumDepthInMeters, sampleSizeValue (the number of cubic meters filtered by the net as reported in the bibliographic resource), sampleSizeUnit, samplingProtocol (following the controlled vocabulary at <http://vocab.nerc.ac.uk/collection/B07/current/>, Wiebe et al. 2014), eventRemarks (name of the sampling gear as reported in the bibliographic reference and mesh size of the net, separated by a pipe), associatedReferences (bibliographic reference associated to the resource), preparations (following ‘Documentation for code table SPECIMEN\_PART\_NAME’ at [http://arctos.database.museum/info/ctDocumentation.cfm?table=CTSPECIMEN\\_PART\\_NAME](http://arctos.database.museum/info/ctDocumentation.cfm?table=CTSPECIMEN_PART_NAME)), catalogNumber (museum voucher code for the specimen). Most of the sampling stations have two sets of coordinates: the starting and ending points. In such cases, the coordinates reported in the dataset refer to the starting point of the sampling event. For some museum records, the net number, which corresponds to a specific depth stratum investigated, was not available. For these records, the minimum depth was omitted, while for the maximum depth the value recorded for the corresponding sampling station was reported.

## Taxonomic coverage

The Copepoda diversity of the dataset is displayed in 6,027 records, among which Calanoida represent the most frequent (80%), followed by Cyclopoida (15.3%) and unidentified Copepoda (4.6%). Only five records belong to Harpacticoida and one to Siphonostomatoida. Regarding the life stages identification, the data set is composed of most adults (52.4%), followed by copepodites (45.5%), nauplii (0.7%), and unreported (1.4%). The three campaigns (III<sup>rd</sup>, V<sup>th</sup>, and X<sup>th</sup>) data report analysis produced a combined total of 5,306 literature reports divided among 52 morphological units. Among

these, 26 species belong to three orders (Calanoida, Cyclopoida, Harpacticoida) and 17 families. Overall, Calanoida were the most frequently found (78.5%), followed by Cyclopoida (16.25%) and Harpacticoida (0.07%). In terms of sampling frequency, among the determined specimens, members of family Metridinidae were the most common (25.56%), followed by Euchaetidae (23.11%), Calanidae (21.19%), and Oithonidae (10.6%); the other 14 families accounted for the remaining 19.53% (Fig. 3). Overall, 721 museum vouchers were acquired from the National Antarctic Museum (MNA collection records), among which Calanoida represented the major contributors (91.6%), followed by Cyclopoida (8.2%) and two records belonging to Harpacticoida and Siphonostomatoida, respectively. Calanoid diversity spans 19 families, among which we find a relevant percentage of Euchaetidae (22.8%), Calanidae (17.8%), Metridinidae (16.2%), Aetideidae (13.9%), Scolecithridae (8.5%), Lucicutiidae (3.8%), and others (17%). Cyclopoida diversity accounts for three families and four genera, while Harpacticoida and Siphonostomatoida are represented by one species each (Fig. 4).

## Taxonomic rank

**Kingdom:** Animalia

**Phylum:** Arthropoda

**Class:** Maxillopoda

**Order:** Calanoida, Cyclopoida, Harpacticoida, Siphonostomatoida

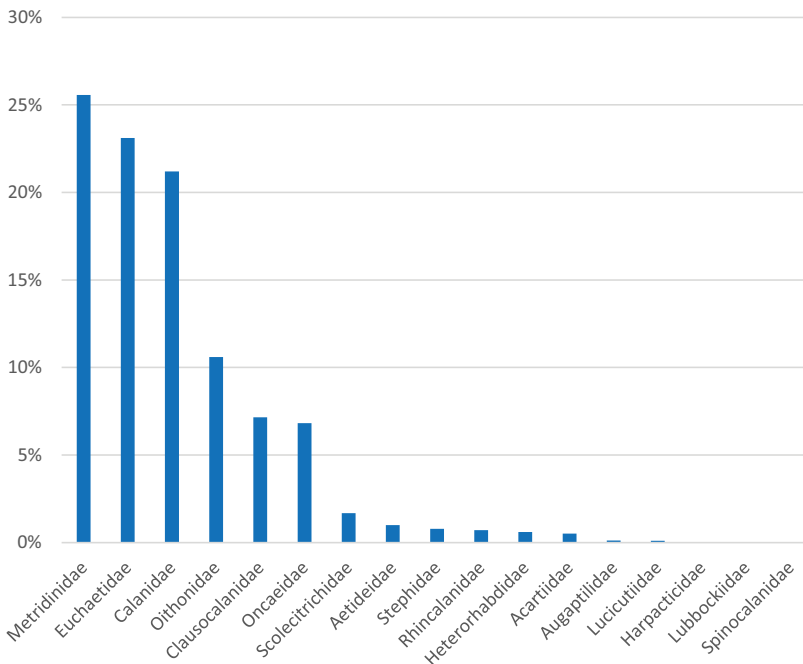


**Figure 3.** Taxonomic diversity for data report analysis.

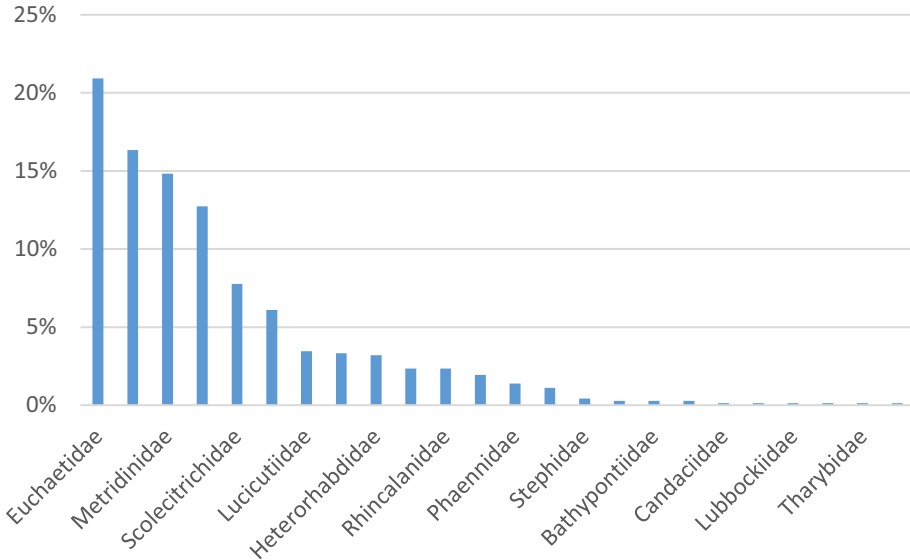


**Figure 4.** Taxonomic diversity for museum vouchers.

**Families:** Acartiidae, Aetideidae, Augaptilidae, Bathypontiidae, Calanidae, Candaciidae, Clausocalanidae, Eucalanidae, Euchaetidae, Harpacticidae, Heterorhabdidae, Lubbockiidae, Lucicutiidae, Metridinidae, Oithonidae, Oncaeiidae, Paracalanidae, Phaennidae, Rataniidae, Rhincalanidae, Scolecitrichidae, Spinocalanidae, Stephidae, Tharybidae, Tisbidae

**Genera:** *Aetideopsis*, *Aetideus*, *Amallothrix*, *Calanoides*, *Calanus*, *Calocalanus*, *Candacia*, *Cephalophanes*, *Chiridiella*, *Chiridius*, *Chirundina*, *Clausocalanus*, *Cornucalanus*, *Ctenocalanus*, *Euaugaptilus*, *Eucalanus*, *Euchirella*, *Farrania*, *Gaetanus*, *Haloptilus*, *Harpacticus*, *Heterorhabdus*, *Lubbockia*, *Lucicutia*, *Metridia*, *Microcalanus*, *Oithona*, *Oncaea*, *Onchocalanus*, *Paracalanus*, *Paracomantenna*, *Paraeuchaeta*, *Paraheterorhabdus*, *Paralabidocera*, *Phaenna*, *Pleuromamma*, *Pontoptilus*, *Pseudeuchaeta*, *Pseudhaloptilus*, *Pseudoamallothrix*, *Pseudochirella*, *Racovitzanus*, *Ratania*, *Rhincalanus*, *Scaphocalanus*, *Scolecithricella*, *Spinocalanus*, *Stephos*, *Temorites*, *Tisbe*, *Triconia*, *Undinella*

**Species:** *Aetideopsis antarctica*, *Aetideopsis minor*, *Aetideus australis*, *Aetideus pseudarmatus*, *Amallothrix gracilis*, *Amallothrix dentipes*, *Calanoides acutus*, *Calanoides carinatus*, *Calanus propinquus*, *Candacia falcifera*, *Cornucalanus robustus*, *Ctenocalanus vanus*, *Euaugaptilus laticeps*, *Euchirella rostromagna*, *Euchirella rostrata*, *Farrania frigida*, *Gaetanus tenuispinus*, *Gaetanus inermis*, *Gaetanus brevispinus*, *Gaetanus minor*, *Haloptilus ocellatus*, *Harpacticus furcifer*, *Heterorhabdus austrinus*, *Heterorhabdus pustulifer*, *Heterorhabdus tanneri*, *Lucicutia ovalis*, *Lucicutia wolfendeni*, *Lucicutia magna*, *Lucicutia intermedia*, *Lucicutia curta*, *Lucicutia macrocera*, *Metridia gerlachei*, *Metridia curticauda*, *Microcalanus pygmaeus*, *Oithona frigida*, *Oithona similis*, *Oncaea curvata*, *Onchocalanus magnus*, *Paraeuchaeta antarctica*, *Paraeuchaeta similis*, *Paraeuchaeta exigua*, *Paraeuchaeta comosa*, *Paraeuchaeta kurilensis*, *Paraheterorhabdus farrani*, *Paralabidocera antarctica*, *Pleuromamma robusta*, *Pleuromamma*

*gracilis*, *Pleuromamma abdominalis*, *Pontoptilus ovalis*, *Pseudhaloptilus eurygnathus*, *Pseudoamallothrix ovata*, *Pseudochirella hirsuta*, *Pseudochirella notacantha*, *Racovitzanus antarcticus*, *Ratania atlantica*, *Rhincalanus gigas*, *Scaphocalanus subbrevicornis*, *Scaphocalanus magnus*, *Scaphocalanus verwoorti*, *Scaphocalanus affinis*, *Scaphocalanus brevicornis*, *Scolecithricella minor*, *Spinocalanus abyssalis*, *Spinocalanus magnus*, *Spinocalanus horridus*, *Spinocalanus brevicaudatus*, *Stephos longipes*, *Temorites brevis*, *Triconia conifera*, *Triconia antarctica*, *Undinella simplex*

## History of the Copepoda collection

The Antarctic copepods sampled during the three expeditions were studied by different research groups and experts in different times. The III<sup>rd</sup> expedition samples were determined and studied by T.Z. Sertorio, P. Salemi Picone, P. Bernat, E. Cattini, C. Ossola, A. M. Carli, L. Pane, and G.L. Mariottini (Carli et al. 1990; Zunini Sertorio et al. 1990). Samples from the V<sup>th</sup> expedition were examined by T.Z. Sertorio, P. Licandro, F. Ricci, M. Giallain, A. Artegiani, L. Pane, A. Carli, G.L. Mariottini, and M. Feletti (Carli et al. 1992; Zunini Sertorio et al. 1992). Samples from the X<sup>th</sup> expedition were studied by L. Pane, A. Carli, M. Feletti, and B. Francomacaro (Pane et al. 2004).

Other samples from the V<sup>th</sup> expedition were also studied and later published by (Zunini Sertorio et al. 2000). In this case, with the aid of Dr Elena Markhaseva and Dr Nina Vyskvartzeva of the Zoological Institute of the Russian Academy of Sciences of St Petersburg, new determinations and records of species were added. However, these records were grouped by family and reported only with a general indication of the sampling station without details about depth or abundance. The fate of these samples is unknown and are therefore not available in the MNA collections. For this reason, these latter records were not included in the present dataset but just listed here with the classification reported in the original paper (Zunini Sertorio et al. 2000):

*Mimocalanus cultrifer* (Farran, 1908); *Mimocalanus inflatus* (Davis, 1949); *Spinocalanus antarcticus* (Wolfenden, 1906); *Spinocalanus spinipes* (Brodsky, 1950); *Spinocalanus spinosus* (Farran, 1908); *Chiridiella megadactyla* (Bradford, 1971); *Gaetanus antarcticus* (Wolfenden, 1905); *Pseudochirella elongata* (Wolfenden, 1905); *Cornucalanus antarcticus* (Brodsky & Zvereva, 1950); *Lophotrix simplex* (Wolfenden, 1911); *Mixtocalanus alter* (Farran, 1929); *Mixtocalanus verwoorti* (Park, 1980); *Scaphocalanus antarcticus* (Park, 1982); *Scaphocalanus echinatus* (Farran, 1905); *Scaphocalanus farrani* (Park, 1982); *Scaphocalanus parantarcticus* (Park, 1982); *Scolecithricella cenotelis* (Park, 1980); *Scolecithricella dentipes* (Verwoort, 1951); *Scolecithricella emarginata* (Farran, 1905); *Scolecithricella ovata* (Farran, 1905); *Temora* sp.; *Undinella acuta* (Vaupel-Klein, 1970); *Hemirhabdus* sp.; *Heterostylites longicornis* (Giesbrecht, 1889); *Euaugaptilus antarcticus* (Wolfenden, 1911); *Euaugaptilus nodifrons* (Sars, 1905); *Haloptilus oxycephalus* (Giesbrecht, 1889); *Pachyptilus pacificus* (Johnson, 1936).

Finally, the whole MNA copepod collection was recently reorganized and taxonomically revised at the lowest possible taxonomic level for the present contribution by G. Bonello and M. Grillo under a research contract with the MNA. For this final check, species identifications were based on the Banyuls sur Mer marine Copepoda

database (Razouls et al. 2020; <https://copepodes.obs-banyuls.fr>), while the current taxonomical state was cross-checked with the Register of Antarctic Marine Species, RAMS (De Broyer et al. 2020) (last accessed 02 December 2019). For all 82 species present in the MNA collections, a collection of permanent slides for microscopy were prepared by mounting specimens within plastic adhesive rings, filled with Glycerol, to avoid undesired flattening. When possible, multiple specimens were acquired in both ventral and lateral view to ease eventual future analysis (Kihara and da Rocha 2009). Transparent varnish was used to seal the slides after mounting them.

### Copepod image acquisition

For all the species listed in this data paper, a selection of complete specimens was prepared to produce high-quality images and highlight taxonomical characters necessary for species identification. For this purpose, different imaging techniques were applied: i) Scanning Electron Microscopy (SEM) after gold coating (e.g., for *Paraeuchaeta exigua*



**Figure 5.** *Paraeuchaeta exigua* (Copepoda, Calanoida; female, MNA-12333) acquired with scanning electron microscopy (SEM). This is one of the most common species in the coastal area of Terra Nova Bay. It plays a key role in the neritic trophic chain and highly contributes to the total mesozooplanktic biomass.

(Wolfenden, 1911), Fig. 5); ii) fluorescence microscopy after staining. In this latter case, Copepoda specimens were stained with 1.5 mg/ml Congo Red solution following the methods of Michels and Büntzow (2010) and with different Congo Red and Fuchsin dilutions (Ivanenko et al. 2012). Images were then acquired with an Olympus IX70 (200×) inverted microscope (e.g., *Metridia gerlachei* (Giesbrecht, 1902), Fig. 6) provided with a fluorescent light apparatus. Image post-processing and cleaning were performed with Adobe Photoshop CC 2015 and Nik Collection filters (Sharpener and Silver Efex).

### Geographic data and new distributional records

To evaluate the number of potential new records for a given area, defined as new occurrences in the Global Biodiversity Information Facility repository (GBIF, <https://www.gbif.org>) for that area, we have used the *spocc* (version 1.0.8) R package, as well as the online Copepod database provided by the Banyuls sur mer observatory (Razouls et al. 2020; <https://copepodes.obs-banyuls.fr>). For the analysis with *spocc* we selected

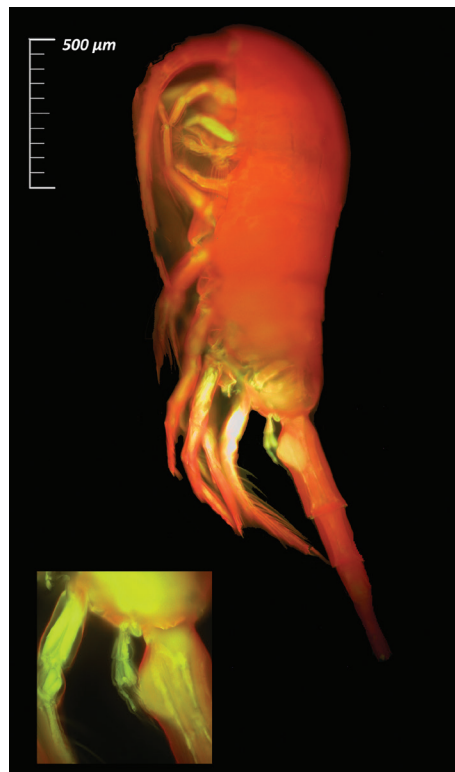


**Figure 6.** *Metridia gerlachei* (Copepoda, Calanoida; female, MNA-12439) acquired with fluorescence microscopy (Congo Red, 1.5 mg/ml). This species is one of the most adapted species in the Antarctic region and can perform diel vertical migrations that highly influence the surrounding waters in terms of trophic relationships in Terra Nova Bay.

the sources ‘gbif’, ‘obis’, ‘ecoengine’, ‘inat’, ‘idigbio’ and produced a distributional map for each single species. The Banyuls sur mer observatory interactive database gathers information on diversity and distribution of planktic Copepoda from the available literature and is continuously updated with the latest research.

To our knowledge, regarding the Ross Sea area and its boundaries, 62% of the species reported ( $n = 71$ ) in this data paper represent new records for GBIF for the Western Ross Sea sector and 28% for the whole Antarctic region. It must be considered that some of the sampling stations were close to the northern boundaries of the circumpolar current and the Ross Sea Gyre, hence the presence of pelagic copepods typical for sub-Antarctic areas.

## Acknowledgements

We thank Dr Gritta Veit-Köhler (German Centre for Marine Biodiversity Research) and an anonymous reviewer for their precious suggestions and comments that greatly improved the initial manuscript version.

## References

- Amato E (1990) Environmental impact assessment at sea. National Scientific Commission for Antarctica, Oceanographic Campaign 1987–1988. In: Cervellati R, Dall’Oglio G, Ramorino MC, Testa M (Eds) Rapporto preliminare sulla campagna antartica Estate Australe 1987–88. PNRA, Roma, 95–99.
- Benassi G, Ferrari I, Gentile G, Menozzi P, McKenzie KG (1992) Planktonic Ostracoda in the Southern Ocean and in the Ross Sea: 1989–90 Campaign. In: National Scientific Commission for Antarctica (Ed.) Oceanographic Campaign 1989–90, Data Report Part II. National Scientific Commission for Antarctica, Genova, 247–300.
- Boldrin C, Stocchino C (1990) On the hydrological characteristics of Terra Nova Bay (Ross Sea-Antarctica). In: National Scientific Commission for Antarctica (Ed.) Oceanographic Campaign 1987–88, Data Report Part I. National Scientific Commission for Antarctica, Genova, 11–57.
- Bruni V, Maugeri TL, Acosta Pomar L, Grasso S, Moio L (1990) Preliminary data on marine microflora in Terra Nova Bay (Antarctica). In: National Scientific Commission for Antarctica (Ed.) Oceanographic Campaign 1987–88, Data Report Part I. National Scientific Commission for Antarctica, Genova, 87–104.
- Carli A, Mariottini GL, Pane L (1990) Contribution to the study of copepods collected in Terra Nova Bay (Ross Sea). In: National Scientific Commission for Antarctica (Ed.) Oceanographic Campaign 1987–88, Data Report Part II. National Scientific Commission for Antarctica, Genova, 129–167.
- Carli A, Feletti M, Mariottini GL, Pane L (1992) Contribution to the study of copepods collected during the italian oceanographic campaign in Antarctica 1989–90. In: National Scientific Commission for Antarctica (Ed.) Oceanographic Campaign 1989–90, Data Report Part II. National Scientific Commission for Antarctica, Genova, 179–210.

- Carli A, Pane L, Stocchino C (2000) Planktonic copepods in Terra Nova Bay (Ross Sea): distribution and relationship with environmental factors. In: Faranda FM, Guglielmo L, Ianora A (Eds) *Ross Sea Ecology*. Springer, Berlin, 309–321. [https://doi.org/10.1007/978-3-642-59607-0\\_24](https://doi.org/10.1007/978-3-642-59607-0_24)
- Carli A, Feletti M, Pane L (2002) Zooplankton biomass and copepod abundance of Terra Nova Bay, Ross Sea Antarctic Campaign 1994/1995. *Terra Antarctica Reports B1* 51–55.
- Catalano G, Benedetti F (1990) Distributions of nutrients in the Terra Nova Bay and in the Ross Sea. National Scientific Commission for Antarctica (Ed.) *Oceanographic Campaign 1987–88, Data Report Part I*. National Scientific Commission for Antarctica, Genova, 61–83.
- Catalano G, Benedetti F, Iorio M (1991a) Coastal oceanography from Cape Russel to Campbell Ice Tongue (Terra Nova Bay). Dissolved oxygen, nutrients, pH, total alkalinity and total inorganic carbon distribution. National Scientific Commission for Antarctica (Ed.) *Oceanographic Campaign 1989–90, Data Report Part I*. National Scientific Commission for Antarctica, Genova, 25–32.
- Catalano G, Benedetti F, Goffart A, Iorio M (1991b) Distribution of dissolved oxygen, pH, total alkalinity and nutrients in Southern Ocean and Ross Sea (R/V “Cariboo” 1989–90 cruise). In: National Scientific Commission for Antarctica (Ed.) *Oceanographic Campaign 1989–90, Data Report Part I*. National Scientific Commission for Antarctica, Genova, 11–23.
- Catalano G (1992) The activity of the Chemical Oceanography Group in the Italian Antarctic Oceanographic Expeditions. *Oceanografia in Antartide*. ENEA-Progetto Antartide, Italia/Centro EULA, Universidad de Concepcion, 59–70.
- Cecchetto M, Alvaro MC, Ghiglione C, Guzzi A, Mazzoli C, Piazza P, Schiaparelli S (2017) Distributional records of Antarctic and sub-Antarctic Ophiuroidea from samples curated at the Italian National Antarctic Museum (MNA): check-list update of the group in the terra nova bay area (Ross Sea) and launch of the MNA 3D model “Virtual gallery.” *ZooKeys* 705: 61–79. <https://doi.org/10.3897/zookeys.705.13712>
- Cecchetto M, Lombardi C, Canese S, Cocito S, Kuklinski P, Mazzoli C, Schiaparelli S (2019) The bryozoa collection of the Italian National Antarctic Museum, with an updated check-list from Terra Nova Bay, Ross Sea. *ZooKeys* 812: 1–22. <https://doi.org/10.3897/zookeys.812.26964>
- Dearborn JH, Ferrari FD, Edwards KC (2011) Can pelagic aggregations cause benthic satiation? Feeding biology of the Antarctic brittle star *Astrotoma agassizii* (Echinodermata: Ophiuroidea). *Antarctic Research Series* 44: 1–28. <https://doi.org/10.1029/AR044p0001>
- De Broyer C, Clarke A, Koubbi P, Pakhomov E, Scott F, Vanden Berghe E, Danis B (2020) Register of Antarctic Marine Species. <http://www.marinespecies.org/rams> [accessed on 2020-07-16]
- Fabiano M, Povero P, Medica D, Bruzzone R (1991a) Distribution of particulate organic matter in Antarctic waters. In: National Scientific Commission for Antarctica (Ed.) *Oceanographic Campaign 1989–90, Data Report Part I*. National Scientific Commission for Antarctica, Genova, 113–137.
- Fabiano M, Povero P, Catalano G, Benedetti F (1991b) Hydrological data collected during the biological, chemical and geological sampling in Terra Nova Bay. In: National Scientific Commission for Antarctica (Ed.) *Oceanographic Campaign 1989–90, Data Report Part I*. National Scientific Commission for Antarctica, Genova, 35–71.

- Fabiano M, Povero P, Danovaro R, Medica D, Bruzzone R (1991c) Particulate organic matter in Terra Nova Bay. In: National Scientific Commission for Antarctica (Ed.) Oceanographic Campaign 1989–90, Data Report Part I. National Scientific Commission for Antarctica, Genova, 73–112.
- Fabiano M (1992) Observations on the Particulate Organic Matter in Antarctic waters. *Oceanografia in Antartide*. ENEA-Progetto Antartide, Italia/Centro EULA, Universidad de Concepcion, 145–148.
- Fabiano M, Povero P, Medica D, Danovaro R (1992) Distribution and composition of the particulate organic matter in Antarctic waters (Oceanographic Expedition 1989–90). *Oceanografia in Antartide*. ENEA-Progetto Antartide, Italia/Centro EULA, Universidad de Concepcion: 133–143.
- Faranda FM, Guglielmo L, Ianora A (2000) The Italian Oceanographic Cruises in the Ross Sea (1987–95): strategy, general considerations and description of the sampling sites. In: Faranda FM, Guglielmo L, Ianora A (Eds) *Ross Sea Ecology*. Springer, Berlin, Heidelberg, 1–13. [https://doi.org/10.1007/978-3-642-59607-0\\_1](https://doi.org/10.1007/978-3-642-59607-0_1)
- Fonda Umani S, Monti M (1990) Microzooplanktonic populations in Terra Nova Bay. In: National Scientific Commission for Antarctica (Ed.) Oceanographic Campaign 1987–88, Data Report Part I. National Scientific Commission for Antarctica, Genova, 241–254.
- Fraser JH (1966) Zooplankton sampling. *Nature* 211: 915–916. <https://doi.org/10.1038/211915a0>
- Garlasché G, Karimullah K, Iakovenko N, Velasco-Castrillón A, Janko K, Guidetti R, Rebecchi L, Cecchetto M, Schiaparelli S, Jersabek CD (2020) A data set on the distribution of Rotifera in Antarctica. *Biogeographia* 35: 17–25. <https://doi.org/10.21426/B635044786>
- Ghiglione C, Alvaro MC, Griffiths HJ, Linse K, Schiaparelli S (2013) Ross Sea Mollusca from the Latitudinal Gradient Program: R/V *Italica* 2004 Rauschert dredge samples. *ZooKeys* 341: 37–48. <https://doi.org/10.3897/zookeys.341.6031>
- Ghiglione C, Alvaro MC, Cecchetto M, Canese S, Downey R, Guzzi A, Mazzoli C, Piazza P, Rapp HT, Sarà A, Schiaparelli S (2018) Porifera collection of the Italian National Antarctic Museum (MNA), with an updated checklist from Terra Nova Bay (Ross Sea). *ZooKeys* 758: 137–156. <https://doi.org/10.3897/zookeys.758.23485>
- Goffart A, Catalano G, Magazzù G, Hecq J (1992) Some Examples of the Influence of Hydrodynamic Constraints on the Phytoplanktonic Biomass Distribution in the Southern Ocean. *Oceanografia in Antartide*. ENEA-Progetto Antartide, Italia/Centro EULA, Universidad de Concepcion: 265–271.
- Guglielmo L, Costanzo G, Manganaro A, Zagami G (1990) Spatial and vertical distribution of zooplanktonic communities in the Terra Nova Bay (Ross Sea). In: National Scientific Commission for Antarctica (Ed.), Data Report Part I. National Scientific Commission for Antarctica, Genova, 257–398.
- Guglielmo L, Costanzo G, Zagami G, Manganaro A, Arena G (1992) Zooplankton ecology in the Southern Ocean. In: National Scientific Commission for Antarctica (Ed.), Data Report Part II. National Scientific Commission for Antarctica, Genova, 30–468.
- Guglielmo L, Zagami G, Saggiomo V, Catalano G, Granata A (2007) Copepods in spring annual sea ice at Terra Nova Bay (Ross Sea, Antarctica). *Polar Biology* 30: 747–758. <https://doi.org/10.1007/s00300-006-0234-2>

- Hagen W, Kattner G, Graeve M (1993) *Calanoides acutus* and *Calanus propinquus*, Antarctic copepods with different lipid storage modes via wax esters or triacylglycerols. *Marine Ecology Progress Series* 97: 135–142. <https://doi.org/10.3354/meps097135>
- Hagen W, Schnack-Schiel SB (1996) Seasonal lipid dynamics in dominant Antarctic copepods: energy for overwintering or reproduction? *Deep-Sea Research Part I: Oceanographic Research Papers* 43: 139–158. [https://doi.org/10.1016/0967-0637\(96\)00001-5](https://doi.org/10.1016/0967-0637(96)00001-5)
- Hecq JH, Guglielmo L (1992) Structure and functioning of the Ross Sea pelagic ecosystem: an interdisciplinary approach. *Oceanografía en Antártica*. Gallardo VA, O. Ferrati O, Moyano H (Eds) *Proyecto Antártica-Italia*. Centro EULA, Concepción, Chile, 227–233.
- Hopkins TL (1985) Food web of an Antarctic midwater ecosystem. *Marine Biology* 89: 197–212. <https://doi.org/10.1007/BF00392890>
- WoRMS Editorial Board (2020) World Register of Marine Species. <http://www.marinespecies.org> [accessed on: 2020-07-16]
- ICES (2000) ICES Zooplankton Methodology Manual ICES Zooplankton Methodology Manual. Harris RP, Wiebe PH, Lenz J, Skjoldal HR, Huntley M (Eds). Academic Press. <https://doi.org/10.1016/B978-0-12-327645-2.X5000-2>
- Innamorati M, Mori G, Lazzara L, Nuccio C, Lici M, Vanucci S (1990) Ecology of phytoplankton. In: National Scientific Commission for Antarctica (Ed.), *Oceanographic Campaign 1987–88, Data Report Part I*. National Scientific Commission for Antarctica, Genova, 161–238.
- Innamorati M, Lazzara L, Mori G, Nuccio C, Saggiomo V (1991) Phytoplankton Ecology. In: National Scientific Commission for Antarctica (Ed.) *Oceanographic Campaign 1989–90, Data Report Part I*. National Scientific Commission for Antarctica, Genova, 141–252.
- Innamorati M, Lazzara L, Massi L, Mori G, Nuccio C, Saggiomo EV (1992) Research on the Phytoplankton Biomass in the Ross Sea in Relation to Environmental Factors. *Oceanografía in Antártide*. ENEA-Progetto Antartide, Italia/Centro EULA, Universidad de Concepcion, 235–252.
- Ivanenko VN, Corgosinho PHC, Ferrari F, Sarradin PM, Sarrazin J (2012) Microhabitat distribution of *Smacigastes micheli* (Copepoda: Harpacticoida: Tegastidae) from deep-sea hydrothermal vents at the Mid-Atlantic Ridge, 37°N (Lucky Strike), with a morphological description of its nauplius. *Marine Ecology* 33 (2): 246–256. <https://doi.org/10.1111/j.1439-0485.2011.00484.x>
- Kellermann A (1987) Food and feeding ecology of postlarval and juvenile *Pleuragramma antarcticum* (Pisces; Notothenioidei) in the seasonal pack ice zone off the Antarctic peninsula. *Polar Biology* 7: 307–315. <https://doi.org/10.1007/BF00443949>
- Kihara TC, da Rocha CEF (2009) Técnicas para estudos taxonômico de copépodes harpacticóides da meiofauna marinha. Editora Asterisco, Porto Alegre, 94 pp.
- La Ferla R, Acosta Pomar L, Allegra A, Bruni, V (1992) Microbial Distribution in Coastal Stations of Terra Nova Bay. *Oceanografía in Antártide*. ENEA-Progetto Antartide, Italia/Centro EULA, Universidad de Concepcion, 149–153.
- Loots C, Swadling KM, Koubbi P (2009) Annual cycle of distribution of three ice-associated copepods along the coast near Dumont d'Urville, Terre Adélie (Antarctica). *Journal of Marine Systems* 78: 599–605. <https://doi.org/10.1016/j.jmarsys.2009.01.003>
- Magazzù G, Decembrini F (1990) Primary Production and Picoplankton C assimilation in the Ross sea (Antarctica). National Scientific Commission for Antarctica (Ed.) *Oceanographic*

- Campaign 1987–88, Data Report Part I. National Scientific Commission for Antarctica, Genova, 107–157.
- Magazzù G, Decembrini F (1991) Primary Production in the Southern Ocean. In: National Scientific Commission for Antarctica (Ed.) Oceanographic Campaign 1989–90, Data Report Part I. National Scientific Commission for Antarctica, Genova, 255–310.
- Magazzù G, Decembrini F (1992) Results on Primary Production of the Oceanographic Expedition of 1987–88 and 1989–90 of the National Antarctic Research Program. Oceanografia in Antartide. ENEA-Progetto Antartide, Italia/Centro EULA, Universidad de Concepcion, 273–284.
- Matsuoka K, Skoglund A, Roth G, Tronstad S, Melvær Y (2017) Quantarctica: A unique, open, standalone GIS package for Antarctic Research and Education. In: EGU General Assembly Conference Abstracts (Ed.). Vienna, Austria, April 2017.
- Maugeri T. (1992) Microbiological Research in the Antarctic Oceanographic Expeditions 1987/88 and 1989/90. Oceanografia in Antartide. ENEA-Progetto Antartide, Italia/Centro EULA, Universidad de Concepcion, 173–186.
- Mazzocchi MG, Zagami G, Ianora A, Guglielmo L, Crescenti N, Hure J (1995) Atlas of Marine Zooplankton Straits of Magellan Atlas of Marine Zooplankton Straits of Magellan. Springer, Berlin, Heidelberg, 245 pp. <https://doi.org/10.1007/978-3-642-79139-0>
- McKenzie KG, Benassi G, Naldi M, Ferrari I, Menozzi P (1990) Report on planktic Ostracoda from Ross Sea, Antarctica. In: National Scientific Commission for Antarctica (Ed.) Oceanographic Campaign 1987–88, Data Report Part II, Genova, 171–229.
- Michels J, Büntzow M (2010) Assessment of Congo red as a fluorescence marker for the exoskeleton of small crustaceans and the cuticle of polychaetes. Journal of Microscopy 238(2): 95–101. <https://doi.org/10.1111/j.1365-2818.2009.03360.x>
- Minutoli R, Brugnano C, Granata A, Zagami G, Guglielmo L (2017) Zooplankton electron transport system activity and biomass in the western Ross Sea (Antarctica) during austral summer 2014. Polar Biology 40: 1197–1209. <https://doi.org/10.1007/s00300-016-2043-6>
- Nuccio C, Innamorati M, Lazzara L, Mori G (1992) Phytoplankton populations in Terra Nova Bay, Ross Sea. Oceanografia in Antartide. ENEA-Progetto Antartide, Italia/Centro EULA, Universidad de Concepcion, 253–262.
- Oresland V (1991) Feeding of the carnivorous copepod *Euchaeta antarctica* in Antarctic waters. Marine Ecology Progress Series 78: 41–47. <https://doi.org/10.3354/meps078041>
- Oresland V, Ward P (1993) Summer and winter diet of four carnivorous copepod species around South Georgia. Marine Ecology Progress Series 98: 73–78. <https://doi.org/10.3354/meps098073>
- Oresland V (1995) Winter population structure and feeding of the chaetognath *Eukrohnia hamata* and the copepod *Euchaeta antarctica* in Gerlache Strait, Antarctic Peninsula. Marine Ecology Progress Series 19 (1–3): 77–86. <https://doi.org/10.3354/meps19077>
- Pane L, Feletti M, Francomacaro B, Mariottini GL (2004) Summer coastal zooplankton biomass and copepod community structure near the Italian Terra Nova Base (Terra Nova Bay, Ross Sea, Antarctica). Journal of Plankton Research 26(12): 1479–1488. <https://doi.org/10.1093/plankt/fbh135>
- Piazza P, Błazewicz-Paszkowycz M, Ghiglione C, Alvaro MC, Schnabel K, Schiaparelli S (2014) Distributional records of Ross Sea (Antarctica) Tanaidacea from museum samples stored

- in the collections of the Italian National Antarctic Museum (MNA) and the New Zealand National Institute of Water and Atmospheric Research (NIWA). *ZooKeys* 451: 49–60. <https://doi.org/10.3897/zookeys.451.8373>
- Pusceddu A, Dell'anno A, Vezzulli L, Fabiano M, Saggiomo V, Cozzi S, Catalano G, Guglielmo L (2009) Microbial loop malfunctioning in the annual sea ice at Terra Nova Bay (Antarctica). *Polar Biology* 32: 337–346. <https://doi.org/10.1007/s00300-008-0539-4>
- Razouls C, de Bovée F, Kouwenberg J, Desreumaux N (2020) 2005–2020. Diversity and Geographic Distribution of Marine Planktonic Copepods. Sorbonne University, CNRS. <http://copepodes.obs-banyuls.fr/en> [accessed on: 2020-07-17]
- Reinhardt SB, Van Vleet ES (1986) Lipid composition of twenty-two species of Antarctic midwater zooplankton and fish. *Marine Biology* 91: 149–159. <https://doi.org/10.1007/BF00569431>
- Saggiomo V, Massi L, Modigh M, Innamorati M (1992) Size-Fractionated Primary Production in Terra Nova Bay (Ross Sea) During the Austral Summer (1989–90). *Oceanografia in Antartide*. ENEA-Progetto Antartide, Italia/Centro EULA, Universidad de Concepcion, 289–294.
- Sameoto DD, Jaroszynski LO, Fraser WB (1980) BIONESS, a new design in multiple net zooplankton samplers. *Canadian Journal of Fisheries and Aquatic Sciences* 37: 722–724. <https://doi.org/10.1139/f80-093>
- Schnack-schiel SB, Hagen W (1994) Life cycle strategies and seasonal variations in distribution and population structure of four dominant calanoid copepod species in the eastern Weddell Sea, Antarctica. *Journal of Plankton Research* 16(11): 1543–1566. <https://doi.org/10.1093/plankt/16.11.1543>
- Schnack-Schiel SB, Thomas D, Dieckmann GS, Eicken H, Gradinger R, Spindler M, Weisenberger J, Mizdalski E, Beyer K (1995) Life cycle strategy of the Antarctic calanoid copepod *Stephos longipes*. *Progress in Oceanography* 36: 45–75. [https://doi.org/10.1016/0079-6611\(95\)00014-3](https://doi.org/10.1016/0079-6611(95)00014-3)
- Schnack-Schiel SB, Thomas DN, Haas C, Dieckmann GS, Alheit R (2001) The occurrence of the copepods *Stephos longipes* (Calanoida) and *Drescheriella glacialis* (Haracticoida) in summer sea ice in the Weddell Sea, Antarctica. *Antarctic Science* 13: 150–157. <https://doi.org/10.1017/S0954102001000232>
- Selbmann L, Onofri S, Zucconi L, Isola D, Rottigni M, Ghiglione C, Piazza P, Alvaro MC, Schiaparelli S (2015) Distributional records of Antarctic fungi based on strains preserved in the culture collection of fungi from extreme environments (CCFEE) mycological section associated with the Italian national Antarctic museum (MNA). *MycKeys* 10: 57–71. <https://doi.org/10.3897/mycokeys.10.5343>
- Sigovini M, Keppel E, Tagliapietra D (2016) Open nomenclature in the biodiversity era. *Methods in Ecology and Evolution* 7(10): 1217–1225. <https://doi.org/10.1111/2041-210X.12594>
- Swadling K (2001) Population structure of two Antarctic ice-associated copepods, *Drescheriella glacialis* and *Paralabidocera antarctica*, in winter sea ice. *Marine Biology* 139: 597–603. <https://doi.org/10.1007/s002270100610>
- Tanimura A, Hoshiai T, Fukuchi M (1996) The life cycle strategy of the ice-associated copepod, *Paralabidocera antarctica* (Calanoida, Copepoda), at Syowa Station, Antarctica. *Antarctic Science* 8: 257–266. <https://doi.org/10.1017/S0954102096000363>

- Wiebe PH, Allison D, Kennedy M, Moncoiffé G (2014) A vocabulary for the configuration of nets for collecting plankton and micronekton. *Journal of Plankton Research* 37(1): 21–27. <https://doi.org/10.1093/plankt/fbu101>
- Wieczorek J, Bloom D, Guralnick R, Blum S, Döring M, Giovanni R, Robertson T, Vieglais D (2012) Darwin core: an evolving community-developed biodiversity data standard. *PLoS ONE* 7(1): e29715. <https://doi.org/10.1371/journal.pone.0029715>
- Williams R (1985) Trophic relationships between pelagic fish and euphausiids in Antarctic waters. Antarctic nutrient cycles and food webs. In: Siegfried WR, Condy PR, Laws RM (Eds) *Antarctic Nutrient Cycles and Food Webs*. Springer, Berlin, Heidelberg, 452–459. [https://doi.org/10.1007/978-3-642-82275-9\\_63](https://doi.org/10.1007/978-3-642-82275-9_63)
- Zmijewska MI (1993) Seasonal and spatial variations in the population structure and life histories of the Antarctic copepod species *Calanoides acutus*, *Calanus propinquus*, *Rhincalanus gigas*, *Metridia gerlachei* and *Euchaeta antarctica* (Calanoida) in Croker Passage (Antarctic Peninsula). *Oceanologia* 35: 73–100.
- Zunini Sertorio T, Salemi Piccone P, Bernat P, Cattini E, Ossola C (1990) Copepods collected in sixteen stations during the Italian Antarctic Expedition 1987–1988. In: National Scientific Commission for Antarctica (Ed.) *Oceanographic Campaign 1987–88, Data Report Part II*, Genova, 67–125.
- Zunini Sertorio T, Licandro P, Ricci F, Giallain M (1992) A study on Ross Sea copepods. In: National Scientific Commission for Antarctica (Ed.) *Oceanographic Campaign 1989–90, Data Report Part II*, Genova, 217–246.
- Zunini Sertorio T, Licandro P, Ossola C, Artegiani A (2000) Copepod Communities in the Pacific Sector of the Southern Ocean in Early Summer. In: Faranda FM, Guglielmo L, Ianora A (Eds) *Ross Sea Ecology*. Springer, Berlin, 291–307. [https://doi.org/10.1007/978-3-642-59607-0\\_23](https://doi.org/10.1007/978-3-642-59607-0_23)

# Comparative mitochondrial genomes of four species of *Sinopodisma* and phylogenetic implications (Orthoptera, Melanoplinae)

Qiu Zhongying<sup>1\*</sup>, Chang Huihui<sup>2\*</sup>, Yuan Hao<sup>2</sup>, Huang Yuan<sup>2</sup>,  
Lu Huimeng<sup>3</sup>, Li Xia<sup>4</sup>, Gou Xingchun<sup>1</sup>

**1** Shaanxi Key Laboratory of Brain Disorders & School of Basic Medical Sciences, Xi'an Medical University, Xi'an, 710021, China **2** College of Life Sciences, Shaanxi Normal University, Xi'an 710062, China **3** Key Laboratory for Space Bioscience & Biotechnology, School of Life Sciences, Northwestern Polytechnical University, Xi'an 710072, China **4** Huizhou No.8 High School, Huizhou 516001, China

Corresponding author: Gou Xingchun ([gouxingchun@189.cn](mailto:gouxingchun@189.cn))

Academic editor: Tony Robillard | Received 11 December 2019 | Accepted 14 August 2020 | Published 17 September 2020

<http://zoobank.org/B1B57760-9151-4018-AEC3-E212C4104818>

**Citation:** Zhongying Q, Huihui C, Hao Y, Yuan H, Huimeng L, Xia L, Xingchun G (2020) Comparative mitochondrial genomes of four species of *Sinopodisma* and phylogenetic implications (Orthoptera, Melanoplinae). ZooKeys 969: 23–42. <https://doi.org/10.3897/zookeys.969.49278>

## Abstract

In this study, the whole mitochondrial genomes (mitogenomes) from four species were sequenced. The complete mitochondrial genomes of *Sinopodisma pieli*, *S. houshana*, *S. qinlingensis*, and *S. wulingshanensis* are 15,857 bp, 15,818 bp, 15,843 bp, and 15,872 bp in size, respectively. The 13 protein-coding genes (PCGs) begin with typical ATN codons, except for COXI in *S. qinlingensis*, which begins with ACC. The highest A+T content in all the sequenced orthopteran mitogenomes is 76.8% (*S. qinlingensis*), followed by 76.5% (*S. wulingshanensis*), 76.4% (*S. pieli*) and 76.4% (*S. houshana*) (measured on the major strand). The long polythymine stretches (T-stretch) in the A+T-rich region of the four species are not adjacent to the trnI locus but are inside the stem-loop sequences on the major strand. Moreover, several repeated elements are found in the A+T-rich region of the four species. Phylogenetic analysis based on 53 mitochondrial genomes using Bayesian Inference (BI) and Maximum Likelihood (ML) revealed that Melanoplinae (Podismini) was a monophyletic group; however, the monophyly of *Sinopodisma* was not supported. These data will provide important information for a better understanding of the phylogenetic relationship of Melanoplinae.

\* Contributed equally as the first authors.

**Keywords**

mitogenome, phylogeny, *Sinopodisma*

**Introduction**

The insect mitochondrial genome (mitogenome) is a circular double-stranded covalently closed DNA molecule, with maternal genetic characteristics of relatively small molecular mass, simple structure, high copy number, relatively conservative gene arrangement, and rapid rate of gene evolution. The mitogenome contains 13 protein-coding genes (PCGs), two ribosomal RNA genes (rRNAs), 22 transfer RNA genes (tRNAs), and one A+T-rich region. The mitochondrial genes have been widely used in identifying species, estimating evolutionary relationships and recognising both the population structure and phylogeography (Flook and Rowell 1997a; Liu et al. 2013; Cameron 2014; Song et al. 2015; Du et al. 2017; Li et al. 2017; Sun et al. 2017; Zhou et al. 2017; Tang et al. 2018; Zhang et al. 2018; Chang et al. 2020). With the advancement of high-throughput sequencing technology, more and more mitogenome sequences have been sequenced. Many species systems, especially insect phylogenetic relationships, were constructed through the complete sequences of mitogenomes, complementing morphological classification (Gen 2015; Song et al. 2015; Li et al. 2017; Zhou et al. 2017; Li et al. 2020). Comparison of mitogenomes may reveal important genome-level characteristics, helping us understanding the genome structure, gene order, and evolutionary lineages. Moreover, the addition of newly complete mitogenomes will contribute to our understanding of phylogenetic relationships. Regarding the relationships among families or subfamilies within Acrididae, a few hypotheses based on morphology have been presented (Flook and Rowell 1997b, 1998; Flook et al. 1999, 2000; Fenn et al. 2008; Ma et al. 2009; Sun et al. 2010; Zhao et al. 2010; Zhao et al. 2011; Li et al. 2012; Huang et al. 2013), but they were not always consistent with each other (Li et al. 2011; Chintauan-Marquier et al. 2014; Song et al. 2015). The lack of a consensus about phylogeny based only on morphology makes it especially critical to use DNA data from highly polymorphic genetic regions such as mitogenome sequences. The taxonomic and phylogenetic relationships of Melanoiplinae have been studied by morphological and molecular data, but the systematics of the Podismini is still controversial (Litzenberger and Chapco 2001; Litzenberger and Chapco 2003; Shengquan et al. 2003; Chintauan-Marquier et al. 2011; Li et al. 2011; Chintauan-Marquier et al. 2014; Gen 2015; Grzywacz and Tatsuta 2017; Liu et al. 2017). The clades proposed by previous studies of the Podismini of Eurasian taxa do not fit the older morphological or cytological classifications but are in agreement with molecular studies (Litzenberger and Chapco 2001; Chintauan-Marquier et al. 2011; Chintauan-Marquier et al. 2014). However, some studies using different molecular markers may also give inconsistent results (Litzenberger and Chapco 2003; Grzywacz and Tatsuta 2017). The topological structure based on morphological data of Podismini was similar to that of the mtDNA and/or rDNA tree proposed previously (Gen 2015).

The genus *Sinopodisma* Chang, 1940 belongs to Melanoplineae, Acrididae, and Caelifera (Cigliano et al. 2019) based on the Orthoptera Species File (OSF). Approximately 42 species of *Sinopodisma* have been described and are mostly distributed in eastern Asia (Huang et al. 2013; Gen 2015). *Sinopodisma* grasshoppers are small in size, with degenerate wings; they mostly live in mountains 850 m above sea level (Wang et al. 2004). Based on morphological characters, *Sinopodisma* from China were divided into four groups (Shengquan et al. 2003). The results obtained from different data types failed to reach a consistent conclusion on the classification and evolutionary relationship of *Sinopodisma*, which needs further discussion. (Storozhenko 1993; Li et al. 2006; Li et al. 2011; Huang et al. 2013; Grzywacz and Tatsuta 2017; Liu et al. 2017; Chang et al. 2020).

In order to better understand the phylogenetic relationship of Melanoplineae, we obtained complete mitogenome sequences of *S. pieli*, *S. houshana*, *S. qinlingensis*, and *S. wulingshanensis* and compared them in detail. The new mitogenomes data not only helped us understand the characteristics of mitogenome of this group and the differences among different species, but also provided the basis for better exploring their evolutionary relationships. Combined with the new data and the existing data, we reconstructed the phylogeny of 53 Acrididae species based on a dataset of 37 complete mitochondrial genes, which may provide new angle for discussing the relationships within the Melanoplineae.

## Materials and methods

### Sample collection and DNA extraction

Information on the samples analysed in the present study is summarised in Suppl. material 1: Table S1. The samples were preserved in 100 % ethanol and stored at -20 °C freezer in Institute of Zoology of Shaanxi Normal University. Total genomic DNA was extracted from the muscle tissue of single individuals using the phenol/chloroform/isoamylalcohol method (Zhou et al. 2007), and then stored at -20 °C.

### DNA sequencing and annotations

High-Throughput Sequencing Technique was used to sequence *S. wulingshanensis*. We first fragmented DNA using an ultrasonic mechanical method. Then, we built DNA library and used Illumina HiSeq 2500 to sequence the whole genome, including the mitogenomes. The average read length was approximately 125 bp. The DNA library and sequencing were supported by the Biomarker Company (Kawahara and Breinholt 2014). At the same time, we obtained the mitogenome sequences of *S. pieli*, *S. houshana*, and *S. qinlingensis* by Sanger sequencing. We first synthesised Long-PCR(L-PCR) primers according to our own design, which divided the entire mitochondrial ring into six overlapping segments, each 3,000 bp to 4,500 bp long, covering the entire length of the whole mitochondrion, which is approximately 16,000 bp long (Suppl. mate-

rial 1: Table S2) (Liu et al. 2006). Next, we used the mitochondrial universal primer sequences published by Simon (Simon et al. 1994; Simon et al. 2006) to perform sub-PCR, using the products of L-PCR as templates. The L-PCR was performed in a total volume of 25  $\mu\text{L}$  including 11.25  $\mu\text{L}$  ddH<sub>2</sub>O, 2.5  $\mu\text{L}$  forward primer (10  $\mu\text{M}$ ), 2.5  $\mu\text{L}$  reverse primer (10  $\mu\text{M}$ ), 1  $\mu\text{L}$  template DNA (50 ng/ $\mu\text{L}$ ), 2.5  $\mu\text{L}$  dNTP Mixture (2.5 mM), 10  $\mu\text{L}$  10 $\times$ LA PCR BufferII (Mg+Plus), and 0.25  $\mu\text{L}$  TaKaRa LATaq DNA polymerase (5  $\mu\text{U}/\mu\text{L}$ ). The PCR reaction was under the following conditions: initial denaturation at 93 °C for 2 min  $\rightarrow$  (92 °C for 10 sec, 52.5 °C for 30 sec, 68 °C for 8 min)  $\times$  20 cycles  $\rightarrow$  (92 °C for 10 sec, 52.5 °C for 30 sec, 68 °C for 8 min + 20 sec)  $\times$  20 cycles  $\rightarrow$  72 °C for 7 min  $\rightarrow$  decrease to 4 °C.

The sub-PCR was performed in a total volume of 40  $\mu\text{L}$  including 14  $\mu\text{L}$  of ddH<sub>2</sub>O, 2  $\mu\text{L}$  of forward primer (10  $\mu\text{M}$ ), 2  $\mu\text{L}$  of reverse primer (10  $\mu\text{M}$ ), 2  $\mu\text{L}$  of template DNA (50 ng/ $\mu\text{L}$ ), and 20  $\mu\text{L}$  of 2 $\times$ Taq PCRStar Mix. The sub-PCR was under the following conditions: initial denaturation at 96 °C for 2 min  $\rightarrow$  (96 °C for 10 sec, 51.5 °C for 35 sec, 60 °C for 4 min)  $\times$  35 cycles  $\rightarrow$  72 °C for 7 min  $\rightarrow$  decrease to 4 °C. Most sub-PCR products were directly sequenced by means of primer walking, and other fragments were cloned into the pGEM-T Easy vector (Promega, USA) prior to sequencing.

The Standen Package (Staden et al. 2000) was used for sequence assembly and annotation. Transfer RNAs were identified by tRNAscan-SE1.21 (Lowe and Eddy 1997), and the other genes were determined by comparison with other related mitogenome sequences. The sequences of PCGs were translated based on the invertebrate mtDNA genetic code. Sequence information analysis was performed using MEGA 6.0 (Tamura et al. 2013) and ClustalX2 (Larkin et al. 2007). With *S. wulingshanensis*, after sequencing the genomes of the two species, the raw reads were inserted in the CLC Genomics Workbench 9.0 (CLC Bio, Aarhus, Denmark) to trim reads and then saved as a fastq file. We used the mitogenome of *S. pieli* as the reference and assembled the mitogenome of *S. wulingshanensis* using Mira 4.0.2 and MITObim 1.7 (Hahn et al. 2013). We used Geneious Prime (Kearse et al. 2012) (Biomatters Ltd., Auckland, New Zealand) for mitogenome annotation. Tandem Repeats Finder (Benson 1999) online software (<http://tandem.bu.edu/trf/trf.html>) was used to predict repeat elements in A+T-rich region. The four mitogenome sequences are available at GenBank, accession numbers: KX857633, KX857634, KX857636, KX857637.

## Phylogenetic analyses

Fifty-three available insect mitogenomes were used the phylogenetic analyses of Acrididae. The mitogenomes of *Asiotmethis jubatus* (NC\_025904), *Filchnerella beicki* (NC\_024923) and *Humphalotropis culaishanensis* (NC\_023535) were downloaded and used as outgroup (Taxonomy of all species is based on Orthoptera Species File (Version 5.0/5.0) (Cigliano et al. 2019), Suppl. material 1: Table S3). We inferred phylogenies using all 37 gene sequences. Alignments of individual genes were concatenated using SequenceMatrix v1.7.8 (Gaurav et al. 2011). The concatenated matrix

removing the stop codons was analysed by Bayesian Inference (BI) and Maximum Likelihood (ML) methods. Before phylogenetic analyses, the phylogenetic signals were assessed by MEGA6.0 (Tamura et al. 2013). For the ML analyses, PartitionFinder (Lanfear et al. 2012) was used to find the best-fit partitioning scheme for the 13 PCGs + 2 rRNAs + 22 tRNAs data set. ModelFinder (Kalyaanamoorthy et al. 2017) was used to find best-fit partition models and phylogenetic tree were reconstructed by IQ-TREE 1.7 (Nguyen et al. 2015) with 1000 bootstrap replicates. For the BI analyses, we used the best-fit partitioning scheme and partition-specific models recommended by PartitionFinder (Lanfear et al. 2012) and analysed using MrBayes 3.2.6 (Ronquist and Huelsenbeck 2003) with the MCMC analysis run for 2,000,000 generations and sampling every 1000 trees. After discarding the first 25% samples as burn-in, posterior probabilities (PP) were calculated in a consensus tree.

## Results and discussion

### Mitogenome organisation

The complete mitogenomes of *S. pieli*, *S. houshana*, *S. wulingshanensis* and *S. qinlingensis* are 15,857 bp, 15,818 bp, 15,872 bp and 15,843 bp in size, respectively (Figure 1, Suppl. material 1: Tables S4, S5). All mitogenomes contain a conserved set of 37 genes, including 13 PCGs (ATP6, ATP8, COXI, COXII, COXIII, CYTB, ND1, ND2, ND3, ND4, ND5, ND6, and ND4L), rRNAs (*rrnL* and *rrnS*), 22 tRNAs and a large non-coding region called the A+T-rich region. All four species have the arrangement order translocation of *trnK* and *trnD* (Figure 1). The gene overlapping between the four mitogenomes ranges from 1 to 8 bp in size. The longest overlapping region in the four mitogenomes, with a length of 33 bp, is located between *trnY* and COXI, except in *S. pieli*, where it is located between *trnY*-COXI and *trnW*-*trnC*. Intergenic regions (IGRs) of the four species range from 1 to 16 bp in size, with the longest IGRs located between *trnSUCN* and ND1. The A+T content, AT skew and GC skew exhibit similar characteristics in the four species (Table 1).

### Nucleotide compositions

Generally, A % > T % and C % > G % are common characteristics in all insects (Li et al. 2012). The nucleotide compositions of the four species' mitogenomes are significantly biased towards A and T (A+T > 76 %, see Table 1). All four mitogenomes (measured on the major strand) favour A-skew and C-skew. The A+T content (as measured on the major strand) among the four sequenced mitogenomes is 76.8 % (*S. qinlingensis*), followed by 76.5 % (*S. wulingshanensis*), 76.4 % (*S. pieli*) and 76.4 % (*S. houshana*) (Suppl. material 2: Figure S1). The lowest A+T content of orthopteran mitogenomes is 63.3 % in *Gampsocleis gratiosa*. Compared to the mitogenomes of other insects, they have very high contents of AT bases. In addition to the important effect of the GC



biased codon usage drives the evolution of tRNA anticodons, but those patterns cannot be generalised to invertebrate mitogenomes due to the differences between vertebrate and invertebrate mtDNA; therefore, this assumption is not final conclusion (Xia 2005). Furthermore, the GC content of the mitogenome does not reflect taxonomic characteristics or evolutionary relationships.

### Protein-coding genes

A total of nine PCGs (ND2, COXI, COXII, ATP8, ATP6, COXIII, ND3, ND6 and CYTB) are located on the J-strand, while the others (ND5, ND4, ND4L and ND1) are located on the N-strand. The 13 PCGs start with typical ATN codons in all four species, except COXI in *S. qinlingensis*, which begins with ACC. Many nonstandard initiation codons have previously been reported (Nardi et al. 2003; Kim et al. 2005; Samuels et al. 2005; Fenn et al. 2007; Ma et al. 2009; Liu and Huang 2010; Sheffield et al. 2010; Yang and Huang 2011; Ye et al. 2012; Zhang et al. 2013; Kim et al. 2014), including ATTTAA (Nardi et al. 2003), ATTA (Ye et al. 2012), TTAA and ATTA (Fenn et al. 2007), CCG (Zhang et al. 2013), CGA, AAA (Liu and Huang 2010), GTG (Samuels et al. 2005). The 13 PCGs of the four species all terminate with the conventional stop codons TAG or TAA.

The A+T content of the 13 PCGs, excluding stop codons, is observed to be 76.1%, 75.7%, 75.8% and 75.6% in *S. qinlingensis*, *S. wulingshanensis*, *S. pieli* and *S. houshana*, respectively (Table 1). The highest A+T content is found in the third codon position (93.8% in *S. qinlingensis*, 93.2% in *S. wulingshanensis* and 93.3% in *S. houshana*), but in *S. pieli*, the highest A+T content is in the second position (86.8%). The most obvious T-skew is recovered in the second codon position, except *S. pieli*. Additionally, the three codon positions show different GC-skews. In all four species other than *S. pieli*, the first codon position exhibits G-skew, and the other two codon positions exhibit C-skew. In *S. pieli* PCGs, the first and second codon positions exhibit C-skew, and the third codon position exhibits G-skew.

Codon usage bias (codon bias) is a phenomenon in which specific codons are used more frequently than other synonymous codons by certain organisms during the translation of genes to proteins. With rapid progress in whole-genome sequencing, analysis of codon usage bias at the genome level, rather than for a single gene or a set of genes, has gained attention. Genome-wide investigations on the variations in codon use and codon context bias are important for understanding the functional evolution of genomes within and between species (Lu et al. 2002; Fenn et al. 2007; Sun et al. 2017; Xu et al. 2019). Relative synonymous codon usage (RSCU) analysis indicated that in katydids, codons including A or T at the third position are always overused compared with other synonymous codons. The biased usage of AT nucleotides is also reflected in the form of codon usage, with RSCU values negatively correlating with the C and G contents in codons. The relatively synonymous codon frequencies of the four species' PCGs were summarised in Figure 2. Among the 64 available codons, the most frequently used codons are TTA (Leu), ATT (Ile), TTT (Phe), and ATA (Met), which

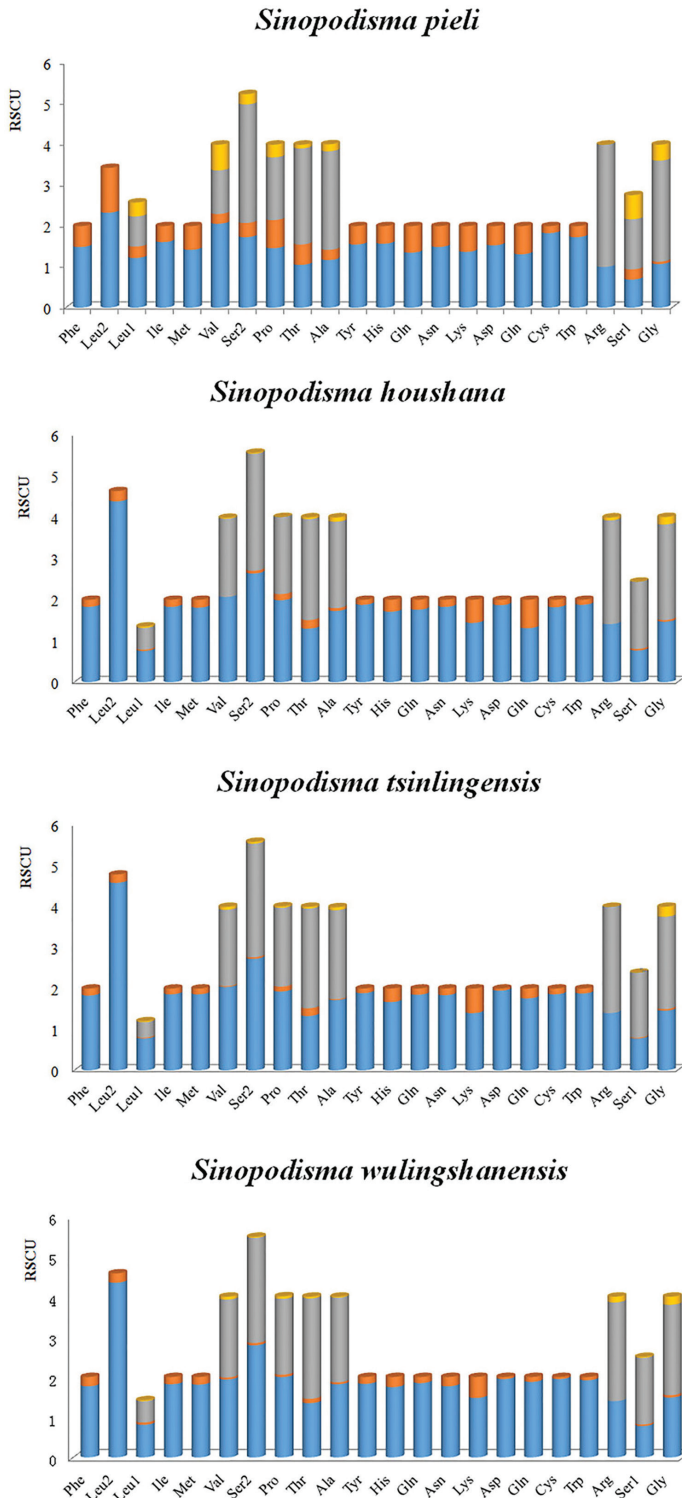


**Figure 2.** The relative synonymous codon frequencies from the four species.

are composed entirely of AT nucleotides. The codon CGC (Arg) is not used by the PCGs of *S. pieli*, *S. qinlingensis*, *S. wulingshanensis* or *S. houshana* mitogenomes. The codon CGG (Arg) is not found in *S. pieli* or *S. qinlingensis* mitogenomes. The codon AGG (Ser) is not exist in *S. qinlingensis* or *S. houshana* mitogenomes. The codons CCG (Pro) and GCU (Val) do not appear in the *S. houshana* mitogenome. To adapt to different living habits or types of resistance, different species require different functions of proteins, inevitably resulting in the preferential use of amino acids. In order from most to least frequent, the four mostly used amino acids in *S. houshana*, *S. wulingshanensis* and *S. qinlingensis* are Leu, Ile, Ser, and Phe; by contrast, the four mostly used amino acids in *S. pieli* are Leu, Phe, Tyr and Ile (Suppl. material 2: Figure S2).

### Transfer RNA genes

A total of 14 tRNAs (trnI, trnM, trnW, trnL<sup>UUR</sup>, trnD, trnK, trnG, trnA, trnR, trnN, trnS<sup>AGN</sup>, trnE, trnT, trnS<sup>UCN</sup>) are located on the J-strand, while the remaining tRNAs (trnQ, trnC, trnY, trnF, trnH, trnP, trnL<sup>CUN</sup>, trnV) are located on the N-strand. Moreover, 21 of the 22 tRNAs are well folded into a clover-leaf-like secondary structure, except trnS<sup>AGN</sup>, which lacks the DHU stem in all four species (Suppl. material 2: Figure S3). This phenomenon is considered to be a typical feature of metazoan mitogenomes (Wolstenholme 1992). In *S. houshana*, trnP is only 58 bp, and its variable (V) loop and TΨC arm are incomplete. Due to the stereoscopic limitations, it could not form a stable hydrogen bond in the TΨC arm. Therefore, the stereoscopic structure of this tRNA apparently only contains three arms, and the variable (V) loop and TΨC arm merged into an armband structure with 10 bp using a weaker hydrogen bond (Suppl. material 2: Figure S3). Additionally, trnK and trnD are translocated with each other in four mitogenomes. The tRNA translocation trnD-trnK seems to be a synapomorphy of the caeliferan group Acridomorpha (Song et al. 2015).

The lengths of the 22 tRNAs in the four species range from 64 to 71 bp in *S. pieli*, *S. qinlingensis* and *S. wulingshanensis*, and from 58 to 71 bp in *S. houshana*. According to the secondary structures and sequence alignments, the most conserved tRNAs in the four mitogenomes is trnF (Suppl. material 2: Figure S3), with the same nucleotide, trnG with one nucleotide insertion, and trnL<sup>CUN</sup>, with one nucleotide substitution.

In the remaining tRNAs, nucleotide substitutions are mainly restricted to loops, with obvious insertion-deletion polymorphisms. In *S. pieli*, there are 27 non-canonical base pairs, consisting of 17 G-U pairs and 1 A-A, 2 A-G, 1 A-C, 1 U-C and 5 U-U mismatches. In *S. qinlingensis*, there are 21 non-canonical base pairs, consisting of 17 G-U pairs and 1 A-A, 1 A-G and 2 U-U mismatches. In *S. wulingshanensis*, there are 22 non-canonical base pairs, consisting of 18 G-U pairs and 1 A-A, 1 A-G and 2 U-U mismatches. In *S. houshana*, there are 27 non-canonical base pairs, consisting of 19 G-U pairs and 1 A-A, 2 A-G, 2 A-C, 1 U-C and 2 U-U mismatches. The possession of aberrant mismatches, loops, or extremely short arms for tRNA is common in metazoan mitogenomes (Wolstenholme 1992). Although it remains unknown whether the aberrant tRNAs lose their respective functions, that could be corrected by post-transcriptional RNA editing processes (Masta and Boore 2004).

## Ribosomal RNA genes

Similar to other insect mitogenomes, *rrnL* is located between *trnL*<sup>CUN</sup> and *trnV*, and *rrnS* is located between *trnV* and the A+T-rich region. The lengths of *rrnL* are 1,343 bp, 1,313 bp, 1,369 bp and 1,313 bp in the *S. pieli*, *S. houshana*, *S. wulingshanensis* and *S. qinlingensis* mitogenomes, respectively, and the lengths of *rrnS* are 792 bp, 797 bp, 797 bp, and 797 bp, respectively. In the other orthopteran mitogenomes in GenBank, the lengths of *rrnL* range from 1,236 bp (*Gryllotalpa pluvialis*, NC\_011302) to 1,371 bp (*Pseudoxya diminuta*, NC\_025765), and the lengths of *rrnS* range from 461 bp (*Ceracris kiangsu*, NC\_019994) to 882 bp (*Ruspolia dubia*, NC\_009876). Therefore, the lengths of *rrnL* and *rrnS* from these four species are within the normal range. The A+T content ranges from 72.5% to 77.7% in the rRNA genes, and both rRNA genes exhibit T-skew and G-skew (Table 1).

## A+T-rich region

The A+T-rich region is the major noncoding region in insect mitogenome, which is located in the conserved position between the *rrnS* and *trnI* genes and has an A+T content of 86.5% in *S. pieli* and *S. houshana*, 86.6% in *S. wulingshanensis* and 86.3% in *S. qinlingensis*. In addition, the A+T-rich regions of all four mitogenomes favour A-skew and C-skew (Suppl. material 1: Table S5). The A+T-rich region is considered to be involved in the regulation of mtDNA transcription and replication, and there is a long polythymine stretch (T-stretch) adjacent to the *trnI* gene. A similar T-stretch has been found in some other insects, including *A. zacharjini* (17 bp), *F. helanshanensis* (14 bp) and *P. rubimarginis* (14 bp) (Zhang et al. 2013). The T-stretches on the major strand are also found in the A+T-rich region in our four sequenced mitogenomes, with a length of 11 bp but with two Cs inserted. However, they are not adjacent to the *trnI* locus but are instead inside the stem-loop sequence in the major strand (Figure 3).

Some tandem repetition and conserved structural elements have been observed in the insect A+T-rich region. Comparison of our four species with *Schistocerca gregaria* and *Oxya chinensis* revealed some conserved blocks. Indeed, these A+T-rich regions have eight conserved blocks (Figure 3). Blocks E1 and E2 can form a highly conserved stem-loop secondary structure in which the stem consists of 12 base pairs (Suppl. material 2: Figure S4). However, we do not find the motif “TATA” at the 5' end or the motif “G(A)nT” at the 3' end. The A+T-rich region of mitogenome may have evolved to have some alternative flanking sequence forms, if it had been present for a functional role (Yang et al. 2011).

The presence of a variable number of tandem repeat units may be useful for inferring the genetic structures of populations among closely related taxa and individuals of the same species (Mancini et al. 2008). Two repeated elements are found in the A+T-rich region of the *S. pieli* mitogenome. The A+T-rich regions of *S. houshana* and *S. qinlingensis* have six repeated elements, whereas the A+T-rich region in *S. wulingshanensis* contains three repeated elements (Suppl. material 1: Table S6). Tandem repeats may



**Figure 3.** The long polythymine stretch and conserved sequence blocks in the A+T rich regions from four species. Note: The long polythymine stretch. T-stretch sequence was labelled with box, located in the majority strand. Within each block, nucleotides identical in the two sequences are bottom-marked with asterisks.

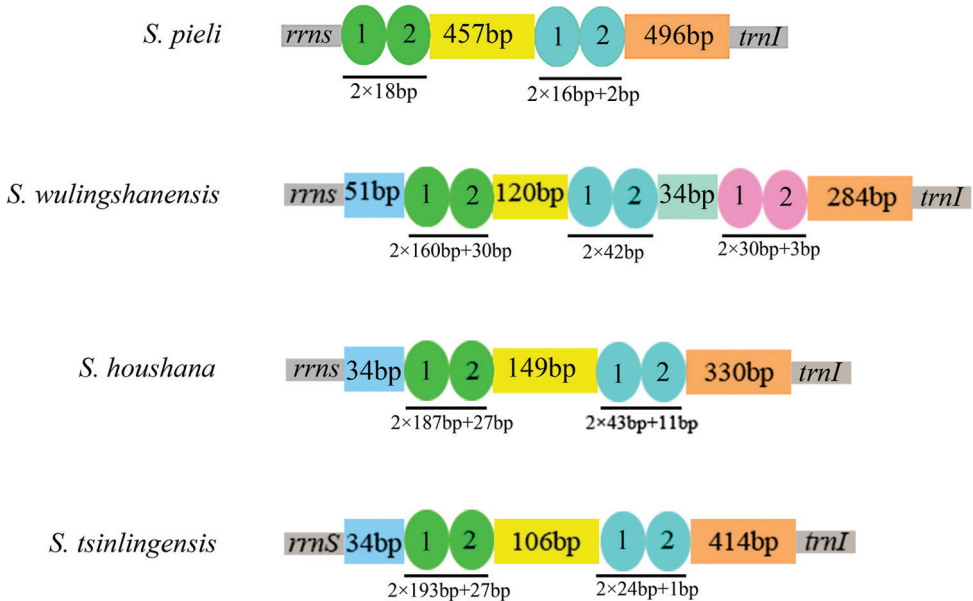


**Figure 4.** The main repeat elements in A+T-rich regions from four species.

play various regulatory and evolutionary roles (Armour et al. 1996; Benson 1999); the main tandem repeats of the four species are shown in Figure 4.

### Phylogenetic relationships

The dataset of all 37 mitochondrial genes was used to perform phylogenetic analyses based on 53 Acrididae mitogenome sequences, including the four newly generated sequences, 49 other Acrididae sequences from GenBank and three outgroup sequences (Suppl. mate-

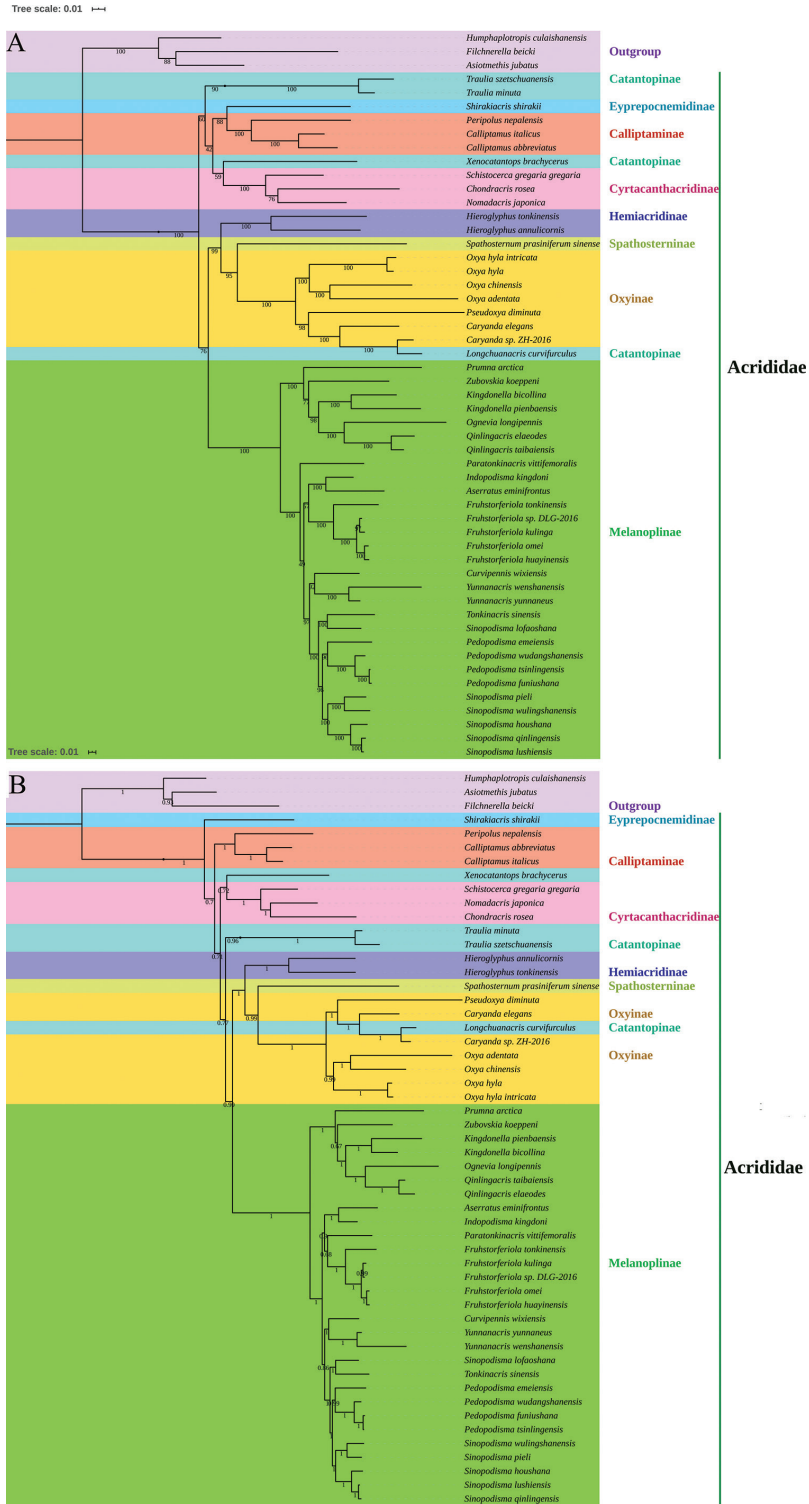


**Figure 5.** The phylogenetic tree based on 37 mitochondrial genes. **(A)** ML tree; **(B)** BI tree.

rial 1: Table S3). The partition of dataset and their optimal models were shown in Suppl. material 1: Table S7. There were some differences in the topologies of ML and BI trees (Figure 5). The relationships between Cyrtacanthacridinae, Eyprepocnemidinae, Calliptaminae, and Catantopinae and the relationships between the four subfamilies and other subfamilies were quite different in the two trees. Based on the tree topologies, Melanoplinae species clustered together, supporting the monophyly of this subfamily. Among the other subfamilies, the monophyly of Hemiacridinae, Cyrtacanthacridinae, and Calliptaminae could be supported, but the monophyly of the other four subfamilies (Catantopinae, Oxyinae, Spathosterninae, and Eyprepocnemidinae) could not be tested (Figure 5).

In Melanoplinae, the topological relationships between the genera were the same in the two trees and all species belong to the tribe Podismini. The phylogenetic results in this study supported the monophyly of Podismini. The same inference could be found in other phylogenies based on mitogenome data (Zhang and Lin 2016; Zhang et al. 2017), but the topology based on single gene did not support the monophyly of Podismini (Chintauan-Marquier et al. 2014; Grzywacz and Tatsuta 2017). Our topologies showed that *Sinopodisma* clustered two groups: (1) group 1: (((*S.lushienensis* + *S. qinlingensis*) + *S. houshana*) + (*S. pieli* + *S. wulingshanensis*)) and (2) group 2: (*S. lushiensis*+ *Tonkinacris sinensis*). So *Sinopodisma* do not cluster a monophyletic taxon, which was consistent with the results of Liu et al. (2017). But it was not agreement with other research results (Huang et al. 2013; Grzywacz and Tatsuta 2017). The present phylogenetic trees placed *Sinopodisma* as an apical node sister to *Pedopodisma*. *Sinopodisma*, and *Pedopodisma* are similar in morphology and distinguished only by slight differences (Huang et al. 2013; Cigliano et al. 2019). *Pedopodisma*, a genus endemic to China, was synonymized by Storozhenko (1993), which caused confusion on the classification of genus *Sinopodisma*. Storozhenko's treatment has not been accepted by Chinese acridologists (Li et al. 2006) because tegmina are completely absent in *Pedopodisma* but distinct though reduced in *Sinopodisma* (Huang et al. 2013). Clearly, we only obtained six mitogenomes of *Sinopodisma*, and four of *Pedopodisma*, so additional sampling of the taxa *Sinopodisma* and *Pedopodisma* is needed to obtain sufficient mitogenome data to clarify the monophyly between *Sinopodisma* and the phylogenetic relationship of *Sinopodisma* and *Pedopodisma*.

## Conclusions

The complete mitochondrial genomes of *Sinopodisma pieli*, *S. houshana*, *S. qinlingensis*, and *S. wulingshanensis* were obtained. The mitogenomes of four species have typical genome organisation and gene arrangement order, compared to other caeliferan mitogenomes. We focused on comparative analyses of four *Sinopodisma* mitogenomes to find the characteristics of base composition, overlapping and intergenic regions, and tRNA secondary structures. All 13 PCGs have typical starting ATN codons, except for COXI in *S. qinlingensis*, which start with ACC. A+T contents in four mitogenomes are high and we found several repeated elements in the A+T-rich region of the four species. Moreover, 53 mitogenome data were used to build the phylogenetic relationship. The

phylogenetic tree supported the monophyly of Melanoplinae, but do not support the monophyly of *Sinopodisma*.

## Acknowledgments

The authors have declared that no competing interest exists. This paper received assistance from the Project of Shaanxi Key Laboratory of Brain Disorders (18NBZD10), the National Natural Science Foundation of China (81800211) and Xi'an medical university doctoral research fund (2017DOC20). We would like to thank Jianhua Huang for kindly providing us with samples.

## References

- Armour JA, Anttinen T, May CA, Vega EE, Sajantila A, Kidd JR, Kidd KK, Bertranpetit J, Pääbo S, Jeffreys AJ (1996) Minisatellite diversity supports a recent African origin for modern humans. *Nature Genetics* 13(2): 154–160. <https://doi.org/10.1038/ng0696-154>
- Benson G (1999) Tandem repeats finder: a program to analyze DNA sequences. *Nucleic Acids Research* 27(2): 573–580. <https://doi.org/10.1093/nar/27.2.573>
- Cameron SL (2014) How to sequence and annotate insect mitochondrial genomes for systematic and comparative genomics research. *Systematic Entomology* 39(3): 400–411. <https://doi.org/10.1111/syen.12071>
- Chang H, Qiu Z, Yuan H, Wang X, Li X, Sun H, Guo X, Lu Y, Feng X, Majid M, Huang Y (2020) Evolutionary rates of and selective constraints on the mitochondrial genomes of Orthoptera insects with different wing types. *Molecular Phylogenetics and Evolution* 145: 106734. <https://doi.org/10.1016/j.ympev.2020.106734>
- Chintauan-Marquier IC, Amédégnato C, Nichols RA, Pompanon F, Grandcolas-P, Desutter-Grandcolas L (2014) Inside the Melanoplinae: new molecular evidence for the evolutionary history of the Eurasian Podismini (Orthoptera:Acrididae). *Molecular Phylogenetics and Evolution* 71: 224–233. <https://doi.org/10.1016/j.ympev.2013.09.009>
- Chintauan-Marquier IC, Jordan S, Berthier P, Amedegnato C, Pompanon F (2011) Evolutionary history and taxonomy of a short-horned grasshopper subfamily: the Melanoplinae (Orthoptera: Acrididae). *Molecular Phylogenetics and Evolution* 58(1): 22–32. <https://doi.org/10.1016/j.ympev.2010.07.003>
- Cigliano MM, Braun H, Eades DC, Otte D (2019) Orthoptera Species File. Version 5.0/5.0. <http://Orthoptera.SpeciesFile.org>
- Consortium THGS (2006) Insights into social insects from the genome of the honeybee *Apis mellifera*. *Nature* 443(7114): 931–949. <https://doi.org/10.1038/nature05260>
- Du Y, Zhang C, Dietrich C, Zhang Y, Dai W (2017) Characterization of the complete mitochondrial genomes of *Maiestas dorsalis* and *Japananus hyalineus* (Hemiptera: Cicadellidae) and comparison with other Membracoide. *Scientific Reports* 7(1): 14197. <https://doi.org/10.1038/s41598-017-14703-3>

- Fenn JD, Cameron SL, Whiting MF (2007) The complete mitochondrial genome sequence of the Mormon cricket (*Anabrus simplex*: Tettigoniidae: Orthoptera) and an analysis of control region variability. *Insect Molecular Biology* 16(2): 239–52. <https://doi.org/10.1111/j.1365-2583.2006.00721.x>
- Fenn JD, Song H, Cameron SL, Whiting MF (2008) A preliminary mitochondrial genome phylogeny of Orthoptera (Insecta) and approaches to maximizing phylogenetic signal found within mitochondrial genome data. *Molecular Phylogenetics and Evolution* 49(1): 59–68. <https://doi.org/10.1016/j.ympev.2008.07.004>
- Flook PK, Klee S, Rowell CH (1999) Combined molecular phylogenetic analysis of the Orthoptera (Arthropoda, Insecta) and implications for their higher systematics. *System Biology* 48(2): 233–253. <https://doi.org/10.1080/106351599260274>
- Flook PK, Klee S, Rowell CH (2000) Molecular phylogenetic analysis of the basal Acridomorpha (Orthoptera, Caelifera): resolving morphological character conflicts with molecular data. *Molecular Phylogenetics and Evolution* 15(3): 345–354. <https://doi.org/10.1080/106351599260274>
- Flook PK, Rowell CH (1998) Inferences about orthopteroid phylogeny and molecular evolution from small subunit nuclear ribosomal DNA sequences. *Insect Molecular Biology* 7(2): 163–178. <https://doi.org/10.1046/j.1365-2583.1998.72060.x>
- Flook PK, Rowell CH (1997a) The effectiveness of mitochondrial rRNA gene sequences for the reconstruction of the phylogeny of an insect order (Orthoptera). *Molecular Phylogenetics and Evolution* 8(2): 177–192. <https://doi.org/10.1006/mpev.1997.0425>
- Flook PK, Rowell CH (1997b) The phylogeny of the Caelifera (Insecta, Orthoptera) as deduced from mtrRNA gene sequences. *Molecular Phylogenetics and Evolution* 8(1): 89–103. <https://doi.org/10.1006/mpev.1997.0412>
- Gaurav V, Lohman DJ, Meier R (2011) SequenceMatrix: concatenation software for the fast assembly of multi-gene datasets with character set and codon information. *Cladistics* 27(2): 171–180. <https://doi.org/10.1111/j.1096-0031.2010.00329.x>
- Gen I (2015) A systematic study of the grasshopper tribe Podismini in Japan (Orthoptera: Acrididae). *Insecta matsumurana Series entomology: Journal of the Faculty of Agriculture Hokkaido University, series entomology* 71: 1–119. <https://hdl.handle.net/2115/60241>
- Grzywacz B, Tatsuta H (2017) Phylogenetic relationship of Japanese Podismini species (Orthoptera: Acrididae: Melanoplinae) inferred from a partial sequence of cytochrome c oxidase subunit I gene. *Journal of Orthoptera Research* 26(1): 11–19. <https://doi.org/10.3897/jor.26.14547>
- Hahn C, Bachmann L, Chevreaux B (2013) Reconstructing mitochondrial genomes directly from genomic next-generation sequencing reads—a baiting and iterative mapping approach. *Nucleic Acids Research* 41(13): e129. <https://doi.org/10.1093/nar/gkt371>
- Huang J, Zhang A, Mao S, Huang Y (2013) DNA barcoding and species boundary delimitation of selected species of Chinese Acridoidea (Orthoptera: Caelifera). *PLoS ONE* 8(12): e82400. <https://doi.org/10.1371/journal.pone.0082400>
- Kalyaanamoorthy S, Minh BQ, Wong TKF, von Haeseler A, Jermiin LS (2017) ModelFinder: fast model selection for accurate phylogenetic estimates. *Nature Methods* 14(6): 587–589. <https://doi.org/10.1038/nmeth.4285>

- Kawahara AY, Breinholt JW (2014) Phylogenomics provides strong evidence for relationships of butterflies and moths. *Proceeding Biology Science* 281(1788): 20140970. <https://doi.org/10.1098/rspb.2014.0970>
- Kearse M, Moir R, Wilson A, Stones-Havas S, Cheung M, Sturrock S, Buxton S, Cooper A, Markowitz S, Duran C, Thierer T, Ashton B, Meintjes P, Drummond A (2012) Geneious Basic: an integrated and extendable desktop software platform for the organization and analysis of sequence data. *Bioinformatics* 28(12): 1647–1649. <https://doi.org/10.1093/bioinformatics/bts199>
- Kim I, Cha SY, Yoon MH, Hwang JS, Lee SM, Sohn HD, Jin BR (2005) The complete nucleotide sequence and gene organization of the mitochondrial genome of the oriental mole cricket, *Gryllotalpa orientalis* (Orthoptera: Gryllotalpidae). *Gene* 353(2): 155–168. <https://doi.org/10.1016/j.gene.2005.04.019>
- Kim MJ, Wang AR, Park JS, Kim I (2014) Complete mitochondrial genomes of five skippers (Lepidoptera: Hesperidae) and phylogenetic reconstruction of Lepidoptera. *Gene* 549(1): 97–112. <https://doi.org/10.1016/j.gene.2014.07.052>
- Lanfear R, Calcott B, Ho SY, Guindon S (2012) Partitionfinder: combined selection of partitioning schemes and substitution models for phylogenetic analyses. *Molecular Biology and Evolution* 29(6): 1695–1701. <https://doi.org/10.1093/molbev/mss020>
- Larkin MA, Blackshields G, Brown NP, Chenna R, McGettigan PA, McWilliam H, Valentin F, Wallace IM, Wilm A, Lopez R, Thompson JD, Gibson TJ, Higgins DG (2007) Clustal W and Clustal X version 2.0. *Bioinformatics* 23(21): 2947–2948. <https://doi.org/10.1093/bioinformatics/btm404>
- Li B, Liu Z, Zheng ZM (2011) Phylogeny and classification of the Catantopidae at the tribal level (Orthoptera, Acridoidea). *ZooKeys* (148): 209–255. <https://doi.org/10.3897/zookeys.148.2081>
- Li H, Leavengood Jr JM, Chapman EG, Burkhardt D, Song F, Jiang P, Liu J, Zhou X, Cai W (2017) Mitochondrial phylogenomics of Hemiptera reveals adaptive innovations driving the diversification of true bugs. *Proceedings of the Japan Academy Series B-Physical and Biological Sciences* 284(1862): 20171223. <https://doi.org/10.1098/rspb.2017.1223>
- Li H, Liu H, Song F, Shi A, Zhou X, Cai W (2012) Comparative mitogenome analysis of damselfly bugs representing three tribes in the family Nabidae (Insecta: Hemiptera). *PLoS ONE* 7(9): e45925. <https://doi.org/10.1371/journal.pone.0045925>
- Li R, Wang Y, Shu X, Meng L, Li B (2020) Complete mitochondrial genomes of three *Oxya* grasshoppers (Orthoptera) and their implications for phylogenetic reconstruction. *Genomics* 112(1): 289–296. <https://doi.org/10.1016/j.ygeno.2019.02.008>
- Litzenberger G, Chapco W (2001) Molecular Phylogeny of Selected Eurasian *Podismine* Grasshoppers (Orthoptera: Acrididae). *Annals of the Entomological Society of America* 4: 505–511. [https://doi.org/10.1603/0013-8746\(2001\)094\[0505:MPOSEP\]2.0.CO;2](https://doi.org/10.1603/0013-8746(2001)094[0505:MPOSEP]2.0.CO;2)
- Litzenberger G, Chapco W (2003) The North American Melanoplinae (Orthoptera: Acrididae): A Molecular Phylogenetic Study of Their Origins and Taxonomic Relationships. *Annals of the Entomological Society of America* 96(4): 491–497. [https://doi.org/10.1603/0013-8746\(2003\)096\[0491:TNAMOA\]2.0.CO;2](https://doi.org/10.1603/0013-8746(2003)096[0491:TNAMOA]2.0.CO;2)

- Liu H, Yan L, Jiang G (2017) The complete mitochondrial genome of the jumping grasshopper *Sinopodisma pieli* (Orthoptera: Acrididae) and the phylogenetic analysis of Melanoplinae. *Zootaxa* 4363(4): 506–520. <https://doi.org/10.11646/zootaxa.4363.4.3>
- Liu N, Hu J, Huang Y (2006) Amplification of grasshoppers complete mitochondrial genomes using long PCR. *Chinese Journal of Zoology* 41(2): 61–65. [https://doi.org/10.1016/S1872-2040\(06\)60043-1](https://doi.org/10.1016/S1872-2040(06)60043-1)
- Liu N, Huang Y (2010) Complete Mitochondrial Genome Sequence of Acridacinae (Acrididae: Orthoptera) and Comparative Analysis of Mitochondrial Genomes in Orthoptera. *Comparative and Functional Genomics* 2010: 319–486. <https://doi.org/10.1155/2010/319486>
- Liu QN, Zhu BJ, Dai LS, Liu CL (2013) The complete mitogenome of *Bombyx mori* strain Dazao (Lepidoptera: Bombycidae) and comparison with other lepidopteran insects. *Genomics* 101(1): 64–73. <https://doi.org/10.1016/j.ygeno.2012.10.002>
- Lowe TM, Eddy SR (1997) tRNAscan-SE: a program for improved detection of transfer RNA genes in genomic sequence. *Nucleic Acids Research* 25: 955–964. <https://doi.org/10.1093/nar/25.5.955>
- Ma C, Liu C, Yang P, Kang L (2009) The complete mitochondrial genomes of two band-winged grasshoppers, *Gastrimargus marmoratus* and *Oedaleus asiaticus*. *BMC Genomics* 10: 1–156. <https://doi.org/10.1186/1471-2164-10-1>
- Mancini E, De Biase A, Mariottini P, Bellini A, Audisio P (2008) Structure and evolution of the mitochondrial control region of the pollen beetle *Meligethes thalassophilus* (Coleoptera: Nitidulidae). *Genome* 51(3): 196–207. <https://doi.org/10.1139/G07-116>
- Masta SE, Boore JL (2004) The complete mitochondrial genome sequence of the spider *Habronattus oregonensis* reveals rearranged and extremely truncated tRNAs. *Molecular Biology and Evolution* 21(5): 893–902. <https://doi.org/10.1093/molbev/msh096>
- Nardi F, Spinsanti G, Boore JL, Carapelli A, Dallai R, Frati F (2003) Hexapod origins: monophyletic or paraphyletic? *Science* 299(5614): 1887–1889. <https://doi.org/10.1126/science.1078607>
- Nguyen LT, Schmidt HA, von Haeseler A, Minh BQ (2015) IQ-TREE: a fast and effective stochastic algorithm for estimating maximum-likelihood phylogenies. *Molecular Biology and Evolution* 32(1): 268–274. <https://doi.org/10.1093/molbev/msu300>
- Ronquist F, Huelsenbeck JP (2003) MrBayes 3: Bayesian phylogenetic inference under mixed models. *Bioinformatics* 19(12): 1572–1574. <https://doi.org/10.1093/bioinformatics/btg180>
- Samuels AK, Weisrock DW, Smith JJ, France KJ, Walker JA, Putta S, Voss SR (2005) Transcriptional and phylogenetic analysis of five complete ambystomatid salamander mitochondrial genomes. *Gene* 349: 43–53. <https://doi.org/10.1016/j.gene.2004.12.037>
- Sheffield NC, Hiatt KD, Valentine MC, Song H, Whiting MF (2010) Mitochondrial genomics in Orthoptera using MOSAS. *Mitochondrial DNA* 21(3–4): 87–104. <https://doi.org/10.3109/19401736.2010.500812>
- Shengquan X, Takeda M, Zheng Z (2003) Phylogeny of *Sinopodisma* (Orthoptera: Acridoidea) inferred from cladistic analysis, species distributions and geological events. *Oriental Insects* 37(1): 335–342. <https://doi.org/10.1080/00305316.2003.10417353>

- Simon C, Buckley TR, Frati F, Stewart JB, Beckenbach AT (2006) Incorporating Molecular Evolution into Phylogenetic Analysis, and a New Compilation of Conserved Polymerase Chain Reaction Primers for Animal Mitochondrial DNA. *Annual Review of Ecology, Evolution, and Systematics* 37(2006): 545–579. <https://doi.org/10.1146/annurev.ecolsys.37.091305.110018>
- Simon C, Rati FF, Beckenbach A, Crespi B, Liu H, Flook P (1994) Evolution, weighting, and phylogenetic utility of mitochondrial gene sequences and a compilation of conserved polymerase chain reaction primers. *Annals of the Entomological Society of America* 87(6): 651–701. <https://doi.org/10.1093/aesa/87.6.651>
- Song H, Amédégnato C, Cigliano MM, Desutter-Grandcolas L, Heads SW, Huang Y, Otte D, Whiting MF (2015) 300 million years of diversification: elucidating the patterns of orthopteran evolution based on comprehensive taxon and gene sampling. *Cladistics* 31(6): 621–651. <https://doi.org/10.1111/cla.12116>
- Staden R, Beal KF, Bonfield JK (2000) The Staden package, 1998. *Bioinformatics Methods and Protocols* 132: 115–130. <https://doi.org/10.1385/1-59259-192-2:115>
- Storozhenko SY (1993) To the knowledge of the tribe Melanoplinae (Orthoptera, Acrididae: Catantopinae) of the Eastern Palearctica. *Articulata* 8: 1–22.
- Sun H, Zheng Z, Huang Y (2010) Sequence and phylogenetic analysis of complete mitochondrial DNA genomes of two grasshopper species *Gomphoceris rufus* (Linnaeus, 1758) and *Primnoa arctica* (Zhang and Jin, 1985) (Orthoptera: Acridoidea). *Mitochondrial DNA* 21(3–4): 115–131. <https://doi.org/10.3109/19401736.2010.482585>
- Sun S, Hui M, Wang M, Sha Z (2017) The complete mitochondrial genome of the alvinocaridid shrimp *Shinkaicaris leurokolos* (Decapoda, Caridea): Insight into the mitochondrial genetic basis of deep-sea hydrothermal vent adaptation in the shrimp. *Comparative Biochemistry and Physiology Part D: Genomics and Proteomics* 25: 42–52. <https://doi.org/10.1016/j.cbd.2017.11.002>
- Tamura K, Stecher G, Peterson D, Filipski A, Kumar S (2013) MEGA6: Molecular Evolutionary Genetics Analysis version 6.0. *Molecular Biology Evolution* 30(12): 2725–2729. <https://doi.org/10.1093/molbev/mst197>
- Tang JM, Li F, Cheng TY, Duan DY, Liu GH (2018) Comparative analyses of the mitochondrial genome of the sheep ked *Melophagus ovinus* (Diptera: Hippoboscidae) from different geographical origins in China. *Parasitology Research* 117(8): 2677–2683. <https://doi.org/10.1007/s00436-018-5925-4>
- Wang W, Li X, Yin X (2004) Taxonomic study on *Sinopodisma* Chang from China (Orthoptera: Acridoidea: Catantopidae). *Journal of Hebei University* 24: 99–106. <https://doi.org/10.1109/JLT.2003.821766>
- Wolstenholme DR (1992) Animal Mitochondrial DNA: Structure and Evolution. *International Review of Cytology* 141: 173–216. [https://doi.org/10.1016/S0074-7696\(08\)62066-5](https://doi.org/10.1016/S0074-7696(08)62066-5)
- Xia X (2005) Mutation and selection on the anticodon of tRNA genes in vertebrate mitochondrial genomes. *Gene* 345(1): 13–20. <https://doi.org/10.1016/j.gene.2004.11.019>
- Xu SY, Long JK, Chen XS (2019) Comparative analysis of the complete mitochondrial genomes of five Achilidae species (Hemiptera: Fulgoroidea) and other Fulgoroidea reveals

- conserved mitochondrial genome organization. Peer J 7: e6659. <https://doi.org/10.7717/peerj.6659>
- Yang F, Du YZ, Wang LP, Cao JM, Yu WW (2011) The complete mitochondrial genome of the leafminer *Liriomyza sativae* (Diptera: Agromyzidae): great difference in the A+T-rich region compared to *Liriomyza trifolii*. Gene 485(1): 7–15. <https://doi.org/10.1016/j.gene.2011.05.030>
- Yang H, Huang Y (2011) Analysis of the complete mitochondrial genome sequence of *Pielomastax zhengi*. Zoological Research 32(4): 353–362.
- Ye HY, Xiao LL, Zhou ZJ, Huang Y (2012) Complete mitochondrial genome of *Locusta migratoria migratoria* (Orthoptera: Oedipodidae): three tRNA-like sequences on the N-strand. Zoological Science 29(2): 90–96. <https://doi.org/10.2108/zsj.29.90>
- Zhang HL, Huang Y, Lin LL, Wang XY, Zheng ZM (2013) The phylogeny of the Orthoptera (Insecta) as deduced from mitogenomic gene sequences. Zoological Studies 52: 1–37. <https://doi.org/10.1186/1810-522X-52-37>
- Zhang HL, Zeng HH, Huang Y, Zheng ZM (2013) The complete mitochondrial genomes of three grasshoppers, *Asiotmethis zacharjini*, *Filchnerella belanshanensis* and *Pseudotmethis rubimarginis* (Orthoptera: Pamphagidae). Gene 517(1): 89–98. <https://doi.org/10.1016/j.gene.2012.12.080>
- Zhang QL, Yang XZ, Zhang L, Feng RQ, Zhu QH, Chen JY, Yuan ML (2019) Adaptive evidence of mitochondrial genomes in *Dolycoris baccarum* (Hemiptera: Pentatomidae) to divergent altitude environments. Mitochondrial DNA Part A 30(1): 9–15. <https://doi.org/10.1080/24701394.2018.1446951>
- Zhang XM, Li X, Liu F, Yuan H, Huang Y (2017) The complete mitochondrial genome of *Tonkinacris sinensis* (Orthoptera: Acrididae): A tRNA-like sequence and its implications for phylogeny. Biochemical Systematics and Ecology 70: 147–154. <https://doi.org/10.1016/j.bse.2016.11.002>
- Zhang XM, Lin LL (2016) The complete mitochondrial genome of *Fruhstorferiola tonkinensis* (Orthoptera: Catantopidae). Mitochondrial DNA Part B 1(1): 434–435. <https://doi.org/10.1080/23802359.2016.1180555>
- Zhao L, Zheng ZM, Huang Y, Sun HM (2010) A comparative analysis of mitochondrial genomes in Orthoptera (Arthropoda: Insecta) and genome descriptions of three grasshopper species. Zoological Science 27(8): 662–672. <https://doi.org/10.2108/zsj.27.662>
- Zhao L, Zheng ZM, Huang Y, Zhou ZJ, Wang L (2011) Comparative analysis of the mitochondrial control region in Orthoptera. Zoological Studies 50(3): 386–396. <https://zoolog-stud.sinica.edu.tw/501.html>
- Zhou ZJ, Huang Y, Shi FM (2007) The mitochondrial genome of *Ruspolia dubia* (Orthoptera: Conocephalidae) contains a short A + T-rich region of 70-bp in length. Genome 50(9): 855–866. <https://doi.org/10.1139/G07-057>
- Zhou Z, Zhao L, Liu N, Guo H, Guan B, Di J, Shi F (2017) Towards a higher-level Ensifera phylogeny inferred from mitogenome sequences. Molecular Phylogenetics and Evolution 108: 22–33. <https://doi.org/10.1016/j.ympev.2017.01.014>

## Supplementary material 1

### Tables S1–S7

Authors: Qiu Zhongying, Chang Huihui, Yuan Hao, Huang Yuan, Lu Huimeng, Li Xia, Gou Xingchun

Data type: table excel

Explanation note: **Table S1.** Information on the samples analysed in the present study.

**Table S2.** List of L-PCR primers used in this study. **Table S3.** Taxonomic information and GenBank accession numbers for the 53 taxa used for the phylogenetic analysis in this study. **Table S4.** Annotation and gene organisation of four mitochondrial genomes. **Table S5.** Base composition and length features of the four mitochondrial genomes used in this study. **Table S6.** The repeat elements in A+T-rich regions of four species. **Table S7.** Subset partition and its optimal model of datasets.

Copyright notice: This dataset is made available under the Open Database License (<http://opendatacommons.org/licenses/odbl/1.0/>). The Open Database License (ODbL) is a license agreement intended to allow users to freely share, modify, and use this Dataset while maintaining this same freedom for others, provided that the original source and author(s) are credited.

Link: <https://doi.org/10.3897/zookeys.969.49278.suppl1>

## Supplementary material 2

### Figures S1–S4

Authors: Qiu Zhongying, Chang Huihui, Yuan Hao, Huang Yuan, Lu Huimeng, Li Xia, Gou Xingchun

Data type: images

Explanation note: **Figure S1.** The A+T content of mitogenomes in orthopteran species.

**Figure S2.** The amino acid composition from *S. pieli*, *S. houshana*, *S. wulingshanensis*, and *S. qinlingensis*. **Figure S3.** Inferred secondary structure of tRNA families in *S. pieli*, *S. houshana*, *S. wulingshanensis* and *S. qinlingensis* mitochondrial genomes. Note: The nucleotide substitution pattern for each tRNA family is modeled using as the reference the structure determined for *S. pieli*. Because of the special secondary structure of trnP in *S. houshana*, the trnP in Figure S3 is presented separately. In nucleotide substitutions and insertions, we used different colours to represent different species (one or several). The colour of some substitutions and insertions only represent some species, which means base deletions in the location of other species. **Figure S4.** Putative stem-loop structures found in A+T-rich region from four species.

Copyright notice: This dataset is made available under the Open Database License (<http://opendatacommons.org/licenses/odbl/1.0/>). The Open Database License (ODbL) is a license agreement intended to allow users to freely share, modify, and use this Dataset while maintaining this same freedom for others, provided that the original source and author(s) are credited.

Link: <https://doi.org/10.3897/zookeys.969.49278.suppl2>

# Lost lovers linked at long last: elusive female *Nanophyllium* mystery solved after a century of being placed in a different genus (Phasmatodea, Phylliidae)

Royce T. Cumming<sup>1,2,3</sup>, Stéphane Le Tirant<sup>4</sup>, Sierra N. Teemsa<sup>1</sup>,  
Frank H. Hennemann<sup>5</sup>, Luc Willems<sup>6</sup>, Thies H. Büscher<sup>7</sup>

**1** Associate Researcher, Montreal Insectarium, 4581 rue Sherbrooke est, Montréal, Québec, H1X 2B2, Canada **2** Ph.D. Student, Richard Gilder Graduate School, American Museum of Natural History, New York, NY 10024, USA **3** Ph.D. program in Biology, Graduate Center, City University of New York, NY, USA **4** Collection manager, Montreal Insectarium, 4581 rue Sherbrooke, Montréal, Québec, H1X 2B2, Canada **5** Tannenwaldallee 53, 61348 Bad Homburg, Germany **6** Naturalis Biodiversity Center, PO Box 9517, NL-2300 RA Leiden, The Netherlands **7** Department of Functional Morphology and Biomechanics, Zoological Institute, Kiel University, Am Botanischen Garten 9, 24118 Kiel, Germany

Corresponding author: Royce T. Cumming ([phylliidae.walkingleaf@gmail.com](mailto:phylliidae.walkingleaf@gmail.com))

Academic editor: Marco Gottardo | Received 6 July 2020 | Accepted 22 August 2020 | Published 17 September 2020

<http://zoobank.org/C26EB0BB-5221-4953-A0AD-0822A9050369>

**Citation:** Cumming RT, Le Tirant S, Teemsa SN, Hennemann FH, Willems L, Büscher TH (2020) Lost lovers linked at long last: elusive female *Nanophyllium* mystery solved after a century of being placed in a different genus (Phasmatodea, Phylliidae). ZooKeys 969: 43–84. <https://doi.org/10.3897/zookeys.969.56214>

## Abstract

After successful laboratory rearing of both males and females from a single clutch of eggs, the genus *Nanophyllium* Redtenbacher, 1906 (described only from males) and the *frondosum* species group within *Phyllium* (*Pulchriphyllium*) Griffini, 1898 (described only from females) are found to be the opposite sexes of the same genus. This rearing observation finally elucidates the relationship of these two small body sized leaf insect groups which, for more than a century, have never been linked before. This paper synonymizes the *frondosum* species group with *Nanophyllium* Redtenbacher, 1906 in order to create a singular and clearly defined taxonomic group. Five species are transferred from the *Phyllium* (*Pulchriphyllium*) *frondosum* species group and create the following new combinations: *Nanophyllium asekiense* (Größer, 2002), **comb. nov.**; *Nanophyllium chitoniscoides* (Größer, 1992), **comb. nov.**; *Nanophyllium frondosum* (Redtenbacher, 1906), **comb. nov.**; *Nanophyllium keyicum* (Karny, 1914), **comb. nov.**; *Nanophyllium suzukii* (Größer, 2008), **comb. nov.** The only taxon from this species group

not transferred from the *frondosum* species group to *Nanophyllum* is *Phyllium* (*Pulchriphyllum*) *groesseri* Zompro, 1998. Based on protibial exterior lobes, this species belongs in the *schultzei* species group as described in Hennemann et al. 2009 and is therefore excluded from further discussion here. The rearing of *Nanophyllum* also yielded the male *Nanophyllum asekiense* (Größer, 2002), **comb. nov.** thus, enabling comparison of this male to the other previously known *Nanophyllum* species. Two new species of nano-leaf insects are described within, *Nanophyllum miyashitai* **sp. nov.**, from Morobe Province, Papua New Guinea, and *Nanophyllum daphne* **sp. nov.**, from Biak Island, Papua Province, Indonesia. With such distinct sexual dimorphism in *Nanophyllum* between sexes, which have only now been matched up via captive rearing, illustrated within are numerous specimens which might represent the unknown opposite sexes of the many currently known species of *Nanophyllum*. Due to pronounced sexual dimorphism in *Nanophyllum*, only future captive rearing or molecular analysis will match up the many unknown sexes. To conclude, with the description of two new *Nanophyllum* species, dichotomous keys to species for known males and females are presented.

### Keywords

Nano-leaf insect, Phasmida, Phylliinae, *Phyllium*, sexual dimorphism, taxonomy, walking leaf, West Papua

## Introduction

The leaf insects (Phylliidae) represent a lineage within the stick insects (Phasmatodea), which are popular as pets and within insect collections due to their impressive leaf-like camouflage. The Phylliidae have an impressive array of morphological adaptations to mimic different types of leaves. Present in many species is the ability for various color forms which allow them to look like living, dying, or dead leaves (Fig. 1). These masters of leaf-like camouflage can be found throughout Southeast Asia, with some of the biodiversity hotspots being Indonesia, Malaysia, and Papua New Guinea (Brock et al. 2020).

Included within the Phylliidae are the *Nanophyllum* Redtenbacher, 1906 a group of small bodied species which for more than 100 years have only been known from rarely collected male specimens. Throughout a majority of those years only the single type species *Nanophyllum pygmaeum* Redtenbacher, 1906 was recognized. It was not until the last couple of decades that a majority of new *Nanophyllum* species began to be described (Brock et al. 2020). With numerous species described throughout the island of New Guinea solely from male specimens, the question begs to be asked, “where are the female *Nanophyllum*?”. Could the lack of females be that they are incredibly elusive, or already well-known and simply not recognized as female *Nanophyllum*?

Brock and Hasenpusch (2003: 203, fig. 6) were the first to suggest and illustrate the unknown *Nanophyllum* female, an individual from Nabire, Irian Jaya, collected along with a male which would later become the holotype of *Nanophyllum hasenpuschi* Brock & Größer, 2008. Unfortunately, however, the female specimen is missing both front legs (an important morphological identification feature frequently used for differentiation) but all other features place it morphologically close to *Phyllium* (*Pulchriphyllum*) *frondosum* Redtenbacher, 1909. Additionally, Brock and Hasenpusch (2003) discuss the subadult female found by G. B. Monteith in 1971 in the Iron Range,

Queensland as additional evidence that a “*frondosum*-like species” is probably the unknown female for the *Nanophyllium*. As it turns out, the *frondosum* species group, as defined by Hennemann et al. (2009), are also somewhat of a quandary since they are only known from female specimens, except for *Phyllium* (*Pulchriphyllium*) *groesseri* Zompro, 1998. In light of the speculation by Brock and Hasenpusch (2003) the authors scoured major collections around the world for additional *Nanophyllium* male specimens and females of the *frondosum* species group looking for shared morphological features which might support the thoughts of Brock and Hasenpusch (2003).

As it so happens, the breakthrough was not due to the exhaustive review of museum specimens, but instead came as a surprise at the Montreal Insectarium, Quebec, Canada. In April 2018 the Insectarium received eggs of *Phyllium* (*Pulchriphyllium*) *asekiense* Größer, 2002 from Morobe Province, Papua New Guinea with the hopes of raising this beautifully variable species in captivity (Fig. 1). The surprise came in early 2019 when the three sole survivors of the very slow developing nymphs reached adulthood; as one female *Phyllium asekiense* and two male ‘*Nanophyllium*’. This breakthrough at long last was the evidence we had been searching for to remove the speculation of these two known, but never associated, taxa.

This pairing of the *frondosum* species group with the *Nanophyllium* morphologically was not surprising given numerous morphological similarities between the taxonomic groups (discussed below). From our extensive review of museum specimens, we found males ranging in length from ~ 27 to 40 mm and females ranging from ~ 46 to 71 mm, a difference which is not outside of the norm with the male to female ratio seen throughout the family.

## Materials and methods

The holotype specimen of *Nanophyllium miyashitai* sp. nov. was loaned to the Montreal Insectarium (Stéphane Le Tirant, collection manager) from the extensive collection of Tetsuo Miyashita, Japan. See the abbreviations section below for a full list of collections (both institutional and large private) in which relevant material was recovered. Photos of specimens that were loaned to/held within the Montreal Insectarium were taken by René Limoges of using a Nikon D810 DSLR camera with Nikon Micro-Nikkor 200 mm f/4 lens on Manfrotto 454 micrometric positioning sliding plate. Lighting was provided by two Nikon SB-25 flash units with a Cameron Digital diffusion photo box. Adobe Photoshop Elements 13 was used as post processing software. The *Nanophyllium miyashitai* sp. nov. holotype specimen is deposited in the Montreal Insectarium (Quebec, Canada) type collection.

Photographs of the female *Nanophyllium chitoniscoides* (Größer, 1992) comb. nov. (Fig. 16A) were taken by Frank Hennemann within his personal collection using a Nikon D7000 camera equipped with a Nikon DX AF-S Micro 40 mm lens and a wireless Nikon SU-800 dual speed light system. Background lightning was provided by a 18W 6000K LED panel light plate.

The photograph of the female holotype *Nanophyllium suzukii* (Größer, 2008) comb. nov. (Fig. 16B) was taken by Mandy Schröter under direction of Stephan Blanke at the Senckenberg German Entomological Institute Müncheberg using a Nikon D7200 digital camera and a Nikon Micro Nikkor 105 mm f/2.8 G ED objective. Lighting was from the Yongnuo Digital Speedlight YN 560 IV reflected by the inner surface of a Styrofoam box set up around the specimen. A grey card was used for white balance. Composite images with an extended depth of field were created using the software StackShot Macro Rail Package (Cognisys Inc., U.S.A.) and Zerene Stacker (release November 7, 2017; Zerene Systems LLC, U.S.A.).

Photographs of the types of *Nanophyllium daphne* sp. nov. (Fig. 21C) and *Nanophyllium keyicum* (= *Phyllium insulanicum*) (Fig. 16D) were taken by Yvonne van Dam at Naturalis using a Nikon D600 with a 60 mm macro lens.

All other photographs were taken by unknown photography equipment/by simple camera phone images, and where photo credit/equipment is known it is stated within the figure caption. Egg orientation terminology follows Clark (1978). Species group organizations follow the classification presented in Hennemann et al. (2009) and Cumming (2017). Wing venation terminology follows Burt (1932) and Ragge (1955). Measurements of the holotype specimens were made to the nearest 0.1 mm using digital calipers.

The following institutional abbreviations are used:

<b>AMNH</b>	American Museum of Natural History, New York, New York, U.S.A.
<b>ANIC</b>	Australian National Insect Collection, Canberra, Australia
<b>ANSP</b>	Academy of Natural Sciences, Philadelphia, Pennsylvania, U.S.A.
<b>CAS</b>	California Academy of Sciences, San Francisco, California, U.S.A.
<b>CFIA</b>	Canadian Food Inspection Agency, Canada
<b>IMQC</b>	Insectarium de Montréal, Montréal, Québec, Canada
<b>MNHU</b>	Museum für Naturkunde der Humboldt-Universität, Berlin, Germany
<b>MSNG</b>	Museo Civico di Storia Naturale, Genova, Italy
<b>MZSF</b>	Strasbourg Zoological Museum, Strasbourg, France
<b>NHMB</b>	Naturhistorisches Museum Basel, Basel, Switzerland
<b>NHMUK</b>	Natural History Museum United Kingdom, London, United Kingdom
<b>RBINS</b>	Royal Belgian Institute of Natural Sciences, Brussels, Belgium
<b>RMNH</b>	Naturalis Biodiversity Center, Leiden, Netherlands
<b>SDEI</b>	Senckenberg Deutsches Entomologisches Institut, Müncheberg, Germany
<b>SDNHM</b>	San Diego Natural History Museum, San Diego, California, U.S.A.
<b>SMTD</b>	Staatliches Museum für Tierkunde, Dresden, Germany
<b>UMMZ</b>	University of Michigan, Museum of Zoology, Ann Arbor, Michigan, U.S.A.
<b>Coll FH</b>	Private collection of Frank H. Hennemann, Bad Homburg, Germany
<b>Coll RC</b>	Private collection of Royce T. Cumming, California, U.S.A.
<b>Coll SLT</b>	Private collection of Stéphane Le Tirant, Montreal, Canada

## Results

### Captive rearing of *Nanophyllum* in the Montreal Insectarium

In January 2018, Stéphane Le Tirant of the Montreal Insectarium applied for a live insect import permit from the CFIA to allow the importation of live eggs to Canada from local insect suppliers in Papua New Guinea. Fortunately, one of those suppliers was able to export a small series of eggs freshly laid by a wild caught female *Phyllium asekiense*, collected in Morobe Province, Papua New Guinea. In April 2018, the Montreal Insectarium received 13 eggs, all black in color, and with the same morphology across the series. Eggs were incubated at room temperature on a plastic screen mesh within a plastic box with coco fiber at the base which was regularly sprayed with water to maintain humidity. Of these thirteen received eggs, during a period of seven to eleven months only five nymphs hatched (Fig. 2D). In an attempt to find at least one species of food which the fresh nymphs would accept, nymphs were offered *Psidium guajava* (Guava), *Rubus* sp. (Bramble), and *Gaultheria shallon* (Salal) to eat. These three plants are commonly accepted host plants regularly used within the Montreal Insectarium. Of these five nymphs, two nymphs refuse to eat any of the host plants offered entirely and died within a few days. The other three nymphs thankfully accepted bramble and during the first few instars all three individuals looked very similar in morphology (Fig. 2E). All three nymphs were quite active both day and night and fed continuously. It was not until the last two molts that the sexual dimorphism became noticeable, and after a period of 90 to 130 days after first hatching all three reached adulthood as two males and one female. Unfortunately, the males became adult (Fig. 2C) whilst the female was still only a subadult (Fig. 2A). The males were active by day and night (readily flying) and lived only for about four months, dying before the female was adult.

The female lived as an adult for about nine months before dying, producing a total of 245 eggs of many different colors (Fig. 3). During the peak of her egg producing life she produced three to four eggs per day, and as many as 112 eggs in a single month. In adulthood, the female was no longer active during the day and only fed at night. In the months since the 245 eggs were laid, they have been incubating and during this period very few nymphs have successfully hatched, and all refused to feed on the three host plant species that were offered and accepted by the original culture. To try and ensure that the species was successfully brought into culture, the Montreal Insectarium shared many eggs with other experienced Phylliidae breeders but they also were unsuccessful with obtaining a subsequent generation.

Despite the failed attempt to bring this species into culture, the successful rearing of both sexes from a batch of eggs from a single female has allowed the much needed definitive evidence to back up the morphological observations that the females of the *frondosum* species group and the males of *Nanophyllum* are simply one and the same. Therefore, the *frondosum* species group of *Phyllium* (*Pulchriphyllum*) is here transferred to the genus *Nanophyllum* (except for *Ph. groesseri*, which instead belongs to

the *Phyllium (Pulchriphyllium) schultzei* species group based in the protibial lobes and is therefore left within the *Phyllium (Pulchriphyllium)* subgenus). The genus *Nanophyllium* is here revised with most species illustrated and a general description for the male, female, and egg morphology after more than 100 years is now summarized together.

## Taxonomic accounts

### *Nanophyllium* Redtenbacher, 1906: 180.

**Type species.** *Nanophyllium pygmaeum* Redtenbacher, 1906, by monotypy.

**Distribution.** East of Weber's biogeographic line of faunal balance (Gressitt, 1982), primarily on the island of New Guinea and surrounding islands, as well as on the northern tip of Australia (Fig. 4).

### Species group checklist and sex which is known

#### *pygmaeum* species group

*Nanophyllium adisi* Zompro & Größer, 2003 (Male)

*Nanophyllium asekiense* (Größer, 2002) comb. nov. (Female, Egg, Male)

*Nanophyllium australianum* Cumming, Le Tirant, & Teemsma, 2018 (Male)

*Nanophyllium chitoniscoides* (Größer, 1992) comb. nov. (Female, Egg)

*Nanophyllium frondosum* (Redtenbacher, 1906) comb. nov. (Female)

*Nanophyllium hasenpuschi* Brock & Größer, 2008 (Male)

*Nanophyllium keyicum* (Karny, 1914) comb. nov. (Female, Egg)

*Nanophyllium pygmaeum* Redtenbacher, 1906 (Male)

*Nanophyllium rentzi* Brock & Größer, 2008 (Male)

*Nanophyllium suzukii* (Größer, 2008) comb. nov. (Female, Egg)

*Nanophyllium daphne* Cumming, Willemsse, Le Tirant, Teemsma, Hennemann and Büscher, sp. nov. (Female)

#### *stellae* species group

*Nanophyllium stellae* Cumming, 2016 (Male)

*Nanophyllium larsoni* Cumming, 2017 (Male)

*Nanophyllium miyashitai* Cumming, Le Tirant, Teemsma, Hennemann, Willemsse and Büscher, sp. nov. (Male)

### Female *Nanophyllium* general morphology

1. Antennae: consisting of nine or ten segments (Fig. 5).
2. Posteriormedial tubercle of the head capsule, split into two points (Fig. 6A–C) not a single tubercle as is present in most of the remaining Phylliidae (Fig. 6D).
3. Thorax: mesopleurae on their anterior end are notably wider than the prescutum anterior width. Mesopleurae always with prominent tubercles. Prescutum length

to width ratio from 1 : 1.8 (more typical) to 1 : 3.4 (in the more extreme width like which is seen in *N. suzukii*) (Fig. 7).

4. Tegmina: within the *Nanophyllium* there are three primary venation patterns (Fig. 8).
  - a. In the smallest species (individuals ~ 56.0 mm or less), the radial bend occurs before the splitting of the first radial and the radial sector, therefore the radial sector is straight (for example see *N. chitoniscoides* comb. nov.; Fig. 8A). These females also have a radius and medial crossvein present on the radial bend at or before the splitting of the first radial (Fig. 8A). The cubitus at its terminus is clearly split into the anterior cubitus and posterior cubitus veins with a clearly defined gap between them (Fig. 8A). Example species are *N. chitoniscoides* comb. nov., *N. daphne* sp. nov.
  - b. For the larger species, the bend in the radial vein happens on the radial sector after the splitting of the first radial from the radius (Fig. 8B). Also, the radius and medial crossvein occurs after the splitting of the first radial, instead originating on the radial sector (Fig. 8B). The cubitus at its terminus can be weakly split into the anterior cubitus and posterior cubitus, but in many specimens this vein is simple and unbranched (it is never clearly split with a large gap between the anterior cubitus and posterior cubitus like is seen in the smaller species; Fig. 8A). Example species are *N. asekiense* comb. nov., *N. frondosum* comb. nov., or *N. suzukii* comb. nov.
  - c. The final venation pattern is found in *Nanophyllium keyicum* comb. nov., the only species in this genus which has a wide gap between the media and cubitus veins which persists throughout the entire length of the media, this gap is several times wider than a single vein width. This feature is only seen on this species from Kei Island, Indonesia (Fig. 8C). All other examined *Nanophyllium* species have the media and cubitus veins running side by side throughout the entire length, no farther than a single vein width apart (for example in the larger species like *N. asekiense* comb. nov. or *N. suzukii* comb. nov.; Fig. 8B), or with veins moderately wide for the anterior portion (at most two or three vein widths apart) but as they reach the splitting of the media posterior the width between the media and cubitus veins is reduced and the veins are side by side (this example can be seen in the smaller species like *N. daphne* sp. nov.). Also, in *N. keyicum* comb. nov., the radius and medial crossvein occurs after the splitting of the first radial, instead originating on the radial sector (Fig. 8C). Similar to the larger species, the cubitus at its terminus can be weakly split into the anterior cubitus and posterior cubitus (like those seen in Fig. 8B), but in most specimens of *N. keyicum* comb. nov. this vein is simple and unbranched (as illustrated in Fig. 8C).
5. Alae: absent.
6. Genitalia: gonapophyses protruding from abdominal segment VIII as long as the terminal abdominal segment, gonapophyses protruding from abdominal segment IX thinner and shorter, not exceeding the terminal abdominal segment, and subgenital plate short and moderately broad with the point just reaching the anterior margin of the terminal abdominal segment (Fig. 9).

### Male *Nanophyllium* general morphology

The *Nanophyllium* based on male morphology can be separated into two distinct species groups, the *pygmaeum* species group (Fig. 10A) and the *stellae* species group (Fig. 10B). Males of several species for the two species groups are known, but females and eggs are only known for the *pygmaeum* species group, the female and eggs are not yet known for the *stellae* species group.

Easily observed morphological features which differentiate the species groups are the femoral lobes. The *pygmaeum* species group has profemoral interior lobes which are angular (Fig. 11D–H) and mesofemoral interior lobes which do not reach from end to end of the shaft and have distinct serrate teeth. The *stellae* species group has profemoral interior lobes which are rounded without a sharp angle (Fig. 11A–C) and mesofemoral interior lobes which are a large rounded triangle, reaching from end to end without prominent spination.

1. Profemoral interior lobe, in both species groups with most often three small teeth, but occasionally four teeth (rarely), never more than four teeth (Fig. 11A–H).
2. Posteromedial tubercle of the head capsule split into two points (Fig. 7A–C) not a single tubercle as is present in most of the remaining Phylliidae (Fig. 7D).
3. Thorax: mesopleurae on their anterior end are moderately wider than the prescutum anterior width (Fig. 12). Prescutum length to width ratio ranges from 1 : 2.6 to 1 : 3.3 (Fig. 12).
4. Tegmina short, length never exceeding the posterior of the metathorax. The venation of the tegmina appears to be rather simple/too sclerotized to identify details of venation. From a review of several different species it appears as though the subcostal vein is lost within an area that is highly sclerotized. The radial vein is moderately present and runs along the edge of the highly sclerotized patch. The medial vein is the most prominent and runs through the center of the tegmina and occasionally has a weak vein splitting from it, but for most observed specimens the medial vein was not prominently branched. The cubitus and first anal are only moderately formed and give stability to the other half of the tegmina and are not notably branched.
5. A unique feature of the alae which appears to be a symplesiomorphy for the *Nanophyllium* is that the radius splits into the first radial and the radial sector on the distal half of the wing and these two veins run separately to the wing margin without fusing to others (the only other group which also has the radial split on the distal half is the *Pulchriphyllium*, but their radial sector fuses with the media anterior, media posterior, and the cubitus instead of running by itself to the wing margin; all other leaf insect genera have the radial split happening on the proximal half of the wing). Within the *Nanophyllium* the alae venation differs between the two species groups.
  - a. In the *pygmaeum* species group the key differences are that the media posterior fuses back to the media anterior before reaching the wing margin, and then

the fused media runs on its own to the wing margin without fusing with the radial sector (Fig. 13A).

- b. In the *stellae* species group the media anterior and the media posterior do not fuse, instead they both run to the wing margin, and the cubitus after splitting from the first anterior anal fuses with the media posterior near the wing margin and then they run fused to the margin as one (Fig. 13B).
6. Vomer long and slender with a single apical hook (Fig. 19C).

### ***Nanophyllium* egg general morphology**

Figure 14

Fortunately, there are several *Nanophyllium* species with the egg morphology known.

These species include: *Nanophyllium asekiense* (Figs 3, 14A–C) comb. nov.; *Nanophyllium chitoniscoides* (Größer, 1992: 165, fig. 3), comb. nov.; *Nanophyllium keyicum* (Karny, 1914: see Größer, 2008: 123, fig. 146), comb. nov.; *Nanophyllium suzukii* (Größer, 2008: 137, fig. 171), comb. nov.; and the unidentified *Nanophyllium* female from the NHMUK 012497230, has a single egg mounted to a card below the specimen (Fig. 14D–F). From these known eggs a generalized list of morphological features can be compiled.

1. Cross-section is roundly pentagonal (Fig. 14C, F).
2. Surface is roughly textured, with pitting of various sizes throughout the capsule surface. Surface lacks pinnae. Pits on the capsule surface depending on the species can either have significant depth to them or in other species can have shallow pits.
3. Operculum has distinct pitting surrounding the central gently raised apex (Fig. 14C, F).
4. Micropylar plate is elongate, nearly reaching from end to end of the capsule and with an approximately uniform width throughout except for around the micropylar cup where it is slightly wider. Running parallel along the micropylar plate margin are pits, which vary in number from species to species (Fig. 14A, D).
5. Lateral surface with irregular pitting in no detectable pattern, with some pits very near each other or touching to form wider irregular shapes (Fig. 14B, E).

### ***Nanophyllium* Distribution**

Figures 4, 15

#### INDONESIA

North Maluku Province:

Batjan Island (*N. suzukii*: SDEI, Fig. 16B)

Maluku Province:

Buru Island (*Nanophyllium* sp. Undetermined female)

Kei Island (*Nanophyllium keyicum*: NHMUK; RMNH; SDEI; FH Coll, Fig. 16D)

West Papua Province:

- Fak Fak (*Nanophyllium rentzi*: NHMUK, Fig. 18A; Coll SLT, Fig. 18B)  
 Aiduma Island (*Nanophyllium* sp. Undetermined male, Fig. 22)  
 Papua Province:  
 Biak Numfor Regency, Biak Island (*N. daphne* sp. nov., RMNH, Fig. 21C)  
 Nabire Regency (*N. hasenpuschi*: NHMUK)  
 Dogiyai Regency, Mapia (*Nanophyllium* sp. Undetermined female: Coll SLT, Fig. 24F)  
 Mimika Regency, Utakwa River (*Nanophyllium* sp. Undetermined male, Wollaston Expedition, NHMUK)  
 Nduga Regency “Hoofdbivak” (*N. adisi*, Stirling Expedition, SMTD)  
 Nduga Regency “Kloofbivak” (Third South New Guinea Expedition, *Nanophyllium* sp. Undetermined nymph, ANSP)  
 Central Mamberamo Regency, Kobakma (*Nanophyllium* sp. Undetermined female, CAS, Fig. 24E)  
 Jayapura Regency, Cyclops Mts. (*N. stellae* (Fig. 10B and *N. larssoni*, SDNHM)

## PAPUA NEW GUINEA

### Western Province:

Katau (*N. pygmaeum*: MSNG)

Daru Island (*Nanophyllium* sp. Undetermined female, CAS, Fig. 24D)

### Chimbu Province:

Kerowagi District (*N. frondosum*, Coll RC, Fig. 16C)

### Eastern Highlands Province:

Mt. Otto (*Nanophyllium* sp. Undetermined female nymph, Sixth Archbold Expedition, AMNH, Fig. 24A)

Buntibasa dist., N. Guinea, Kratke Mts, 4,000–5,000', February 1933. (F. Shaw Mayer), (*Nanophyllium* sp. Undetermined male nymph, NHMUK)

Herowana Village (observational record for *N. asekiense* by Daniel Levitis, USA)

### Gulf Province:

Kerema (*N. asekiense*, Coll RC)

### Morobe Province:

Wau (*N. miyashitai* sp. nov., IMQC, Fig. 20)

Lae (*N. asekiense*, Coll RC)

Sattelberg (*N. frondosum*, UMMZ)

Menyama District, Aseki (*N. frondosum* and *N. asekiense*, Coll RC; *N. chitoniscoides*, Miyashita Private collection, and Coll FH Fig. 16A)

Watut (*N. chitoniscoides*, paratype in the Detlef Größer private collection)

### Central Province:

Vanama River (*Nanophyllium* sp. Undetermined female, Coll RC, Fig. 24B)

Port Moresby (*Nanophyllium* sp. Undetermined female, NHMUK, Fig. 24C)

### Northern Province:

Popondetta (*Nanophyllium* sp. Undetermined female, NHMUK)

### Milne Bay Province:

Normanby Island (*Nanophyllium* sp. Undetermined female)

## AUSTRALIA

## Queensland:

Iron Range National Park (*N. australianum*, ANIC)Lockhart (*N. australianum*, Fig. 23)***Nanophyllium asekiense* (Größer, 2002), comb. nov.**

Figures 1, 2, 3, 6A, 10A, 11E, 12B, 14A–C, 17, 19

**Discussion.** Female *N. asekiense* comb. nov. is most often confused with the sympatric species *N. frondosum* comb. nov., but *N. asekiense* comb. nov. can be differentiated by the presence of small exterior pro- and meso-tibial spurs, which *N. frondosum* comb. nov. lacks.

Only two male *N. asekiense* comb. nov. are known at present, but their morphology is consistent between them for all features except for the abdominal shape (see Fig. 17E, F for side by side comparison of these two males). An additional specimen of *Nanophyllium rentzi* also shows how variable male abdominal morphology can be within the same species while the other morphological features remain stable (Fig. 18A, B). *Nanophyllium asekiense* comb. nov. males can be differentiated from the other known *Nanophyllium* males based on the profemoral lobe morphology. In *N. asekiense* comb. nov. the interior profemoral lobe is distinctly right-angled (a feature present in all species of the *pygmaeum* species group (Fig. 11E–H) except *N. australianum* which has a thinner, obtuse angle; Fig. 11D), but the exterior profemoral lobe of *N. asekiense* comb. nov. is narrow, only about the same width as the profemoral shaft; Fig. 11E (more like *N. australianum* than any other species, as the other spe-

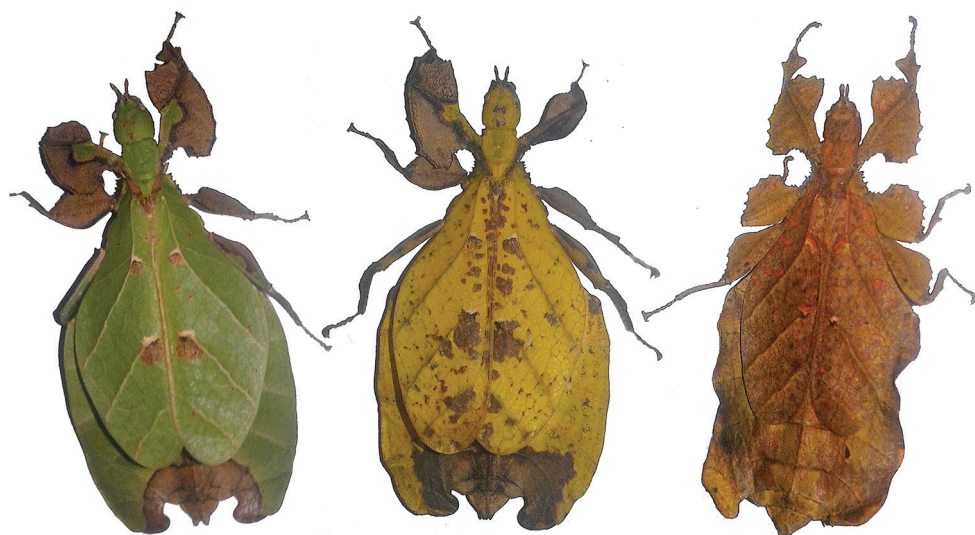


**Figure 1.** Live *Nanophyllium asekiense* (Größer, 2002), comb. nov. females, three primary color forms photographed in Morobe Province, Papua New Guinea.

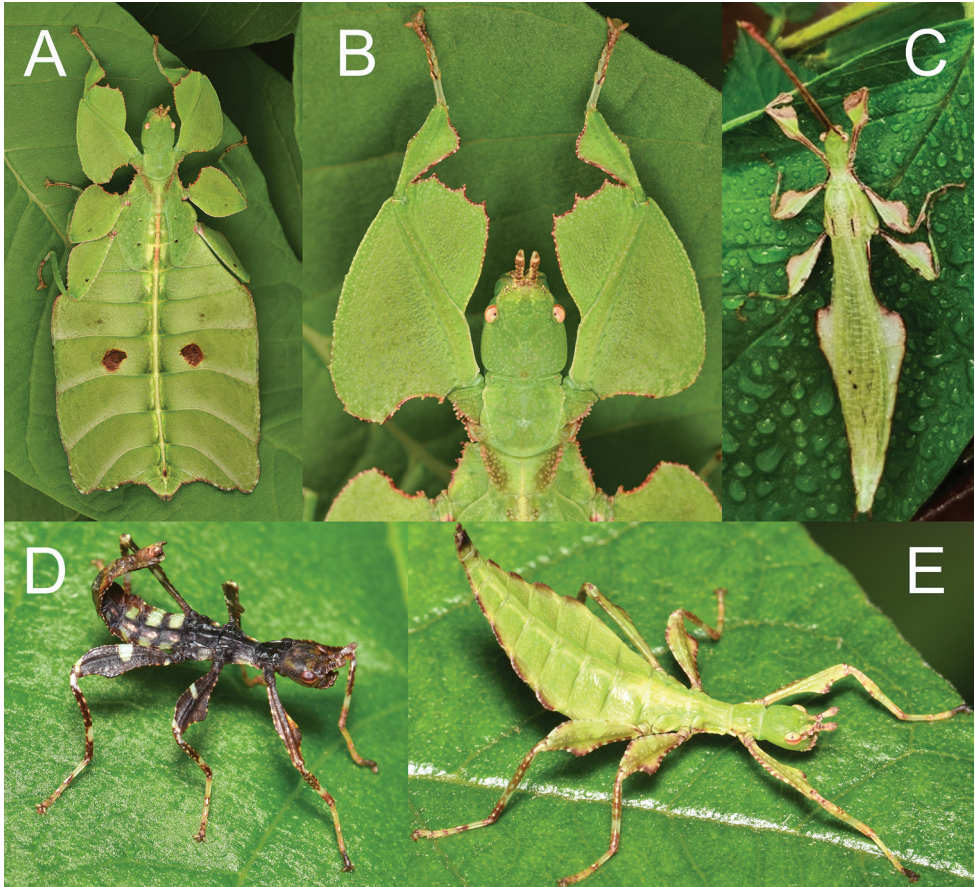


**Figure 2.** Live *Nanophyllium asekiense* (Größer, 2002), comb. nov. raised in the Montreal Insectarium **A** subadult female, full body dorsal **B** subadult female, head and front legs, dorsal **C** adult male, full body dorsal **D** freshly hatched nymph **E** nymph, later instar.

cies instead have an exterior profemoral lobe which is broader than the width of the profemoral shaft; Fig. 11F–H).

**Description. Male. Coloration.** Each antennal segment with dark brown and tan coloration. The rest of the body and legs are of a yellow-green based color, with variable brown margins. In the two males bred by the Montreal Insectarium the individual with the undulating abdomen has minimal brown markings, with only brown along the leg margins and the abdomen margins (Fig. 17E). The male with the straight abdominal margins has more prominent brown markings throughout, with around half of the leg lobes marked with brown and a wider brown abdominal margin (Fig. 17F). The alae and tegmina on both males are a translucent pale green, with small flecks of dark brown along the prominent veins.

**Morphology. Head.** Head capsule about as long as wide, with a vertex that is lumpy without notable granulation, two posteromedial tubercles are not notably large but are



**Figure 3.** *Nanophyllium asekiense* (Größer, 2002), comb. nov. eggs laid by the single adult female which made it to adulthood in the Montreal Insectarium; note the variability of color within the eggs laid by this singular female.

present with a slight furrow between them (Fig. 19D). Compound eyes are notably protruding from the head capsule and there are three well-developed ocelli between and slightly posterior to them (Fig. 19D). *Antennae.* The antennae are longer than the outstretched forelegs and consist of 23 antennomeres (Fig. 19D). The scapus and pedicellus are nearly bare, with only a few short clear setae. All segments beyond the scapus and pedicellus except for the terminal four are covered in stiff dark setae which are each longer than the segment they are on is wide. The terminal four antennal segments also have dark setae, but these setae are shorter than the segments are wide (Fig. 19D). *Thorax.* Pronotum as wide as it is long with moderately formed rims on the lateral margins that are mostly parallel and only gently converging near the posterior, the anterior



**Figure 4.** Distribution map showing localities for the known and herein described species.

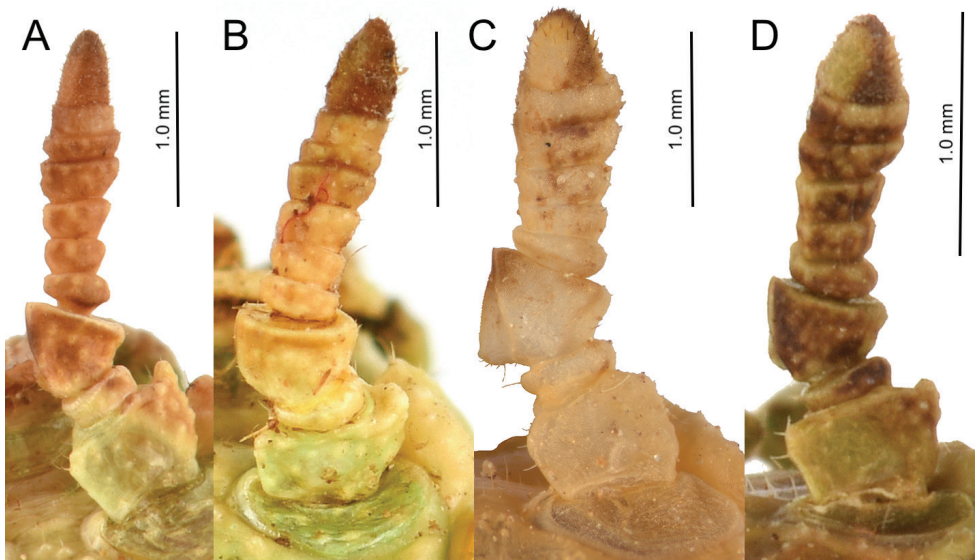


**Figure 5.** Female *Nanophyllium* antennae, dorsal view **A** *Nanophyllium asekiense* Coll SLT **B** *Nanophyllium* species, Indonesia, West Papua, Mapia, Coll SLT **C** *Nanophyllium daphne* sp. nov., RMNH **D** *Nanophyllium* species NHMUK 012497230.

margin is slightly curved with a prominent rim, and the posterior margin is weakly formed (Fig. 19B). Surface of the pronotum has a distinct sagittal furrow and central lateral furrow, and the surface is irregularly lumpy, but not granular (Fig. 19B). Prescutum significantly wider than long, at its widest on the anterior it is 2.5 times wider than long. The prescutum margins evenly converge toward the posterior and have two or three notable nodes on the anterior portion, and the remainder of the margin is irregularly lumpy. Surface of prescutum is nearly smooth without significant features,



**Figure 6.** Head capsule posteriomedial tubercles compared between select genera/species **A** *Nanophyllium* species female NHMUK 012497230 **B** *Nanophyllium frondosum* female, Coll SLT **C** *Nanophyllium miyashitai* sp. nov. holotype male **D** *Phyllium letiranti* Cumming & Teesma, 2018 female, Coll SLT (note the singular tubercle in this *Phyllium* species versus the double tubercles of *Nanophyllium*).

and the anterior prescutum margin is simple, also lacking nodes or spines (Fig. 19B). Mesopleurae gradually diverging wider from anterior to the posterior, and marked with irregularly shaped tubercles throughout, with around four notably larger ones and smaller nodes intermixed (Fig. 19B). Mesopleurae surface irregularly lumpy with a single distinct pit in the center and no notable nodes. Pro-, meso-, and meta-sternum with irregularly spaced granules mostly along the sagittal plane but with the margins occasionally with sparse granules. *Wings.* Tegmina short, not exceeding the posterior of the metathorax. The subcostal vein and any splitting of the radius is obscured within an area of the wing that is highly sclerotized. The radius is the most prominent vein and runs through the center of the tegmina to the posterior margin (along the edge of the highly sclerotized patch). The medial vein is also prominent and runs through the center of the tegmina parallel with the radius and does not appear as though the media has any notable splits. The cubitus and first anal are moderately formed and give stability to the other half of the tegmina, are not notably branched, and this half of the tegmina is not as heavily sclerotized as the other half. The first anal fuses with the cu-



**Figure 7.** Thorax of various *Nanophyllium* females, dorsal **A** *Nanophyllium* species female Coll RC 16-224 **B** *Nanophyllium frondosum* female Coll RC 16-049 **C** *Nanophyllium chitoniscoides* Coll FH **D** *Nanophyllium* species NHMUK 012497230.

bitus around two thirds of the length, and the cubitus runs nearly to the wing margin. Alae developed, with the exposed section of folded alae slightly sclerotized, but not as sclerotized as the alae. The costa runs along the wing margin with a weak subcosta running along and eventually fusing with it. The radius splits into the first radial and the radial sector just distal to the wing midline and these two veins run separately to the wing margin without fusing to others. The media splits into the media anterior and the media posterior almost immediately near the base of the wing. The media posterior fuses back to the media anterior near the distal one fifth of the wing, and then the fused medial veins run to the wing margin (Fig. 13A). The cubitus runs with the first anterior anal for most of the length and then near the distal one fifth of the wing they split and the cubitus runs unbranched and unfused to the wing margin. There are seven anterior anals which run simply to the wing margin and four or five well-formed posterior anals which run simply to the wing margin. *Abdomen.* Abdominal segment II with parallel sides, segment III widening in a smooth arc, segment IV widening slightly for the first half, then gently curving in for the second half, segments V through VIII variable with margins that are either straight and converging uniformly to the apex which

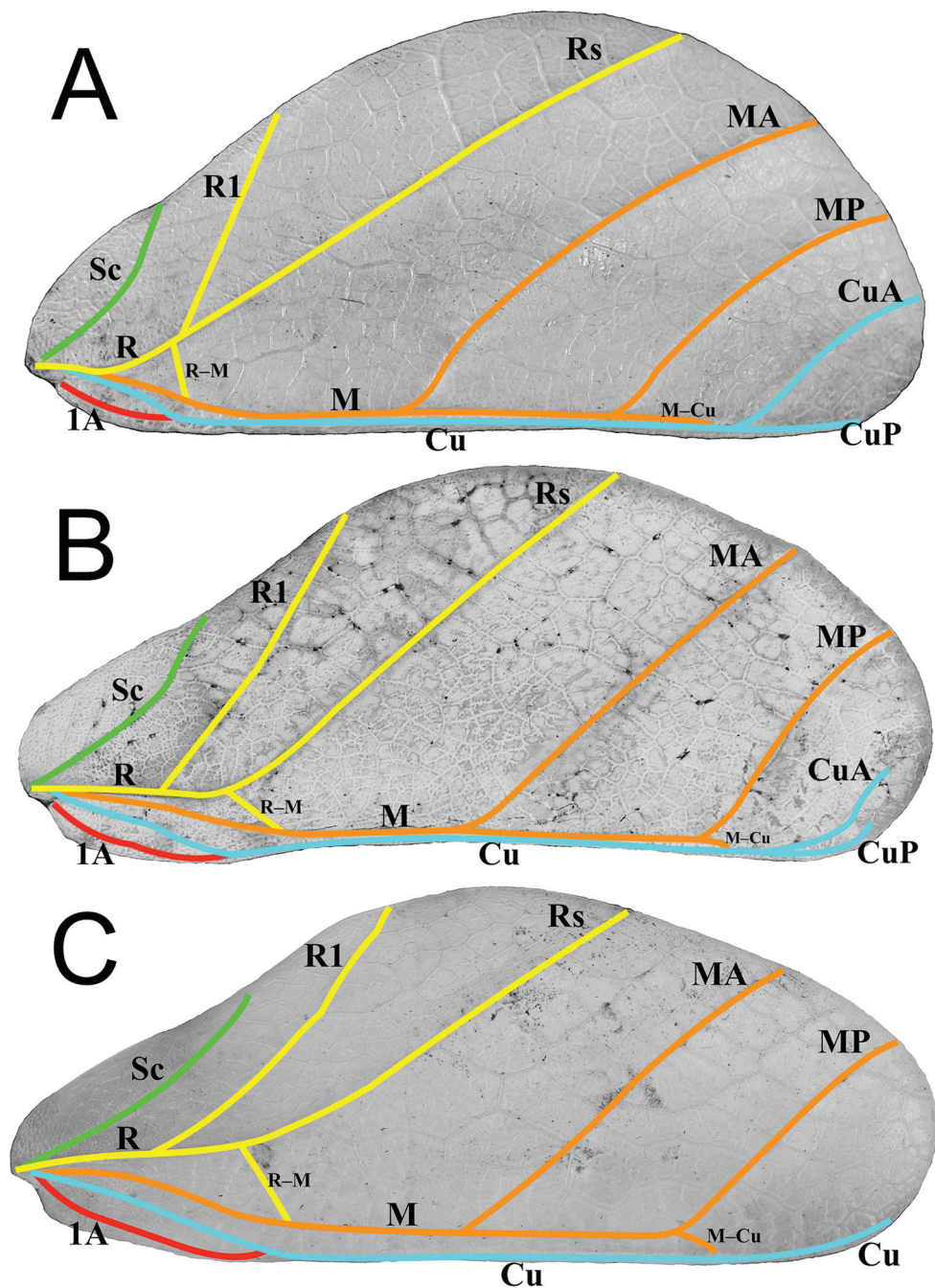


**Figure 8.** Three primary venation patterns seen in female *Nanophyllium* tegmina, dorsal view **A** *Nanophyllium chitoniscoides* Coll FH **B** *Nanophyllium suzukii* holotype, SDEI **C** *Nanophyllium keyicum* Coll FH. Abbreviations used: Sc (subcosta); R (radius); R1 (radius 1); Rs (radial sector); R-M (radius and medial crossvein); M (media); MA (media anterior); MP (media posterior); Cu (cubitus); CuA (cubitus anterior); CuP (cubitus posterior); 1A (first anal).

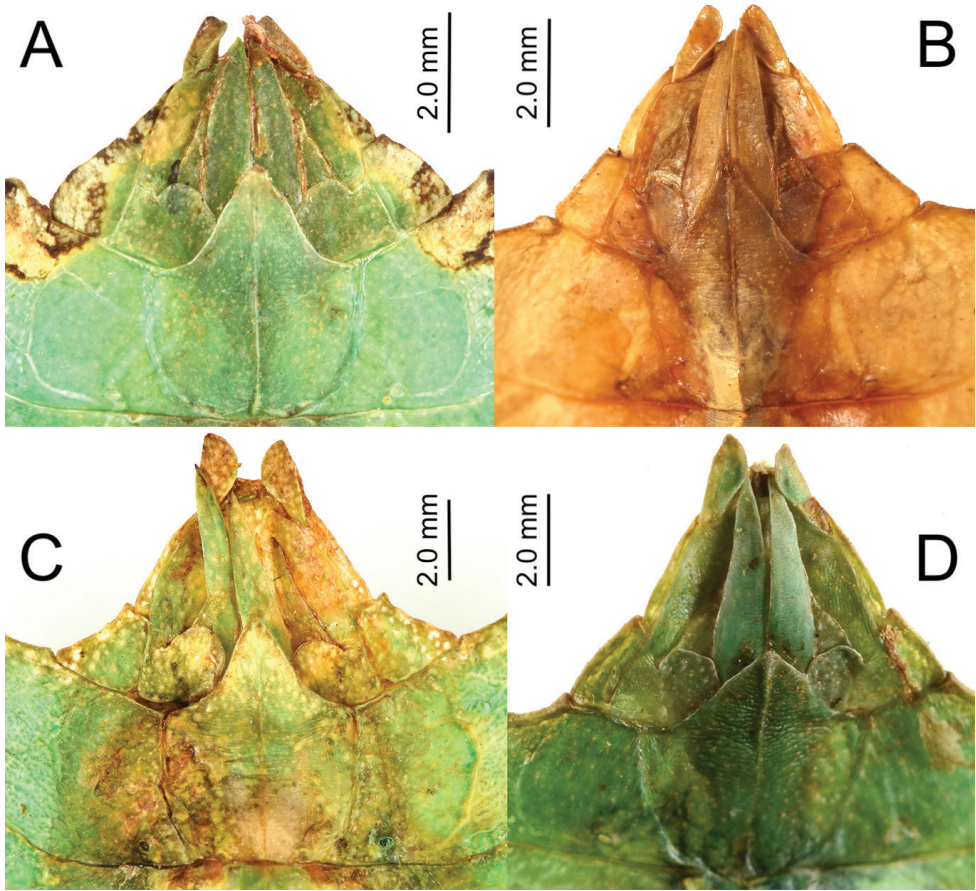


**Figure 9.** Female *Nanophyllium* genitalia, ventral view **A** *Nanophyllium* species NHMUK 012497230 **B** *Nanophyllium* species, Papua New Guinea, Central Province, Coll RC 16-224 **C** *Nanophyllium* species, Indonesia, West Papua, Mapia, Coll SLT **D** *Nanophyllium chitoniscoides*, Coll FH.

gives the abdomen a straight spade-shaped appearance or with margins which each expand and then contract which gives the abdomen a lobed appearance. Abdominal segment IX with margins which slightly converge to the abdominal segment X which is longer than wide and ends in a rounded apex. *Genitalia*. Poculum broad and ending in a slightly cleft apex that reaches the anterior margin of segment X (Fig. 19C). Cerci densely covered in nodes throughout the surface and short setae mostly on the distal half (Fig. 19C). Vomer long, and slightly bending to the side, not perfectly straight; with sides gradually converging to the upward hooked apex (Fig. 19C). *Legs*. Profemoral interior lobe angular (approximately 90 degrees) with three small evenly spaced teeth with a nearly straight gap between each tooth (Fig. 19A). Exterior profemoral lobe significantly thinner than the interior lobe (about as wide as the profemoral shaft), only present as a smoothly curved lobe just distal to the midline, not spanning the entire length (Fig. 19A). Protibiae with lobes only present on the proximal half, the distal



**Figure 10.** Side by side *Nanophyllium* males of the two species groups **A** *pygmaeum* species group, *Nanophyllium asekiense* male from Morobe Province, Papua New Guinea **B** *stellae* species group, *Nanophyllium stellae* HT from Jayapura, Indonesia.

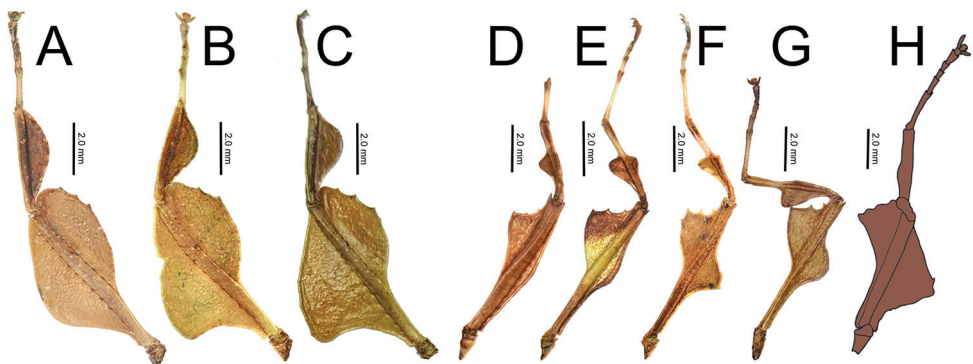


**Figure 11.** Front legs and lobes of males of the *stellae* species group (**A–C**) and the *pygmaeum* species group (**D–H**) **A** *Nanophyllium stellae* **B** *Nanophyllium miyashitai* sp. nov. **C** *Nanophyllium larsoni* **D** *Nanophyllium australianum* **E** *Nanophyllium asekiense* comb. nov. **F** *Nanophyllium rentzi* Coll SLT **G** *Nanophyllium hasenpuschi* **H** *Nanophyllium adisi* line drawing based on holotype.



**Figure 12.** Pronotum and thorax of males for the two species groups, dorsal **A** *Nanophyllium stellae* (*stellae* species group) **B** *Nanophyllium asekiense* comb. nov. (*pygmaeum* species group).

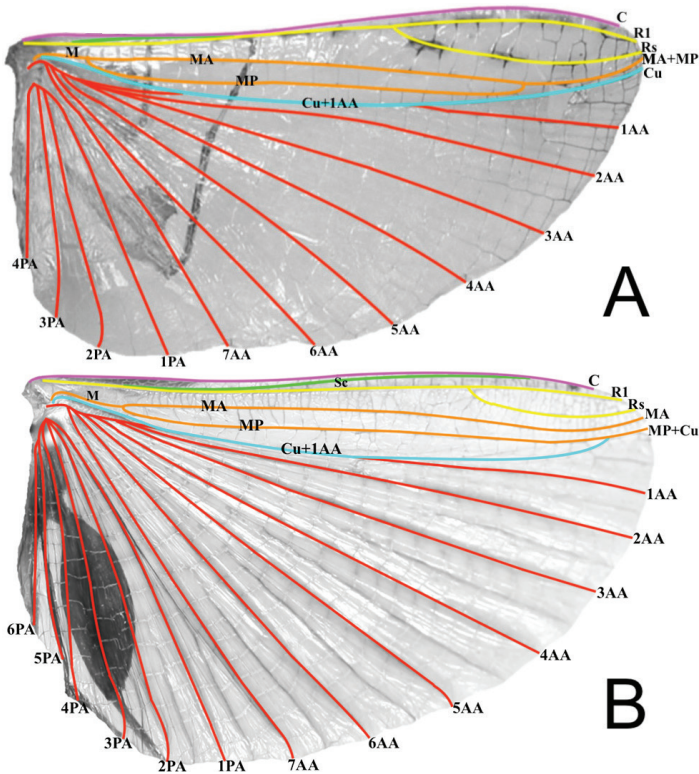


**Figure 13.** Alae wing venation of males for the two species groups, dorsal **A** *Nanophyllium rentzi* (*pygmaeum* species group) **B** *Nanophyllium stellae* (*stellae* species group). Abbreviations used: C (costa); Sc (subcosta); R (radius); R1 (radius 1); Rs (radial sector); M (media); MA (media anterior); MP (media posterior); Cu (cubitus); Cu+1AA (cubitus and first anterior anal); 1AA–7AA (first through seventh anterior anal); 1PA–6PA (first through fifth posterior anal).

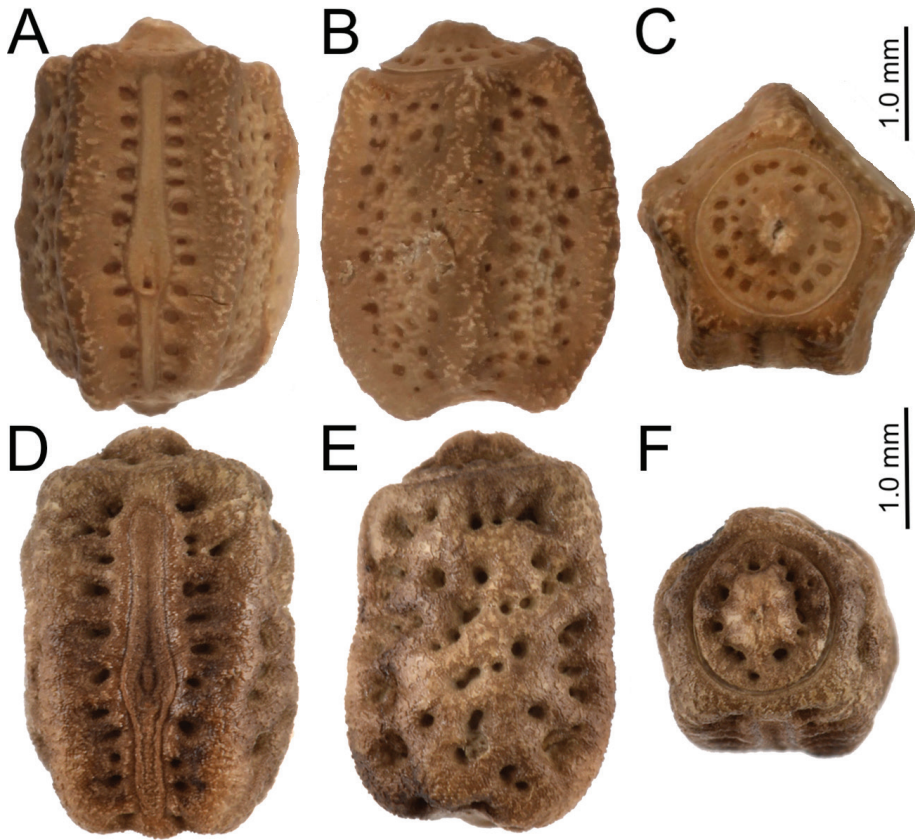


**Figure 14.** A–C *Nanophyllium asekiense* Coll RC 18-046 **A** dorsal view **B** lateral view **C** Opercular (anterior) view **D–F** egg from *Nanophyllium* sp. NHMUK 012497230 **D** dorsal view **E** lateral view **F** opercular (anterior) view.



**Figure 15.** Distribution map showing the undetermined *Nanophyllium* specimens with mappable localities.

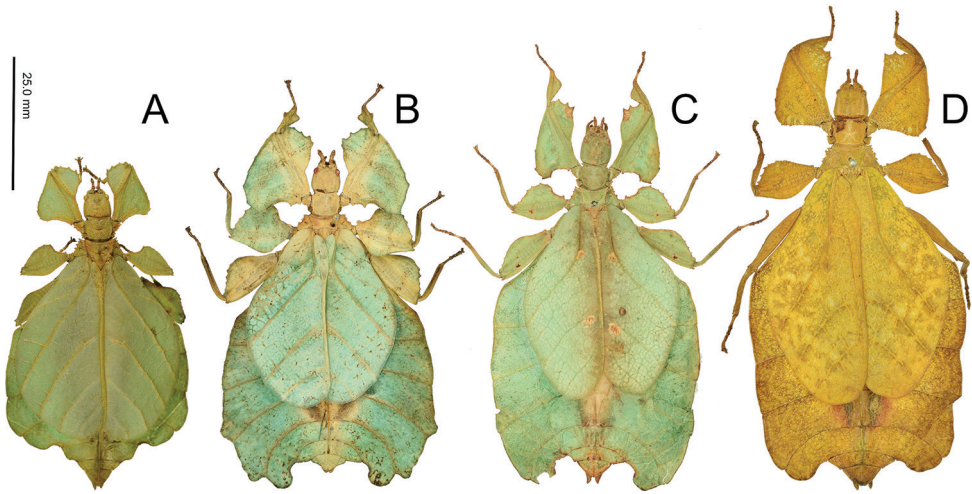


**Figure 16.** Notable known *Nanophyllium* females scaled to relative size **A** *Nanophyllium chitoniscoides* comb. nov. Coll FH **B** *Nanophyllium suzukii* comb. nov. **C** *Nanophyllium frondosum* comb. nov. **D** *Nanophyllium keyicum* comb. nov. (RMNH).

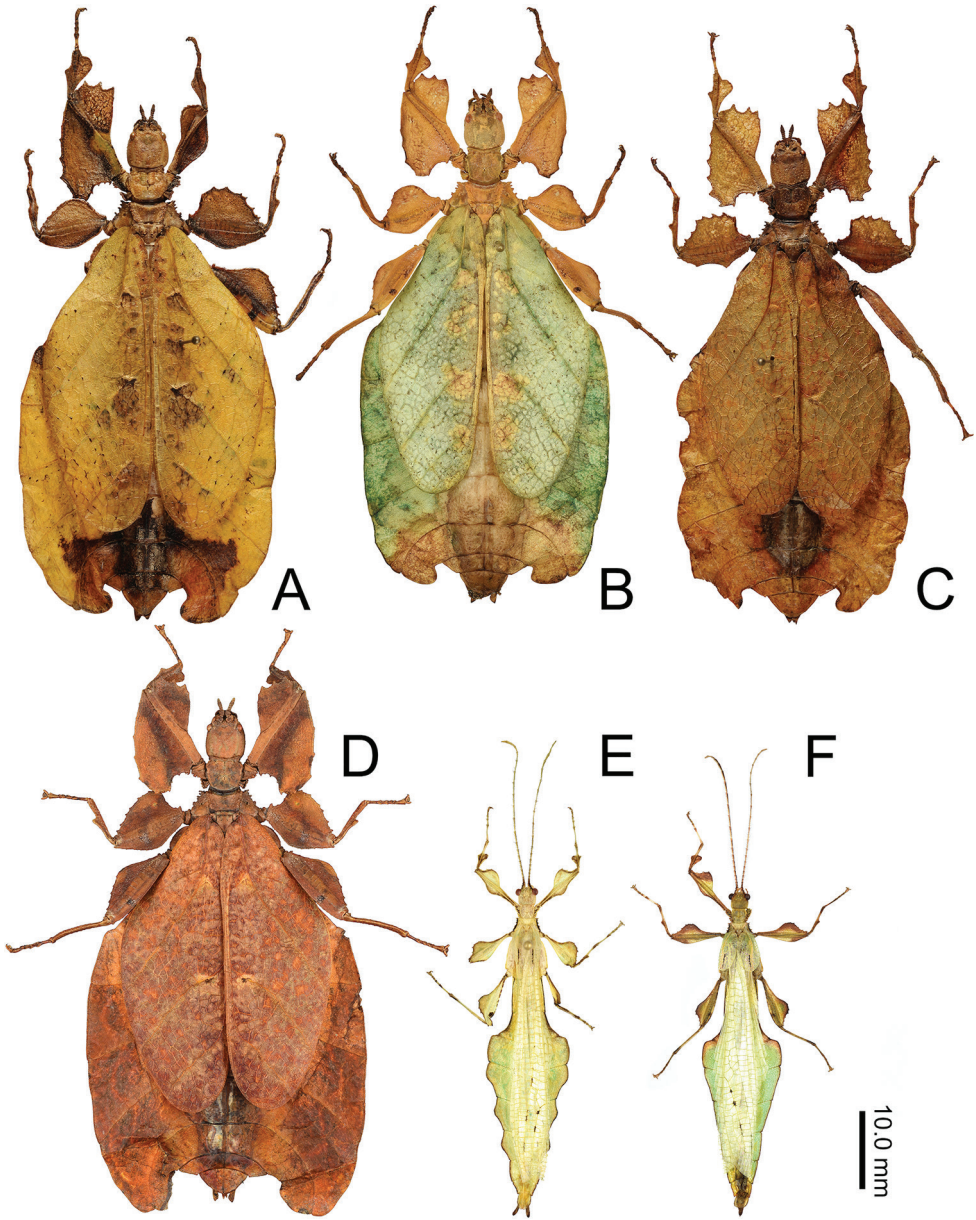
half is bare. The protibial exterior lobe is a scalene triangle only as wide as the protibial shaft. The interior lobe is also a scalene triangle and about two times as wide as the exterior lobe (Fig. 19A). Mesofemoral exterior lobe smoothly arcing the full length, with the widest portion on the distal half and only about one and a half times as wide as the mesofemoral shaft, with fine serration on the widest portion only. Mesofemoral interior lobe with the majority of the lobe on the distal half, the proximal half with only a sliver of the lobe and lacks teeth versus the wide proximal expanse (about three times as wide as the mesofemoral shaft) has four to five notable serrate teeth. Interior metafemoral lobe with the majority of the lobe on the distal half, with only a thin sliver on the proximal half. The distal half of the metafemoral lobe is two and a half times as wide as the shaft and has five to six serrated teeth. Exterior metafemoral lobe slightly thinner than the metafemoral shaft, spanning the full length, and lacking serration. Mesotibial exterior has a small roundly triangular lobe near the midline which is only about as wide as the mesotibial shaft. Metatibiae lacking exterior and interior lobes.

***Nanophyllium miyashitai* sp. nov.**

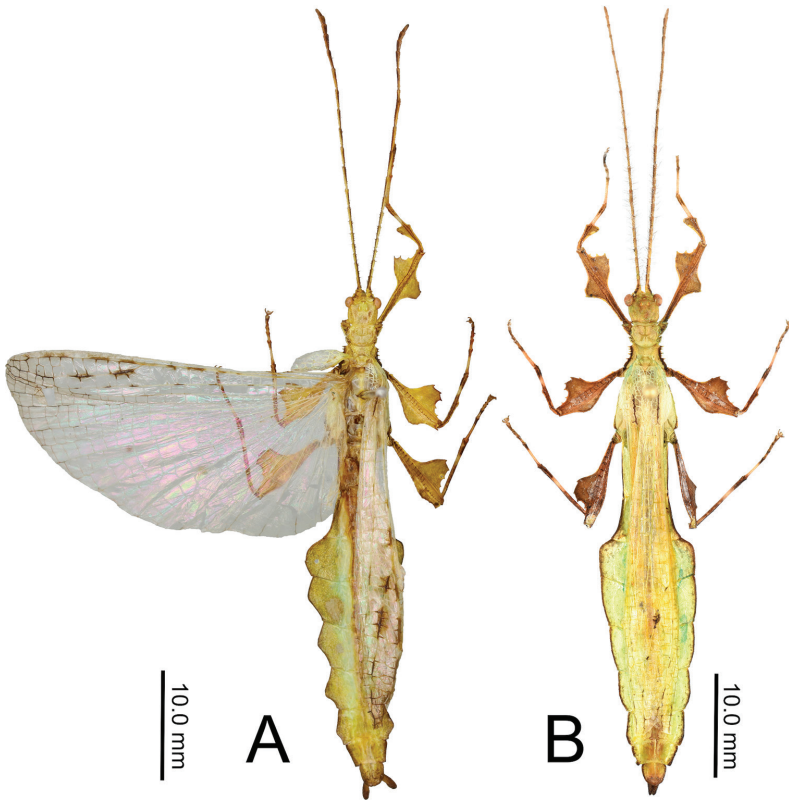
<http://zoobank.org/2C3C5029-9E78-4687-A680-BDC9645DD3CB>

Figure 20

**Type material. Holotype:** ♂, PAPUA NEW GUINEA: Morobe Province, Wau: IX, 2000. From the collection of Tetsuo Miyashita, Japan. Deposited in the Montreal Insectarium (Quebec, Canada) type collection.



**Figure 17.** *Nanophyllium asekiense* (Größer, 2002), comb. nov. males and females, all originating from Papua New Guinea, Morobe Province. Note the variation in the male abdominal shape and the female abdominal, color, and femoral lobe variability **A** yellow form female, Morobe Province, Aseki, Oiwa Village, July, 2016, Coll RC 16-268 **B** green form female, Papua New Guinea, Morobe, Aseki (Oiwa), Nov. 2000, Coll SLT **C** brown form female, Morobe Province, Aseki, Oiwa Village, July, 2016, Coll RC 16-264 **D** red/brown form female, Papua New Guinea, Morobe, Aseki (Oiwa), Nov. 2000, Coll SLT **E** serrate abdominal male bred by the Montreal Insectarium, IMQC **F** spade shaped male bred by the Montreal Insectarium, Coll RC 19-055.



**Figure 18.** *Nanophyllium rentzi* males dorsal, note the variation in abdominal shape **A** holotype in the NHMUK (copyright NHMUK 2020 online Data Portal; <https://data.nhm.ac.uk/object/b03f481f-1a1c-4ccd-8558-505668fc78f3/1591228800000>) **B** male from Fak Fak, Indonesia, Coll SLT.

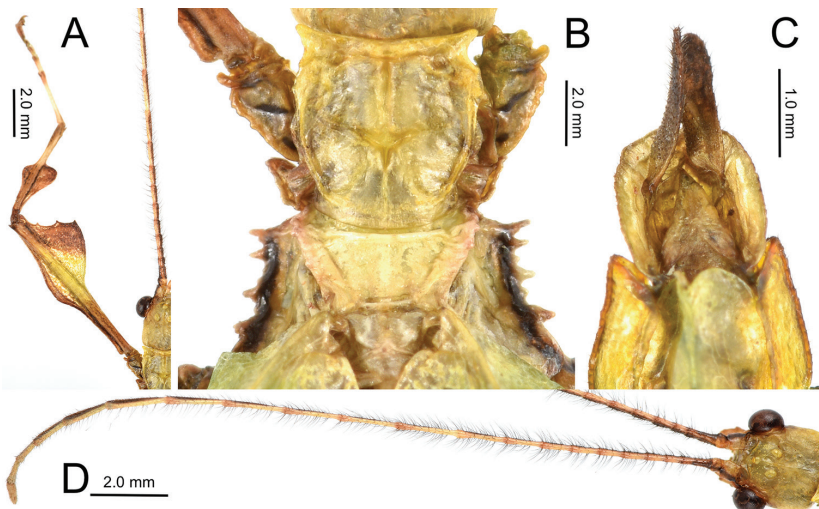


**Figure 19.** Male *Nanophyllium asekiense* (Größler, 2002), comb. nov. morphological details **A** profemoral and protibial lobes **B** dorsal thorax spination **C** ventral view of the genitalia **D** dorsal view of the head and antennae.

**Differentiation.** With the interior lobe of the profemora rounded, not angular, and the mesofemoral interior lobe broad and reaching fully end to end in a rounded triangle, this new species falls within the *stellae* species group. This is the first species from the *stellae* species group recorded from Papua New Guinea. The other two species are known from Jayapura, Irian Jaya, Indonesia (very near the border with Papua New Guinea so it is likely they also occur there but to date, we have not confirmed any specimens). This new species can be differentiated from the other two species in the *stellae* species group by the mesopleurae which have a prominent anterior tubercle followed by four additional small tubercles (only a single anterior tubercle in the other two species) and tegmina that are shorter, only about half the length of the metathorax (almost the length of the metathorax in the other two species).

Like the other members of the *Nanophyllium stellae* species group, the holotype is a male specimen and the female is unknown. It is expected that the female is larger than other known female *Nanophyllium* as the *stellae* species group members are larger than the *pygmaeum* species group members.

**Description. Male. Coloration.** Antennae dark brown, a similar brown to that found throughout the head and thorax. The majority of the dorsal aspect throughout the remainder of the body and legs is of a similar lighter brown, but not a light as the stripe of light brown running along the sagittal plane along the head and thorax. Alae and tegmina have a similar dark brown to that found on the antennae. Throughout the ventral surface the coloration is the same as that found on the legs. Granulation on the body is mostly of a lighter brown than the surface it is found on.

**Morphology. Head.** Head capsule slightly longer than wide, with a vertex that is heavily granulose, which includes the two posteromedian tubercles which are no larger than the surrounding granulation around them (Fig. 20F). Three well-developed ocelli are slightly posterior to the compound eyes which are ovular and slightly protrude from the head capsule (Fig. 20F). **Antennae.** Antennae in the holotype are both damaged and repaired so the original number of antennomeres is unknown. The antennae are longer than the outstretched forelegs and the left antennae consist of 21 antennomeres and the right of 19 (including the scapus and pedicellus). Scapus and pedicellus with short clear setae and the scapus has a notable spur on the anterior rim lateral side. All segments beyond the scapus and pedicellus covered in stiff dark setae each longer than the segment is wide until the terminal four segments where the setae begin to steadily decrease in size until the terminal segment which has dense short setae. **Thorax.** Pronotum wider than long (width to length, 1 : 0.75) with parallel lateral margins, and all margins slightly granulose. Surface of the pronotum heavily granulose like the vertex of the head capsule. Prescutum significantly wider than long (width to length, 3.3 : 1), with converging lateral margins with a granular surface of at least five nodes (Fig. 20F). Surface of prescutum slightly granular but lacking significant features. Mesopleurae gently diverging, anterior edge armed with a single tubercle, remainder of the rim with four small tubercles with a single seta protruding from the tip of each. Mesopleurae surface irregularly granular with a single distinct pit in the center. Pro-, meso-, and metasternum covered in irregularly spaced granules. **Wings.** Tegmina short, only reaching about halfway through the metathorax. Alae developed; exposed section

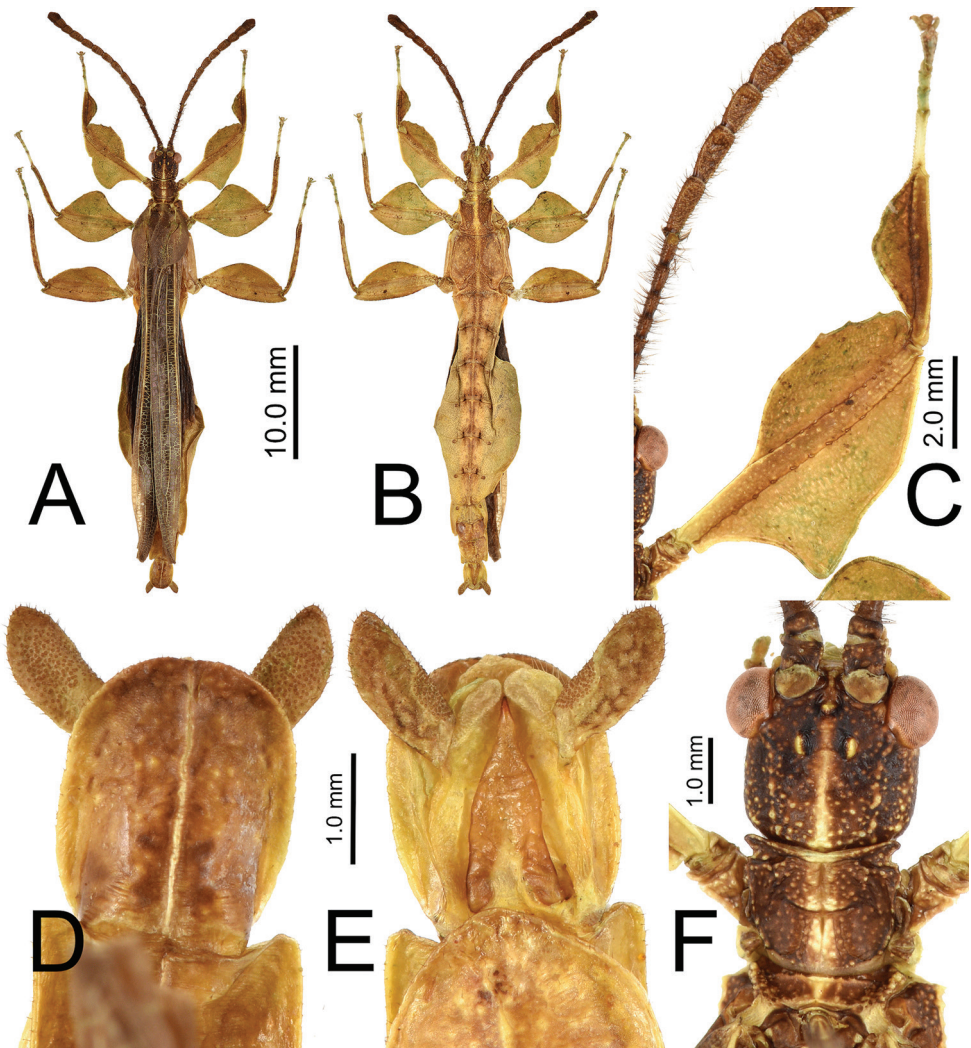


**Figure 20.** Holotype male *Nanophyllium miyashitai* sp. nov. **A** full body dorsal **B** full body ventral **C** right front leg **D** abdominal segment X and dorsal view of cerci **E** genitalia, ventral **F** head through thorax, dorsal.

of folded alae moderately sclerotized. *Abdomen.* Abdominal segments with folding in the holotype so shape description is only approximate. Abdominal segment II slightly tapering, III gradually widening, IV widening for the first quarter, then parallel, V through the first half of VI parallel, VII converging, VIII–IX parallel to subparallel. Anal abdominal segment X longer than wide with a broad rounded apex (Fig. 20D). Poculum broad, about as broad as segment IX, ending in a broad rounded apex that reaches the anterior margin of segment X (Fig. 20E). Cercus about as wide as the vomer but slightly shorter, margins marked with a row of thin tan setae and a dorsal surface that is heavily granular. Vomer long, reaching the majority of the length to the

apex, with sides gradually converging to the hooked apex (Fig. 20E). *Legs*. Profemora, interior lobe rounded with three small nubby, evenly spaced teeth (Fig. 20C). Exterior lobe wider than the interior lobe and with a slight recurve and an edge that is smooth with a row of single stout setae along the entire length. Protibiae lacking an exterior lobe, interior lobe a rounded scalene triangle spanning the entire length of the protibia (Fig. 20C). Mesofemora, exterior lobe smoothly arcing the length of the mesofemora, interior lobe smoothly triangular with five to six small nubby teeth on the distal half and about one and a half times as wide as exterior lobe. Interior and exterior lobe of metafemora smoothly arcing with interior lobe about twice as wide as the exterior lobe and the interior with a few small nubby teeth near the distal end. Meso- and metatibiae lacking exterior and interior lobes.

**Measurements of holotype [mm].** Length of body (including cerci and head, excluding antennae) 40.0, length/width of head 2.6/2.5, antennae (repaired) 16.4, pronotum 1.8, mesonotum 1.8, length of tegmina 5.9, length of alae 30.5, greatest width of abdomen 8.0, profemora 7.4, mesofemora 6.8, metafemora 7.3, protibiae 3.9, mesotibiae 5.0, metatibiae 6.7.

**Distribution.** Currently only known from the type locality of Wau, Morobe Province, Papua New Guinea (Fig. 4).

**Etymology.** Patronym. This species is dedicated to Mr. Tetsuo Miyashita (Japan). Miyashita is a major private collector who has amassed one of the largest insect collections in the world. Miyashita and the specimens from his collection have allowed the description of several new beetle taxa over the years with this being the first phasmid described from his collection.

### *Nanophyllium daphne* sp. nov.

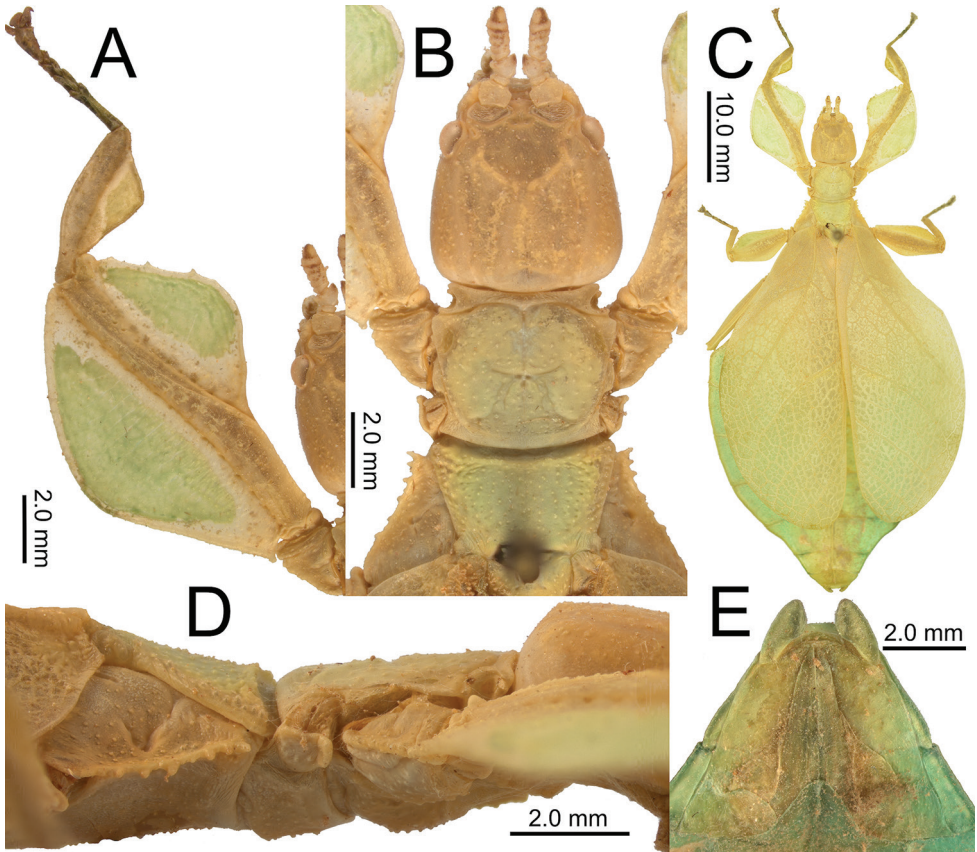
<http://zoobank.org/A5CB1FE9-AA0A-4141-A291-C20654161E50>

Figure 21

**Type material. Holotype** ♀: INDONESIA: Biak. 16/9.54; NNM-Leiden, ex collectie A. Veldhuyzen. In the collection RMNH, Leiden, Netherlands.

**Discussion and differentiation.** This small species (body length of the holotype only 54.0 mm) has several interesting morphological features which differentiate it from other known *Nanophyllium* females. The tegmina venation places this species most closely aligned to *N. chitoniscoides* due to the venation pattern having the radial bend occurring before the splitting of the first radial and the radial sector, therefore the radial sector is straight (Fig. 9A). Additionally, a radial and medial crossvein is present on the radial bend at or before the splitting of the first radial (Fig. 9A).

This new species can be differentiated from all other *Nanophyllium* by several morphological features. First, it is the only species which has exterior profemoral lobes which are obtuse (Fig. 21A), not right angles like in *N. keyicum* (Fig. 16D) or recurved acute angles like in all other known *Nanophyllium* species (for example Fig. 16C). Additionally, this is the only species known where the female has the abdomen tapering



**Figure 21.** Female holotype of *Nanophyllum daphne* sp. nov. **A** front left leg showing lobes and serration **B** antennae, head, and thorax dorsal details **C** full body dorsal **D** thorax, lateral view **E** genitalia, ventral.

towards the posterior, giving the abdomen a spade-shaped appearance (Fig. 21C), all other known species have females with abdominal segments VI and VII either parallel sided (like in *N. frondosum* and *N. keyicum*, Fig. 16C, D respectively) or as the broadest segments (like in *N. chitoniscoides* and *N. suzukii*, Fig. 16A, B, respectively).

These unique morphological features coupled with the geographic isolation from the mainland makes it unlikely that this female represents the unknown female sex of one of the many species which are only known from males from the mainland (Fig. 4). Instead, we here describe this species as *Nanophyllum daphne* sp. nov. as the first recorded Phylliidae species from Biak Island, Indonesia.

**Description. Female. Coloration.** Presently, only the dried holotype specimen is known, which is fairly well-preserved with only minimal discoloration along the mid-line due to a lack of gutting. The majority of the body is of a pale light green coloration, with the areas of discoloration (such as the head, thorax, and shafts of the legs) being a pale brown/tan in coloration. Leaf insects are more vibrantly colored in life and it can be assumed that this specimen was a brighter green in life.

**Morphology.** *Head.* Head capsule slightly longer than wide, vertex with small granulation throughout the surface and unevenly spaced in no detectable pattern (some right next to each other some with more spacing). The posteromedial tubercle is small, only slightly noticeable and split into two lobes. Frontal convexity stout, not prominently protruding, with a lumpy surface which is marked by numerous pale setae. *Antennae.* Antennae consisting of nine segments. The terminal segment has a narrower base than segment VIII, instead with a width only about as wide as segments IV or V, and it is about as long as the previous two segments combined length. All segments have setae present; segments I through III have sparse but long pale setae; segments IV through VIII have sparse, stout, tan setae; and the terminal segment IX has dense, stout, dark setae. Compound eyes slender and tightly formed to the head, only reaching across one quarter of the head capsule length. Ocelli absent. Antennal fields approximately the same dimensions as the compound eyes, wider than the base of the first antennomere, and not protruding back farther than the frontal suture. *Thorax.* Pronotum with anterior margin that is slightly concave and lateral margins that are straight that slightly converge to a broad, slightly convex posterior margin that is about the same width as the anterior rim (Fig. 21B). The pronotum surface has moderate granulation throughout that is evenly spaced, and the pronotum surface has a moderate pit in the center and furrows along the sagittal and lateral planes (Fig. 21B). Pronotum lacks prominent rims, with only the anterior rim moderately formed and with a rough texture (but no features as prominent as actual granulation present). Pro-, meso-, and metasternum with granulation throughout, with all granules evenly spaced and of even size. Prescutum wider than long, with an anterior margin 1.3 times wider than the posterior margin (Fig. 21B). Prescutum lateral rims and surface of the prescutum with granulation throughout, but no prominent spination. No prescutum crest present, the surface is only slightly raised so it is not perfectly flat, but it is not prominent. Prescutum anterior rim slightly raised in the center but not prominent, and lacks a sagittal spine, instead there is only weak granulation throughout the rim which is similar to the granulation found on the prescutum surface. Mesopleurae start near the anterior margin but not flush with it, instead they begin notably wider than the prescutum anterior margin. Mesopleurae are nearly straight and diverge evenly along their length (Fig. 21B). Mesopleurae margins on their anterior margin are marked by a prominent tubercle immediately adjacent to two more which are medium sized and followed by three small tubercles that are nearly evenly spaced throughout the remainder of the length of the mesopleurae with slight granulation interspersed (Fig. 21B). Face of the mesopleurae has a granular surface similar to the texture of the prescutum disk and marked with a distinct pit near the middle of the surface. *Wings.* Tegmina long, reaching past the anterior margin of abdominal segment VIII. The subcosta (Sc) is the first vein in the forewing and arcs smoothly unbranched towards the wing margin. The radius (R) gently bends towards the wing margin almost immediately and along this bend (first on the medial side) there is a notable radius to media crossvein (R-M), then following this first branching, the radius branches (on the distal side) into the first radius (R1) which runs unbranched to the wing margin, and the remainder

of the radius as the radial sector (Rs) runs unbent to the wing margin, terminating slightly past the wings mid-length. The media (M) runs nearly parallel with the cubitus along the wing margin (there is a slightly wider than side by side gap near the anterior, but the veins are almost touching throughout a majority of their length). The media anterior (MA) diverges near the wing mid-length and arcs smoothly towards the wing margin where it terminates approximately three-quarters of the way through the length of the wing; this is followed by a splitting of the media posterior (MP) which runs parallel with the media anterior as it smoothly arcs towards the wing posterior margin. Following the media posterior split there is a small media to cubitus crossvein (M-Cu) which runs briefly parallel side by side with and then fuses to the cubitus. The cubitus (Cu) is bifurcate, branching into the cubitus anterior (CuA) and cubitus posterior (CuP) which diverge evenly, and both terminate at or near the wing posterior apex. The first anal vein (1A) is simple and fuses with the cubitus near the wing anterior margin. *Alae rudimentary.* *Abdomen.* Abdominal segments II through the anterior one third of IV uniformly diverging, posterior two thirds of IV through the anterior half of V parallel, the remainder of the abdominal segments are roundly converging to the broad rounded apex giving the abdomen an overall rounded appearance. *Genitalia.* Subgenital plate short and rounded, starting at the anterior margin of segment VIII and extending only about halfway onto segment IX, with straight, uniformly converging margins. Subgenital plate is only about a third the length of the gonapophyses, leaving a significant amount of the gonapophyses exposed. Gonapophyses are long and slender, not quite reaching the apex of the terminal abdominal segment (Fig. 21E). Cerci broad and slightly cupped, with a surface throughout that is rough in texture, and margins with only a few short setae, none prominent. *Legs.* Profemoral exterior lobe broad with a rounded obtuse angle, and slightly wider than the interior lobe. Edge of the profemoral exterior lobe without notable teeth but with a margin that is granular throughout the length (Fig. 21A). Profemoral interior lobe narrower than the exterior and shaped as a slightly obtuse angle marked with four small teeth (Fig. 21A). The proximal most tooth is very small, not much more than a bump along the margin, this is followed by a narrow gap, the first prominent tooth, then a larger gap twice as wide as the first, another prominent tooth the same size as the previous, a gap the same size as the first small gap, and then one more prominent tooth at the distal end which is about the same size as the previous two teeth. The gaps between teeth are not deep and looping, instead they are straight and shallow between each tooth (Fig. 21A). Mesofemoral exterior lobe arcs smoothly from end to end and lacks dentition. The interior and exterior mesofemoral lobes are of a similar width. Mesofemoral interior lobe arcs end to end with three serrate teeth only on the distal quarter of the lobe, which is slightly wider than the proximal portion of the lobe. Metafemoral interior lobe arcs end to end with the distal end wider than the proximal, and seven to eight irregularly shaped teeth on the distal third of the lobe only. Metafemoral exterior lobe is thin, smooth, and hugs the metafemoral shaft without teeth. Protibiae lacking an exterior lobe. Protibiae interior lobe spans the entire length of the protibiae and is not particularly wide, only about the same width as the protibial shaft itself. The lobe is smoothly

triangular and is slightly wider towards the distal half. Mesotibiae and metatibiae lacking exterior and interior lobes.

**Measurements of holotype [mm].** Length of body (including cerci and head, excluding antennae) 54.0, length/width of head 5.7/5.1, antennae 2.9, pronotum 4.0, mesonotum 2.7, length of tegmina 36.0, greatest width of abdomen 28.0, profemora 10.0, mesofemora 8.3, metafemora 9.9, protibiae 5.7, mesotibiae 6.4, metatibiae 8.2.

**Etymology.** Noun. Named for the nymph Daphne of Greek mythology who was pursued tirelessly by the god Apollo and was eventually after pleading with her father for a way to escape the relentlessness of Apollo, was turned into a laurel tree. Derived from Greek, Δάφνη.

**Distribution.** Currently only known from Biak Island, Papua Province, Indonesia.

### **Possible unconfirmed sexes of known *Nanophyllium* species/ notable specimens which cannot be identified to species**

#### ***Nanophyllium* species (male)**

Figure 22A

**Collection data.** One male, observed and collected by Mike Wild (USA/Indonesia) in 2015. **INDONESIA:** Papua Province, Puncak Jaya Regency, Mokndoma, around 2,180 meters elevation.

**Discussion.** This individual was observed and photographed by Mike Wild, who notes that despite living in the area for more than 14 years, and actively observing and collecting insects there the entire time, this is the only leaf insect he has ever seen. This species has highly reduced exterior profemoral lobes, which places it morphologically most similar to *N. australianum* (Fig. 11D) from Australia. This particular feature is not observed in other New Guinea known males to such a slender degree. This unknown species can be differentiated from *N. australianum* by the orange head, pronotum, and mesonotum (Fig. 22A) a unique feature in and of itself as all other known *Nanophyllium* males have the head and thorax the same color as the rest of the body. It is possible that this male may represent the unknown sex of one of the known female *Nanophyllium* or represent an undescribed species, but at this time it cannot be determined with so many species only known from a single sex.

Originally proposed by Rentz (1988) we agree that these darker and slightly metallic *Nanophyllium* males appear to not mimic foliage, but to instead be mimicking a wasp. Easily observed in this individual from Mokndoma and noted by Rentz (1988) the dark coloration is “shining black with a bluish overcast”. This coloration is common within Scoliidae and Pompilidae, both of which are large and intimidating wasps within the correct size range of a *Nanophyllium* male. Additionally, this particular specimen from Mokndoma has a bright orange head, pronotum, and mesonotum, and many species of these large wasps also have yellow, orange, or red segments of their bodies. We hope that examination of wasp species from this region and additional *Nanophyllium* males will help to identify possible species models.



**Figure 22.** Live observations of unidentifiable male *Nanophyllum* **A** individual observed by Mike Wild in Mokndoma, Indonesia **B** individual observed by Achmad Rian Dietra, May, 2017 on Aiduma Island, Indonesia.

*Nanophyllum* species (male)

Figure 22B

**Observational collection data.** One male, observed by Achmad Rian Dietra (Indonesia) in May of 2017. **INDONESIA:** West Papua Province, Kaimana Regency, Aiduma Island.

**Discussion.** This is only known from photographs of a live individual taken by Achmad Rian Dietra (Indonesia). Based on pro- and mesofemoral lobes being strongly angular and not smoothly arcing from end to end, this individual belongs to the *pygmaeum* species group. This species group only has males known for six species: *N. pygmaeum* Redtenbacher, 1906, *N. asekiense* (Größer, 2002), comb. nov., *N. adisi* Zompro & Größer, 2003, *N. rentzi* Brock & Größer, 2008, *N. hasenpuschi* Brock & Größer, 2008, and *N. australianum* Cumming, Le Tirant & Teemsma, 2018.

Based on the profemoral exterior lobe that is wider than the shaft width and not larger than the interior lobe, that rules out *N. australianum* (exterior lobe of profemora same width as shaft width; Fig. 11D) and *N. adisi* (exterior lobe of profemora larger than interior lobe; Fig. 11H). *Nanophyllum rentzi* (Fig. 18) and *N. asekiense* (Größer, 2002), comb. nov. (Fig. 17E, F), can also be ruled out as possible identifications, as their entire body coloration is green and the alae are completely transparent, in contrast this specimen from Aiduma Island has a brown body and dark tegmina and alae. The two remaining identification possibilities are *N. pygmaeum* and *N. hasenpuschi* which can easily be morphologically separated by the coloration of the alae, solid brown in *N. pygmaeum* or alae with a large transparent patch in *N. hasenpuschi*. Unfortunately, this individual has its wings closed so the interior color is impossible to see. A definitive identification is unfortunately not possible at this time. Geographically this individual is located near collection sites of both *N. hasenpuschi* and *N. pygmaeum* so no inference can be drawn from locality (Fig. 4). This is however a unique opportunity to share photos of a live individual and to add a new distribution checkpoint to the map of *Nanophyllum* collection/observation localities (Fig. 15). It is also possible that this individual represents an undescribed species on its own, or the male for an undescribed species based on one of the below females illustrated.

### **Presumed records for female *Nanophyllum australianum* Cumming, Le Tirant, & Teemsma, 2018**

*Nanophyllum australianum* specimens are exceedingly rare (likely due to a lack of extensive collecting in the area they are found in), with only four collections/observations known to the authors to date and all known from in/near Iron Range National Park of Northern Queensland, Australia (Fig. 4).

The first known record is a subadult female discovered by G. B. Monteith in June 1971 while he was collecting along the edge of the rainforest of Iron Range. Monteith recognized this individual as a second species for Australia and likened the species to a specimen from Popondetta, Papua New Guinea (Fig. 23A; Monteith 1971). This species was again referenced in Key (1974) but this time as “*P. frondosum*” based on the subadult nymph collected by Monteith (Monteith 1978).

The second collection record we are aware of is an early instar nymph collected by G. B. Monteith in February 1976, near Gordon’s Mine Area, Iron Range (see Cumming et al. 2018: fig. 2 for an image of this nymph, note the shape of the femoral lobes which are angled with distinct teeth like which can be seen in the adults).

The third record was the holotype male which was collected as a nymph by D. C. F. Rentz near Mt. Tozer within the Iron Range in December 1986 and which matured to adult in January 1987 (see Rentz (1988) for notes and photographs of the nymph when it was caught, and see Cumming et al. (2018) for images of the resulting adult and species description).

The only other individual we are aware of is a subadult female which was photographed by Chien C. Lee in July 2014 in Lockhart, Queensland (Fig. 23B, C). This female matches the morphology of the first nymph which was collected as a subadult by Monteith in 1971, and with it observed near the same general collecting locality as the holotype male *N. australianum*, coupled with the similarity in femoral shapes to the male, we expect these females represent the female *Nanophyllium australianum*. The authors hope that future collection efforts in the Iron Range area will yield additional specimens so we can better review the intraspecific variation of this rarely collected species and allow the morphological description of the female adult morphology.

### Unidentified *Nanophyllium* species (females) (listed from the smallest to the largest specimens)

***Nanophyllium* sp. Female NYMPH (35 mm):** PAPUA NEW GUINEA: Eastern Highlands District LJBass, Coll. Sixth Archbold Exped. To Papua New Guinea. No.7, Kotuni, south slopes Mt. Otto, 2200m. Aug. 4–20, 1959. (AMNH). (Fig. 24A).

This subadult could be *N. aseekiense* or *N. frondosum* based on the geographic proximity to *N. aseekiense* and *N. frondosum* known localities and how large it might be if it had reached adulthood. It is likely too large to have been one of the smaller species like *N. pygmaeum*.

***Nanophyllium* sp. Female (46.7 mm):** PAPUA NEW GUINEA: Central Province, Along Hiritano Highway, East of Vanapa River crossing. June 21<sup>st</sup>, 1989. Collected by L. M. Munsey, previously from the collection of Jerri Larsson (California), (Coll RC 16-224). (Fig. 24B).

**Habitat.** From the notes of L. M. Munsey the collector of the two specimens: “Daytime beating in a 1 to 3 acre area of cuttings with few small and large downed trees remaining”.

***Nanophyllium* sp. Female (54.0 mm):** PAPUA NEW GUINEA: Central Province, 20Km SE Port Moresby “bushes” 26.i.1985 J.W.Ismay. Ex Papua New Guinea DPI-CRIC Konedobu. C.I.E. COLL. A. 17440. NHMUK 012497230. (Fig. 24C).

***Nanophyllium* sp. Female (59.6 mm):** PAPUA NEW GUINEA: Daru, Papua (New Guinea) Mouth of Fly R. VII-1941. Collector RG Wind. Van Dyke Collection. (CAS). (Fig. 24D).

These three small adult females possibly represent the unknown female for *Nanophyllium pygmaeum* as they are the correct size and geographically are from southern Papua New Guinea, with the female from CAS from nearby the Fly River, which is the *N. pygmaeum* type locality.

***Nanophyllium* sp. Female (70.5 mm):** INDONESIA: New Guinea: West Irian, Kobakma, North Slope of Central Range N. of Baliem Valley 3500' October 1971,

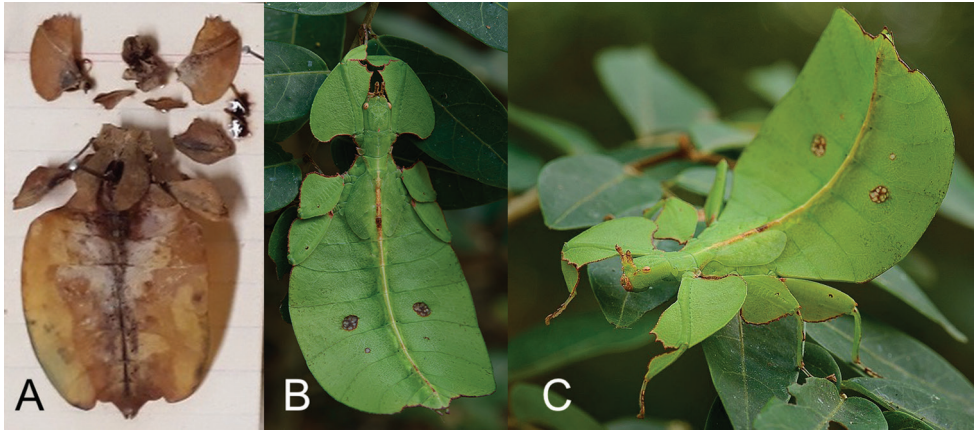


**Figure 23.** Likely *N. australianum* subadult females **A** preserved specimen which was collected by G. B. Monteith in June 1971 on the edge of Iron Range, Queensland (photograph by Susan Wright, collections manager, Queensland Museum) **B** dorsal, live individual photographed by Chien C. Lee (Malaysia) in July 2014; Lockhart, Queensland **C** same individual as in B but viewed from the lateral aspect.

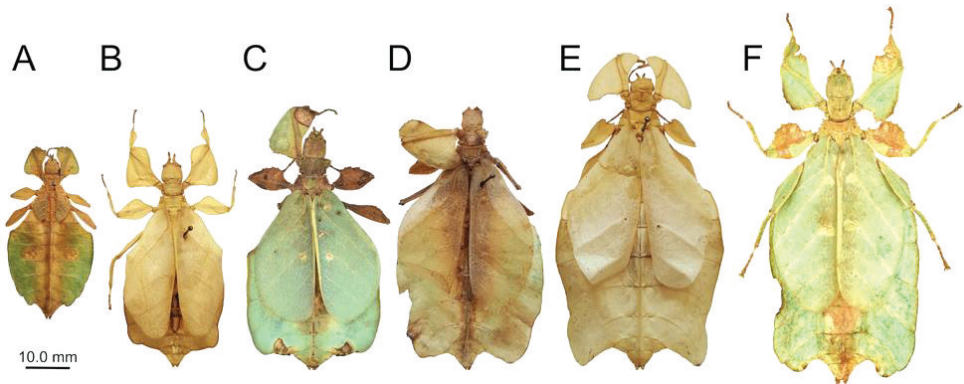


**Figure 24.** *Nanophyllium* females and their collection data which likely represent the unknown female *Nanophyllium rentzi*, *Nanophyllium hasenpuschi*, *Nanophyllium pygmaeum*, *Nanophyllium adisi*, or possibly undescribed species, scaled to relative size **A** Eastern Highlands District LJB Brass, Coll., Sixth Archbold Exped. To Papua New Guinea, No. 7, Kotuni, south slopes Mt. Otto, 2200m. Aug.4–20.1959, AMNH **B** Papua New Guinea, Central Province, Along Hiritano HWY., E. of Vanama River Crossing: June 1989, Coll RC 16-224 **C** Papua New Guinea, Central, 20 km SE Port Moresby, I.1985, NHMUK 012497230 **D** Daru, Papua (New Guinea) Mouth of Fly R., VII-1941, Collector RG Wind, CAS **E** New Guinea, West Irian, Kobakma, North Slope of Central Range N. of Baliem Valley 3500' October 1971, Robert Mitton Coll, CAS **F** Indonesia, West Papua, Mapia, May 1999, Coll SLT.

Robert Mitton, Coll., Presented by H. Vannoy Davis, C.A.S. Accession. (CAS). (Fig. 24E).

Based on the size and morphology this female from Kobakma is similar to *N. frondosum* females which are known from other distant localities in Papua New Guinea. Unfortunately, the holotype *N. frondosum* has no other locality information other than

“Neu-Guinea” (Redtenbacher, 1906) and therefore we cannot determine if *N. frondosum* is a wide-ranging species or if there is a complex of *N. frondosum*-like species. Hopefully future molecular comparison of freshly collected material can reveal the extent of *N. frondosum*.

An additional possibility is that this female could be the opposite sex of *Nanophyllium adisi*, which is known from nearby this collection location from “Hoofdbivak, 250 m Datum IX” from the Stirling Expedition of 1926 (present day Indonesia: Papua Province, Nduga Regency). This possibility is in our opinion unlikely as these localities are separated by the expansive Maoke Mountains which are most likely a geographic barrier between these populations.

***Nanophyllium* sp. Female (75.0 mm):** INDONESIA, West Papua, Mapia, V.1999 (Coll SLT) (Fig. 24F).

This female is from very near the type locality of *N. hasenpuschi* and could possibly represent the unknown female. Hopefully the holotype *N. hasenpuschi* can be sequenced one day to be compared and possibly matched with this female. Morphologically this female is similar to *N. aseekiense* as it has slight exterior tibial lobes and similar prominent serration of the femoral lobes.

## Biogeography

Figures 4, 15

Phylliidae arose according to Bradler et al. (2015) in the Eocene approximately 55–65 mya ago. However, other phylogenetic approaches (Goldberg et al. 2015; Büscher et al. 2018a, b; Robertson et al. 2018) discuss monophyletic Phylliidae in various different relationships to other groups, which would suggest a later origin of the lineage. The early radiation of the extant *Phyllium* and *Chitoniscus* species is dated ~30–35 mya ago (Bradler et al. 2015; Robertson et al. 2018). The report of the fossil *Eophyllium messeleense* Wedmann, Bradler & Rust, 2007 gives further indication that Phylliidae arose more than 47 mya ago and estimates the splitting of *Nanophyllium* from the remaining Phylliidae ~ 20 mya ago (Wedmann et al. 2007). Assuming an approximate splitting of *Nanophyllium* 20–35 mya from the remaining Phylliidae some conclusions on the biogeographical history of *Nanophyllium* can be drawn. Ancestors of *Nanophyllium* probably settled New Guinea close to that timeframe, after New Guinea emerged in the Eocene (~ 40 mya) and was separated from Australia during the Oligocene (~25 mya) after the New Guinea Passive Margin collided with the leading edge of the Eastern Philippines-Halmahera-New Guinea Arc System (Hall 2001). As extant phylliids inhabit most parts of the Oriental and Australian region, but *Nanophyllium*, so far known, is restricted to New Guinea, including the surrounding islands, and Australia (Fig. 4), this lineage probably evolved on New Guinea and later migrated to northern Australia. *Nanophyllium* likely diversified on New Guinea due to geographic isolation by the Central Cordillera (Chisholm 1911) and the Foja Mountain Ranges in the north (Richards et al. 2009; Oliver et al. 2011). During the Pleistocene (2.6 mya–

11.7 ka) Australia and New Guinea were interconnected many times, due to climatic oscillation resulting in sea level fluctuations (Pillans et al. 1998), but the remaining parts of Indonesia remained separated from New Guinea (Ludt and Rocha 2015). The southernmost population of *Nanophyllum* possibly distributed to Australia and became separated, resulting in the speciation of *N. pygmaeum* and *N. australianum* after the Last Glacial Maximum ~ 17–19 ka ago (Ludt and Rocha 2015). The distributional records of the known *Nanophyllum* specimens suggest a well-established isolation of the distributions of *N. miyashitai* sp. nov. from other *Nanophyllum* by the Central Cordillera. As this formation arose quite early (probably during the Oligocene (Hall 2001), this population potentially has been isolated for a comparatively long time, that likely led to allopatric speciation. Likewise, most of the other *Nanophyllum* species are probably a result of allopatric isolation caused by this mountain range. *Nanophyllum keyicum* and *N. daphne* sp. nov. in contrast, are probably a result of the isolation on the islands they are found, which became separated from mainland New Guinea.

**Key to known *Nanophyllum* males\***

- 1 Profemoral interior lobes which are rounded without a sharp angle; mesofemoral interior lobes which are a large rounded triangle, reaching from end to end without prominent spination; (alae) the media anterior and the media posterior do not fuse, instead they both run to the wing margin, and the cubitus after splitting from the first anterior anal fuses with the media posterior near the wing margin and then they run fused to the margin as one; (*stellae* species group) ..... **1**
- Profemoral interior lobe angular; mesofemoral interior lobes which do not reach from end to end of the shaft and have distinct serrate teeth; (alae) the media posterior fuses back to the media anterior before reaching the wing margin, and then the fused media runs on its own to the wing margin without fusing with the radial sector; (*pygmaeum* species group) ..... **4**
- 2 Mesopleurae with a single anterior tubercle, remainder lacking tubercles; tegmina longer (almost the length of the metathorax) ..... **3**
- Mesopleurae with a prominent anterior tubercle followed by four additional small tubercles; tegmina shorter (only about half the length of the metathorax) ..... ***N. miyashitai* sp. nov.**
- 3 Exterior profemoral lobe smoothly rounded with an obtuse angle; abdominal segments with smooth edges creating a clean, spade-shaped abdomen ..... ***N. stellae***
- Exterior profemoral lobe slightly recurved creating an overall acute angle; abdominal segment V with two large clear spots; segments V–VII each with margins that extend and then contract creating a scalloped edge ..... ***N. larssoni***

---

\* Adapted from Cumming et al. 2018.

- 4 Alae completely transparent, not fully brown in color or with a brown band along the margin; tegmina transparent..... **5**
- Alae color either completely brown or with a transparent center and brown margin; tegmina completely brown..... **6**
- 5 Profemoral interior lobe notably larger than the exterior lobe .. *N. aseekiense*
- Profemoral interior lobe equal width to the exterior lobe .....*N. rentzi*
- 6 Exterior profemoral lobe distinct, wider than the width of the profemoral shaft.....**7**
- Exterior lobe of profemora greatly reduced, not wider than the width of the profemoral shaft..... *N. australianum*
- 7 Exterior profemoral lobe notably tapered on the distal and proximal ends; the interior profemoral lobe can be of the same size as the exterior lobe or larger than the exterior lobe..... **8**
- Exterior profemoral lobe only notably tapered on the proximal end, with the distal nearly reaching the end of the profemoral shaft; profemoral interior lobe always smaller than the exterior lobe ..... *N. adisi*
- 8 Alae almost completely brown, or completely brown in color .*N. pygmaeum*
- Only the alae margin and sclerotized section brown, interior half of the alae transparent.....*N. hasenpuschi*

Key to known Nanophyllium females

- 1 Small species (~ 56.0 mm or less); (tegmina) the radial bend occurs before the splitting of the first radial and the radial sector, therefore the radial sector is straight; the radius and medial crossvein is present on the radial bend at or before the splitting of the first radial ..... **2**
- Larger species (> 56.0 mm); (tegmina) the bend in the radial vein happens on the radial sector after the splitting of the first radial from the radius; the radius and medial crossvein occurs after the splitting of the first radial, instead originating on the radial sector..... **3**
- 2 Profemoral exterior lobe broad, with a slight recurve, giving the exterior angle an acute or right angle; mesofemoral interior lobe with the widest portion on the proximal half..... *N. chitoniscoides* **comb. nov.**
- Profemoral exterior lobe narrow, smoothly arcing from end to end with the exterior angle distinctly obtuse; mesofemoral interior lobe with the widest portion on the distal half .....*N. daphne* **sp. nov.**
- 3 (Tegmina) there is a wide gap between the media and cubitus veins which persists throughout their entire length, this gap is several times wider than a single vein width; profemoral exterior lobe proximal margin is straight, not recurved..... *N. keyicum* **comb. nov.**
- (Tegmina) the media and cubitus veins run side by side throughout the entire length either touching or no farther than a single vein width apart; profemoral exterior lobe proximal margin is recurved, not straight..... **4**

- 4 Prescutum width more than two times the length; mesofemoral exterior lobe broad, notably wider than the mesofemoral shaft..... *N. suzukii* **comb. nov.**
- Prescutum width less than two times the length; mesofemoral exterior lobe as wide as or thinner than the mesofemoral shaft ..... **5**
- 5 No protibial exterior lobes and no mesotibial exterior lobes, exteriors simple ..... *N. frondosum* **comb. nov.**
- Distinct protibial exterior lobes and mesotibial exterior lobes, present as small spurs ..... *N. asekiense* **comb. nov.**

## Conclusions

Review of a wide number of institution and private collections as well as the successful rearing by the Montreal Insectarium has revealed the identity of a previously unconfirmed female *Nanophyllum*. This has allowed us to synonymize the *frondosum* species group (only known from females) with the *Nanophyllum* (only known from males) into a single genus.

Unfortunately, due to the striking sexual dimorphism in *Nanophyllum*, this leaves many females and males with unknown opposite sexes and the possibility that some of the presently described species of either group might simply be the opposite sex of an already known species. Hopefully future collections of fresh material from throughout the region will either allow successful rearing of species to elucidate the unknown sex or allow pairing of sexes on a molecular basis. Additionally, we eagerly await extensive molecular analysis for the Phylliidae as a whole to elucidate the higher taxonomy within the family and the placement of the *Nanophyllum*.

## Acknowledgments

Mr. Tetsuo Miyashita who recognized the importance of describing this new *Nanophyllum* species from his personal collection. Alexandre Banko for his collaboration and transportation of the holotype *Nanophyllum miyashitai* specimen. René Limoges, entomological technician at the Montreal Insectarium for taking many of the photos for this work, as well as for many professional courtesies. Paul Harrison, Mario Bonneau, Thierry Boislard, Thomas Théry, Jennifer De Almeida, and Dominic Ouellette, entomological technicians at the Montreal Insectarium for caring for the live Phylliidae cultures and for taking photos of the live *Nanophyllum*. Lorraine Bluteau, horticulturist at the Montreal Insectarium for growing the host plants for the breeding laboratory for many years. Maxim Larrivée (director of the Montreal Insectarium) and Michel Saint-Germain (head of research and entomological collections at the Montreal Insectarium) for their support to “Team Phyllies”. Stephan Blanke and Mandy Schröter at the Senckenberg German Entomological Institute Müncheberg (SDEI) for supplying photos of the holotype female *Phyllum suzukii*. Achmad Rian Dietra (Indonesia) for allowing us to use his photograph

of a live *Nanophyllium* male he observed on Aiduma Island. Mike Wild (USA/Indonesia) for allowing us to use his photo of a live *Nanophyllium* male he found in Mokndoma. Jim Berrian (SDNHM) for assistance with the museum's camera equipment and much support over the years. Judith Marshall and Benjamin Price (NHMUK) for processing the loan of the Phylliidae specimens despite the lack of an Orthopteroid collection curator. Paul Brock for reading the first working draft and offering suggestions. Jason Weintraub (ANSP) for searching the collection for relevant specimens for this study and for information about the "Third South New Guinea Expedition". Susan Wright, collection manager at the Queensland Museum for photos of their collection. Yvonne van Dam (RMNH) for preparing photographs of type material of *Nanophyllium daphne* sp. nov. and *Phyllium insulanicum* (newly accepted name: *Nanophyllium keyicum*). Chien C. Lee (Malaysia) for sharing images of a wild female *Nanophyllium australianum*. Thank you to our peer reviewers for valuable feedback on this article.

## References

- Bradler S, Cliquennois N, Buckley TR (2015) Single origin of Mascarene stick insects: ancient radiation on sunken islands? *BMC Evolutionary Biology* 15: 1–196. <https://doi.org/10.1186/s12862-015-0478-y>
- Brock PD (1999) *The Amazing World of Stick and Leaf-Insects*. The Amateur Entomologists' Society, Orpington, Kent, England. *The Amateur Entomologist* 26: 1–165.
- Brock PD, Hasenpusch J (2003) Studies on the leaf insects (Phasmida: Phylliidae) of Australia. *Journal of Orthoptera Research* 11: 199–205. [https://doi.org/10.1665/1082-6467\(2002\)011\[0199:SOTLIP\]2.0.CO;2](https://doi.org/10.1665/1082-6467(2002)011[0199:SOTLIP]2.0.CO;2)
- Brock PD, Büscher TH, Baker E (2020) Phasmida SF: Phasmida Species File Version 5.0/5.0. In: Roskov Y (Eds) *Species 2000 & ITIS Catalogue of Life*. Species 2000: Naturalis, Leiden. <https://www.catalogueoflife.org/col>
- Buckley TR, Attanayake D, Bradler S (2009) Extreme convergence in stick insect evolution: phylogenetic placement of the Lord Howe Island tree lobster. *Proceedings of the Royal Society B* 276: 1055–1062. <https://doi.org/10.1098/rspb.2008.1552>
- Büscher TH, Buckley TR, Grohmann C, Gorb SN, Bradler S (2018a) The evolution of tarsal adhesive microstructures in stick and leaf insects (Phasmatodea). *Frontiers in Ecology and Evolution* 6: 1–11. <https://doi.org/10.3389/fevo.2018.00069>
- Büscher TH, Kryuchkov M, Katanaev VL, Gorb SN (2018b) Versatility of Turing patterns potentiate rapid evolution in the attachment microstructures of stick and leaf insects (Phasmatodea). *Journal of the Royal Society Interface* 15: 1–7. <https://doi.org/10.1098/rsif.2018.0281>
- Chisholm H (1911) New Guinea. In: Chisholm H (Ed.) *Encyclopædia Britannica* 19 (11<sup>th</sup> edn.). Cambridge University Press, Cambridge, 486–490.
- Clark JT (1978) The eggs of leaf insects (Insecta: Phasmida). *Zoological Journal of the Linnean Society* 63: 249–258. <https://doi.org/10.1111/j.1096-3642.1978.tb02562.x>

- Cumming RT, Leong JV, Lohman DJ (2017) Leaf insects from Luzon, Philippines, with descriptions of four new species, the new genus *Pseudomicrophyllium*, and redescription of *Phyllium* (*Phyllium*) *geryon* Gray, 1843, (Phasmida: Phylliidae). *Zootaxa* 4365: 101–131. <https://doi.org/10.11646/zootaxa.4365.2.1>
- Cumming RT, Le Tirant S, Teemsa SN (2018) Northeastern Australia record of *Nanophyllium pygmaeum* Redtenbacher, 1906, now recognized as a new species, *Nanophyllium australianum* n. sp. (Phasmida, Phylliidae). *Faunitaxys* 6: 1–5.
- Cumming RT, Teemsa SN (2018) *Phyllium* (*Phyllium*) *letiranti* sp. nov. (Phasmida, Phylliidae) a new leaf insect from Peleng Island, Indonesia. *Insecta Mundi* 0618: 1–16.
- Cumming RT (2016) A new species of *Nanophyllium* Redtenbacher, 1906 from the northern coast of New Guinea (Phasmida, Phylliidae). *Zootaxa* 4147: 089–091. <https://doi.org/10.11646/zootaxa.4147.1.7>
- Cumming RT (2017) A second new species of *Nanophyllium* Redtenbacher, 1906 from the northern coast of New Guinea (Phasmida, Phylliidae). *Zootaxa* 4238: 246–248. <https://doi.org/10.11646/zootaxa.4238.2.3>
- Goldberg J, Bresseel J, Constant J, Kneubühler B, Leubner F, Michalik P, Bradler S (2015) Extreme convergence in egg-laying strategy across insect orders. *Scientific Reports* 5(7825): 1–7. <https://doi.org/10.1038/srep07825>
- Gressitt JL (1982) Ecology and biogeography of New Guinean Coleoptera (beetles). In: Gressitt JL (Eds) *Monographiae Biologicae 42, Biogeography and Ecology in New Guinea*. Dr W. Junk Publishers, The Hague, 709–734. [https://doi.org/10.1007/978-94-009-8632-9\\_36](https://doi.org/10.1007/978-94-009-8632-9_36)
- Größer D (1992) Zwei neue Arten der Gattung *Phyllium* aus Neugenia (Phasmatodea: Phylliidae). *Entomologische Zeitschrift* 102: 162–167.
- Größer D (2008) Wandelnde Blätter. Ein Katalog aller bisher beschriebenen Phylliinae-Arten und deren Eier mit drei Neubeschreibungen (2<sup>nd</sup> edn.). Chimaira, Frankfurt am Main, 175 pp.
- Hall R (2001) Cenozoic reconstructions of SE Asia and the SW Pacific: changing patterns of land and sea. In: Metcalfe I, Smith JMB, Morwood M, Davidson ID (Eds) *Faunal and Floral Migrations and Evolution in SE Asia-Australasia*, Swets & Zeitlinger, Lisse, 35–56.
- Hennemann FH, Conle OV, Gottardo M, Bresseel J (2009) On certain species of the genus *Phyllium* Illiger, 1798, with proposals for an intra-generic systematization and the descriptions of five new species from the Philippines and Palawan (Phasmida: Phylliidae: Phylliinae: Phylliini). *Zootaxa* 2322: 1–83. <https://doi.org/10.11646/zootaxa.2322.1.1>
- Herwaarden HCM (1998) A guide to the genera of stick- and leaf-insects (Insecta: Phasmida) of New Guinea and the surrounding islands. *Science in New Guinea* 24: 55–117.
- Illiger JKW (1798) Verzeichnis der Käfer Preussens. Johann Jacob Gebauer, Halle, 510 pp. <https://biodiversitylibrary.org/page/52579286>
- Key KHL (1974) Phasmatodea (Stick-insects). In: CSIRO (Ed.) *The Insects of Australia*. Supplement 1974. Melbourne University Press, Australia, 48–49.
- Ludt WB, Rocha LA (2015) Shifting seas: the impacts of Pleistocene sea-level fluctuations on the evolution of tropical marine taxa. *Journal of Biogeography* 42: 25–38. <https://doi.org/10.1111/jbi.12416>

- Monteith GB (1971) Leaf Insects from Australia. The Entomological Society of Queensland 78: 14–15.
- Monteith GB (1978) The First Male Leaf Insect from Australia. The Entomological Society of Queensland 5: 138–139.
- Oliver P, Krey K, Richards S (2011) A new species of bent-toed gecko (*Cyrtodactylus*, Gekkonidae) from the North Papuan Mountains. *Zootaxa* 2930: 22–32. <https://doi.org/10.11646/zootaxa.4671.1.9>
- Pillans B, Chappell J, Naish TR (1998) A review of the Milankovitch climatic beat: template for Plio-Pleistocene sea-level changes and sequence stratigraphy. *Sedimentary Geology* 122: 5–21. [https://doi.org/10.1016/S0037-0738\(98\)00095-5](https://doi.org/10.1016/S0037-0738(98)00095-5)
- Redtenbacher J (1906) Die Insektenfamilie der Phasmiden. I. Phasmidae, Areolatae. Verlag W. Engelmann, Leipzig, 180 pp.
- Rentz DCF (1988) *Nanophyllum pygmaeum* Redtenbacher (Phasmatodea: Phylliidae: Phyllinae), a leaf insect recently recognized in Australia. *Australian Entomological Magazine* 15: 1–3. <http://hdl.handle.net/102.100.100/266346?index=1>
- Robertson JA, Bradler S, Whiting MF (2018) Evolution of Oviposition Techniques in Stick and Leaf Insects (Phasmatodea). *Frontiers in Ecology and Evolution* 6: 1–216. <https://doi.org/10.3389/fevo.2018.00216>
- Richards SJ, Oliver PM, Krey K, Tjaturadi B (2009) A new species of *Litoria* (Amphibia: Anura: Hylidae) from the foothills of the Foja Mountains, Papua Province, Indonesia. *Zootaxa* 2277: 1–13. <https://doi.org/10.11646/zootaxa.2277.1.1>
- Stål C (1875) Öfversigt af Kongliga Vetenskaps-Akademiens Förhandlingar. Recensio Orthopterorum. *Revue critique des Orthopteres*, Decricts Par, Linne De Geer et Thunberg. P. A. Norstedt & Söner, Stockholm, Sweden, 32(III), 105 pp.
- Wedmann S, Bradler S, Rust J (2007) The first fossil leaf insect: 47 million years of specialized cryptic morphology and behavior. *Proceedings of the National Academy of Sciences of the United States of America* 104: 565–569. <https://doi.org/10.1073/pnas.0606937104>
- Zompro O, Größler D (2003) A generic revision of the insect order Phasmatodea: The genera of the areolate stick insect family Phylliidae (Walking Leaves). *Spixiana* 26: 129–141. [https://www.zobodat.at/pdf/Spixiana\\_026\\_0129-0141.pdf](https://www.zobodat.at/pdf/Spixiana_026_0129-0141.pdf)
- Zompro O (2001) Philippine phasmids from the collection of the Staatliches Museums für Tierkunde, Dresden (Insecta: Phasmatodea). *Reichenbachia* 34: 49–56.

# On the Plakobranchidae (Gastropoda, Sacoglossa) from soft sediment habitats of Koh Tao, Gulf of Thailand, with descriptions of two new species

Rahul Mehrotra<sup>1,2</sup>, Manuel Caballer Gutiérrez<sup>3,4</sup>, Chad M. Scott<sup>2</sup>, Spencer Arnold<sup>2</sup>,  
Coline Monchanin<sup>2,5</sup>, Suchana Chavanich<sup>1,6</sup>

**1** Reef Biology Research Group, Department of Marine Science, Faculty of Science, Chulalongkorn University, Bangkok 10330, Thailand **2** Conservation Diver, 7321 Timber Trail Road, Evergreen, Colorado, 80439, USA **3** The American University of Paris, Department of Computer Science Math and Environmental Science, 6 rue du Colonel Combes, 75007 Paris, France **4** Muséum national d'Histoire naturelle, 55 rue de Buffon, 75005 Paris, France **5** Research Center on Animal Cognition (CRCA), Center for Integrative Biology (CBI); CNRS, University Paul Sabatier – Toulouse III, France **6** Center of Excellence for Marine Biotechnology, Department of Marine Science, Faculty of Science, Chulalongkorn University, Bangkok 10330, Thailand

Corresponding author: Suchana Chavanich ([Suchana.C@chula.ac.th](mailto:Suchana.C@chula.ac.th))

---

Academic editor: Nathalie Yonow | Received 6 April 2020 | Accepted 24 July 2020 | Published 17 September 2020

---

<http://zoobank.org/6D442A10-F351-4B9C-8364-41B47A0B145A>

---

**Citation:** Mehrotra R, Caballer Gutiérrez M, Scott CM, Arnold S, Monchanin C, Chavanich S (2020) On the Plakobranchidae (Gastropoda, Sacoglossa) from soft sediment habitats of Koh Tao, Gulf of Thailand, with descriptions of two new species. ZooKeys 969: 85–121. <https://doi.org/10.3897/zookeys.969.52941>

---

## Abstract

Research in recent years have provided rapid advances in biogeographic and taxonomic documentation of sea slugs around the world. However, efforts are lacking in surveying most coastlines and habitats in South-East Asia. Recent studies from the Gulf of Thailand have indicated that a wealth of unexplored sea slug diversity and ecology may be gained from an investigation of soft sediment habitats beyond the reef slopes. Additionally, the waters of Koh Tao have been found to host regionally high levels of sea slug diversity with several species awaiting taxonomic clarification. In this work the initial findings of an expanded survey effort from the waters around Koh Tao are provided, with the identity of two soft sediment-associated sacoglossan species in the family Plakobranchidae being investigated. By integrating morphological and molecular analyses, the species *Plakobranchus noctisstellatus* **sp. nov.** and *Elysia aowthai* **sp. nov.** are described and species complexes surrounding *Plakobranchus ocellatus* van Hasselt, 1824 and *Elysia japonica* Eliot, 1913 are discussed. The topics of morphological variability and the cryptic species problem are also discussed.

## Keywords

biodiversity exploration, cryptic species, *Elysia*, Heterobranchia, *Plakobranchus*

## Introduction

In Thailand, most of the research carried out on sacoglossan sea slugs occurred in the last 30 years, after the description of *Cylindrobulla phuketi* Jensen, 1989. Since then, a total of 21 species have been recorded in Thailand (Andaman Sea and Gulf of Thailand combined), with seven of these being described within Thai waters. These include *C. phuketi*, *Elysia siamensis* Swennen, 1998, and *E. bangtawaensis* Swennen, 1998; *Gascoignella nukuli* Swennen, 2001 and *Swennenia jabae* (Swennen 2001); *Costasiella coronata* Swennen, 2007, and *Ercolania halophilae* Jensen, Kohnert, Bendell & Schrödl, 2014. Of the 21 species, six are recorded only from the Andaman Sea in western Thailand, ten exclusively within the Gulf of Thailand, and the remaining are known either from both seas or their precise collection location is unknown.

A recent inventory of traditional ‘opisthobranch’ sea slugs from the island of Koh Tao, Gulf of Thailand, yielded 87 species and documented 32 new records for the Gulf of Thailand region (25 of which for all Thai waters), particularly highlighting the remarkable role of soft sediment habitats in the local sea slug diversity (Mehrotra and Scott 2016). It was found that 37% of all species recorded around Koh Tao were recorded exclusively from the soft sediment habitats outside of the coral reef, including the majority of species found at the time to be as yet undescribed, and rarely observed by the local recreational diving community. As part of this study, two species of *Plakobranchnus* van Hasselt, 1824 were identified from the island’s waters, *Plakobranchnus ocellatus* van Hasselt, 1824 and *Plakobranchnus ianthobaptus* Gould, 1852, later amended to *Plakobranchnus* cf. *ocellatus* and *Plakobranchnus* cf. *papua* respectively (Mehrotra et al. 2019). Molecular evidence has shown that the species historically identified as *P. ocellatus* represents a complex of multiple species (Krug et al. 2013) and thus at present the recently described *Plakobranchnus papua* Meyers-Muñoz et al., 2016 is the only species that is considered taxonomically stable (see discussion).

The analysis of soft sediment sea slugs of the island also included a species of the genus *Elysia* Risso, 1818 that was found to bear characteristics corresponding to different species and was recorded as *Elysia* sp. Later, during trials on the ingestive capabilities of scleractinian corals, the same species was referred to as *Elysia* cf. *japonica* (Mehrotra et al. 2019), due to the resemblance with the species described by Eliot (1913) from Japan. Since the original description of *Elysia japonica* Eliot, 1913, numerous authors have described other morphologically similar species, based on a variety of characters which were missing in the description of *E. japonica*, whose type appears to be lost (Trowbridge et al. 2011). The taxonomic uncertainty of these species has been raised numerous times over the decades (see Jensen 1985; Rudman 2001; Trowbridge et al. 2011; Takano et al. 2013 and others), with *Elysia abei* Baba, 1955, *E. amakusana* Baba, 1955, and *E. furvacauda* Burn, 1958, all at one point or another being suggested as synonyms of *E. japonica*.

Such cases as those of *Plakobranchnus ocellatus* and *Elysia japonica* are part of a rapidly growing subset of taxonomic murkiness referred to as the ‘cryptic species’ problem. These are often characterised by discrepancies between morphological and molecular analyses (Korshunova et al. 2019), with increasing access to molecular technologies

allowing for growing documentation of genetic divergence within groups with overlapping external morphologies (Jörger and Schrödl 2013; Korshunova et al. 2019). Incidences of molecular analyses revealing previously undocumented species complexes or challenging historic synonymisations are abundant within the family Plakobranchidae Gray, 1840 (i.e., Krug et al. 2013, 2016). It is therefore apparent that comprehensive and integrated analyses are needed in the description of such species, including aspects of internal and external morphology, genetics, as well as ecology.

Since the initial findings recorded by Mehrotra and Scott (2016), more extensive surveys on sea slug biodiversity and ecology have been carried out, with a focus on the soft sediment habitats. In this work we conducted a molecular analysis to clarify the status of the species in the genus *Plakobranchus* from Koh Tao, as a result describing a new species exclusive to deeper soft sediment habitats from the island. We also provide an integrated molecular analysis of a species belonging to the complex surrounding *E. japonica*, discussing its long and complex taxonomic history, and providing detailed morphological information for the species inhabiting Thai waters, which is described as a new taxon based on genetic and geographical criteria.

## Materials and methods

### Sampling and anatomical studies

Specimens of *Plakobranchus* and specimens of *Elysia* resembling *E. japonica* were collected by SCUBA diving at Koh Tao, Thailand, on soft sediment habitats at depths ranging from 1 to 25 meters and photographed in-situ with an Olympus TG-4 camera with an underwater housing. When specimens were collected, 95% ethanol was used for preservation for both molecular and morphological analysis. Anatomical studies were performed using an Olympus SZX16 stereomicroscope, which was also used for the preparation of glycerine slides for light microscopy of radula, eyes, and penial apparatus. A TESCAN-VEGA-II-LSU scanning electron microscope (**SEM**) belonging to the Plateau Technique de Microscopie Electronique of the Muséum national d'Histoire naturelle, Paris, France (**MNHN**) was used for this study. The SEM observations were performed on dried and gold-coated samples with an accelerating voltage of 15 kV. Images were taken with an Everhart-Thornley detector. Type specimens are deposited at the MNHN. No permissions were required for sample collection and all permissions for analyses were acquired through Chulalongkorn University, Thailand. Some paratypes of the described species are also stored at the Reef Biology Research Group (**RBRG**) in the Department of Marine Science, Chulalongkorn University.

### DNA extraction, amplification, and sequencing

Tissue was taken from the ventral region of the foot of each specimen and DNA extracted using Quiagen DNeasy Tissue Kits. Primer sequences for partial sequences of cytochrome c oxidase subunit I (COI) were sourced from Folmer et al. (1994) us-

ing pairs LCO1490 (5'-GGTCAACAAATCATAAAGATATTTGG-3') and HC02198 (5'-TAAACTTCAGGGTGACCAAAAAATCA-3'). Partial sequences of the 16S rRNA region were amplified using the forward primer 16Sar-L (5'-CGCCTGTTTATCAAAAACAT-3') from Palumbi et al. (1991) and reverse primer 16s-xH (5'-CCG-GTYTGAAMYYAGATCACGTAGG3') from Mehrotra et al. (2020). Primers for the Histone 3 region were taken from Colgan et al. (2000) using the primers H3F (5'-ATGGCTCGTACCAAGCAGACVGC-3') and H3R (5'-ATATCCTTRGGC-ATRATRGTGAC-3'). PCR was carried out using BioRads MJ Mini™ Personal Thermal Cycler with a reaction volume of 20 µl. PCR protocol for the COI region was as follows: an initial denaturing step at 94 °C for 3 minutes; 40 cycles of denaturing at 94 °C for 30 seconds, annealing at 45 °C for 30 seconds, an extension at 72 °C for 1 minute, followed by a final extension at 72 °C for 10 minutes. PCR protocol for the partial 16S region and the nuclear H3 region was: an initial denaturing step at 94 °C for 3 minutes; 40 cycles of denaturing at 94 °C for 30 seconds, annealing at 53 °C for 30 seconds, an extension at 72 °C for 1 minute, followed by a final extension at 72 °C for 10 minutes. The same protocol was used for both 16S primer combinations. Electrophoresis was carried out using 0.5% TBE agarose gel. Purified aliquots were sent to Macrogen (Macrogen Sequencing Services: <http://dna.macrogen.com/eng/>) for sequencing.

## Sequence and phylogenetic analyses

Available sequences for multiple species (Table 1) of *Plakobranchnus* and of multiple species of *Elysia*, including numerous sequences from those species which are cryptic with *Elysia japonica*, were used for phylogenetic analysis. Sequences were sourced from published material (specifically Bass 2006; Krug et al. 2013; Takano et al. 2013; Krug et al. 2015, 2016) and GenBank (NCBI). All sequence metadata such as sample identifier and location were verified based on published material as primary quality control, with GenBank metadata used if sequences were unpublished or unverified. All sequences were aligned and edited using BioEdit 7.2.5 (Hall 1999) and then reviewed manually. Primers were trimmed from the resulting alignment. The pairwise distances for COI, 16S, and H3 genes were calculated using the Kimura 2 parameters model implemented in MEGA 5.1 (Tamura et al. 2011). We applied a liberal 7% (COI) threshold to suggest a possible species delimitation criterion; however, only a closer morphological analysis of more specimens will yield a clearer picture of an appropriate molecular stringency in the discussed clades. Automatic Barcode Gap Discovery (ABGD) analyses (Puillandre et al. 2012) were conducted on the complete COI dataset without the outgroup. Three different ABGD analyses were performed to delineate species within the COI dataset. Each analysis was run using a different nucleotide substitution model, JC69, K80 2.0, and Simple Distance, with the settings Pmin = 0.001, Pmax = 0.1, Steps = 10, X = 1.5, Nb bins = 20. Phylogenetic analyses were carried out by using both Maximum Likelihood (ML), and Bayesian Inference (BI) methods. Analysis for each was conducted on sequences from the COI region independently, followed by an analysis of concatenated sequences of COI and 16S and H3 regions. Optimum evolutionary models were selected using the model test feature

within MEGA 7.0.14 (Kumar et al. 2016). The optimum model used for analyses of COI and concatenated sequences was GTR+G+I. Analysis was conducted with 1000 bootstrap replicates and random starting trees. All sequences were additionally analysed using Bayesian Inference via MrBayes 3.2 (Ronquist et al. 2012). Analysis was conducted with 50,000,000 generations and four chains with Markov chains being sampled every 1000 generations. The first 25% generations were removed as burn-in with the rest being used to produce the 50% consensus tree.

**Table 1.** Sequences used in this study. New sequences are in bold, the remainder were obtained from GenBank.

Species	Location	COI	16S	H3
<i>Elysia abei</i>	Japan	KM086374	JN819137	JN819171
<i>Elysia abei</i>	Japan	KC573711	–	–
<i>Elysia abei</i>	Japan	KC573712	–	–
<i>Elysia abei</i>	Japan	KC573713	–	–
<i>Elysia abei</i>	–	JN819115	–	–
<i>Elysia abei</i>	Japan	AB758953	AB759022	–
<i>Elysia abei</i>	Japan	AB758954	AB759023	–
<i>Elysia abei</i>	Japan	AB758955	AB759024	–
<i>Elysia amakusana</i>	Japan	AB758956	AB759025	–
<i>Elysia amakusana</i>	Australia	GQ996686	EU140851	–
<i>Elysia asbecki</i>	Vanuatu	KM086360	KM204200	KM040808
<i>Elysia bangtawaensis</i>	Thailand	KM086375	KM204224	KM040826
<i>Elysia chlorotica</i>	Massachusetts, USA	KM086377	KM204226	JN819183
<i>Elysia diomedea</i>	Panama	KM086379	KM204228	KM040830
<i>Elysia furvacauda</i>	Australia	KM086369	KM204218	KM040821
<i>Elysia hamatani</i>	Japan	JN819110	JN819143	JN819177
<b><i>Elysia aowthai</i> sp. nov.</b>	<b>Gulf of Thailand</b>	<b>MK835779</b>	<b>MK835763</b>	<b>MK835771</b>
<b><i>Elysia aowthai</i> sp. nov.</b>	<b>Gulf of Thailand</b>	<b>MK835780</b>	<b>MK835764</b>	<b>MK835772</b>
<b><i>Elysia aowthai</i> sp. nov.</b>	<b>Gulf of Thailand</b>	<b>MK835781</b>	<b>MK835765</b>	<b>MK835773</b>
<i>Elysia marginata</i>	Guam	JN819100	–	–
<i>Elysia obtusa</i>	Japan	KM086387	KM204236	KM040840
<i>Elysia rufescens</i>	Japan	AB758961	–	–
<i>Elysia singaporensis</i>	Singapore	KM086398	KM204249	KM040847
<i>Elysia</i> sp. 5	Hawaii	JN819113	JN819138	JN819172
<i>Elysia</i> cf. <i>japonica</i>	Japan	AB758952	–	–
<i>Elysia</i> cf. <i>japonica</i>	Guam	DQ471255	DQ480176	DQ534772
<i>Plakobranthus ocellatus</i>	Australia	GQ996680	–	–
<i>Plakobranthus ocellatus</i>	Philippines	JX272720	–	–
<i>Plakobranthus ocellatus</i>	Philippines	JX272696	–	–
<i>Plakobranthus ocellatus</i>	Philippines	JX272695	–	–
<i>Plakobranthus ocellatus</i>	Philippines	JX272688	–	–
<i>Plakobranthus ocellatus</i> (black)	Japan	KC573718	–	–
<i>Plakobranthus ocellatus</i> (black)	Japan	AB758971	–	–
<i>Plakobranthus ocellatus</i> (blue)	Japan	KC573714	–	–
<i>Plakobranthus ocellatus</i> (blue)	Japan	AB758968	–	–
<i>Plakobranthus ocellatus</i> (blue)	Guam	KC573717	KM204279	KM040891
<i>Plakobranthus ocellatus</i> (purple)	Japan	KC573727	KM204280	KC597161
<i>Plakobranthus ocellatus</i> (purple)	Japan	KC573726	–	–

Species	Location	COI	16S	H3
<i>Plakobranchnus ocellatus</i> (purple)	Japan	AB758969	–	–
<i>Plakobranchnus</i> sp. (aff. purple)	French Polynesia	KC573729	KM204276	KM040890
<i>Plakobranchnus</i> sp. (aff. purple)	Guam	KC573730	–	–
<i>Plakobranchnus</i> sp. (spotless)	Japan	KC573731	KM204283	KM040893
<i>Plakobranchnus ocellatus</i>	Guam	HM187634	KM204284	KM040894
<i>Plakobranchnus ocellatus</i> (white)	Japan	AB758970	–	–
<i>Plakobranchnus ocellatus</i> (white)	Japan	KC573719	–	–
<i>Plakobranchnus ocellatus</i> (white)	Guam	KC573722	–	–
<i>Plakobranchnus ocellatus</i> (white)	Thailand	KC573723	–	–
<i>Plakobranchnus ocellatus</i> (white)	Australia	KC573725	–	–
<b><i>Plakobranchnus ocellatus</i></b>	<b>Gulf of Thailand</b>	<b>MK835784</b>	<b>MK835768</b>	<b>MK835776</b>
<b><i>Plakobranchnus papua</i></b>	<b>Gulf of Thailand</b>	<b>MK835785</b>	<b>MK835769</b>	<b>MK835777</b>
<b><i>Plakobranchnus papua</i></b>	<b>Gulf of Thailand</b>	<b>MK835786</b>	<b>MK835770</b>	<b>MK835778</b>
<i>Plakobranchnus papua</i>	Indonesia	KC573732	KM204281	KC597163
<i>Plakobranchnus papua</i>	Indonesia	KU934191	–	–
<i>Plakobranchnus papua</i>	Indonesia	KU934192	–	–
<i>Plakobranchnus papua</i>	Indonesia	KU934193	–	–
<b><i>Plakobranchnus noctisstellatus</i> sp. nov.</b>	<b>Gulf of Thailand</b>	<b>MK835782</b>	<b>MK835766</b>	<b>MK835774</b>
<b><i>Plakobranchnus noctisstellatus</i> sp. nov.</b>	<b>Gulf of Thailand</b>	<b>MK835783</b>	<b>MK835767</b>	<b>MK835775</b>
<i>Plakobranchnus</i> (aff. sp. 1)	Papua New Guinea	KC573734	KM204277	KC597165
<i>Plakobranchnus</i> (sp. 2)	Philippines	KC573736	KM204282	KM040892
<i>Plakobranchnus</i> sp.	Hawaii	KY012787	–	–
<i>Plakobranchnus</i> sp.	Hawaii	KY012788	–	–
<i>Plakobranchnus</i> sp.	Hawaii	KC573738	–	–
<i>Thuridilla albopustulosa</i>	Guam	KM086443	KM204302	KM040916
<i>Thuridilla gracilis</i>	Guam	KM086444	KM204304	KM040917
<i>Thuridilla hopei</i>	Italy	KC573743	KM204305	KC597170
<i>Thuridilla livida</i>	Malaysia	KC573745	KM204307	KC597172
<i>Thuridilla splendens</i>	Japan	KM086445	KM204310	KM040920
<i>Costasiella coronata</i>	Hong Kong	KJ610067	KJ610027	KJ610054
<i>Costasiella usagi</i>	Guam	KJ610071	KJ610031	KJ610058
<i>Cyerce elegans</i>	Vanuatu	KM086353	KM204193	KM040801

## Results

### Phylogenetic analyses

All molecular analyses (Fig. 1) consistently place *Plakobranchnus noctisstellatus* sp. nov. as not only distinct from all other sequenced species and morphs belonging to the genus *Plakobranchnus* with strong support, but also basal to the genus in both stand-alone COI and concatenated phylogenies (100% PP and BS values). Uncorrected pairwise distances for each gene for *Plakobranchnus noctisstellatus* were found to have a minimum distance of 12%, 10%, and 7% for COI, 16S, and H3 respectively when compared to its congeners (Table 2). Distances for COI were also calculated for other available *Plakobranchnus* sequences which were then informally separated into clades with a liberal minimum distance threshold of 7%. Concatenated phylogenies of the combined sequences also rendered *Plakobranchnus* as monophyletic with high support (100% PP and 99% BS). Initial approaches of ABGD analyses consistently indicated nine partitions (Fig. 1, Table 2); however, recursive

analyses using JC69 and K80 models indicated a tenth partition separating *Plakobranthus papua* from Koh Tao as sister to those from the type locality. In all analyses, *Plakobranthus noctisstellatus* sp. nov. was distinct from all other clades of the genus.

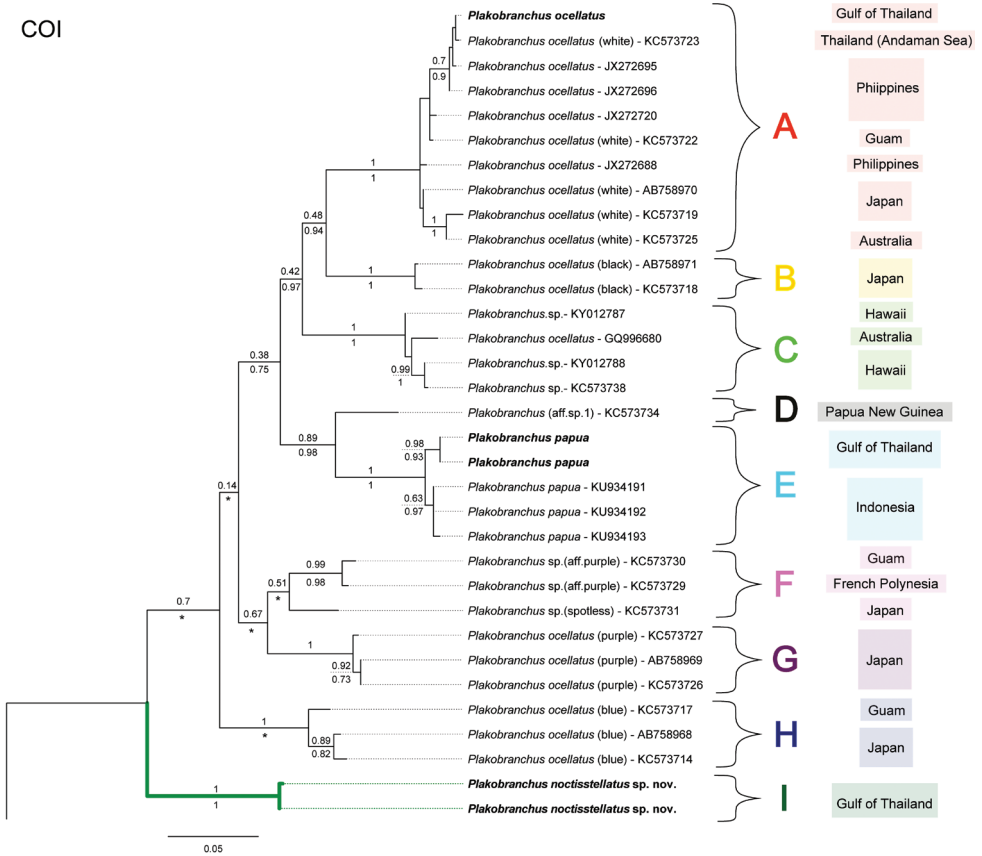


**Figure 1.** Phylogenetic hypothesis of *Plakobranthus* based on COI sequences. Bootstrap values from ML shown above branch and posterior probability (PP) values below branch. Sequences obtained in this study in bold. Missing PP values, or those that support branch placements that deviate from the ML tree are denoted with an asterisk \* and are due to the discrepancy between ML and BI topologies (see Suppl. material 1). Tree rooted to *Costasiella coronata* (not shown).

**Table 2.** Distance values within and between clades corresponding to the COI phylogeny of *Plakobranthus*.

Clade	In-clade min	In-clade max	Out-clade min
A	0%	4%	10%
B	–	1%	9%
C	0%	2%	10%
D	–	–	7%
E	0%	2%	7%
F	1%	6%	8%
G	0%	1%	7%
H	1%	3%	9%
I	0%	0%	12%

Strong support was also found for *Elysia aowthai* sp. nov. as a distinct species in both stand-alone COI (100% PP and 96% BS) and concatenated phylogenies (100% PP and BS values). Distances for *E. aowthai* sp. nov. were calculated within the clade (Clade A in Fig. 2), and minimum distances for species outside the clade for each gene. The maximum intra-clade distance for each gene was found to be 6% (COI), 7% (16S), and 0% (H3), with the minimum distance for specimens outside the clade being 11% (COI), 9% (16S), and 6% (H3) (Table 3). All three ABGD analyses with all *Elysia* sequences used outputted consistent results, revealing 13 stable different partitions within the dataset via the initial approach. However, all three also suggested a 14<sup>th</sup> partition via the recursive approach. The *E. japonica* complex divided into four clades (Fig. 2, Table 3) in the initial approach, with the recursive approach separating *Elysia* cf. *japonica* (from Japan) into a fifth distinct part. Nonetheless, in all analyses the *Elysia aowthai* sp. nov. clade (Clade A) was well supported as distinct from all others, including the two specimens identified as *E. cf. japonica* from Guam (Bass 2006) and *E. amakusana* from Australia (Wägele et al. 2010).



**Figure 2.** Phylogenetic hypothesis for the *Elysia japonica* complex based on COI sequences. Sequences obtained in this study in bold. Bootstrap values from ML shown above branches and PP values from BI below branches. Tree rooted to *Costasiella coronata* (not shown).

**Table 3.** Distance values within and between clades corresponding to the COI phylogeny of the *Elysia japonica* complex.

Clade	In-clade min	In-clade max	Out-clade min
A	0%	4%	12%
B	–	–	11%
C	–	–	11%
D	1%	6%	12%

Phylogenies documented here largely agree with others (Bass and Karl 2006; Krug et al. 2013; Takano et al. 2013; Krug et al. 2016) with the family Plakobranchidae being separated into two clades. The first clade includes the genera *Plakobranchus* and *Thuridilla*, which form monophyletic sister subclades with strong support, and the species in *Elysia* formed a second well-supported clade (Fig. 3). Likewise, the genus-specific analysis using the COI gene for *Plakobranchus* also agrees with the previous observations (Krug et al. 2013, 2016) that there is indeed an extensive complex of spe-

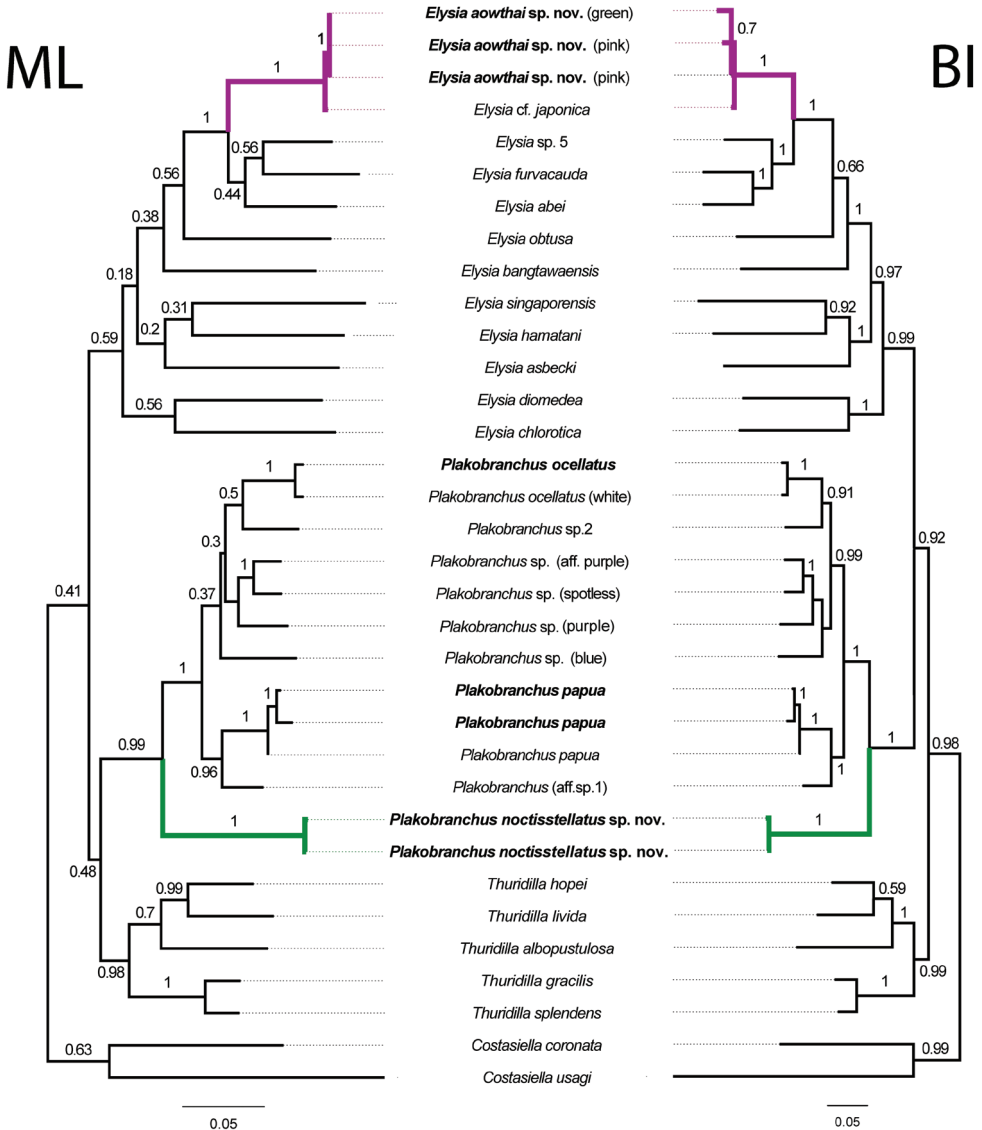


**Figure 3.** Phylogenetic hypotheses of Plakobranchidae based on concatenated sequences of COI, 16S, and H3 regions. Sequences obtained in this study in bold. Bootstrap values from ML topology (left) aligned with PP values from BI topology (right).

cies needing formal description. A similar case is seen for the *Elysia japonicalabei/amakusana/furvacaudalaowthai* complex with numerous cases of mistaken identities and at least four distinct species delimited under analysis of the COI gene (Fig. 2, Table 3).

## Systematics

### Class Gastropoda Cuvier, 1795

#### Subclass Heterobranchia Burmeister, 1837

#### Superorder Panpulmonata Jörger, Stöger, Kano, Fukuda, Knebelberger & Schrödl, 2010

#### Order Sacoglossa Ihering, 1876

#### Suborder Plakobranchea Gray, 1840

#### Superfamily Plakobranchoidea Gray, 1840

#### Family Plakobrancheidae Rang, 1829

### Genus *Plakobrancheus* van Hasselt, 1824

**Diagnosis.** Body wide, dorsoventrally flattened with broad parapodial flaps folding along dorsal midline, tail truncate. Head broad and flattened with a pair of small, raised, median eyes and rolled, laterally originating, rhinophores. Parapodial lamellae with digestive gland branches and dorsal haemolymph sinuses. Anus anterodorsal and penis armed with curved stylet. Radular teeth denticulate.

### *Plakobrancheus ocellatus* van Hasselt, 1824

Figure 4, Suppl. material 2

*Plakobrancheus ocellatus*: Christa et al. 2013: 560, fig. 1A, D (Luminau, Guam; Australia)

*Plakobrancheus ocellatus* (white): Krug et al. 2013: (Andaman Sea, Thailand; Japan; Australia; Guam)

*Plakobrancheus ocellatus* (white): Takano et al. 2013: fig. 3K (Japan)

? *Plakobrancheus ocellatus* s. s.: Meyers-Muñoz et al. 2016: 91, Table 2

*Plakobrancheus ocellatus*: Tanamura and Hirose 2016: 5, fig. 3A (Ryuku Archipelago, Japan)

*Plakobrancheus* sp. 6: Gosliner et al. 2018: 434 (Philippines)

*Plakobrancheus ocellatus*: Yonow and Jensen 2018: 20, fig. 5I (Bohol, Philippines)

**Material examined.** Three specimens 25–32 mm Chalok Bay, 10°3'44.77"N, 99°49'30.35"E, Koh Tao, Thailand.

**Supplementary observations.** More than 100 individuals, ranging in size 5 mm–45 mm, observed in regular diving surveys between 2012 and 2019, Chalok Bay, 10°3'44.77"N, 99°49'30.35"E, Shark Bay 10°3'39.75"N, 99°50'4.43"E; Tao Tong 10°3'58.13"N, 99°49'4.76"E; Sai Nuan 10°4'43.24"N, 99°48'48.51"E; Twins 10°7'1.93"N, 99°48'44.26"E; Hin Wong Bay 10°6'12.30"N, 99°50'58.63"E, Koh Tao, Thailand; not collected.

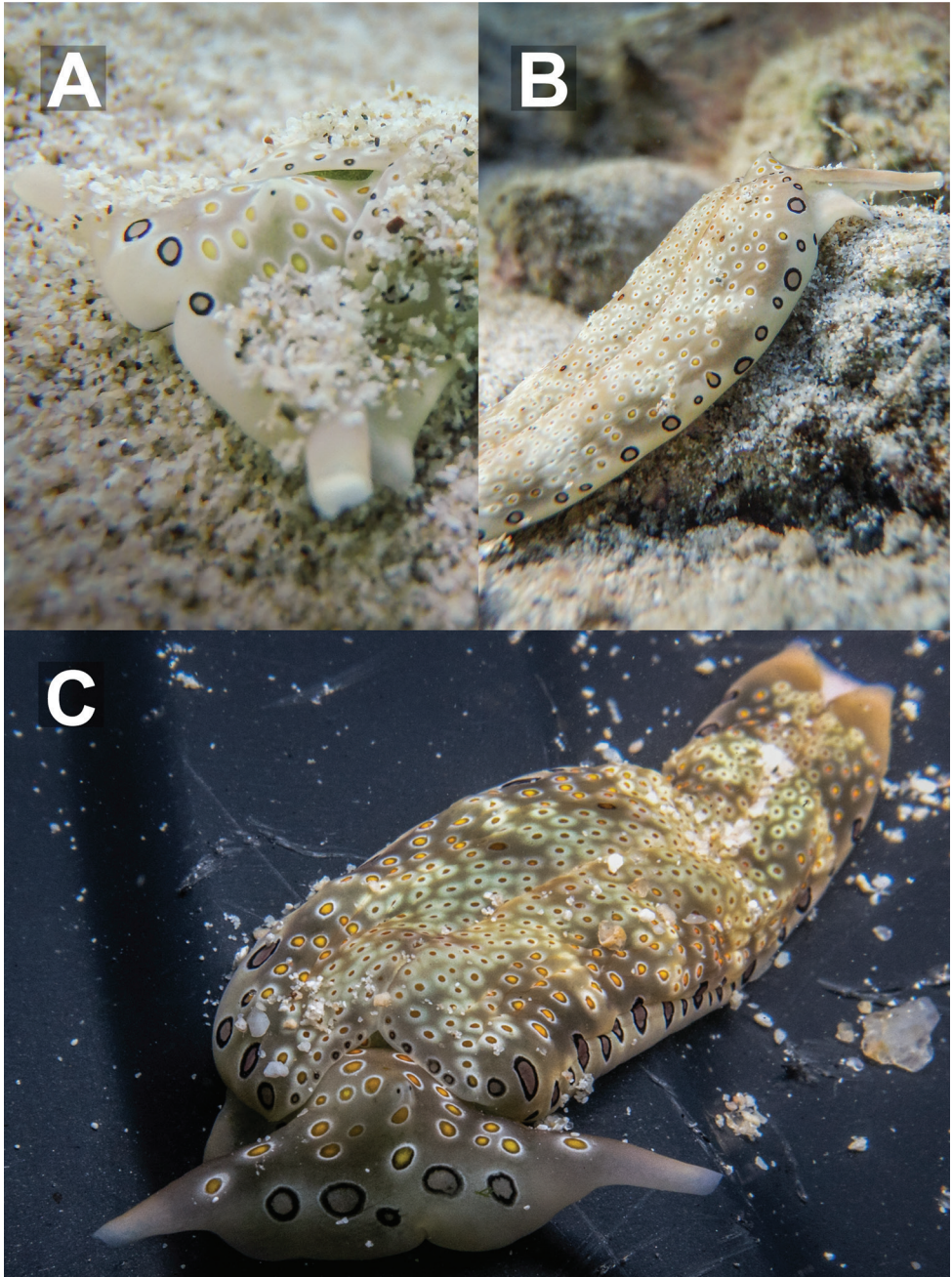


**Figure 4.** Living specimens of *Plakobranchus ocellatus* from Koh Tao. **A, B** close-up of head with retracted rhinophores and dorsolateral view, 25 mm **C** sequenced specimen, 32 mm.

**Description.** Length alive up to 45 mm. Background colour pale yellowish white to pale brown, covered in ocelli, increasing in size laterally from parapodial margins. Dorsal ocelli small, brown or brown with yellow centres, surrounded by a diffuse ring

of white. Dorso-laterally, ocelli that have a yellow centre and a brown ring followed by a white diffuse ring are also found on the head between rhinophores. Lateral ocelli large with a grey centre, thick black ring followed by thin diffuse white ring; 3–7 of these are also found on the anteriormost part of the head. Tips of rhinophores translucent bluish grey, not easily visible upon retraction, followed by white diffusing to the same pale colour as the dorsum. Rhinophores rolled, long, extending laterally from the head, curved like bull horns.

Parapodial margins translucent when opened, with yellowish white spots visible along the edge beneath the tissue surface. Internally parapodial ridges thick, bright green, with no visible spots. Eyes black, very close together, placed centrally on the head, held raised above the rest of the head when crawling. Oral prominences globose with a very fine black line on the edge of the upper lip. Anterior foot corners and tail edged in the same translucent bluish grey as rhinophore tips. Male genital opening located behind the right rhinophore, above the foot corner, in front of the anterior part of the parapodia. Penis translucent white when extended in living specimens. Foot sole white with numerous black spots throughout.

**Ecology.** From shallow soft sediments to sandy areas along the reef edge. Rarely in deeper soft sediment habitats beyond the reef edge. Depth 0.5–11 m.

**Distribution.** *Plakobranchnus ocellatus sensu lato* is currently considered widespread across the Indo-Pacific including Kenya, Zanzibar, the Red Sea, Maldives, Seychelles, Reunion (Yonow 2012), India (Sheeja and Padma Kumar 2014), the Philippines (Christa et al. 2013), Indonesia (Eisenbarth et al. 2018; Yonow and Jensen 2018), Japan (Maeda et al. 2012), Australia, Papua New Guinea (Yonow and Jensen 2018), Guam (Wägele et al. 2011), Vanuatu (Krug et al. 2013), Hawaii (Wade and Sherwood 2016), Tanzania, Madagascar, Malaysia and Palau (Gosliner et al. 2008). Specimens considered as *P. ocellatus* have been previously recorded from the Andaman and Gulf waters of Thailand (Jensen 1992; Nabhitabhata 2009).

**Remarks.** The genus *Plakobranchnus* has undergone dramatic changes over the past two centuries with more than a dozen species being described in the 1800's and all being synonymised with the type taxon *Plakobranchnus ocellatus* by numerous authors in later years (e.g., Bergh 1887; Jensen 1992). *Plakobranchnus ocellatus* was described based on blue spots with yellow centres seen dorsally and laterally on a pale ground colour and some information on the pericardial and reproductive anatomy. The species has regularly been recognised/identified by numerous authors based on many of these external characteristics (Rao 1960; Mercier and Hamel 2005; Wägele et al. 2010; Maeda et al. 2012; Sheeja and Padma Kumar 2014; Mehrotra and Scott 2016; Wade and Sherwood 2016). Recent research suggests that the dramatic synonymisation of species under the name *P. ocellatus* may have been premature, with molecular evidence suggesting at least ten independent clades within the complex of *P. ocellatus* (Krug et al. 2013, 2016). This supports the findings of previous authors who have observed different morphs of *P. ocellatus* which appeared to be externally distinguishable based on the general colouration and the distribution of the ocelli or the spots on the dorsal or ventral surface (Ono 2005; Trowbridge et al. 2011; Krug et al. 2013; Yonow and

Jensen 2018). While Krug et al. (2013) were able to provide evidence that multiple species historically identified as *P. ocellatus* are likely different, no images nor detailed morphological descriptions or comparisons were provided. It is assumed, however, that all morphotypes identified therein bear some external resemblance to *P. ocellatus sensu stricto*, in particular a white or pale ground dorsal colour.

***Plakobranthus papua* Meyers-Muñoz & van der Velde, 2016**

Figure 5, Suppl. material 3

*Plakobranthus ocellatus*: Coleman 2008: 88 (Milne Bay, Papua New Guinea; Uepi Island, Solomon Islands)

*Plakobranthus* sp. 1: Gosliner et al. 2008: 94 (Philippines; Indonesia; Papua New Guinea)

*Plakobranthus papua* Meyers-Muñoz & van der Velde in Meyers-Muñoz et al. 2016: 80–88, figs 2–7a (West Papua, Indonesia).

*Plakobranthus papua*: Gosliner et al. 2018: 434 (Indonesia)

*Plakobranthus* cf. *papua*: Yonow and Jensen 2018: 21, 27–30, figs 6C, D, 12, 13C, D, 14C, D (Ambon, Indonesia).

**Material examined.** Three specimens 19–30 mm Sai Nuan, 10°4'43.24"N, 99°48'48.51"E, Koh Tao, Thailand.

**Supplementary observations.** 27 individuals, ranging in size 12 mm–35 mm, observed in regular diving surveys between 2012 and 2019, Chalok Bay, 10°3'44.77"N, 99°49'30.35"E, Shark Bay 10°3'39.75"N, 99°50'4.43"E; Tao Tong 10°3'58.13"N, 99°49'4.76"E; Sai Nuan 10°4'43.24"N, 99°48'48.51"E, Koh Tao, Thailand; not collected.

**Description.** Length alive up to 35 mm. Background colour varies from pale yellow to an almost translucent greyish white, lacking the brownish/ochre background in the original description (Meyers-Muñoz et al. 2016: fig. 3a–c) and other Indonesian material (Yonow and Jensen 2018). Dorsally covered in white dots of varying sizes from the anterior-most part of the head to posterior edge of parapodia. These are also visible dorsally on the blunt anterior foot corners. There are prominent spots on the dorsum where no white dots are present and only the background colour is present. Rhinophores are translucent white with a diffuse band of deep blue to dark purple before the translucent tips. Rhinophores rolled, long, extending laterally from the head, curved like bull horns.

Parapodial margin with distinct white rod-like spots, almost identical to but more continuous than those in the Indonesian specimens (Meyers-Muñoz et al. 2016: fig. 3a; Yonow and Jensen 2018). Internal parapodial ridges bright to dark green, slightly thinner than in *P. ocellatus*, with no visible spots. Eyes black, very close together, centrally on the head, held slightly raised above the rest of the head when crawling. Tail tip dark blueish purple, almost black, diffusing to white anteriorly. Male genital opening located behind the right rhinophore, above the foot corner, in front of the anterior part of

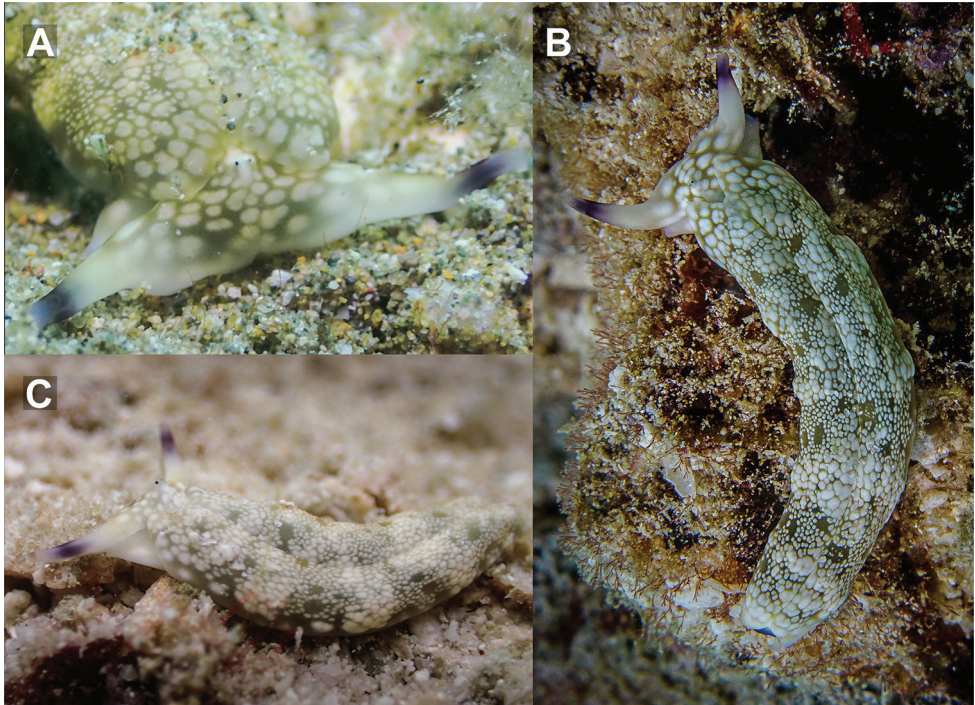


**Figure 5.** Living specimens of *Plakobranthus papua* from Koh Tao **A** close-up of head, 28 mm specimen **B** dorsal view, 30 mm (photograph by Pau Urgell Plaza) **C** dorsolateral view of sequenced specimen, 27 mm.

the parapodia. Penis transparent to translucent with a bluish white tip when extended in living specimens, penile bulb and ducts clearly visible inside. Foot sole completely white with no spots, posteriorly tinged in deep purple visible dorsally on the tail tip.

**Ecology.** Abundant in shallow soft sediment habitats and among the corals and soft sediments of the reef edge. Uncommon, but present in dense coral reef habitats; rare in deeper soft sediment habitats outside the coral reef. Has been observed being ingested naturally by the scleractinian coral *Pleuraectis paumotensis* but is mostly considered unpalatable by such corals (Mehrotra et al. 2015, 2019).

**Distribution.** Known only from the Philippines, Malaysia, Indonesia, and Papua New Guinea (Meyers-Muñoz et al. 2016; Yonow and Jensen 2018). Known from Gulf waters of Thailand (Mehrotra et al. 2015).

**Remarks.** This species has previously been referred to, erroneously, as *Plakobranthus ianthobaptus* Gould, 1852 (Mehrotra and Scott 2016) and *Plakobranthus* cf. *papua* (Mehrotra et al. 2019). Externally, specimens of *P. papua* from Koh Tao differ from the original description of the species. Specifically, the background pigmentation of the parapodia varies from pale yellow to an almost translucent greyish white, lacking the ochre background tinge and the yellow discontinuous line in the border of the parapodia known to date for the species. Furthermore, the specimens of *P. papua* in the original description show scattered white dots of varying sizes on the surface of the parapodia, whilst in specimens from Koh Tao they almost completely cover the surface. The rhino-

phores and tail from Koh Tao specimens are deep blue to dark purple at the tips (rarely black), rather than almost entirely covered by black pigment as in the specimens from the original description. A very similar variant to that documented from Koh Tao was documented from Ambon, Indonesia, as *Plakobranthus* cf. *papua* by Yonow and Jensen (2018: fig. 6C, D). Minor differences between the Ambon specimens and those from Koh Tao are the paler dorsal colouring and more continuous rod-structures along the parapodial margins in Koh Tao specimens. Additionally, the longitudinal white line visible behind the eyes in Ambon specimens appears to be broken up in specimens from West Papua (Meyers-Muñoz et al. 2016: fig. 3A–D) and scattered in Koh Tao specimens (Fig. 5). Molecular data presented here suggest the present specimens as conspecific with *P. papua* and the additional material highlights the external variation in the species.

***Plakobranthus noctisstellatus* sp. nov.**

<http://zoobank.org/2A0E4A50-5567-4470-86F5-7B21690C9A66>

Figures 6, 7, 10D–F

*Plakobranthus* sp.: Coleman 2008: 89 (Thailand; Gorontalo, Indonesia)

*Plakobranthus* sp. 2: Gosliner et al. 2008: 94 (Vanuatu; Bali, Indonesia); Gosliner et al. 2015: 98 (Papua New Guinea).

*Plakobranthus ocellatus* var. I: Meyers-Muñoz et al. 2016: 91, Table 2

*Plakobranthus* cf. *ocellatus*: Yonow and Jensen 2018: 30 (top of 2<sup>nd</sup> column), fig. 6E (Bali, Indonesia)

**Type material.** *Holotype*: adult, 28 mm long (alive), collected in silty sand at 21 m depth, Sai Nuan, 10°4'43.24"N, 99°48'48.51"E, Koh Tao, Thailand, 06 April 2016, deposited in MNHN (IM-2000- 35324). *Paratype*: adult, 31 mm long (alive), collected in silty sand at 18 m depth, Tao Tong, 10°3'58.13"N, 99°49'4.76"E, Koh Tao, Thailand, 18 March 2017, deposited in MNHN (IM-2000- 35325). Paratype dissected: reproductive system studied, and jaw, radula, and penis mounted for optical microscopy. *Paratype*: adult, 26 mm long (alive), collected in silty sand at 24 m depth, Tao Tong, 10°3'58.13"N, 99°49'4.76"E, Koh Tao, Thailand, 17 February 2020, deposited in RBRG (PkII-NR011).

**Supplementary observations.** More than ten individuals, ranging from 10 mm to up to 45 mm, observed in regular diving surveys between 2016 and 2018, Tao Tong 10°3'58.13"N, 99°49'4.76"E; Sai Nuan 10°4'45.02"N, 99°48'45.23"E; Shark Bay 10°3'39.75"N, 99°50'4.43"E; Koh Tao, Thailand, not collected.

**Description.** Length alive up to 45 mm. Body wide, dorsoventrally flattened with wide parapodial flaps folding along dorsal midline. Background colour bright green to dark green, with scarce black spots, and abundant opaque white spots all over. Some white spots with blue hue, others with yellowish tinge. Five or six prominent black spots similar in size and shape to the eyes found laterally on both sides. Tips of rhinophores and tail are electric blue, followed by a black band, not so evident in the tail. Rhinophores long, rolled, extended from lateral edges of the head, curved like bull

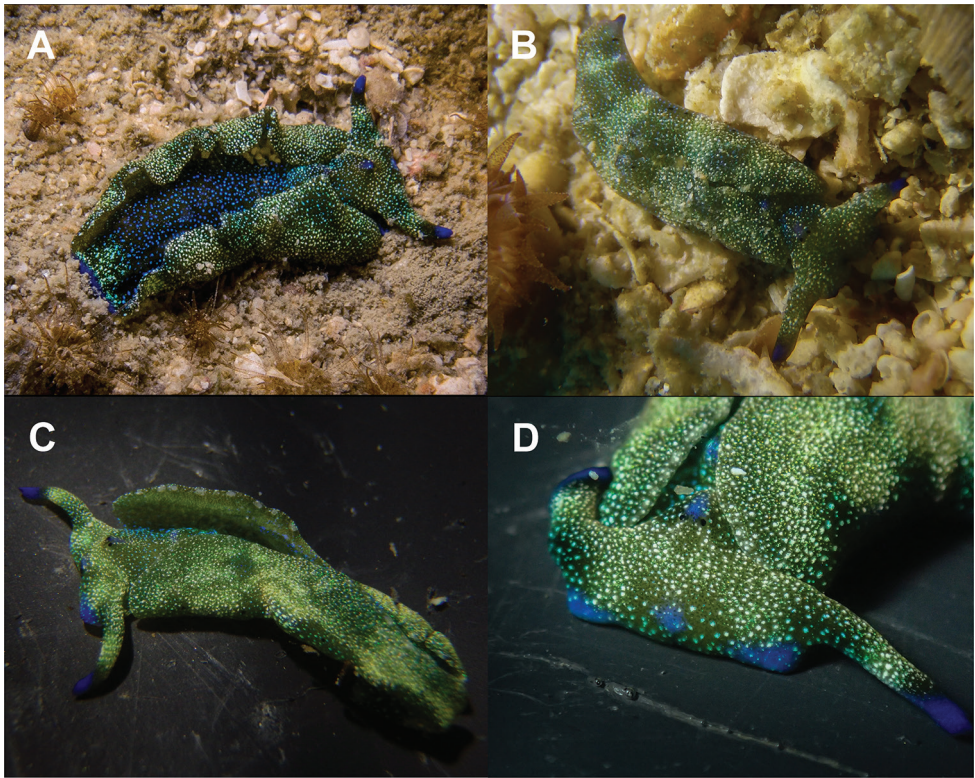


**Figure 6.** Living specimens of *Plakobranchus noctisstellatus* sp. nov. from Koh Tao. **A** 21 mm (photograph by Pau Urgell Plaza) **B** 15 mm **C, D** (paratype) 31 mm.

horns when crawling. Internal parapodial flaps ridges bright green to dark green, with white and electric blue spots. Eyes black, very close to each other, sometimes with a blue hue between them, located in a groove between rhinophores. Oral prominences globose, with a big black patch on each side, and a very fine, undulating black line on the edge of upper lip. Anterior-upper end of the oral prominences green with white spots and the same electric blue as rhinophore tips. Anterior foot corners in preservation blunt. Foot sole the same green as the dorsal surface with several small iridescent light blue spots. A possible transverse foot groove may be present; however, this was not distinct in living specimens and equally as vague upon preservation. Tail truncated. Dorsal region dark green to black, with big opaque white to electric blue spots (Fig. 6).

**Renopericardial** prominence composed of two globose, oval lobes (in preservation). Posterior lobe pointed at the end, with pair of major haemolymph sinuses, both perpendicular to its lateral surface and turning at right angles once in the parapodia. Haemolymph sinuses thick, cord-like, white in preservation, longitudinal, parallel to each other (Fig. 7A), not joining together at the ends. Most external haemolymph sinuses shorter. Internal surface of parapodia smooth in preservation, except for the haemolymph sinuses that externally seem to run from the renopericardial prominence. Anal opening at the right anterior side of the pericardium (Fig. 7A).

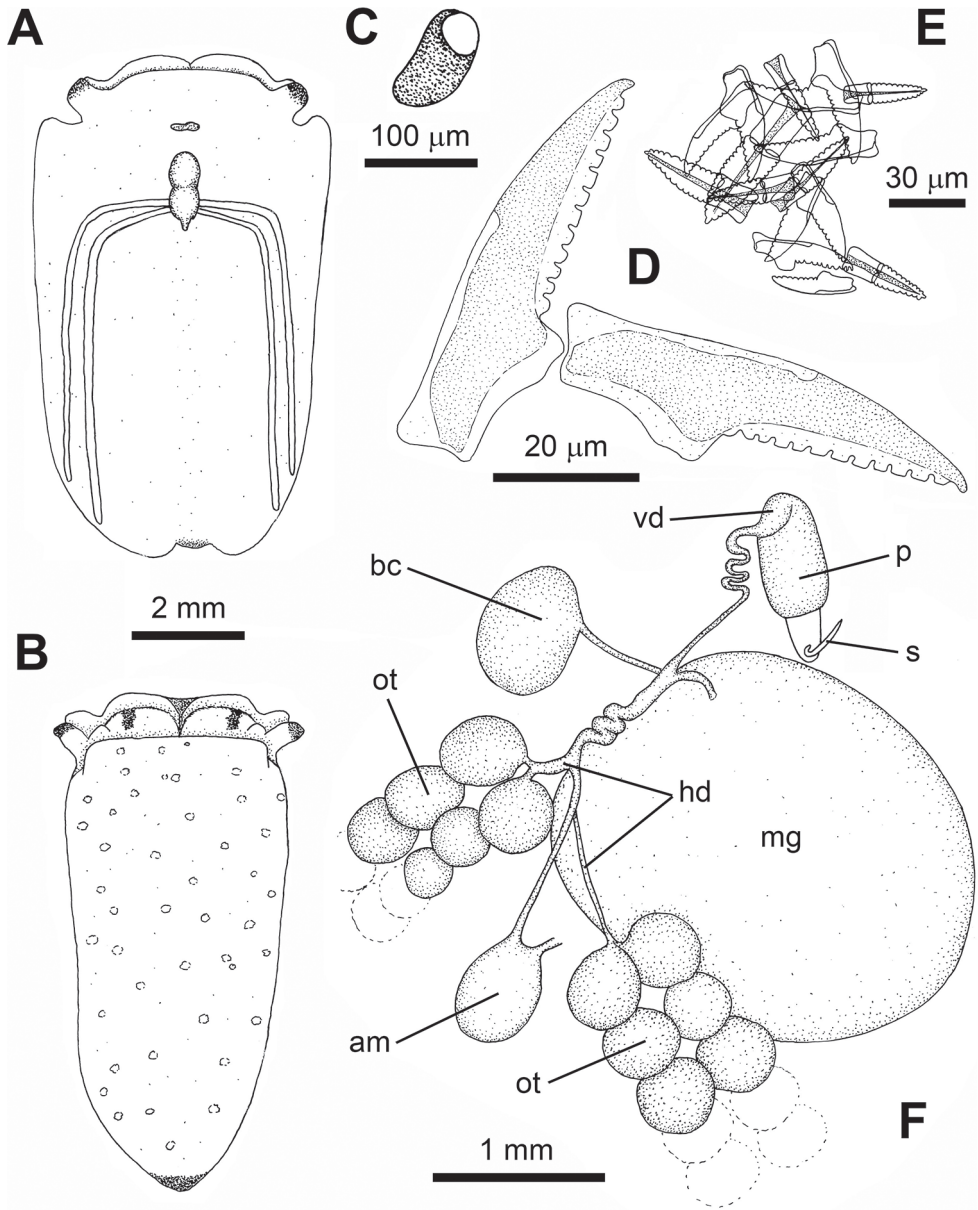


**Figure 7.** *Plakobranchus noctisstellatus* sp. nov. **A** dorsal view of the animal **B** ventral view of the animal, **C** detail of the eye **D** last teeth of the ascending series and active teeth **E** teeth in the ascus **F** reproductive system. Abbreviations: am – ampulla; bc – bursa copulatrix; hd – hermaphrodite duct; mg – mucus gland; ot – ovotestis, p – penis; s – stylet; vd – vas deferens.

*Uniserial radula* (in one 20 mm long specimen) with eight teeth including ghost teeth in ascending row, ten in descending row, 24 in ascus. Teeth triangular, sharp, bearing striations (Fig. 10), and with two cutting edges and 12 or 13 strong and blunt denticles

on each of them. First teeth in ascending series 65  $\mu\text{m}$  long, 18  $\mu\text{m}$  high. Active teeth 60  $\mu\text{m}$  long, 18  $\mu\text{m}$  high. Last teeth in descending series 50  $\mu\text{m}$  long, 17  $\mu\text{m}$  high. Teeth in the ascus in varied stages of degradation, 25–66  $\mu\text{m}$  long, packed haphazardly (Fig. 7E).

**Penial bulb** approximately 1 mm long, below rhinophores, at same level as the eyes, bearing a sharp cuticular stylet. Stylet 280  $\mu\text{m}$  long, hollow, kinked at the base, with the tip like the tip of a hypodermic syringe. Vas deferens connected to penial bulb, curved and strong; medial part thinner and coiled; proximal part straight, over mucus gland, at the end joins a wider conduct. This conduct connected to mucus gland, then coiled and bifurcated to ampulla and to ovotestis. Bursa copulatrix connected to the underside of the central fertilisation area near by the end of the vas deferens (Fig. 7A). Ovotestis grape-shaped, composed of spheres filling the parapodia. Spheres variable in diameter, from 350 to 500  $\mu\text{m}$ . Mucus gland large, globose (Fig. 7F).

**Biology.** All animals were observed year-round at different locations around the island, exclusively in deeper soft sediment habitats at Koh Tao. Animals found either partially buried in or moving across the open silt and sand dominated habitats beyond the fringing coral reefs of the island. Animals found at depths from 15–25 m with no indication of seasonal variation. No observations made shallower than 15 m depth or in the vicinity of coral reef or reef edge habitats. Not observed to be in association with any particular prey algae, nor any other organism in particular, and as such, its prey remains unknown. While multiple individuals have been recorded in close proximity, mating was never observed, nor egg masses identified.

**Derivatio nominis.** *Plakobranchnus noctisstellatus* from the Latin words *noctis* (night) and *stellatus* (stellate), in reference to the small iridescent blue and green spots hidden under the dark parapodia that each resemble stars at night.

**Distribution.** *Plakobranchnus noctisstellatus* sp. nov. is known from Thailand and has been recorded under different names in Vanuatu, Indonesia, and Papua New Guinea (Gosliner et al. 2008, 2015).

**Remarks.** *Plakobranchnus papua* Meyers-Muñoz and van der Velde, 2016, was described based on morphological and molecular evidence, distinguishing it from *P. ocellatus*. Specimens of *P. papua* are characterised by an ochre body with white non-ocellated spots, black rhinophores and tail, and a foot sole without spots. Additionally, the radular teeth of *P. papua* were described as more ‘arched’ than those shown in descriptions provided of *Plakobranchnus ocellatus sensu lato*. Molecular evidence in this study sheds some light on the external variation of the species (see Discussion). Meyers-Muñoz et al. (2016) also tackled a visual comparison of multiple *Plakobranchnus* varieties that have historically been identified as *Plakobranchnus ocellatus*, including a species almost identical and likely corresponding to *Plakobranchnus noctisstellatus* sp. nov. being referred to as *Plakobranchnus ocellatus* var. I. Meyers-Muñoz et al. (2016, Table 2) also indicate that an illustration of this animal (similar to *Plakobranchnus noctisstellatus* sp. nov.) may have been provided by Gould (1852: pl. 26, fig. 407a–c, as *Placobranchnus ianthobaptus*) but Yonow and Jensen (2018) refuted this and stated that there was no resemblance between the two. We concur, in that *Placobranchnus ianthobaptus* can in fact be distinguished externally from *P. noctisstellatus* sp. nov. by its pale brown dorsal ground colour.

*Plakobranchnus noctisstellatus* sp. nov. is easily distinguished both externally and internally from both *P. papua* and *P. ocellatus*. Externally *P. noctisstellatus* sp. nov. is most easily separated from its congeners and the variants of *P. ocellatus* by its vibrant green ground colour and electric blue rhinophores and tail, and notably the dense collections of white and electric blue spots under the parapodial flaps. The presence of non-ocellated black spots, prominent laterally, and iridescent blue spots on the green foot sole also make separation between species easy. The present study suggests that rhinophore colouration in *P. papua* may vary from black (as described) to deep purple with white tips such as those from Koh Tao; however, this variation remains distinct from the electric blue tips and black band found in *P. noctisstellatus* sp. nov. While little information on rhinophore colouration was provided for *P. ocellatus* upon description, the original illustrations of the species by van Hasselt (1824) do show rhinophores that are entirely white or cream, much like specimens of *Plakobranchnus ocellatus* from Koh Tao. The range in rhinophore colouration of different morphs and synonyms of *P. ocellatus* vary from white to purple tips or bands and black lines along rhinophore edges, all of which differ from *P. noctisstellatus* sp. nov. While *Placobranchnus guttatus* Stimpson, 1855 was described as bearing a very similar dorsal colour of dark olive, the species was also described as having green ocellated spots with white rings, which are absent from *P. noctisstellatus* sp. nov.

The reproductive system of *P. ocellatus* is distinguished from that of *P. noctisstellatus* sp. nov. by having two bursae copulatrix, a bilobed mucus gland (not rounded), and much smaller ovotestis (follicles). Compared to that of *P. papua*, the reproductive system of *P. noctisstellatus* sp. nov. shows a smaller stylet and much larger acorn-shaped penial bulb, lacking the groove observed in *P. papua*; a curved vas deferens that rapidly decreases in thickness to become convoluted and connects to the ovotestis, the bursa copulatrix and the ampulla, that Meyers-Muñoz et al. (2016) identify as a second bursa copulatrix; the ovotestis, which Meyers-Muñoz et al. (2016) call follicles are much larger in *P. noctisstellatus* sp. nov.

The number of radular teeth seen in *P. noctisstellatus* appears similar to those of its congeners with eight in the ascending limb (eight in *P. papua* and 7–11 in *P. ocellatus* s. l.) and ten in the descending limb (seven in *P. papua* and 7–9 in *P. ocellatus* s. l.). The number of denticles per radular tooth seen in *P. noctisstellatus* sp. nov. (12 or 13) fits within the range of species described thus far (10–14 in *P. papua* and 10–13 in *P. ocellatus* s. l.); however, the overall shape of the teeth appears to show some variation among the species. The teeth of *P. noctisstellatus* sp. nov. have striations and are more curved than those of *P. papua*, which in turn was described to have teeth that appeared to be more arched than those of *P. ocellatus* by Bergh (1873) and Jensen (1997). Additionally, the denticles seen in the SEM image of *P. ocellatus* by Jensen (1992) are more prominent and proportionally larger than those seen in *P. noctisstellatus* sp. nov., which seem to be more uniform and regular in appearance. It should be noted that van Hasselt (1824) provided no information on the radula of *P. ocellatus* in the original description. Additionally, there appears to be significant plasticity in radular morphology based on diet in numerous species of Sacoglossa (Jensen 1993), but conclusive evidence pertaining

to the diet of *P. noctisstellatus* sp. nov. could not be obtained and thus requires further investigation. At Koh Tao, there are significant differences in the ecology of *P. noctisstellatus* when compared to *P. papua* and *P. ocellatus*. While the former exists exclusively in the deeper soft sediment habitats of the island, the latter species are mostly observed among coral reefs and reef flats closer to shore and the soft sediments therein.

Many of these points and observations were also made in the most recent documentation of *P. noctisstellatus* sp. nov. (as *Plakobranchus* sp.), where Yonow and Jensen (2018) also provided a tabulation comparing the morphology of all species thus far synonymised with *P. ocellatus*. Including their sightings, most observations recorded for specimens most likely being *P. noctisstellatus* sp. nov. are from Indonesia, with Gosliner et al. (2008) also recording the species from Vanuatu; therefore, specimens from the Gulf of Thailand represent the western-most range of the species so far.

### Genus *Elysia* Risso, 1818

**Diagnosis.** Body smooth to papillate, with parapodia that may cover much of the dorsal surface; however, parapodia can be highly variable and may not be held close to the body. Head differentiated from the body with eyes behind dorsal rhinophores. Dorsal sinuses usually branched, anus anterodorsal, reproductive system pseudo-diaulic or triaulic, penis normally unarmed although a hollow apical stylet may be present. Radular teeth blade-shaped ranging from denticulate to smooth.

#### *Elysia aowthai* sp. nov.

<http://zoobank.org/2605D690-FD7A-4830-8CD6-5474C050DB26>

Figures 8F–J, 9, 10A–C, 11

*Elysia* cf. *japonica*: Bass 2006 (Guam)

*Elysia amakusana*: Wägele et al. 2010 (Lizard Island, Australia)

*Elysia* sp. 1: Mehrotra and Scott 2016: fig. 2B, C (Koh Tao, Thailand)

*Elysia* cf. *japonica*: Mehrotra et al. 2019: fig. 1C (Koh Tao, Thailand)

**Type material.** **Holotype:** adult, 14 mm long (alive), collected from soft sediment habitats at 12 m depth, Leuk Bay (type locality) 10°4'15.23"N, 99°50'32.86"E, Koh Tao, Thailand, 20 December 2015, deposited in MNHN (IM-2000- 35326). **Paratype:** adult, 16 mm long (alive), collected from soft sediment habitats at 16 m depth, Tao Tong 10°3'58.13"N, 99°49'4.76"E, Koh Tao, Thailand, 19 June 2017, deposited in MNHN (IM-2000- 35327). Paratype dissected: reproductive system studied, and jaw, radula, and penis mounted for optical microscopy.

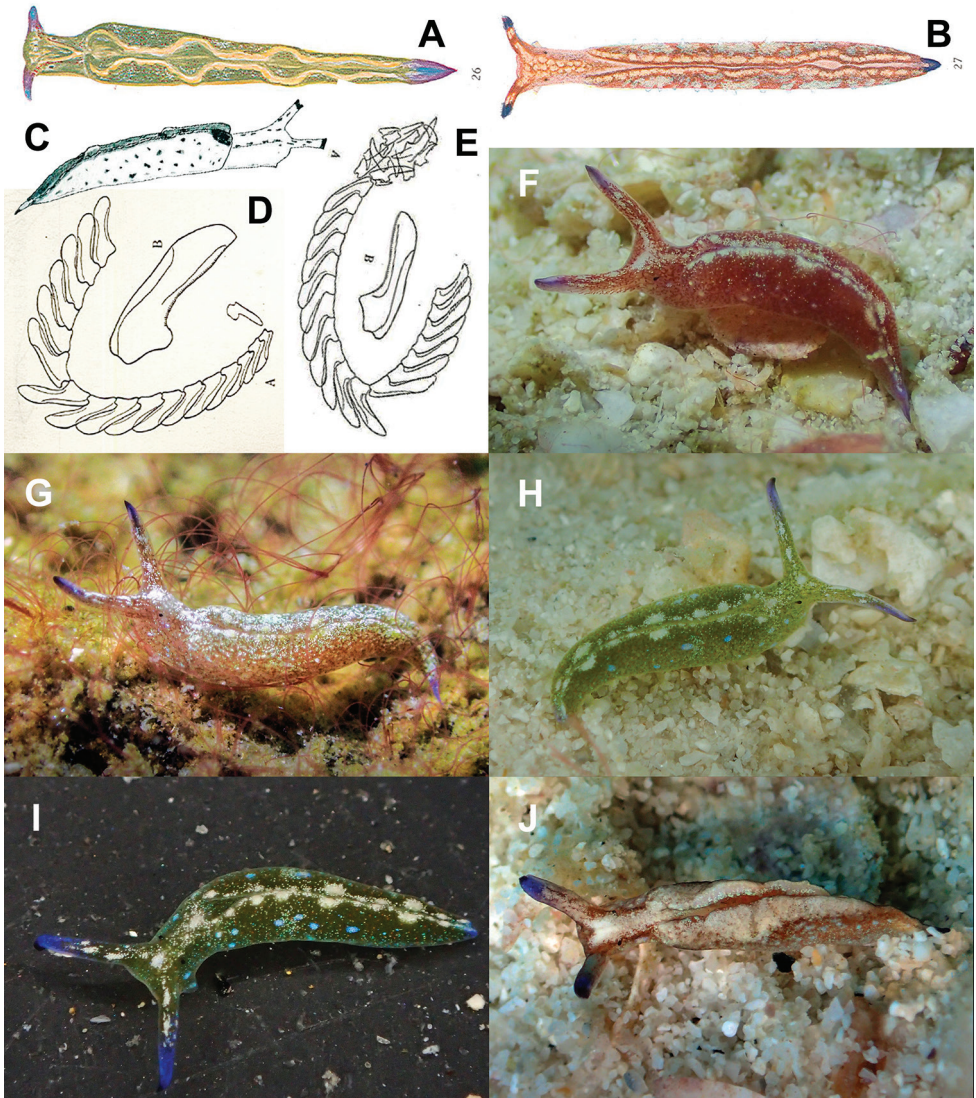


**Figure 8.** Illustrations and images of specimens belong to the *Elysia japonica* complex **A–E** illustrations taken from the original descriptions of species belonging to the *Elysia japonica* complex **A, D** *Elysia abei* Baba, 1955 **B** *Elysia amakusana* Baba, 1955 **C** *Elysia furvacauda* Burn, 1958 **E** illustration of radula of *Elysia japonica* Eliot, 1913 by Baba (1949) **F–J** *Elysia aowthai* sp. nov. showing variation in colouration, 12 mm (**F**), 9 mm (**G**), 11 mm (**H, I**), 8 mm (**J**).

**Paratype:** adult, 14 mm long (alive), collected in silty sand at 25 m depth, Tao Tong, 10°3'58.13"N, 99°49'4.76"E, Koh Tao, Thailand, 17 February 2020, deposited in RBRG (EcjIV-NR012).

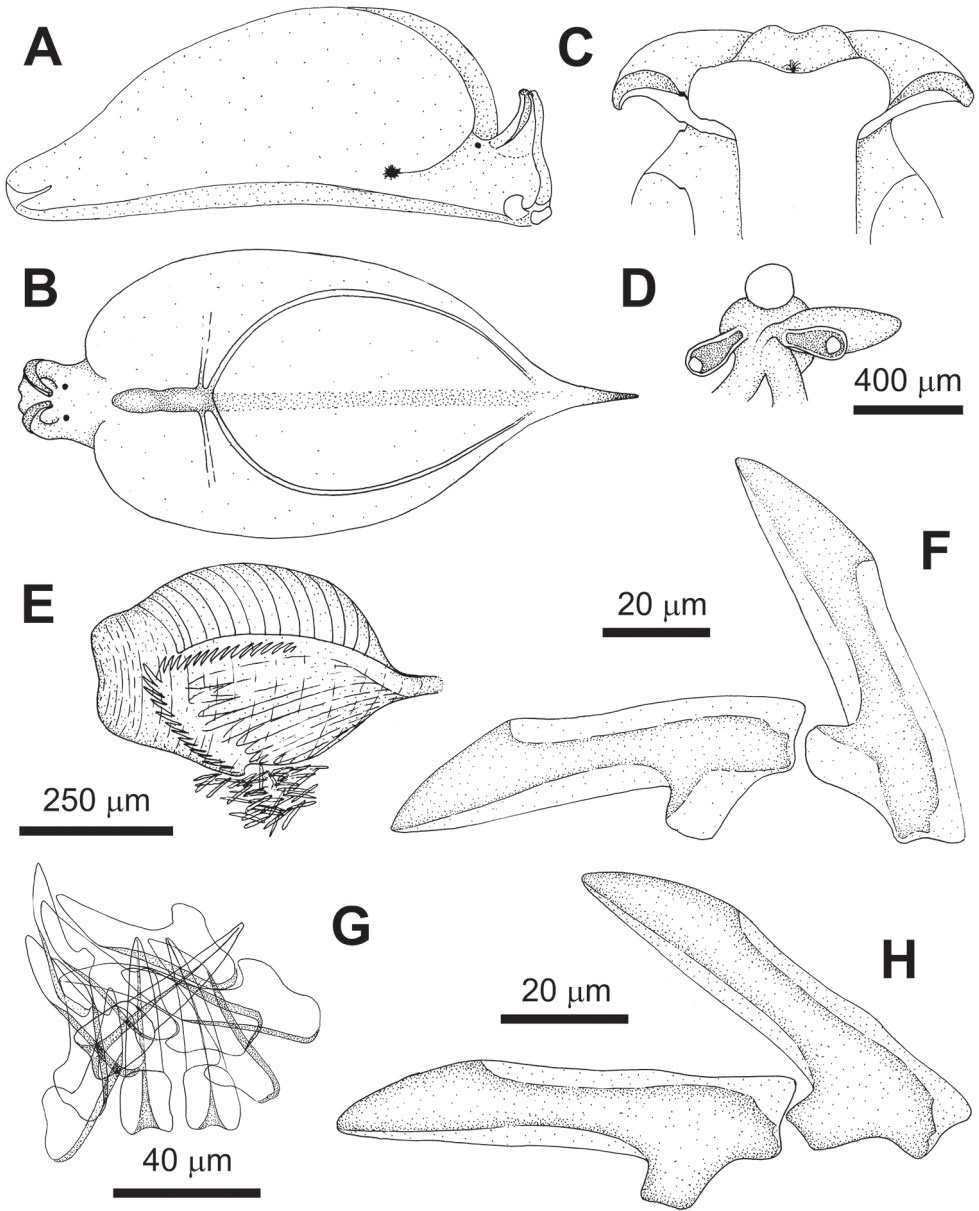


**Figure 9.** *Elysia aowthai* sp. nov., Koh Tao Thailand **A–F** 16 mm alive **A** right side view, the black dot at the end of the parapodia represents the vaginal opening **B** dorsal view, the shaded area probably being the same as that mentioned by Eliot (1913: 47) **C** ventral view with a detail of the head **D** detail of the eyes **E** buccal bulb **F** last teeth of the ascending series and active teeth **G, H** 10 mm alive **G** ascus **H** last teeth of the ascending series and active teeth.

**Supplementary observations.** More than 100 individuals, ranging in size 5 mm–16 mm, observed in regular diving surveys between 2012 and 2019, Leuk Bay 10°4'15.23"N, 99°50'32.86"E; Suan Olan Artificial Reef 10°4'6.70"N, 99°50'26.29"E; Shark Bay 10°3'39.75"N, 99°50'4.43"E; Tao Tong 10°3'58.13"N, 99°49'4.76"E; Sai Nuan 10°4'43.24"N, 99°48'48.51"E; Twins 10°7'1.93"N, 99°48'44.26"E; Hin Wong Bay 10°6'12.30"N, 99°50'58.63"E; Laem Tien 10°5'19.13"N, 99°51'17.64"E Koh Tao, Thailand; not collected.

**Description.** Length alive up to 16 mm. Body translucent white, with tips of rhinophores deep blue to purple, fading to the base and lacking tubules of digestive gland. Opaque white specks all over the body, concentrated on the edge of parapodia, renopericardial prominence, and dorsal surface of head and rhinophores. Digestive gland variable from reddish brown to light green, forming a characteristic reticulated pattern of thin tributaries. Eyes black, conspicuous, comma-shaped, behind rhinophores, bearing 75 µm diameter lentil-shaped crystalline lenses. Rhinophores long, pointed at the tip, with groove along entire length. Lateral groove on right side from anterior border of right parapodium to foot. Foot's transversal groove at same height as end of lateral groove, very subtle, almost invisible, dividing foot in two. Anterior foot corners slightly extended (in preservation), bluntly pointed. Body and parapodia in some specimens with sparse small papillae which disappear upon preservation. Tail pointed, extending beyond parapodia (Fig. 8).

**Renopericardial** prominence long and narrow, oval anteriorly, slightly constricted in the middle, and straight posteriorly. Posterior end with two pairs of major dorsal sinuses: first short, perpendicular, fading at the middle of the parapodium; second long, oblique, curved, orientated towards but not reaching edge of parapodium, ending before the tail. Area between second pair of dorsal sinuses appearing translucent in preserved specimens (Fig. 9B) and probably corresponding to the 'smooth trench' mentioned by Eliot (1913: 47) describing *E. japonica* (KR Jensen, pers. comm.). Renal pore at anterior right side of pericardium. Anus in groove separating the right parapodium from the neck (Fig. 9).

**Buccal bulb** 500 µm long (in three 10, 15, and 16 mm long specimens). Uniserial radula with seven teeth including ghost teeth in ascending row, 8–11 in descending row. Discarded teeth driven out of buccal bulb through a short tube; 12–30 in the ascus, varied in size, some broken, stacked in several groups, some loose. Teeth narrow, blade-shaped. Cutting edges smooth or finely denticulated. Denticulation difficult to observe with the light microscope and random (Fig. 10). First teeth in ascending series 72–76 µm long, 22–25 µm high. Active teeth 71–80 µm long, 27–30 µm high. Last teeth in descending series 50–76 µm long, 20–29 µm high.

**Penis** unarmed, pseudo-conical with a narrow and curved end (chilli-shaped), 500 µm long. Vas deferens long and convoluted, passing through the mucus gland. Male genital opening below right rhinophore, next to right eye. Vagina fusiform, narrow at the extremes, passing through the mucus gland. Bursa copulatrix connected to the vagina. Mucus gland quasi-oval, translucent, 900–1000 µm long, located under the cardiac area. Ducts from the follicles, prostate, and albumen gland coming from the parapodia meet in the mucus gland, but the connections between them are unclear (Fig. 11).

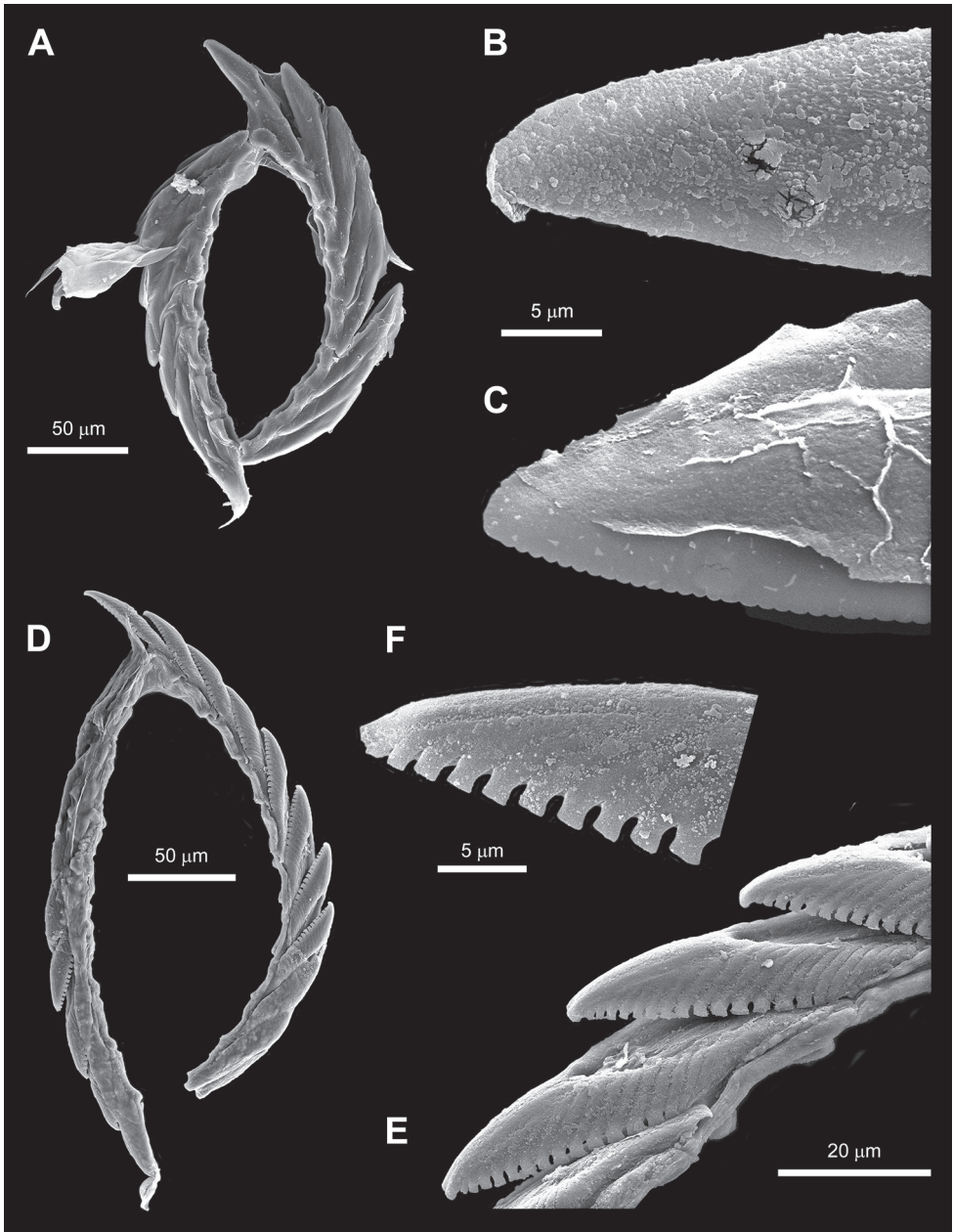


**Figure 10.** SEM images of radulae of *Elysia aowthai* sp. nov. and *Plakobranthus noctisstellatus* sp. nov. **A–C** *Elysia aowthai* sp. nov., Koh Tao, Thailand, 15 mm alive **A** general view of the radula without the ascus **B** active teeth from the radula with smooth cutting edge **C** sixth teeth of the descending series with denticulated cutting edge **D–F** *Plakobranthus noctisstellatus* sp. nov. Koh Tao, Thailand, 21 mm alive **D** general view of the radula without the ascus **E** lateral view of the descending series **F** detail of the cutting edge of a tooth.

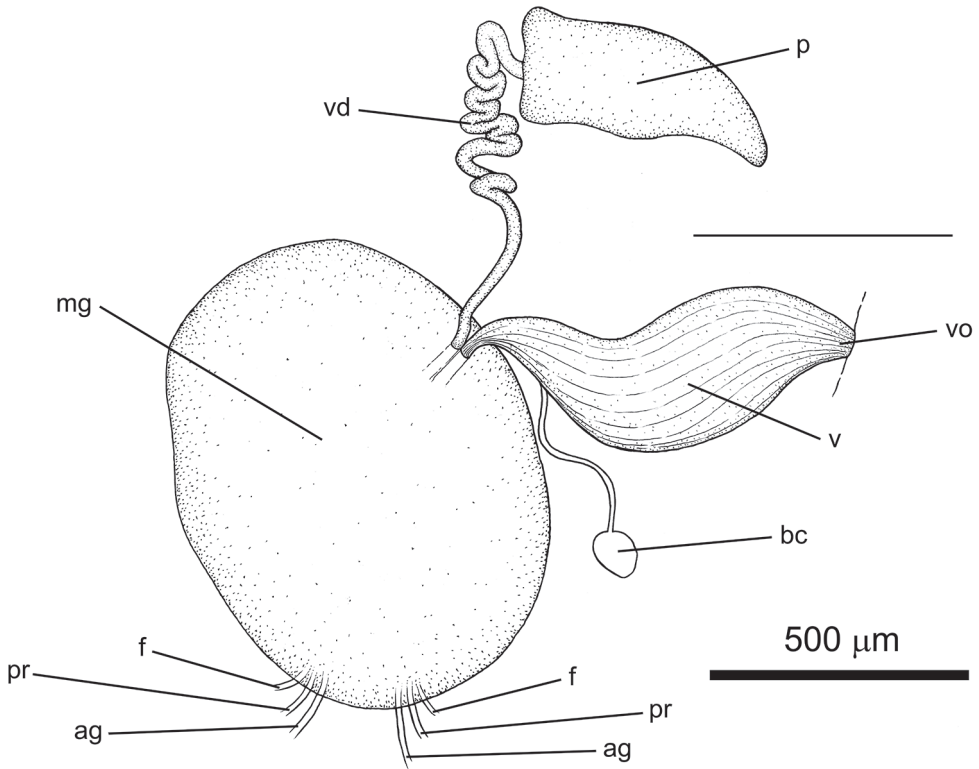


**Figure 11.** Genitalia and reproductive system of *Elysia aowthai* sp. nov., Koh Tao, Thailand, 15 mm alive. Abbreviations: ag – to the albumen gland; bc – bursa copulatrix; f – to the follicles; mg – mucus gland; p – penis; pr – to the prostate; v – vagina; vd – vas deferens; vo – vaginal opening.

**Biology.** All animals were observed year-round at different locations around the island, exclusively in deeper soft sediment habitats at Koh Tao. Animals were always found moving along the surface of the sediments, rarely stationary and with no specific ecological relationship with any other species. Not observed to be in association with any particular prey algae, but often found in the vicinity of a currently unknown filamentous red algae, which may contribute to the reddish colouration seen in most specimens. Specimens with green, brown, purple, and unpigmented digestive glands are likely due to some degree of variability in prey; however, further investigations are required. No observations were made shallower than 10 m depth or in the vicinity of coral reef or reef edge habitats, deeper observations up to 24 m.

**Derivatio nominis.** *Elysia aowthai* in reference to the type locality of the species in the Gulf of Thailand, ‘Aow Thai’ in the local vernacular language, and to honour the local populations that speak it.

**Distribution.** Gulf of Thailand (present study), Guam (as *E. cf. japonica*, Bass 2006), and Australia (as *E. amakusana*, Wägele et al. 2010) based on our molecular analyses.

**Remarks.** The general appearance of *Elysia aowthai* sp. nov. places it within the *E. japonica* species complex. The problem with this complex has its origins in the incomplete description of *E. japonica* itself, but also in the provenance of the type material and the subsequent specimens captured, sometimes associated with descriptions and illustrations and sometimes not. *Elysia japonica* was described based on preserved specimens, which makes the external anatomy and living colouration very difficult to untangle, collected from an unknown location in Japan. The complete description by Eliot (1913) is as follows:

“18 specimens. Locality – unknown. The largest is about 20 mm long and the wings are moderately ample. In two specimens which were dissected, the radula was found to contain 5 teeth in the ascending row, 15 in the descending and about 20 more various sizes lying in a heap. The structure and the shape of the teeth is as usual in the genus. No denticles are to be seen. I think that this form is probably a new species distinguished by the following characters:

1) Colour: In all specimens, the rhinophores and the tip of the tail are conspicuously black or dark brown. Otherwise the colour is uniform and in the best preserved specimens is yellowish brown. The wings have no coloured borders and the head and the pericardium are of the same colour as the dorsal surface.

2) The arrangement of the dorsal surface. This is similar in all specimens and I have not seen it in any other species. The pericardium is not ovate but is constricted in the middle. Its length is greater than its breadth but it is short in comparison with the length of the whole animal. The dorsal ridges which run into it are very distinct and the two hindmost, which run backwards towards the tail, are parallel to one another and enclose an area which is differentiated from the back and forms a smooth trench.”

The first illustration showing the external anatomy of a specimen assumed to be *Elysia japonica* was provided by Baba (1949), with a description of the species. However, this was later changed in a supplement to the previous paper wherein the same specimen (Baba 1949: plate IX, fig. 27) was reidentified and claimed as a new species (Baba 1955), *Elysia amakusana* Baba, 1955, based exclusively on the presence of finely denticulated teeth, which are (theoretically) not present in *E. japonica*. Also, in the same supplement, Baba described *Elysia abei* Baba, 1955, which also has finely denticulated teeth but is differentiated by being green in colour with fine orange-red spots (Baba 1949: plate VIII, fig. 26; Baba 1955). Afterwards, however, Baba determined all three species as valid in a summarised inventory of *Elysia* species from Japan (Baba 1957). A year later, *Elysia furvacauda* Burn, 1958 was described from Australia (Burn 1958), based entirely on the external anatomy (therefore lacking any mention of radular detail), as a red-brown animal with small blue spots and rhinophores, and tail tipped in black. The type material for this species was reported as lost by Jensen (1985), but it is actually deposited in Museums Victoria Collections (MVC 2020, registration number F19467) (KR Jensen, pers. comm.).

Subsequently, Marcus (1980) and later Jensen (1985) both pointed out the similarity in radular teeth between *E. amakusana* and *E. abei*, with Jensen providing a description of three different colour morphs of *E. japonica* from Hong Kong, a comprehensive analysis of the taxonomic confusion to date, and concluding that *E. amakusana* and *E. abei* are junior synonyms of *E. japonica*. Importantly, Jensen showed that the morphology of specimens of three different external colourations was remarkably similar and

that radular teeth have ‘blunt tips and are finely serrulate’. Between 1999 and 2002, discussions on the Sea Slug Forum (hosted by the Australian Museum) between Rudman, Jensen, and others (Rudman 2001) generally supported the view that some or all of *E. abei*, *E. amakusana*, and *E. japonica* were likely synonyms, although Rudman suggested that the name *Elysia japonica* may need to be abandoned due to the lack of type material or information on the type locality. Burn (2006) restated that *E. furvacauda* was distinct from *E. japonica* which was supported by an external illustration of the former (Fig. 8), although no internal anatomy was discussed. Trowbridge et al. (2010, 2011) also discussed in detail the complexity and need for clarification between these species.

The first molecular evidence on any species in the complex was provided by Händeler and Wägele (2007), who sequenced a portion of the mitochondrial 16S rRNA for a species they called *Elysia amakusana* (from Australia) as part of a larger analysis. While this analysis provided no illustration, description, or discussion of the species in particular, an illustration of a specimen identified as *E. amakusana* from Lizard island (Australia) was published a year before by the second author (Wägele et al. 2006: 41, fig. 8H), with this specimen looking similar to *Elysia aowthai* sp. nov. A more thorough molecular assessment regarding the presently discussed species was later provided by Takano et al. (2013), where a comparison between specimens they considered representative of *E. abei*, *E. amakusana*, and *E. cf. japonica* was carried out. These authors provided colour photographs of *E. abei* and *E. amakusana* from Japan (Takano et al. 2013: fig. 3A, B) matching Baba’s (1949: plate VIII, fig. 26; plate IX, fig. 27) illustrations. Takano et al. (2013: fig. 3C) also provided an illustration of a specimen determined as *E. cf. japonica* from Japan that matches the general appearance of a species in the complex of *E. japonica*, and shows a character that could have gone unnoticed in the original description of the species due to the state of preservation of the specimens: big rounded blotches of orange pigment (different from the orange dots of *E. abei*). In their analysis, these authors concluded that *E. abei* and *E. amakusana* were likely synonyms despite their morphological variability, but *E. cf. japonica* appeared distinct. Takano’s et al. (2013) species identifications were based on external colouration and morphology alone. However, if the internal anatomy of their *E. cf. japonica* would match that of the original description, *E. japonica* could be re-described, which would help to clarify the taxonomic/systematic problems around the species complex in the area. Nonetheless, the fact is that there are at least two lineages in Japan corresponding to the external morphology of *E. abei*/*E. amakusana* and (potentially) *E. japonica*. An extensive phylogeny by Krug et al. (2015) showed specimens determined as *E. abei* (Japan), *E. amakusana* (Australia), and *E. furvacauda* (Australia) as distinct species, clustered with species they call *Elysia* sp. 5 (Hawaii) and *Elysia* sp. 30 (Japan), but again the external anatomy of the species is not shown nor discussed, which makes it impossible to draw conclusions on the validity of the different taxa.

After this review it seems clear that, within the complex, several groups may be present based on the external anatomy: one composed of specimens similar to *E. abei* / *E. amakusana* with a wide range of morphological variability, another with unclear characteristics belonging to *E. japonica sensu stricto*, and a third including *E. furvacauda*. However, the reliability of species delimitation using external colouration in this group is questionable when used alone.

On the other hand, the integrated analysis of the COI of numerous species/specimens within the complex conducted here reveals a clear geographical structure. There are at least two separate lineages in Japan (Fig. 2, clade D) corresponding to the true *E. abei*/*E. amakusana* group and (potentially) to the true *E. japonica sensu stricto* (whose type appears to be lost: Trowbridge et al. 2011). The remainder of the groups within the complex (Fig. 2, clades A–C) include *E. furvacauda* from Australia and at least two undescribed species within the range of morphological variability observed for *E. abei*/*E. amakusana* scattered in the Indo-West Pacific (I-WP).

In this work, to contribute to the untangling of the *E. japonica* complex, we describe one of these apparently widely distributed species scattered in the I-WP, *E. aowthai* sp. nov., by providing detailed morphological (external and internal) and molecular evidence. Future findings including precise sampling coordinates, complete diagnoses, colour images, and molecular data will resolve the identities of the members of this species complex and its distribution.

Despite the fact that the radular teeth of *E. aowthai* sp. nov. are indeed finely serrated, two points must be noted: these appear to be rapidly worn away with use leaving smoother edges in older teeth, and this feature is not visible under light microscopy alone and required the use of SEM observations to confirm their presence. Hence, the use of this feature alone does not have enough diagnostic significance in distinguishing the species of the complex.

*Elysia aowthai* sp. nov. is not conspecific to the specimens studied by Jensen (1985) from Hong Kong and determined as *E. japonica*: there are some differences that should be noted such as the morphology of the pericardium which is shorter, wider, and bearing four anastomosed dorsal sinuses in Jensen's specimens, and the shape of the teeth, which are blade-shaped in *E. aowthai* sp. nov. instead of having the rounded blunt tips observed in Jensen's specimens (Jensen 1985: fig. 2C) which appear significantly more rounded than those of *E. aowthai* sp. nov. The reproductive apparatus of Jensen's (1985) specimens were described as 'very similar' to that of *Elysia verrucosa* Jensen 1985, but this statement is insufficient to establish any comparison.

## Discussion

### *Plakobranchus*

*Plakobranchus noctisstellatus* sp. nov. is externally distinctive among its currently described congeners as the only species with bright electric-blue spots under the parapodia and without a pale external colouration. Molecular evidence further supports its distinction from all other species and variants of *Plakobranchus* currently known and places it basal to the rest of the genus. The ecology of the species at its type locality also distinguishes it from *P. ocellatus* and *P. papua* which both appear to favour well-lit shallower (often intertidal) sandy habitats and coral reefs whereas *P. noctisstellatus* sp. nov. is exclusively found beyond the reef slope in deeper soft sediment habitats. There remain several aspects unknown about its biology, including its larval type and ontogenetic development. Its

habitat preference probably plays an important role in its diet and its potential for (or a lack of) kleptoplasty, which is already thoroughly documented in *Plakobranchnus ocellatus* s. l. (Maeda et al. 2012; Christa et al. 2013; Wade and Sherwood 2016).

The recent inventory from Koh Tao (Mehrotra and Scott 2016) documented numerous new sacoglossan records for the Gulf of Thailand. These authors were, however, unable to locate specimens of *P. noctistellatus* sp. nov. due to its absence from shallower reefs and sandy habitats, although they were able to find and record another species of the genus which was misidentified as *Plakobranchnus ianthobaptus* Gould, 1852. The same species has in fact been referred to as *Plakobranchnus* sp. and *Plakobranchnus* cf. *papua* by Mehrotra et al. (2015, 2019) in observations of predation. Although *Plakobranchnus ianthobaptus* has long been considered a synonym of *Plakobranchnus ocellatus* van Hasselt, 1824 (see Jensen 1992; Evertsen et al. 2007 and others). *Plakobranchnus ocellatus* in turn has been recognised as a species complex (Christa et al. 2013; Krug et al. 2013; this paper). The recent description of *Plakobranchnus papua* Meyers-Muñoz and van der Velde, 2016 included an in-depth comparison between the original descriptions of *P. ocellatus* and *P. ianthobaptus*, thus providing the clearest assessment of the latter to date (Meyers-Muñoz et al. 2016).

## *Elysia*

Utilising an integrated approach, combining molecular evidence with a wider understanding of morphological variation, we clarify the identity of a previously documented species as *Elysia aowthai* sp. nov. The wide range of external variation of the species belonging to the complex surrounding *Elysia japonica* highlights the need for a further integrative molecular and morphological investigation into externally similar specimens from Hong Kong, Guam, Australia, Hawaii, and Japan. This should also include similar and undescribed species such as those mentioned by Trowbridge et al. (2010), Takano et al. (2013), and Burn (2006). The variability in colouration is most likely driven by dietary shifts and preferences and is well documented in sea slugs (Harris 1970; Millen and Hermosillo 2012; Ekimova et al. 2017) with variation in sacoglossans usually being driven by the breakdown of ingested products (Jensen 1992; Laetz and Wägele 2018). Jensen (1992) suggested that the pigmentation of some species of *Elysia* with darker colours such as brown and purple may be due to the degradation of algal metabolites as they typically feed on plants with cellulose cell walls such as the Cladophorales.

Specimens of the *Elysia japonica* complex have been documented to be associated with the algae of the genera *Cladophoropsis* (Jensen 1993), *Chaetomorpha* (Jensen 1985; Takano et al. 2013), *Cladophora* (Takano et al. 2013), *Codium*, and *Bryopsis* (Krug et al. 2013). Interestingly, Christa et al. (2014) also identified the algae *Halimeda* sp. as prey for *Elysia amakusana*, but no information was provided on the predator specimen itself, so its precise identity is not clear. The radular morphology provided in the present description of *E. aowthai* sp. nov. does agree with the inferences of structural variation in radulae being based on diet (Jensen 1993) in turn based on the dietary trends documented for the different species in the complex. Furthermore, the discovery of some radular teeth with fine median denticulation along the cutting edge and others lacking it bridges the

single difference used in Baba's descriptions of *E. abei* and *E. amakusana* leaving only one reliable differentiating characteristic: although the tips of the teeth of *E. aowthai* sp. nov. are not really pointed, they are certainly not as rounded as those of *E. japonicalabei* (Fig. 8D, E). Our results do, however, indicate a possible divergence in the clade corresponding to Japanese specimens in the complex, suggesting the presence of two distinct species; therefore, a comprehensive and integrated investigation into these will be needed to assess the identity of *E. abei* and *E. amakusana*. This further supports the need for a closer investigation on the role of dietary plasticity on radular morphology within the *Elysia japonica* complex. Recent findings have also shown that the specimens of *E. aowthai* sp. nov. from Koh Tao are relatively unpalatable to potential scleractinian predators, which may be driven by the toxicity sequestered from their prey (Mehrotra et al. 2019).

## Conclusions

The integration of ecological data, with morphology, ontogeny, and molecular evidence will contribute towards addressing the cryptic species problem increasingly striking in heterobranch sea slugs systematics (Korshunova et al. 2019). Within the Plakobranchidae, the difference in diversity between accepted species (corresponding to external variation) and those suggested by molecular evidence continues to grow. Within *Plakobranchus*, our analyses and those of Krug et al. (2013) suggest that the presently described and delineated species comprise only a third of the possible diversity indicated by molecular means. *Elysia* has also recently been shown to contain several species complexes that require a closer examination, such as *Elysia marginata*, *E. pusilla*, and *E. tomentosa* (Krug et al. 2013, 2016; Yonow and Jensen 2018). As with *Plakobranchus ocellatus* and *Elysia marginata*, evidence that the synonymisation of multiple species and morphotypes under a single name may have been premature has been documented for *Thuridilla gracilis* (Yonow and Jensen 2018; Papu et al. 2020).

Both species documented in this work, *P. noctisstellatus* sp. nov. and *E. aowthai* sp. nov., had been considered unknown or locally rare from Koh Tao until expansion of surveys into deeper soft sediment habitats. Exploration of these same habitats have recently allowed for documentation of previously undescribed species and ecology from Koh Tao (Mehrotra et al. 2017, 2019). Investigation of ecological parameters such as habitat preferences, dietary plasticity, and other interspecies interactions should be included in future attempts studies of species complexes, as they may contribute significantly in the clarification of the cryptic species problems highlighted here.

## Acknowledgements

We would like to thank the survey team for their assistance, in particular Kaitlyn Harris, Kirsty Magson, Pau Urgell Plaza, and Elouise Haskin. We are grateful for comments and input from Dr. Kathe Jensen, Dr. Nathalie Yonow, Dr. Patrick Krug, and Dr.

Bert Hoeksema on several ecological and taxonomic points. This manuscript was also greatly improved thanks to the comments from two anonymous reviewers. We would also like to sincerely thank Françoise Monniot for access provided to light microscopy facilities, and Sylvain Pont and the Plateau Technique de Microscopie Electronique of the Muséum national d'Histoire naturelle (Paris, France) for all the secondary-electron images used in this article. The first author and corresponding author received support from 100<sup>th</sup> Anniversary Chulalongkorn University Fund for Doctoral Scholarship, the 90<sup>th</sup> Anniversary of Chulalongkorn University Fund (Ratchadaphiseksomphot Endowment Fund), NRCT-JSPS Core to Core, UNESCO-IOC/WESTPAC, and UNESCO Japanese Funds-in-Trust. This study was also funded by Mubadala Petroleum (Thailand) Limited, and Conservation Diver (Registered US Charity #20183007707; <http://conservationdiver.com>).

## References

- Baba K (1949) Opisthobranchia of Sagami bay: collected by His Majesty the Emperor of Japan. In: Hattori H (Ed.) Iwanami Shoten, Tokyo, Japan, 194 pp.
- Baba K (1955) Opisthobranchia of Sagami Bay: Supplement: collected by His Majesty the Emperor of Japan. Iwanami Shoten, Tokyo, Japan, 59 pp.
- Baba K (1957) A revised list of the species of Opisthobranchia from the northern part of Japan, with some additional descriptions (with 6 text-figures). *Zoology* 13: 8–14.
- Bass A (2006) Evolutionary genetics of the family Placobranchidae (Mollusca: Gastropoda: Opisthobranchia: Sacoglossa). Ph.D. thesis. University of South Florida. <https://doi.org/10.18195/issn.0313-122x.69.2006.061-068>
- Bass A, Karl S (2006) Molecular phylogenetic analysis of genera in the family Plakobranchidae (Mollusca: Opisthobranchia: Sacoglossa). *Records of the Australian Museum Supplement* 69: 61–68. <https://doi.org/10.18195/issn.0313-122x.69.2006.061-068>
- Bergh R (1873) Neue Nacktschnecken der Südsee, malacologische Untersuchungen. *Journal des Museum Godeffroy* 1: 65–96. <https://doi.org/10.5962/bhl.title.10280>
- Bergh R (1887) Die van Hasselt'schen Nudibranchien. *Notes from the Leiden Museum* 9: 303–323.
- Burn R (1958) Further Victorian Opisthobranchia. *Journal of the Malacological Society of Australia* 1: 20–36. <https://doi.org/10.1080/00852988.1958.10673752>
- Burn R (2006) A checklist and bibliography of the Opisthobranchia (Mollusca: Gastropoda) of Victoria and the Bass Strait area, south-eastern Australia. *Museum Victoria Science Reports* 10: 1–42. <https://doi.org/10.24199/j.mvsr.2006.10>
- Christa G, Händeler K, Schäberle T, König G, Wägele H (2014) Identification of sequestered chloroplasts in photosynthetic and non-photosynthetic sacoglossan sea slugs (Mollusca, Gastropoda). *Frontiers in zoology* 11: 15. <https://doi.org/10.1186/1742-9994-11-15>
- Christa G, Wescott L, Schäberle T, König G, Wägele H (2013) What remains after 2 months of starvation? Analysis of sequestered algae in a photosynthetic slug, *Plakobranchus ocellatus* (Sacoglossa, Opisthobranchia), by barcoding. *Planta* 237: 559–572. <https://doi.org/10.1007/s00425-012-1788-6>

- Coleman N (2008) Nudibranchs Encyclopedia: catalogue of Asia/Indo-Pacific sea slugs. Neville Coleman's Underwater Geographic Pty Ltd., Springwood, 416 pp.
- Colgan DJ, Ponder WF, Egger PE (2000) Gastropod evolutionary rates and phylogenetic relationships assessed using partial 28S rDNA and histone H3 sequences. *Zoologica Scripta* 29: 29–63. <https://doi.org/10.1046/j.1463-6409.2000.00021.x>
- Eisenbarth J-H, Undap N, Papu A, Schillo D, Dialao J, Reumschüssel S, Kaligis F, Bara R, Schäberle T, König G, Yonow N, Wägele H (2018) Marine Heterobranchia (Gastropoda, Mollusca) in Bunaken National Park, North Sulawesi, Indonesia – Follow-Up Diversity Study. *Diversity* 10: 127. <https://doi.org/10.3390/d10040127>
- Ekimova I, Deart Y, Schepetov D (2017) Living with a giant parchment tube worm: a description of a new nudibranch species (Gastropoda: Heterobranchia) associated with the annelid *Chaetopterus*. *Marine Biodiversity* 795. <https://doi.org/10.1007/s12526-017-0795-z>
- Eliot C (1913) Japanese nudibranchs. *Journal of the College of Science, Imperial University of Tokyo* 35: 1–47.
- Evertsen J, Burghardt I, Johnsen G, Wägele H (2007) Retention of functional chloroplasts in some sacoglossans from the Indo-Pacific and Mediterranean. *Marine Biology* 151: 2159–2166. <https://doi.org/10.1007/s00227-007-0648-6>
- Folmer O, Black M, Hoeh W, Lutz R, Vrijenhoek R (1994) DNA primers for amplification of mitochondrial cytochrome c oxidase subunit I from diverse metazoan invertebrates. *Molecular Marine Biology and Biotechnology* 3: 294–299.
- Gosliner TM, Behrens D, Valdés Á (2008) Indo-Pacific nudibranchs and sea slugs: a field guide to the world's most diverse fauna. Sea Challengers Natural History Books., Gig Harbor, WA, 425 pp.
- Gosliner TM, Valdés A, Behrens D (2015) Nudibranch & sea slug identification – Indo-Pacific. New World Publications, Jacksonville, 408 pp.
- Gosliner TM, Valdés A, Behrens D (2018) Nudibranch & Sea Slug Identification – Indo-Pacific. New World Publications, Jacksonville, 451 pp.
- Hall TA (1999) BioEdit: a user-friendly biological sequence alignment editor and analysis program for Windows 95/98/NT. *Nucleic Acids Symposium Series* 41: 95–98.
- Händeler K, Wägele H (2007) Preliminary study on molecular phylogeny of Sacoglossa and a compilation of their food organisms. *Bonner Zoologische Beiträge* 55: 231–254.
- Harris L (1970) Studies on the biology of the aeolid nudibranch *Phestilla melanobranchia* Bergh, 1874. Ph.D. thesis. University of California.
- Jensen KR (1985) Annotated checklist of Hong Kong Ascoglossa (Mollusca: Opisthobranchia), with descriptions of four new species. In: Morton B, Dudgeon D (Eds) Proceedings of the 2<sup>nd</sup> International Workshop on the Malacofauna of Hong Kong and Southern China, Hong Kong, 1983. Hong Kong University Press, Hong Kong, 77–107.
- Jensen KR (1989) A new species of *Cylindrobulla* from Phuket, Thailand, with a discussion of the systematic affiliation of the genus. Phuket Marine Biological Center, Phuket, Thailand, 11 pp.
- Jensen KR (1992) Anatomy of some Indo-Pacific Elysiidae (Opisthobranchia: Sacoglossa (= Ascoglossa)), with a discussion of the generic division and phylogeny. *Journal of Molluscan Studies* 58: 257–296. <https://doi.org/10.1093/mollus/58.3.257>

- Jensen KR (1993) Morphological adaptations and plasticity of radular teeth of the Sacoglossa (= Ascoglossa) (Mollusca: Opisthobranchia) in relation to their food plants. *Biological Journal of the Linnean Society* 48: 135–155. <https://doi.org/10.1111/j.1095-8312.1993.tb00883.x>
- Jensen KR (1997) Sacoglossernes systematik, fylogeni og evolution (Mollusca, Opisthobranchia). (Systematics, phylogeny and evolution of the Sacoglossa (Mollusca, Opisthobranchia)). Vestjydsk Forlag, Copenhagen, 94 pp.
- Jörger KM, Schrödl M (2013) How to describe a cryptic species? Practical challenges of molecular taxonomy. *Frontiers in zoology* 10: 59. <https://doi.org/10.1186/1742-9994-10-59>
- Korshunova T, Mehrotra R, Arnold S, Lundin K, Picton B, Martynov A (2019) The formerly enigmatic Unidentiidae in the limelight again: a new species of the genus *Unidentia* from Thailand (Gastropoda: Nudibranchia). *Zootaxa* 4551: 556–570. <https://doi.org/10.11646/zootaxa.4551.5.4>
- Krug PJ, Vendetti JE, Ellingson RA, Trowbridge CD, Hirano YM, Trathen DY, Rodriguez AK, Swennen C, Wilson NG, Valdés AA (2015) Species selection favors dispersive life histories in sea slugs, but higher per-offspring investment drives shifts to short-lived larvae. *Systematic Biology* 64: 983–999. <https://doi.org/10.1093/sysbio/syv046>
- Krug PJ, Vendetti J, Rodriguez A, Retana J, Hirano Y, Trowbridge C (2013) Integrative species delimitation in photosynthetic sea slugs reveals twenty candidate species in three nominal taxa studied for drug discovery, plastid symbiosis or biological control. *Molecular phylogenetics and evolution* 69: 1101–1119. <https://doi.org/10.1016/j.ympev.2013.07.009>
- Krug PJ, Vendetti J, Valdés A (2016) Molecular and morphological systematics of *Elysia* Risso, 1818 (Heterobranchia: Sacoglossa) from the Caribbean region. *Zootaxa* 4148: 1–137. <https://doi.org/10.11646/zootaxa.4148.1.1>
- Kumar S, Stecher G, Tamura K (2016) MEGA7: Molecular Evolutionary Genetics Analysis version 7.0 for bigger datasets. *Molecular Biology and Evolution* 33: 1870–1874. <https://doi.org/10.1093/molbev/msw054>
- Laetz E, Wägele H (2018) How does temperature affect functional kleptoplasty? Comparing populations of the solar-powered sister-species *Elysia timida* Risso, 1818 and *Elysia cornigera* Nuttall, 1989 (Gastropoda: Sacoglossa). *Frontiers in Zoology* 15: 17. <https://doi.org/10.1186/s12983-018-0264-y>
- Maeda T, Hirose E, Chikaraishi Y, Kawato M, Takishita K, Yoshida T, Verbruggen H, Tanaka J, Shimamura S, Takaki Y, Tsuchiya M, Iwai K, Maruyama T (2012) Algivore or phototroph? *Plakobranchnus ocellatus* (Gastropoda) continuously acquires kleptoplasts and nutrition from multiple algal species in nature. *PloS ONE* 7: e42024. <https://doi.org/10.1371/journal.pone.0042024>
- Marcus ER (1980) Review of western Atlantic Elysiidae (Opisthobranchia Ascoglossa) with a description of a new *Elysia* species. *Bulletin of Marine Science* 30: 54–79.
- Mehrotra R, Arnold S, Wang A, Chavanich S, Hoeksema BW, Caballer Gutierrez M (2020) A new species of coral-feeding nudibranch (Mollusca: Gastropoda) from the Gulf of Thailand. *Marine Biodiversity* 50: 36. <https://doi.org/10.1007/s12526-020-01050-2>
- Mehrotra R, Caballer Gutierrez M, Chavanich S (2017) On the genus *Armina* (Gastropoda: Heterobranchia: Nudibranchia) in Thailand. *Marine Biodiversity* 47: 549–559. <https://doi.org/10.1007/s12526-017-0691-6>

- Mehrotra R, Monchanin C, Scott CM, Phongsuwan N, Caballer Gutierrez M, Chavanich S, Hoeksema BW (2019) Selective consumption of sacoglossan sea slugs (Mollusca: Gastropoda) by scleractinian corals (Cnidaria: Anthozoa). *PLOS ONE* 14: e0215063. <https://doi.org/10.1371/journal.pone.0215063>
- Mehrotra R, Scott CM (2016) Species inventory of sea slugs (Gastropoda: Heterobranchia) for Koh Tao, Thailand, with 25 first records for Thai waters. *Marine Biodiversity* 46: 761–771. <https://doi.org/10.1007/s12526-015-0424-7>
- Mehrotra R, Scott CM, Rohrer J, Hoeksema B (2015) Predation on a sacoglossan gastropod by a mushroom coral. *Coral Reefs* 34: 517. <https://doi.org/10.1007/s00338-015-1285-z>
- Mercier A, Hamel J-F (2005) Note on the association between *Plakobranchnus ocellatus* (Mollusca: Gastropoda: Opisthobranchia) and *Holothuria atra* (Echinodermata: Holothuroidea). *Cahiers de biologie marine* 46: 399–402.
- Meyers-Muñoz MA, van der Velde G, van der Meij SET, Stoffels BEMW, van Alen T, Tuti Y, Hoeksema BW (2016) The phylogenetic position of a new species of *Plakobranchnus* from West Papua, Indonesia (Mollusca, Opisthobranchia, Sacoglossa). *ZooKeys* 594: 98. <https://doi.org/10.3897/zookeys.594.5954>
- Millen S, Hermosillo A (2012) Three new species of aeolid nudibranchs (Opisthobranchia) from the Pacific Coast of Mexico, Panama, and the Indopacific, with a redescription and redesignation of a fourth species. *The Veliger* 51: 145–164.
- Nabhitabhata J (2009) Checklist of Mollusca Fauna in Thailand. Office of Natural Resources and Environmental Policy and Planning, Ministry of Natural Resources and Environment, Bangkok, 576 pp.
- Ono A (2005) *Plakobranchnus* variation – how many species? Sea slug forum, Australian Museum, Sydney. <http://www.seaslugforum.net/find/13970> [10 April, 2019]
- Palumbi SR, Martin AP, Romano SL, McMillan WO, Stice L, Grabowski G (1991) The simple fool's guide to PCR. Dept. of Zoology, University of Hawaii, Honolulu.
- Papu A, Undap N, Martinez NA, Segre MR, Datang IG, Kuada RR, Perin M, Yonow N, Wägele H (2020) First study on marine heterobranchia (Gastropoda, Mollusca) in Bangka Archipelago, North Sulawesi, Indonesia. *Diversity* 12: 52. <https://doi.org/10.3390/d12020052>
- Puillandre N, Lambert A, Brouillet S, Achaz G (2012) ABGD, Automatic Barcode Gap Discovery for primary species delimitation. *Molecular ecology* 21: 1864–1877. <https://doi.org/10.1111/j.1365-294X.2011.05239.x>
- Rao KV (1960) On two opisthobranchiate molluscs, *Placobranchnus ocellatus* Hasselt and *Discodoris boboliensis* Bergh, from Indian waters not hitherto been recorded. *Journal of the Marine Biological Association of India* 3: 253–255.
- Ronquist F, Teslenko M, Mark P, Ayres D, Darling A, Höhna S, Larget B, Liu L, Suchard M, Huelsenbeck J (2012) MrBayes 3.2: efficient bayesian phylogenetic inference and model choice across a large model space. *Systematic biology* 61: 539–542. <https://doi.org/10.1093/sysbio/sys029>
- Rudman WB (2001) *Elysia* cf. *japonica* [In] Sea Slug Forum. Australian Museum, Sydney. <http://www.seaslugforum.net/showall/elyscfjapo> [17 June, 2020]
- Sheeja G, Padma Kumar K (2014) New record of *Plakobranchnus ocellatus* Van Hasselt, 1824 from Kerala Coast, India. *Indian Journal of Life Sciences* 4: 1–5.

- Takano T, Hirano YM, Trowbridge CD, Hirano YJ, Watano Y (2013) Taxonomic clarification in the genus *Elysia* (Gastropoda: Sacoglossa): *E. atroviridis* and *E. setoensis*. American Malacological Bulletin 31: 25–37. <https://doi.org/10.4003/006.031.0114>
- Tamura K, Peterson D, Peterson N, Stecher G, Nei M, Kumar S (2011) MEGA5: Molecular Evolutionary Genetics Analysis using maximum likelihood, evolutionary distance, and maximum parsimony methods. Molecular Biology and Evolution 28: 2731–2739. <https://doi.org/10.1093/molbev/msr121>
- Tanamura D, Hirose E (2016) Population dynamics of the sea slug *Plakobranchnus ocellatus* (Opisthobranch: Sacoglossa: Elysioidea) on a subtropical coral reef off Okinawa-jima Island, Ryukyu Archipelago, Japan. Zoological Studies 55.
- Trowbridge CD, Hirano YJ, Hirano YM (2010) Sacoglossan opisthobranchs on northwestern Pacific shores: *Stiliger berghi* Baba, 1937, and *Elysia* sp. on filamentous red algae. The Veliger 51: 43–62.
- Trowbridge CD, Hirano YM, Hirano YJ (2011) Inventory of Japanese sacoglossan opisthobranchs: historical review, current records, and unresolved issues. American Malacological Bulletin 29: 1–23. <https://doi.org/10.4003/006.029.0201>
- Wade R, Sherwood A (2016) Molecular determination of kleptoplast origins from the sea slug *Plakobranchnus ocellatus* (Sacoglossa, Gastropoda) reveals cryptic bryopsidalean (Chlorophyta) diversity in the Hawaiian Islands. Journal of phycology 53: 467–475. <https://doi.org/10.1111/jpy.12503>
- Wägele H, Burghardt I, Anthes N, Evertsen J, Klussmann-Kolb A, Brodie G (2006) Species diversity of opisthobranch molluscs on Lizard Island, Great Barrier Reef, Australia. Records of the Western Australian Museum, supplement 69: 33–59. <https://doi.org/10.18195/issn.0313-122x.69.2006.033-059>
- Wägele H, Deusch O, Händeler K, Martin M, Schmitt V, Christa G, Pinzger B, Gould S, Dagan T, Klussmann-Kolb A, Martin W (2011) Transcriptomic evidence that longevity of acquired plastids in the photosynthetic slugs *Elysia timida* and *Plakobranchnus ocellatus* does not entail lateral transfer of algal nuclear genes. Molecular biology and evolution 28: 699–706. <https://doi.org/10.1093/molbev/msq239>
- Wägele H, Stemmer K, Burghardt I, Händeler K (2010) Two new sacoglossan sea slug species (Opisthobranchia, Gastropoda): *Ercolania anneyleorum* sp. nov. (Limapontioidea) and *Elysia asbecki* sp. nov. (Plakobranchoidea), with notes on anatomy, histology and biology. Zootaxa 2676: 1–28. <https://doi.org/10.11646/zootaxa.2676.1.1>
- Yonow N (2012) Opisthobranchs from the western Indian Ocean, with descriptions of two new species and ten new records (Mollusca, Gastropoda). ZooKeys 197: 1–130. <https://doi.org/10.3897/zookeys.197.1728>
- Yonow N, Jensen KR (2018) Results of the Rumphius Biohistorical Expedition to Ambon (1990). Part 17. The Cephalaspidea, Anaspidea, Pleurobranchida, and Sacoglossa (Mollusca: Gastropoda: Heterobranchia). Archiv für Molluskenkunde International Journal of Malacology 147: 1–48. <https://doi.org/10.1127/arch.moll/147/001-048>

## Supplementary material 1

### *Plakobranchnus* COI topology difference

Authors: Rahul Mehrotra, Manuel Caballer Gutiérrez, Chad M. Scott, Spencer Arnold, Coline Monchanin, Suchana Chavanich

Data type: Phylogeny

Explanation note: *Plakobranchnus* COI topology difference – Maximum Likelihood (left) and Bayesian Inference (right) phylogenetic analyses of the cytochrome oxidase 1 gene provide very similar topologies. Differences in node and branch placement are here highlighted using Fig. 3 as a baseline for comparison.

Copyright notice: This dataset is made available under the Open Database License (<http://opendatacommons.org/licenses/odbl/1.0/>). The Open Database License (ODbL) is a license agreement intended to allow users to freely share, modify, and use this Dataset while maintaining this same freedom for others, provided that the original source and author(s) are credited.

Link: <https://doi.org/10.3897/zookeys.969.52941.suppl1>

## Supplementary material 2

### *Plakobranchnus ocellatus* mating

Authors: Rahul Mehrotra, Manuel Caballer Gutiérrez, Chad M. Scott, Spencer Arnold, Coline Monchanin, Suchana Chavanich

Data type: multimedia

Explanation note: *Plakobranchnus ocellatus* mating – Two individuals of *Plakobranchnus ocellatus* at Koh Tao, Thailand, exhibit trailing and mating behaviour.

Copyright notice: This dataset is made available under the Open Database License (<http://opendatacommons.org/licenses/odbl/1.0/>). The Open Database License (ODbL) is a license agreement intended to allow users to freely share, modify, and use this Dataset while maintaining this same freedom for others, provided that the original source and author(s) are credited.

Link: <https://doi.org/10.3897/zookeys.969.52941.suppl2>

### Supplementary material 3

#### *Plakobranchnus papua* mating

Authors: Rahul Mehrotra, Manuel Caballer Gutiérrez, Chad M. Scott, Spencer Arnold, Coline Monchanin, Suchana Chavanich

Data type: multimedia

Explanation note: *Plakobranchnus papua* mating – Two individuals of *Plakobranchnus papua* at Koh Tao, Thailand, exhibit trailing and mating behaviour.

Copyright notice: This dataset is made available under the Open Database License (<http://opendatacommons.org/licenses/odbl/1.0/>). The Open Database License (ODbL) is a license agreement intended to allow users to freely share, modify, and use this Dataset while maintaining this same freedom for others, provided that the original source and author(s) are credited.

Link: <https://doi.org/10.3897/zookeys.969.52941.suppl3>



# A new species of *Indoganodes* Selvakumar, Sivaramakrishnan & Jacobus, 2014 (Ephemeroptera, Teloganodidae) from Sri Lanka

Alexander V. Martynov<sup>1</sup>, Dmitry M. Palatov<sup>2,3</sup>

**1** National Museum of Natural History, National Academy of Sciences of Ukraine, Bohdan Khmelnytsky str., 15, 01030, Kyiv, Ukraine **2** Department of Hydrobiology, Biological Faculty, Moscow State University, Leninskie Gory 1/12, 119234, Moscow, Russian Federation **3** A.N. Severtsov Institute of Ecology and Evolution of the Russian Academy of Sciences, Leninskij prosp. 33, 119071, Moscow, Russian Federation

Corresponding author: Alexander V. Martynov ([martynov\\_av@ukr.net](mailto:martynov_av@ukr.net); [centroptilum@gmail.com](mailto:centroptilum@gmail.com))

---

Academic editor: L. Pereira-da-Conceicao | Received 1 July 2020 | Accepted 31 August 2020 | Published 17 September 2020

---

<http://zoobank.org/1EA8A868-0DA8-4146-99EE-F97E7D29263F>

---

**Citation:** Martynov AV, Palatov DM (2020) A new species of *Indoganodes* Selvakumar, Sivaramakrishnan & Jacobus, 2014 (Ephemeroptera, Teloganodidae) from Sri Lanka. ZooKeys 969: 123–135. <https://doi.org/10.3897/zookeys.969.56025>

---

## Abstract

A new species, *Indoganodes tschertoprudi* **sp. nov.** is described from Sri Lanka. The genus *Indoganodes* Selvakumar, Sivaramakrishnan & Jacobus, 2014 was previously known only by one species from the Western Ghats (India). The new species differs from *Indoganodes jobini* Selvakumar, Sivaramakrishnan & Jacobus, 2014 by the number of denticles on the claws, shape of the femora, shape of the chalazae on the femora, absence of any median tubercles on the terga, and presence of posterolateral processes only on segments VI–IX. The diagnosis of *Indoganodes* is also emended. Morphological larval affinities of *Indoganodes* and *Ephemereolina* Lestage, 1924 and the probable origin and diversification of *I. tschertoprudi* **sp. nov.** are discussed.

## Keywords

Indomalayan realm, larva, mayflies, Pannota, type material

## Introduction

Teloganodidae Allen, 1965 is a relatively small family distributed within the Indomalayan realm and southern part of the Afrotropical realm. Endemism is typical for this family, and the many of species in the family have a restricted distribution. Moreover,

the Afrotropical and Indomalayan realms are represented by different genera. Four genera of the family occur in Indomalayan realm: *Teloganodes* Eaton, 1882, *Dudgeodes* Sartori, 2008, *Derlethina* Sartori, 2008, and *Indoganodes* Selvakumar, Sivaramakrishnan & Jacobus, 2014. The family Teloganodidae in the Indomalayan region is currently undergoing a detailed investigation; 22 species and three of four genera mentioned above were described during last 12 years (Sartori et al. 2008; Selvakumar et al. 2014; Anbalagan et al. 2015; Martynov et al. 2016; Garces et al. 2020). The most important progress in the investigation of the group within the region was made by Sartori et al. (2008) who published a revision of Oriental Teloganodidae.

Until now, the genus *Indoganodes* was known only from the Western Ghats (India) and only by the larval stage of the sole species, *Indoganodes jobini* Selvakumar, Sivaramakrishnan & Jacobus, 2014.

In this paper, a new species of *Indoganodes* from Sri Lanka is described based on the larval stage. Detailed observations of the larval features of this new species and its comparison with *I. jobini*, the type species from southern India, allows for the emendation of the generic diagnosis.

## Material and methods

All material were preserved in 80–95% EtOH; some paratypes were mounted with Canada balsam on slides.

Administrative districts and geographical coordinates of localities are given according to Google Earth (<http://earth.google.com>). Photographs were made using a Canon Power Shot A 630 with Ulab XY-B2T microscope in the National Museum of Natural History, National Academy of Sciences of Ukraine (NMNH NASU) and Leica Z16 APO equipped with Leica DFC450 Digital Camera in the I.I. Schmalhausen Institute of Zoology, National Academy of Sciences of Ukraine. Photographs were subsequently processed with LAS Core 3.8 and Helicon Focus.

The type material now is housed in the NMNH NASU in the collection of first author. The inventory numbers (IN) of slides and samples are 672, 673 (*Sri1Insp*) and 674 (*Sri2Insp*).

## Results and discussion

### Taxonomy

#### *Indoganodes tschertoprudi* sp. nov.

<http://zoobank.org/1BC57DCC-5D00-4EB8-8878-14230D74CB06>

Figures 1–5

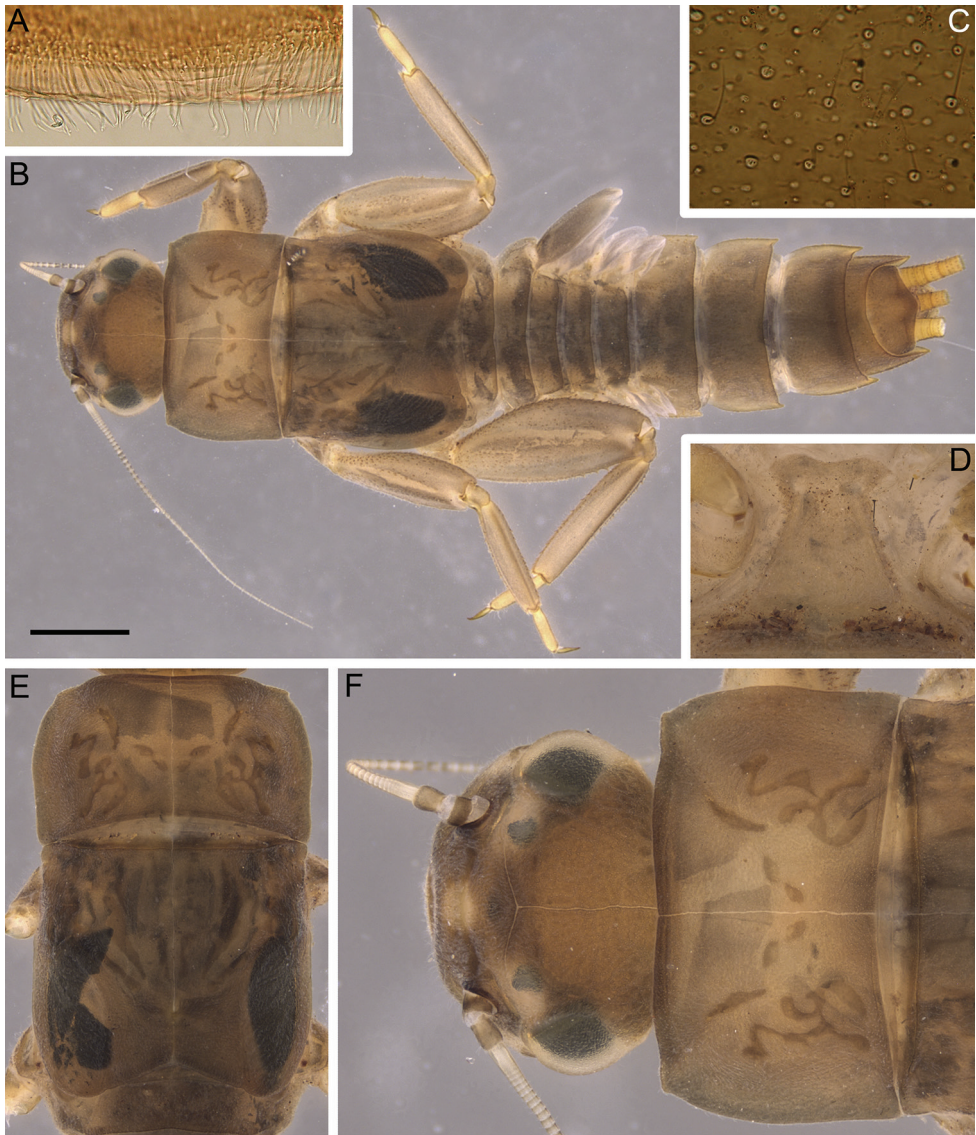


**Figure 1.** *Indoganodes tschertoprudi* sp. nov., larva, type specimens **A** irregular row of stout setae on anterior margin of clypeus, dorsal view **B** total view of larva **C** head surface **D** prosternum, ventral view **E** thorax, dorsal view **F** head and prothorax, dorsal view. Scale bar: 1 mm.

**Material. Holotype:** larva (slide 672, mounted with Canada balsam), Sri Lanka, border of Central and Sabaragamuwa provinces, vicinity of Marathenna village, mountain slope, helocrene in valley of large stream, 6.751333, 80.686167, 1390 m a.s.l., Chertoprud M.V. leg., 5.ii.2017 – *IN Sri1Ingsp.* **Paratypes:** 1 larva (slide 673, mounted with Canada balsam), *ibid.*, Chertoprud M.V. leg., 5.ii.2017 – *IN Sri1Ingsp.* 1 larva (in slide 674 with Euparal), Sri Lanka, Central Province, vicinity of Holmwood Estate, stream

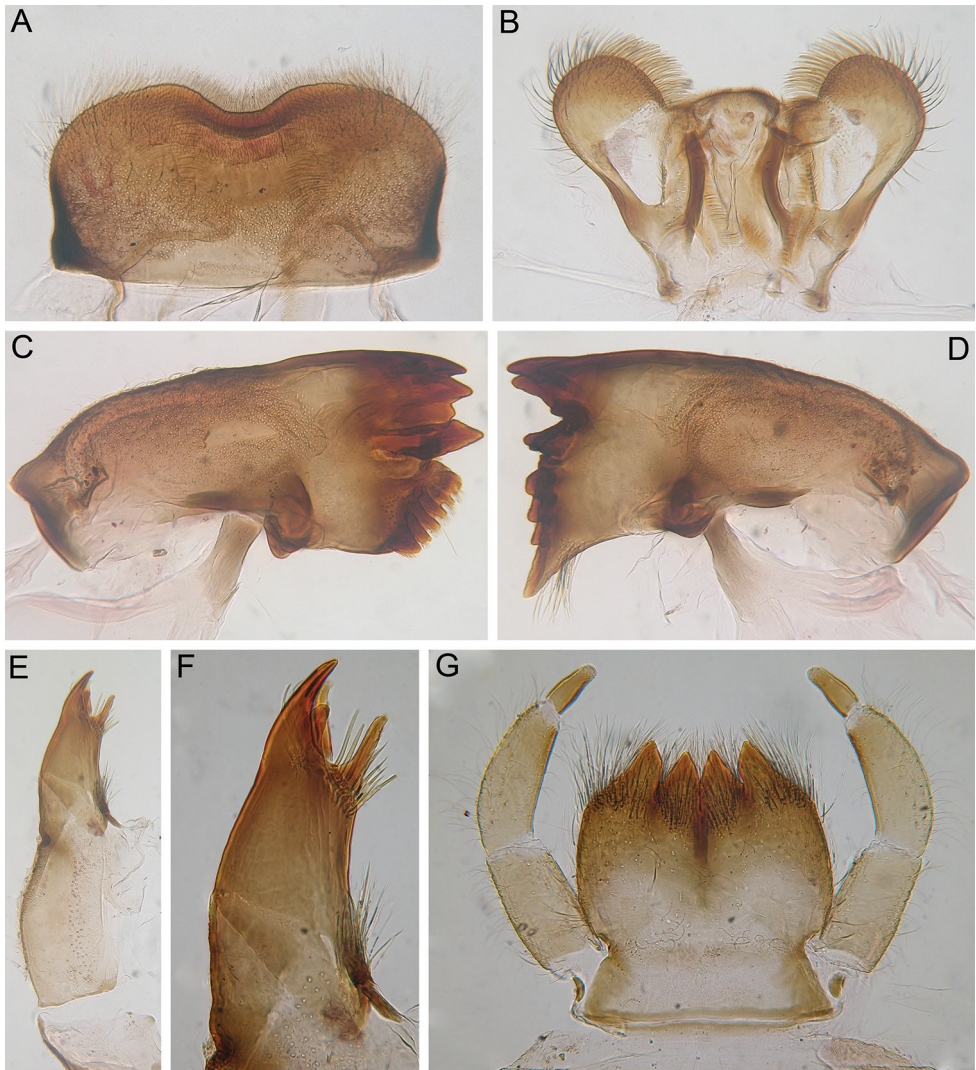


**Figure 2.** *Indoganodes tshertoprudi* sp. nov., larva, type specimens **A** labrum **B** hypopharynx **C** left mandible **D** right mandible **E** maxilla **F** apical half of maxilla **G** labium.

(section with almost no current), 6.826389, 80.724444, 1660 m a.s.l., Chertoprud M.V. leg., 4.ii.2017 – *IN Sri2Insp*.

**Etymology.** This species is named after Dr Mikhail V. Chertoprud (Moscow, Russia), who provided the material for this study.

**Diagnosis.** *Indoganodes tshertoprudi* sp. nov. can be distinguished from the only other known representative of *Indoganodes*, *I. jobini*, by the following combination of characters: (i) tarsal claw with row of 5–8 large, blunt denticles and several (1–3) small, pointed denticles among the large ones (Fig. 3G, H); (ii) several distinct small

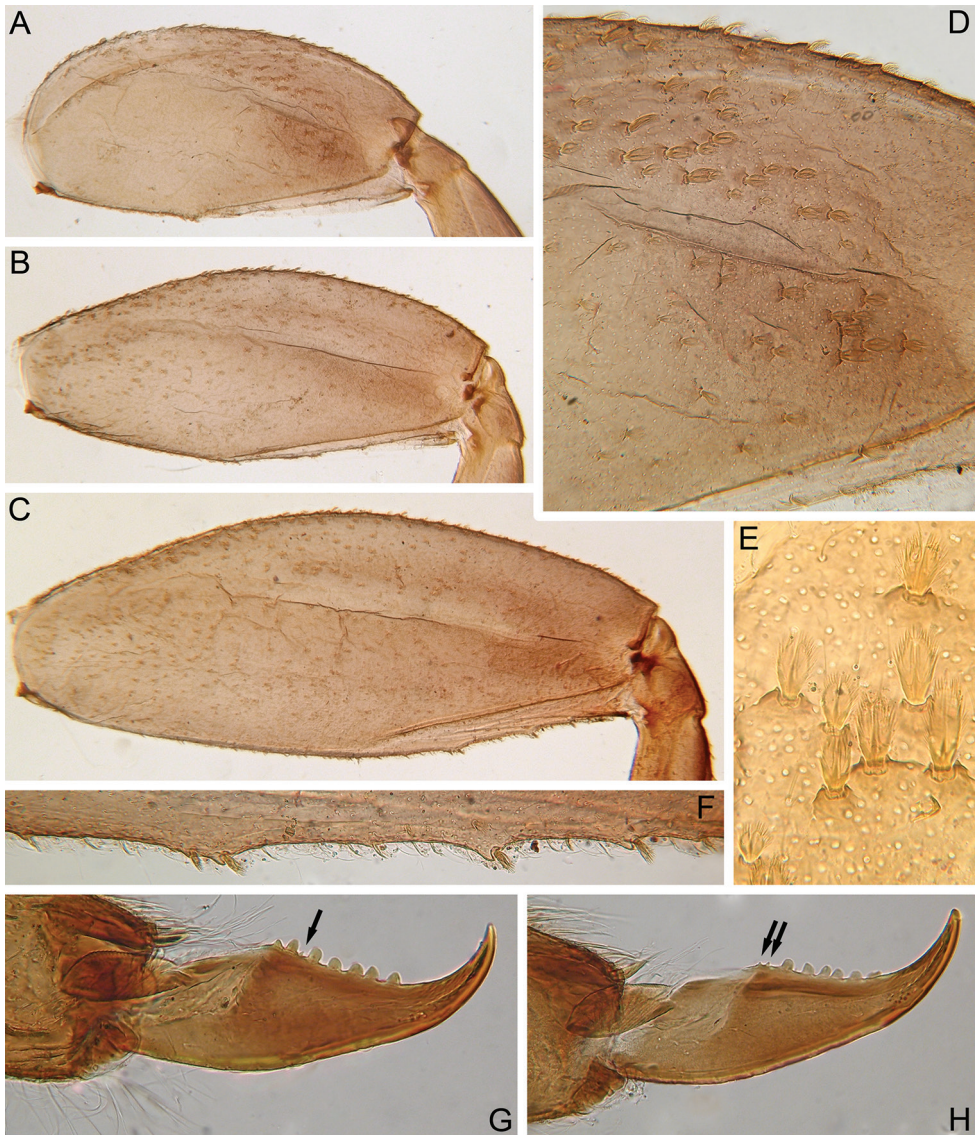


**Figure 3.** *Indoganodes tschertoprudi* sp. nov., larva, type specimens **A** fore femur, dorsal view **B** middle femur, dorsal view **C** hind femur, dorsal view **D** transversal band of stout setae on fore femur, dorsal view **E** stout setae of dorsal surface of fore femur **F** chalazae with stout setae on inner margin of hind femur **G, H** tarsal claws.

chalazae bearing stout setae present only in distal part of inner margin of hind femur (Fig. 3C, F); (iii) shape of femora (Fig. 3A–C); (iv) posterolateral processes present only on segments VI–IX, all of them moderately developed (Fig. 5B); (v) posterior margins of all abdominal terga without any median tubercles (Fig. 5A).

**Description. Larva:** body length 8.7–12.5 mm; caudal filaments partially detached, their length ratio to body unknown, paracercus not rudimental. Body light brown (Fig. 1B); head with yellow spots with unclear margins under ocelli; pronotum and mesonotum with several brown smudges (Fig. 1F); legs light brown; ventral side of body dirty yellow to light brown, without any distinct coloration.

**Head.** Genae small; head without any protuberances; surface of head covered with small hair-like setae and small scale sockets (Fig. 1C); anterior margin of clypeus with dense irregular row of long, stout, hair-like setae with divided apex (Fig. 1A). Labrum (Fig. 2A): wide, anterolateral angles rounded; anterior margin with shallow and wide medial emargination. Dorsal surface (especially anterior part) and anterior margin of labrum densely covered with differently sized (mostly medium-sized and long), thin and stout, hair-like setae. Mostly posterior part of dorsal surface of labrum densely covered with scale sockets. Lateral margins of labrum subparallel, slightly concave. Mandibles (Fig. 2C, D): surface covered with empty scale sockets and scattered short, thin, hair-like setae. Outer margin of mandibles with numerous short and medium-sized hair-like setae. Outer and inner incisors on both mandibles divergent. The molar surface of left mandible composed of three distinct, short, wide ridges; molar surface of right mandible composed of six distinct elongate ridges. Left mandible with bunch of long, hair-like setae under mola; right mandible without setae under mola. Hypopharynx (Fig. 2B): superlinguae with rounded apexes covered by thin and stout, mostly long, hair-like setae; apex of lingua densely covered with short, fine setae. Lingual surface near base with irregular (subparallel to longitudinal axis of body) rows of short, pointed, stout setae (about 18 setae on each side). Maxilla (Fig. 2E, F): palp reduced to small knob, with short, hair-like seta on apex; galea-lacinia with two dentisetae with bristly apexes; galea-lacinia bears one apically rounded, robust denticle on inner margin above dentisetae, ventral surface of maxilla near robust denticle with group of 6 long, stout, hair-like setae; also group of long, stout setae on inner margin near inner dentisetata; base of galea-lacinia with group of long, stout, hair-like setae near inner margin; one or two short or long, pointed, stout setae on dorsal surface near reduced palp. Labium (Fig. 2G): glossae and paraglossae deeply divided, their apexes bluntly pointed, outer margins of paraglossae with deflection. Surfaces of glossae and paraglossae covered with stout and thin, mostly long, hair-like setae; prementum covered with scattered hair-like setae; submentum well developed, covered by same setae and additionally by empty scale sockets. Labial palp 3-segmented; segments II and III robust, but not flattened. Outer margin and adjacent area of dorsal surface of segments I and II covered with long, thin and stout, hair-like setae and several empty scale sockets; several long, hair-like setae on inner margin of segments I and II. Segment III elongated, rounded apically; length/width ratio 2.43–2.75; apex of segment with numerous fine setae, several fine setae present on segment's surface.

**Thorax.** Dorsal surface covered with short, thin, hair-like setae and scattered empty scale sockets; tubercles and ridges absent (Fig. 1E). Anterolateral angles of pronotum with small protuberances (Fig. 1F); prosternum without bilobular, spinous process medially (Fig. 1D).

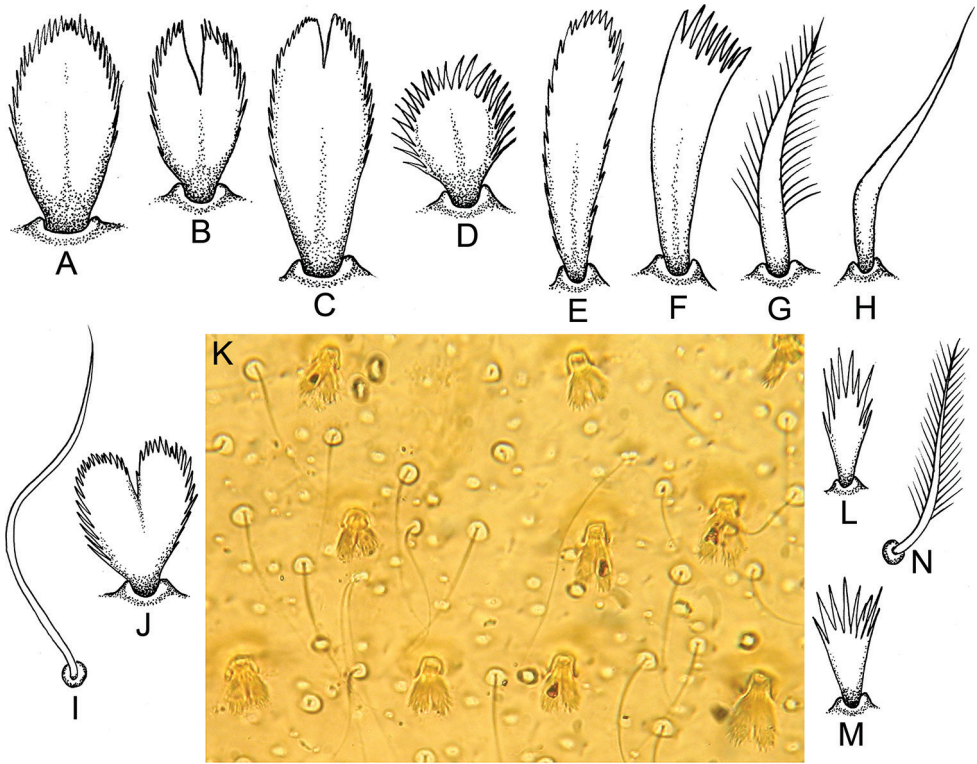


**Figure 4.** *Indoganodes tschertoprudi* sp. nov., larva, type specimens **A–J** different kinds of stout setae from legs (**A–H, J**) and terga (**I, J**) **K** area of dorsal surface of terga **L–N** setae from surface of sterna.

Femora of all legs robust, with longitudinal ridge; outer margin without apical projections (Fig. 3A–C). Fore femur 1.73–2.05 times as long as wide; middle femur 2.27–2.37 times as long as wide; hind femur 2.31–2.58 times as long as wide. Average length ratios of femur, tibia, and tarsus: fore leg 2.13 : 2.24 : 1.00; middle leg 2.78 : 2.85 : 1.00; hind leg 3.48 : 3.51 : 1.00.

Dorsal surface of fore femur with indistinct wide, transversal band of short and medium-sized, oval, stout setae bearing feathered margins and short and medium-sized, feathered, stout setae with divergent margins and cleft at apex (Figs 3A, D, E, 4A–C). Same kind of setae along outer margin and on outer and inner margins (on outer margin, setae more numerous than on inner margin); one stout setae on inner margin on small chalaza. Outer margin of fore femur without chalazae. Entire dorsal surface of fore femur and its margins covered with scattered short, thin, hair-like setae and long, pointed, stout setae with feathered margins.

Ventral surfaces of fore tibia and tarsus with numerous differently shaped, stout setae on inner margin and along it; main types of stout setae are: long, stout setae with feathered margins and pointed apex (Fig. 4G); feathered, stout setae with divergent

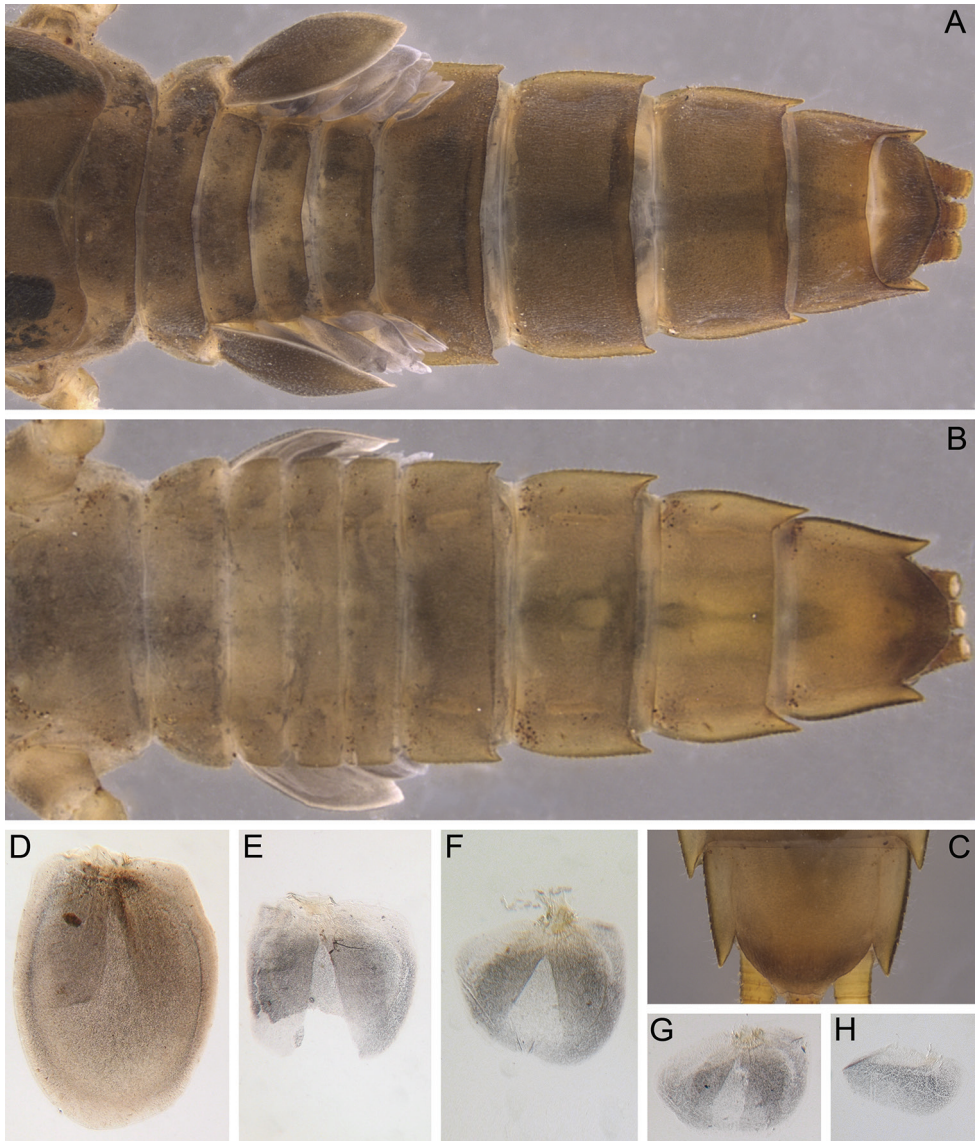


**Figure 5.** *Indoganodes tschertoprudi* sp. nov., larva, type specimens **A** abdomen, dorsal view **B** abdomen, ventral view **C** sternum IX, ventral view **D–H** gills II–VI.

margins and flat apex (some setae with cleft at apex) (Fig. 4F); medium-sized, stout, hair-like setae (Fig. 4H); elongated, feathered, stout setae with slightly divergent margins and rounded apex (Fig. 4E). Dorsal surface of fore tibia and tarsus covered with medium-sized, hair-like setae; dorsal surface of fore tibia along patella-tibial suture also bears row of differently sized, oval or rounded, feathered, stout setae with cleft at apex

in some (Fig. 4A–D). Outer margins of fore tibia and tarsus without stout setae, and only with differently sized, hair-like setae.

Dorsal surfaces of middle and hind femora covered with oval and rounded, medium-sized, feathered, stout setae with cleft at apex in some (Fig. 4B, D), and scattered, short and medium-sized, feathered, stout setae with divergent margins, with cleft at apex (Fig. 4J), and short and medium-sized, oval, stout setae with feathered margins (Fig. 4A–C). Stout setae mostly along outer margin and in central area of femora; stout setae more numerous on outer margins than on inner margins. Additionally, entire dorsal surface and all margins of middle and hind femora covered with a few short, hair-like setae. Middle femur with small, indistinct chalazae bearing stout setae on inner margin (Fig. 3B). Several distinct, small chalazae bearing stout setae present only in distal part of inner margin of hind femur (Fig. 3C, F).

Patella-tibial suture on tibiae of middle and hind legs distinctly shorter than that on fore leg. Setation of middle and hind tibiae and tarsi near that of fore leg, but in contrast to fore leg, outer margins of these tibiae bear short, feathered, oval, stout setae; in immature larvae, row of stout setae more dense and distinct.

Tarsal claw of all legs robust, hooked, its surface covered with several medium-sized, thin, hair-like setae. Claw with row of 5–8 large, blunt denticles and several (1–3) small, pointed denticles among the larger ones (Fig. 3G, H).

**Abdomen.** All terga without any median tubercles (Fig. 5A). Terga I–X covered with: short, feathered, stout setae with divergent margins and a cleft at apex; mostly short, thin, hair-like setae; empty scale sockets (Fig. 4I–K). Posterior margins of all terga without denticles, only with a few short, thin, hair-like setae. Lateral margins of terga I–V covered only with scattered thin, hair-like setae; lateral margins of segments VI–X also with short, feathered, stout setae. Posterolateral processes presented on segments VI–IX; all of them moderately developed; largest processes on segments VI–IX (Fig. 5B, C). All sterna covered with: short, feathered, thin hair-like setae (Fig. 4N); short setae with divergent, feathered margins, and feathered apex (Fig. 4L, M); empty scale sockets.

Segment I without gills; gills present on abdominal segments II–VI (Fig. 5A). Gill II light brown (Fig. 5D), covered with scattered short, thin, hair-like setae and empty scale sockets; dorsal lamella semi-operculate, without transverse band of weakened membrane, incompletely covers other gills. Ventral lobes of gills II–V bifurcated, multifoliate (Fig. 5D–G); gill VI simple, without medial cleft (Fig. 5H).

Basal part of caudal filaments with feathered, stout setae and stout, hair-like setae at articulations; stout setae shorter, mainly oval on dorsal side of the filaments and elongated on ventral side.

**Winged stages:** unknown.

**Distribution and biology.** Larvae of new species were found in wooded gullies in the mountains of Sri Lanka in the subtropical altitudinal zone (altitude 1390–1660 m a.s.l.) (Fig. 6A). Two larvae of *I. tschertoprudi* **sp. nov.** were collected from a helocrene spring in the valley of a large stream (Fig. 6B). The maximum depth of the spring was only 1–2 cm deep; there was no current and the bottom was covered with mud, leaf

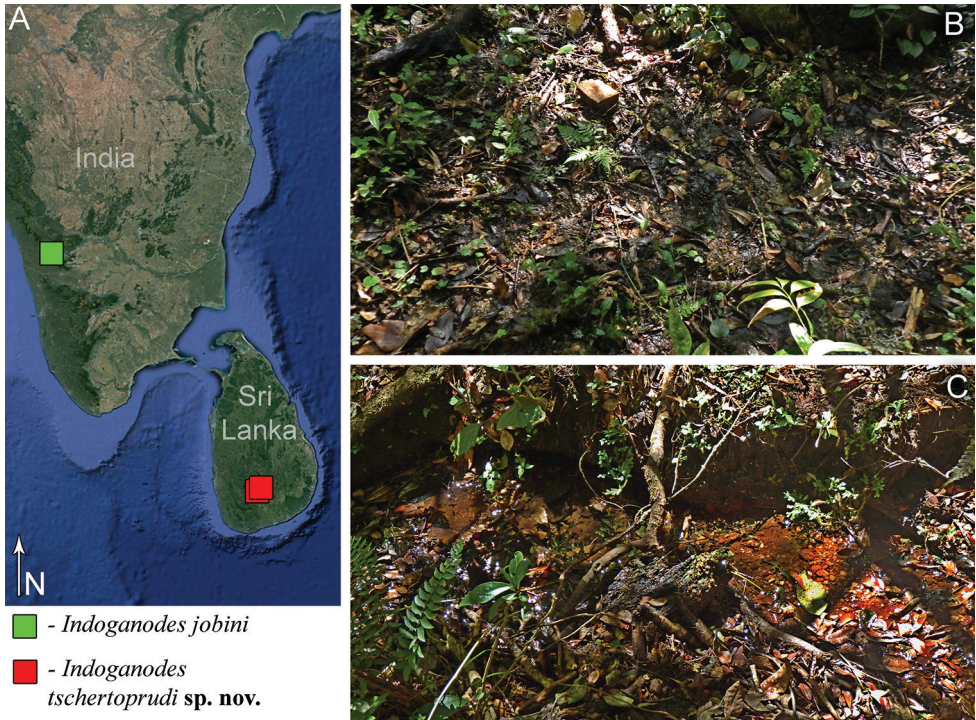


**Figure 6.** Distribution of *Indoganodes* representatives (**A**), and habitats of *Indoganodes tschertoprudi* sp. nov. (**B, C**) **A** map of genus *Indoganodes* distribution **B** type locality, helocrene spring in valley of large stream, vicinity of Marathenna village, border of Central and Sabaragamuwa Provinces, Sri Lanka (February 2017, photo by M.V. Chertoprud) **C** small stream, section with almost no current, vicinity of Holmwood Estate, Central Province, Sri Lanka (February 2017, photo by M.V. Chertoprud).

litter, and detritus. Co-occurring species of mayflies recorded from this habitat were *Ephemera* sp. (Ephemeridae) and *Kimminsula* sp. (Leptophlebiidae). Another larva of this new species was collected along with *Ephemera* sp. from a small stream, in a section with almost no current and having a muddy bottom (Fig. 6C).

## Discussion

Selvakumar et al. (2014) established the genus *Indoganodes* based on the larvae of *I. jobini*. According to the original description, this genus is distinguished from other genera of Teganodidae by the following combination of characters: (i) prosternum without medial bilobular, spinous process; (ii) poorly developed abdominal posterolateral processes on segments I–V and well developed abdominal posterolateral processes on segments VI–IX; (iii) hooked tarsal claw, bearing four small, medial denticles; (iv) labrum subquadrate, approximately twice as broad as long, with short, scattered setae

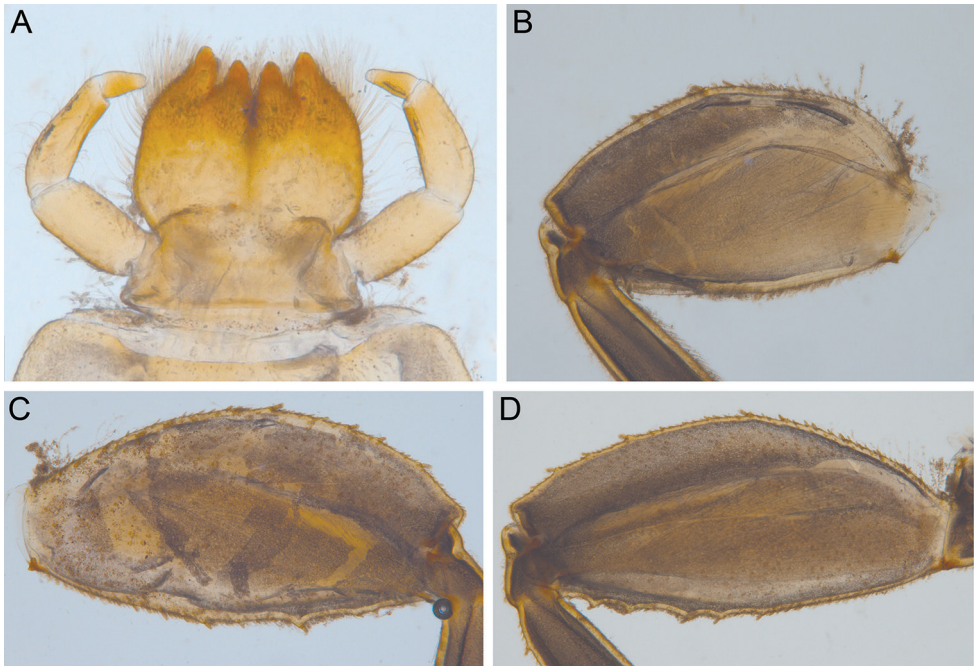


**Figure 7.** *Indoganodes jobini* Selvakumar, Sivaramakrishnan & Jacobus, 2014, larva, type specimen **A** labium **B** fore femur, dorsal view **C** middle femur, dorsal view **D** hind femur, dorsal view (photos by C Selvakumar).

over entire dorsal surface; (v) moderately developed superlinguae of hypopharynx; and (vi) left mandible without medioapicalsetal patch. Several additional figures with distinguishing characters of *I. jobini* are provided in Figure 7A–D.

The new species of *Indoganodes* reveals features that enable us to emend the diagnosis of the genus as follows: characters (i) and (iv–vi) stay unchanged. Emended characters are (ii) abdominal posterolateral processes well developed on segments VI–IX; the processes on segments I–V absent or poorly developed; (iii) claw with one row of denticles, claw with up to eight large denticles and three small denticles, they might alternate in row. Additional characters are: (vii) glossae and paraglossae deeply divided and bluntly pointed; (viii) forefemur not flattened, without distinct and regular, transversal row of stout setae; (ix) outer margin of fore femora without long stout setae; (x) paracercus not reduced.

The Gondwanan origin of the Teloganodidae (McCafferty and Wang 1977) and the close relationship of *Indoganodes* with *Ephemerellina* Lestage 1924 (Selvakumar et al. 2014) apparently hold good, as corroborated by our observations.

The genus *Indoganodes* is most similar to *Ephemerellina* in the combination of some larval characters (winged stages of both *Indoganodes* species are not described): (i) shape of labrum, (ii) fore femur not significantly flattened, (iii) absence of distinct, narrow, transversal row of stout setae on fore femur, (iv) inner margin without a row of setae continuing on dorsal surface near articulation with trochanter, (v) absence of filamen-

tous gill I, (vi) gills present on segments II–VI, (vii) semi-operculate dorsal lobe of gill II, (viii) deep division of glossae and paraglossae, (ix) unreduced paracercus, and some other characters.

*Indoganodes* and *Ephemerellina* are isolated biogeographically, with *Ephemerellina* from the Afrotropical realm and *Indoganodes* from the Indomalayan realm. It is probable that they share a common ancestor from the African continent. After eastern Gondwana, including also India and Sri Lanka, had broken free of Africa about 100 million years ago, these genera evolved separately. Sri Lanka later split from India, and since the Pliocene (5.33–2.58 million years ago), the geographic position of Sri Lanka has been similar to that at present. However, during the periodic low sea levels in the Pleistocene (2.58–0.0117 million years ago), there was a land bridge between India and Sri Lanka, and two-way dispersal of mainly terrestrial fauna was facilitated. The last land bridge was cut off by rising sea levels 5,000–8,000 years ago as the Pleistocene gave way to warmer climates and northern glaciers retreated during the Holocene (Dittus 2017). In our opinion, the morphological proximity of *I. jobini* and *I. tschertoprudi* sp. nov. testify that separation of the species was recent, most probably after the disconnection of India and Sri Lanka at the end of the Pleistocene.

Presently, only the narrow Palk Strait separates Sri Lanka and India. Although mayflies have winged stages capable of dispersal, the teloganodid fauna of the island shares no species with India or other countries of Indian subregion, which is in contrast to the vast number of other mayfly families (Sivaramakrishnan et al. 2009). All species of Teloganodidae found in Sri Lanka are island endemics. These include, in the genus *Teloganodes*, *T. tristis* (Hagen, 1858), *T. insignis* (Wang & McCafferty, 1996), *T. tuberculatus* Sartori, 2008, *T. jacobusi* Sartori, 2008, and *T. hubbardi* Sartori, 2008, and, in the genus *Indoganodes*, *I. tschertoprudi* sp. nov. This teloganodid fauna has no endemic genera. The monotypic genus *Macafertiella* Wang, 1996, which was described from Sri Lanka (Wang and McCafferty 1996), is now considered a junior synonym of *Teloganodes* (Sartori et al. 2008), and the distribution of *Teloganodes* is presently thought to be restricted to southern India (Western and Eastern Ghats) and Sri Lanka (Selvakumar et al. 2014).

## Acknowledgements

The authors are grateful to Dr M.V. Chertoprud (Moscow, Russian Federation) for sampling material on described here species. The authors are also grateful to Dr C. Selvakumar (The Madura College, Madurai, Tamil Nadu, India) for providing additional photographs of the type specimen of *Indoganodes jobini*.

## References

- Anbalagan S, Balachandran C, Kannan M, Dinakaran S, Krishnan M (2015) First record and a new species description of *Dudgeodes* (Ephemeroptera: Teloganodidae) from South India. *Turkish Journal of Zoology* 39: 308–313. <https://doi.org/10.3906/zoo-1401-74>
- Dittus WPJ (2017) The biogeography and ecology of Sri Lankan mammals point to conservation priorities. *Ceylon Journal of Science* 46 (Special Issue): 33–64. <https://doi.org/10.4038/cjs.v46i5.7453>
- Garces JM, Sartori M, Freitag H (2020) Integrative taxonomy of the genus *Dudgeodes* Sartori, 2008 (Insecta, Ephemeroptera, Teloganodidae) from the Philippines with description of new species and supplementary descriptions of Southeast Asian species. *ZooKeys* 910: 93–129. <https://doi.org/10.3897/zookeys.910.48659>
- Martynov AV, Palatov DM, Boonsoong B (2016) A new species of *Dudgeodes* Sartori, 2008 (Ephemeroptera: Teloganodidae) from Thailand. *Zootaxa* 4121(5): 545–554. <https://doi.org/10.11646/zootaxa.4121.5.4>
- McCafferty WP, Wang T-Q (1997) Phylogenetic systematics of the family Teloganodidae (Ephemeroptera: Pannota). *Annals of the Cape Provincial Museums (Natural History)* 19(9): 387–437.
- Sartori M, Peters JG, Hubbard MD (2008) A revision of Oriental Teloganodidae (Insecta, Ephemeroptera, Ephemerelloidea). *Zootaxa* 1957: 1–51. <https://doi.org/10.11646/zootaxa.1957.1.1>
- Selvakumar C, Sivaramakrishnan KG, Jacobus LM, Janarthanan S, Arumugam M (2014) Two new genera and five new species of Teloganodidae (Ephemeroptera) from South India. *Zootaxa* 3846(1): 87Z–104. <https://doi.org/10.11646/zootaxa.3846.1.4>
- Sivaramakrishnan KG, Subramanian KA, Ramamurthy VV (2009) Annotated checklist of Ephemeroptera of the Indian subregion. *Oriental Insects* 43: 315–339. <https://doi.org/10.1080/00305316.2009.10417592>
- Wang T-Q, McCafferty WP (1996) New genus of Teloganodinae (Ephemeroptera: Pannota: Ephemerellidae) from Sri Lanka. *Bulletin de la Société d'Histoire Naturelle de Toulouse* 132: 15–18.



# Pleistocene isolation caused by sea-level fluctuations shaped genetic characterization of *Pampus minor* over a large-scale geographical distribution

Yuan Li<sup>1</sup>, Cheng Liu<sup>1,2</sup>, Longshan Lin<sup>1,2</sup>, Yuanyuan Li<sup>1</sup>,  
Jianguang Xiao<sup>1</sup>, Kar-Hoe Loh<sup>3</sup>

**1** Third Institute of Oceanography, Ministry of Natural Resources, Xiamen 361005, China **2** College of Marine Sciences, Shanghai Ocean University, Shanghai 201306, China **3** Institute of Ocean and Earth Sciences, University of Malaya, Kuala Lumpur 50603, Malaysia

Corresponding author: Longshan Lin ([lshlin@tio.org.cn](mailto:lshlin@tio.org.cn))

---

Academic editor: Maria Elina Bichuette | Received 14 March 2020 | Accepted 28 July 2020 | Published 17 September 2020

---

<http://zoobank.org/8C8AFE36-BD6F-431D-B4E9-7D80E410D7B7>

---

**Citation:** Li Y, Liu C, Lin L, Li Y, Xiao J, Loh K-H (2020) Pleistocene isolation caused by sea-level fluctuations shaped genetic characterization of *Pampus minor* over a large-scale geographical distribution. ZooKeys 969: 137–154. <https://doi.org/10.3897/zookeys.969.52069>

---

## Abstract

The southern lesser pomfret (*Pampus minor*) is an economically important fish, and its numbers are declining because of overfishing and environmental pollution. In addition, owing to the similarities of its external morphological characteristics to other species in the genus *Pampus*, it is often mistaken for grey pomfret (*P. cinereus*) or silver pomfret (*P. argenteus*) juveniles. In this study, the genetic diversity and structure of 264 *P. minor* individuals from 11 populations in China and Malaysia coastal waters were evaluated for the first time, to the best of our knowledge, using mitochondrial cytochrome b fragments. The results showed that *P. minor* had moderate haplotype diversity and low nucleotide diversity. Furthermore, two divergent lineages were detected within the populations, but the phylogenetic structure corresponded imperfectly with geographical location; thus, the populations may have diverged in different glacial refugia during the Pleistocene low sea levels. Analysis of molecular variation (AMOVA) showed that genetic variation originated primarily from individuals within the population. Pairwise  $F_{ST}$  results showed significant differentiation between the Chinese and Malaysian populations. Except for the Xiamen population, which was classified as a marginal population, the genetic differentiation among the other Chinese populations was not significant. During the Late Pleistocene, *P. minor* experienced a population expansion event starting from the South China Sea refugium that expanded outward, and derivative populations quickly occupied and adapted to the new habitat. The results of this study will provide genetic information for the scientific conservation and management of *P. minor* resources.

**Keywords**

Cytochrome b, genetic diversity, genetic structure, South China Sea, southern lesser pomfret

**Introduction**

Because of the rise in fishing pressure, habitat destruction, and global climate change, understanding the level of marine biological variation and its genetic structure is of crucial significance to the protection of marine biological resources and genetic diversity (Butchart et al. 2010). Current research on population genetics mainly includes detecting the level of genetic diversity and population genetic structure within different species, estimating the effective population size, and investigating the mechanisms underlying various evolutionary factors (Ellegren 2014).

*Pampus minor* Liu & Li, 1998 is an offshore warm-water pelagic fish classified under the class Actinopterygii, order Perciformes and family Stromateidae. It is a newly discovered species, distributed primarily south of the mid-southern East China Sea and along the coast of Southeast Asian countries (Li et al. 2019a). Owing to the similarities in the external characteristics of *Pampus* species and the small size of *P. minor* (adults generally do not exceed 150 mm), this species was consistently mistaken for grey pomfret (*P. cinereus*) or silver pomfret (*P. argenteus*) juveniles in early studies (Liu and Li 1998).

The region in which *P. minor* is distributed experienced a series of glacial-interglacial cycles in the Late Quaternary. During glacial periods, fluctuations in sea levels led to massive changes in the area and structure of marginal seas (Wang 1999), which transformed the Western Pacific Ocean into an ideal marine region for studying how glacial periods affected marine life. We postulate that during the Last Glacial Maximum (LGM), *P. minor* was also strongly affected by the Pleistocene glacial period. Thus, under the harsh environmental conditions of the glacial period, most of the individuals within its distribution range went extinct, and only a handful of isolated populations in glacial refugia (such as the South China Sea) survived. As the climate warmed during interglacial periods, sea levels rose, which led to population expansion; hence, the corresponding phylogeographic patterns and population genetic structure may be detected.

There have been few studies on *P. minor* thus far, which have only focused on morphology (Liu and Li 1998; Li et al. 2019a), population genetics (Li et al. 2019b), and phylogenetics (Cui et al. 2010; Guo et al. 2010; Li et al. 2019a). To the best of our knowledge, no basic research has been conducted on the status and distribution of *P. minor* fishery resources, and there have been no reports analyzing the large-scale genetic structure of its distribution range. Given the general decline in fishery resources, *P. minor* resources have also been shrinking, and there is a need to understand its genetic diversity, genetic structure, effective population size, and other population genetic characteristics. These parameters form the basis for formulating strategies for

the effective protection and rational exploitation and utilization of marine fishery resources (Funk et al. 2012).

In this study, mitochondrial DNA sequences (cytochrome b, Cytb) were used to study the genetic diversity, genetic structure, and historical demography of 11 *P. minor* populations in China and Malaysia coastal waters. In addition, the effects of paleoclimatic, paleo-geological, marine geological, environmental and other factors on population formation, distribution and expansion routes, as well as genetic exchange, were revealed. This enabled us to investigate the mechanisms underlying the current phylogeographic patterns of this species, which can serve as a scientific reference for fishery management.

## Materials and methods

### Sample collection

Between May 2016 and December 2017, a total of 264 *P. minor* individuals from 11 geographical populations along the coasts of China (Xiamen, Zhangpu, Taiwan, Zhuhai, Zhanjiang, Beihai, Weizhou Island, Haikou, Sanya) and Malaysia (Kuala Selangor, Mukah) were collected (Fig. 1, Table 1). To ensure the accuracy of the taxonomy, the morphological identification of all specimens was based on Liu and Li (1998). A piece of back muscle tissue was frozen or preserved in 95% alcohol for molecular study.

### DNA extraction, amplification, and sequencing

Genomic DNA of *P. minor* was extracted from muscle tissue using a Qiagen DNeasy kit. The genomic DNA was assessed by electrophoresis with a 1.5% agarose gel and qualified samples were stored at 4 °C for PCR amplification. The mtDNA cytochrome b (Cytb) was amplified with the primers L14734: 5'-AACCACCGTTGT-TATTCAACT-3' (Inoue et al. 2001) and H15149: 5'-CTCAGAATGATATTTGTC-

**Table 1.** Information and molecular indices for *P. minor* based on mitochondrial DNA Cytb sequences.

Country	ID	Population	Number of individuals	Date	NH	NUH	<i>h</i>	$\pi$	<i>k</i>
China	XM	Xiamen Island	24	Apr. 2017	4	3	0.5391±0.1129	0.0007±0.0006	0.2917±0.2500
	ZP	Zhangpu	24	Apr. 2017	3	1	0.5942±0.0537	0.0016±0.0014	0.6667±0.5303
	TW	Taiwan	24	Oct. 2017	3	0	0.5072±0.0929	0.0013±0.0012	0.5507±0.4688
	ZH	Zhuhai	24	Dec. 2016	4	0	0.5326±0.1048	0.0015±0.0013	0.6015±0.4960
	ZJ	Zhanjiang	24	Dec. 2017	3	1	0.5399±0.0619	0.0014±0.0013	0.5725±0.4805
	BH	Beihai	24	Nov. 2016	5	1	0.6377±0.0606	0.0019±0.0016	0.7681±0.5824
	WZ	Weizhou Island	24	Nov. 2016	3	0	0.5543±0.0525	0.0014±0.0013	0.5906±0.4903
	HK	Haikou	24	Dec. 2016	5	1	0.4855±0.1129	0.0013±0.0012	0.5399±0.4629
	SY	Sanya	24	Dec. 2016	3	0	0.4891±0.0843	0.0012±0.0011	0.5145±0.4491
Malaysia	KS	Kuala Selangor	24	May 2016	7	3	0.6341±0.0973	0.49±0.0031	2.0109±1.1731
	SK	Mukah	24	May 2016	7	4	0.6087±0.1115	0.0038±0.0026	1.5652±0.9669
Total			264	-	22	14	0.6763±0.0189	0.0035±0.0023	1.4385±0.8794

Note: NH, number of haplotypes; NUH, number of unique haplotypes; *h*, haplotype diversity;  $\pi$ , nucleotide diversity; *k*, mean number of pairwise differences

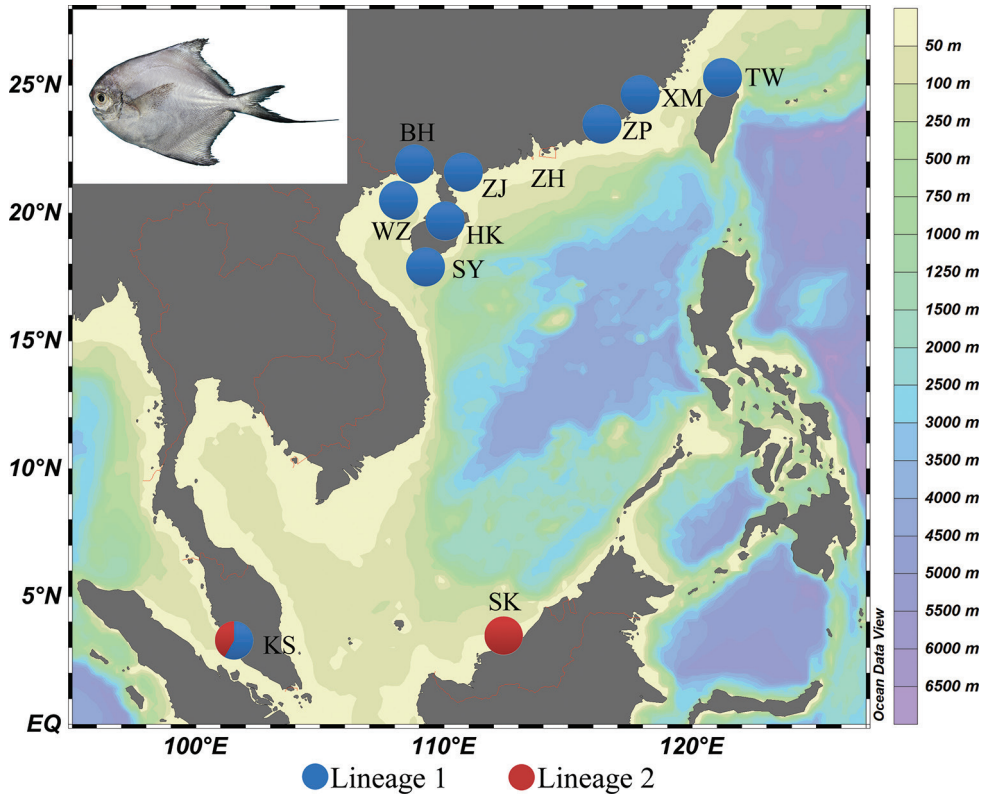


**Figure 1.** Sampling locations of *P. minor*. Populations are marked by abbreviations that correspond to Table 1.

CTCA-3' (Ohdachi et al. 1997). All PCR reactions were carried out in a final mixture of 25  $\mu$ L: 0.15  $\mu$ L Taq polymerase, 2.5  $\mu$ L 10 $\times$  PCR buffer, 17.5  $\mu$ L ultrapure water, 2  $\mu$ L dNTPs, 1  $\mu$ L of forward primer (5  $\mu$ M), 1  $\mu$ L of reverse primer (5  $\mu$ M), and 1  $\mu$ L of template DNA. PCR was carried out by initial denaturation step at 94  $^{\circ}$ C for 4 min, then followed by 32 cycles of denaturation at 94  $^{\circ}$ C for 30 sec, annealing at 50  $^{\circ}$ C for 30 sec, and extension at 72  $^{\circ}$ C for 30 sec, and plus a final extension at 72  $^{\circ}$ C for 10 min. After purification of the PCR products, both DNA strands were sequenced. The newly determined Cytb sequences were deposited in GenBank under the accession numbers (MT303974–MT303978, MF616364–MF616380).

## Data analysis

The Cytb sequences were aligned using the DNASTAR (Madison, WI, USA) software and manually edited. Haplotypes were defined based on sequence data without considering sites with gaps using DnaSP ver. 5.00 (Librado and Rozas 2009). Genetic diversity in each population was assessed as polymorphic sites, haplotype number, mean number of pairwise differences, haplotype diversity, and nucleotide diversity us-

ing ARLEQUIN version 3.5 (Excoffier et al. 2005). Analysis of molecular variation (AMOVA) in ARLEQUIN software was employed to investigate the genetic variation and test population structure. The MEGA 5.0 (Tamura et al. 2011) was applied to reconstruct the neighbor-joining (NJ) tree based on the genetic distance among haplotypes, and implemented with 1000 replicates. The relationships of haplotypes by unrooted minimum spanning tree (MST) was evaluated via the MINSPNET algorithm in ARLEQUIN software (Excoffier et al. 2005), and the MST topological structure was subsequently drawn by hand.

Both neutrality testing and mismatch distribution analysis were used to infer the historical demography expansions, as implemented in ARLEQUIN. Deviations from neutrality, significant negative values of Fu's  $F_s$  and Tajima's  $D$  statistic, were evaluated to experience population growth and spatial range expansion. A molecular clock-based time estimate provided an approximate timeframe for evaluating phylogeographical hypotheses. Historical demographic expansions were further tested by nucleotide mismatch distribution, based on three parameters:  $\theta_0$ ,  $\theta_1$  ( $\theta$  before and after population growth), and  $\tau$  (time since expansion, expressed in units of mutational time) (Rogers and Harpending 1992). The real-time since expansion was computed by the equation  $\tau=2\times\mu\times t$ , where  $\mu$  is the mutation rate for the whole sequence and  $t$  is the time since expansion.

In the present study, a sequence divergence rate of  $0.2\times 10^{-7}$ /site/year (Avice 1998; Sun and Tang 2018) was applied to the Cytb sequences of *P. minor*. Bayesian skyline plots were created using BEAST v.8 (Drummond et al. 2012). However, a molecular clock-based time estimate provided an approximate time frame for evaluating phylogeographic hypotheses.

## Results

### Genetic diversity

A total of 264 sequences were obtained from the 11 *P. minor* populations. After manual alignment, a target fragment of 415 bp was obtained, of which there were 19 polymorphic sites, 12 singleton sites, seven parsimony informative sites, and no indels. A+T content (62.32%) was significantly higher than G+C content, thus showing an AT bias.

A total of 22 Cytb haplotypes were defined in the 264 individuals. The number of haplotypes in each population ranged from three to seven. The number of haplotypes shared by two or more populations was eight (36.4%). There were 14 unique haplotypes (63.6%), and seven populations had unique haplotypes, with the number ranging from one (ZP, ZJ, BH, HK) to four (SK) (Table 1). There were large differences in the composition and distribution of haplotypes between the Chinese and Malaysian populations, with only one haplotype shared between the two. Both the Chinese (7/12=58.3%) and Malaysian (7/11=63.6%) populations were dominated by unique haplotypes (Fig. 2). The haplotype with the highest frequency was Hap\_2, consisting

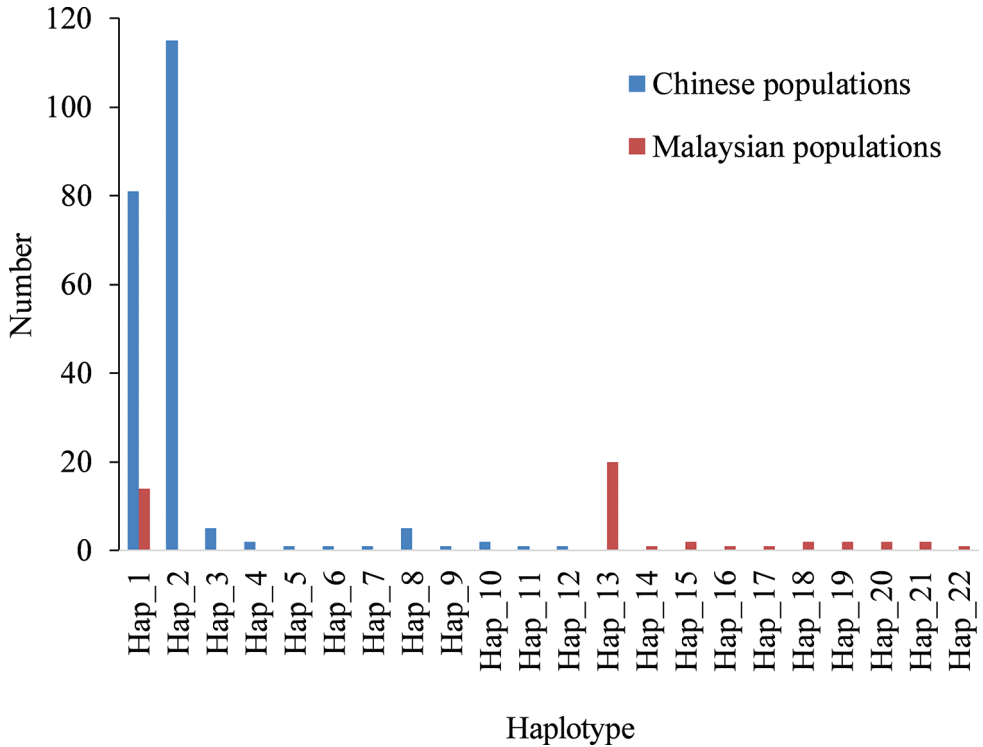


**Figure 2.** Composition and distribution of 22 Cytb haplotypes in the Chinese and Malaysian populations.

of 115 sequences. Hap\_1, consisting of 95 sequences, was the only haplotype shared by the Chinese and Malaysian populations and may be an ancestral haplotype.

In general, the *P. minor* populations exhibited moderate haplotype diversity ( $0.6763 \pm 0.0189$ ) and low nucleotide diversity ( $0.0035 \pm 0.0023$ ). This phenomenon is usually due to bottleneck effects, resulting in population expansion or rapid population growth in small populations, accompanied by the generation of a large number of new mutations (Avice et al. 1984; Grant and Bowen 1998).

## Genetic structure

An NJ tree was constructed based on the 22 *P. minor* Cytb haplotypes. The results showed two divergent lineages detected within the populations but with low bootstrap values. The phylogenetic structure detected corresponded imperfectly to the geographical locations (Fig. 3). Lineage 1 was composed of 12 haplotypes (230 individuals), and lineage 2 was composed of ten haplotypes (34 individuals) (Fig. 3). Lineage 1 was composed of all the Chinese populations and some individuals from Malaysia KS, whereas lineage 2 was composed entirely of Malaysian populations.

An unrooted MST was constructed based on the 22 Cytb haplotypes of the Chinese and Malaysian populations (Fig. 4). All sequences exhibited multiple primary haplotypes, and the other haplotypes were radially distributed around the primary

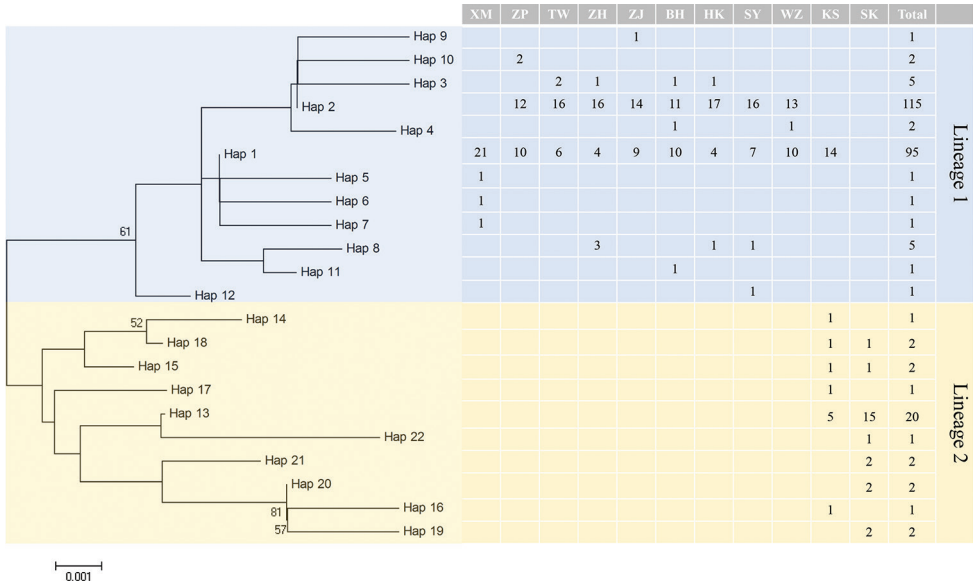


**Figure 3.** NJ tree and distribution of Cytb haplotypes among populations for *P. minor*. Bootstrap supports of > 50 in 1000 replicates are shown.

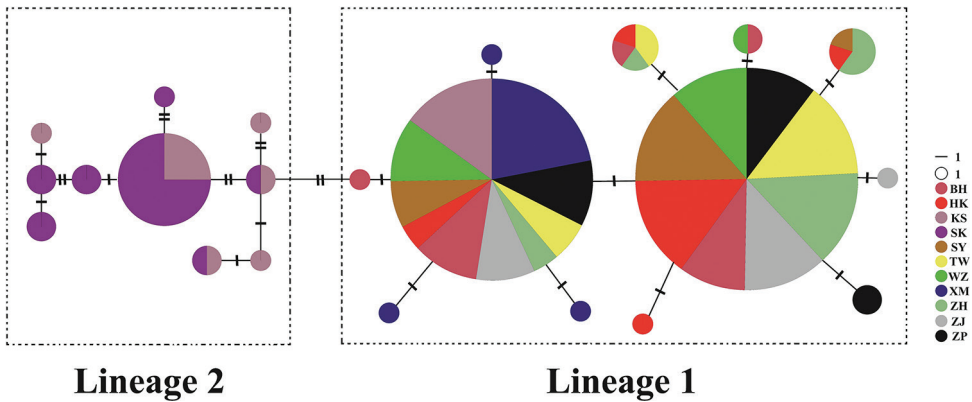


**Figure 4.** Unrooted minimum spanning tree showing the genetic relationships among the Cytb haplotypes of *P. minor*. Circle sizes are proportional to haplotype frequency. Perpendicular tick marks on the lines joining the haplotypes represent the number of nucleotide substitutions.

haplotypes with obvious phylogenetic structures that corresponded to the Chinese and Malaysian populations.

Based on the TrN+G model, the net genetic distance between the two haplotype lineages was 0.006. Based on a mitochondrial Cytb sequence divergence rate of 2% per million years, the time of divergence between lineages 1 and 2 was approximately 300 thousand years ago (Kya).

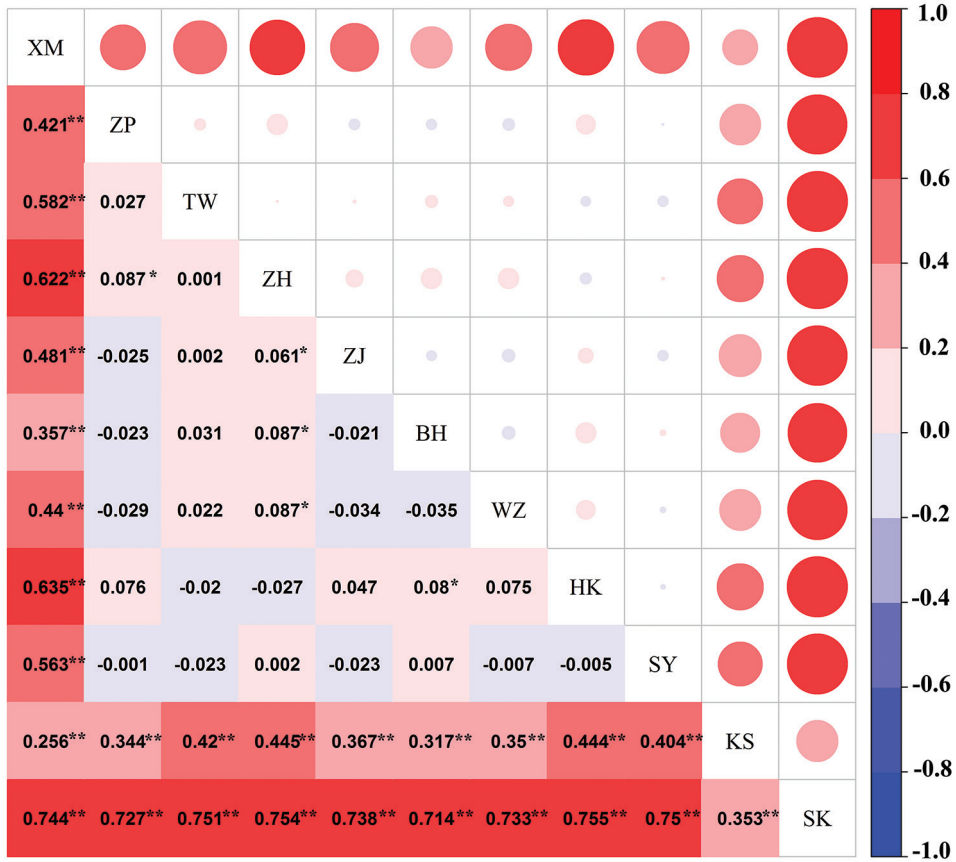


**Figure 5.** Matrix of pairwise  $F_{ST}$  values between 11 *P. minor* populations based on Cytb sequences. \* significant at  $p < 0.05$  by the permutation test, \*\* extremely significant at  $p < 0.01$  by the permutation test.

The fluctuation ranges of pairwise  $F_{ST}$  between populations were relatively large. The  $F_{ST}$  values between the Chinese and Malaysian populations were all above 0.25, and statistical tests indicated significance, thus showing very great differentiation (Wright 1965) (Fig. 5). The  $F_{ST}$  values between the Xiamen and other populations were relatively large, and differentiation was statistically significant. Except for the Xiamen population, the  $F_{ST}$  values between the Chinese populations were below 0.15, thus showing limited differentiation, and most of the statistical tests were not significant. Some  $F_{ST}$  values among the *P. minor* populations were still negative, suggesting that the level of differentiation within *P. minor* populations was greater than that among populations (Aris-Brosou and Excoffier 1996).

AMOVA was used to detect the genetic structure of the populations (Table 2). First, all *P. minor* populations were analyzed as one gene pool. The results showed significant genetic differentiation within each population ( $\Phi_{ST} = 0.477, p < 0.01$ ), ac-

**Table 2.** AMOVA analysis of *P. minor* populations based on mitochondrial Cytb sequences.

Source of variation	Sum of squares	Percentage	$\Phi$ statistic	<i>p</i>
<b>One gene pool</b> (XM, ZP, TW, ZH, ZJ, BH, WZ, HK, SY, KS and SK)				
Among populations	89.92	47.74	$\Phi_{ST}=0.477$	0.00
Within populations	99.25	52.26		
<b>Two gene pools</b> (XM, ZP, TW, ZH, ZJ, BH, WZ, HK and SY) (KS and SK)				
Among groups	64.23	30.74	$\Phi_{CT}=0.612$	0.01
Among populations within groups	25.69	8.04	$\Phi_{SC}=0.207$	0.00
Within populations	99.25	61.23	$\Phi_{ST}=0.693$	0.00
<b>Four gene pools</b> (TW) (XM, ZP, ZH, ZJ, BH and WZ) (HK and SY) (KS and SK)				
Among groups	67.08	40.30	$\Phi_{CT}=0.403$	0.03
Among populations within groups	22.83	13.95	$\Phi_{SC}=0.234$	0.00
Within populations	99.25	45.75	$\Phi_{ST}=0.542$	0.00
<b>Six gene pools</b> (TW) (XM, ZP, ZH and ZJ) (BH and WZ) (HK and SY) (KS) (SK)				
Among groups	79.87	42.54	$\Phi_{CT}=0.425$	0.04
Among populations within groups	10.05	8.43	$\Phi_{SC}=0.147$	0.00
Within populations	99.25	49.03	$\Phi_{ST}=0.510$	0.00

counting for 52.26% of the variation, whereas genetic differentiation among populations accounted for only 47.74% of the variation.

To further confirm the genetic structure of the *P. minor* populations, the 11 populations were grouped into two, four, and six gene pools based on their geographic distribution. The results of all groupings showed that the genetic differentiation among groups was relatively large with statistical significance ( $p < 0.05$ ), whereas genetic differentiation originating primarily within populations was highly significant ( $p < 0.01$ ), and genetic differentiation among populations within groups was also significant ( $p < 0.01$ ).

## Historical demography

Two haplotype lineages were detected in all Chinese and Malaysian populations with imperfect geographic lineage structures. Due to the significant differentiation among all populations, the historical demography of the two haplotype lineages was analyzed. The nucleotide mismatch distribution in all *P. minor* sequences was unimodal, and similar results were found in both lineages (Fig. 6). Neutrality test results showed that the Fu's  $F_s$  tests for each lineage and the overall population yielded negative values, and were statistically significant ( $p < 0.05$ ). Tajima's  $D$  test for each lineage and the

**Table 3.** Summary of molecular diversity, neutral test and goodness-of-fit test for *P. minor*.

	Number	NH	$h \pm SD$	$\pi \pm SD$	$k \pm SD$	Tajima's $D$		Fu's $F_s$			Goodness-of-fit test			
						$D$	$p$	$F_s$	$p$	$\tau$	$\theta_0$	$\theta_1$	SSD	HRI
Lineage 1	230	7	0.5807 $\pm$ 0.0177	0.0016 $\pm$ 0.0013	0.6643 $\pm$ 0.5131	-1.378	0.044	-7.647	0.003	0.836	0.011	83022	0.0258ns	0.1889ns
Lineage 2	34	7	0.6524 $\pm$ 0.0917	0.0042 $\pm$ 0.0028	1.7273 $\pm$ 1.0316	-0.905	0.189	-3.499	0.030	1.813	0.000	2.601	0.0321ns	0.1151ns
All	264	22	0.6763 $\pm$ 0.0189	0.0035 $\pm$ 0.0023	1.4385 $\pm$ 0.8794	-1.379	0.045	-12.923	0.001	1.000	0.000	99999	0.026ns	0.109ns

Note: NH, numbers of haplotypes;  $h$ , haplotype diversity;  $\pi$ , nucleotide diversity;  $k$ , average number of pairwise differences; ns,  $p > 0.05$

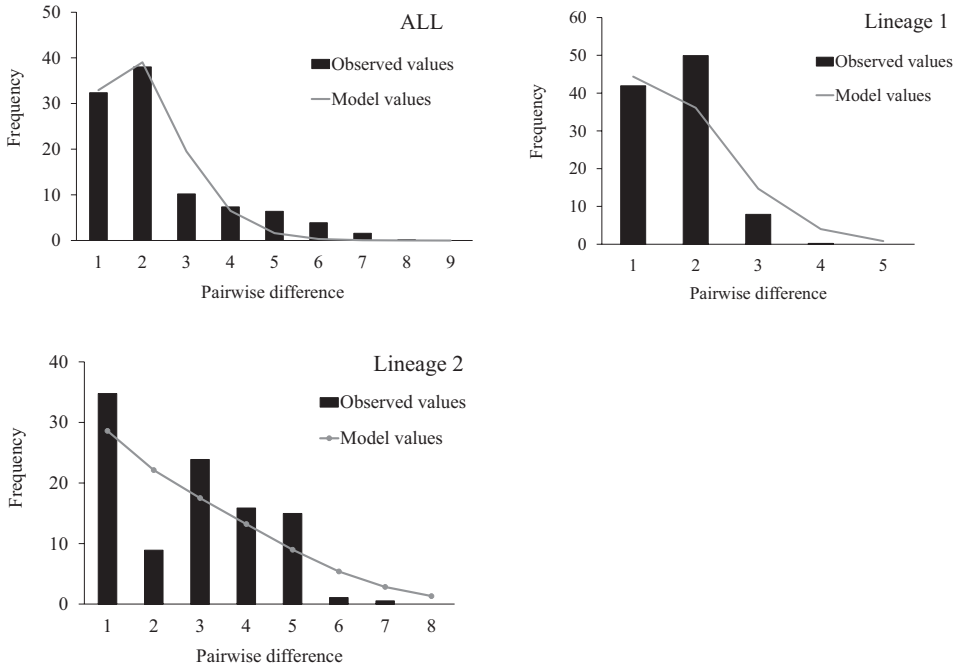


**Figure 6.** The expected mismatch distributions under a sudden expansion model (solid gray line) and the observed pairwise difference (black bars) of Cytb haplotypes of *P. minor*.

overall population yielded negative values, and were all statistically significant, except for lineage 2. In addition, the *SSD* and *HRI* test indices were not significant ( $p > 0.05$ ) (Table 3), indicating that there was no significant deviation from the expected distribution under the population expansion model. Therefore, this can be used to analyze the historical demography of the *P. minor* populations, implying that this species has experienced population expansion events. Simultaneously, the Bayesian skyline plot (BSP) also indicated the same result (Fig. 7).

The  $\tau$  value of the nucleotide mismatch distribution provides a time point for estimating population expansion. The  $\tau$  value of lineage 2 was 1.813 (95% CI: 0.059–5.600), which was larger than that of lineage 1 (0.836, 95% CI: 0.572–1.357) (Table 3). Based on a divergence rate of  $0.2 \times 10^{-7}$ /site/year and  $\tau$ , the population expansion time points of lineages 1 and 2 were estimated to be 101 and 218 Kya, respectively, which was during the Late Pleistocene. The ratio of  $\theta_1$  after expansion to  $\theta_0$  before expansion is infinite, indicating a sharp increase in the size of the effective maternal population of *P. minor* after population expansion. BSPs for lineage 1 and lineage 2 showed that both lineages have undergone the Late Pleistocene demographic expansion (Fig. 7), which started at different times. The effective population size of lineage 2 increased slowly, while the effective population size of lineage 1 increased sharply after the LGM.

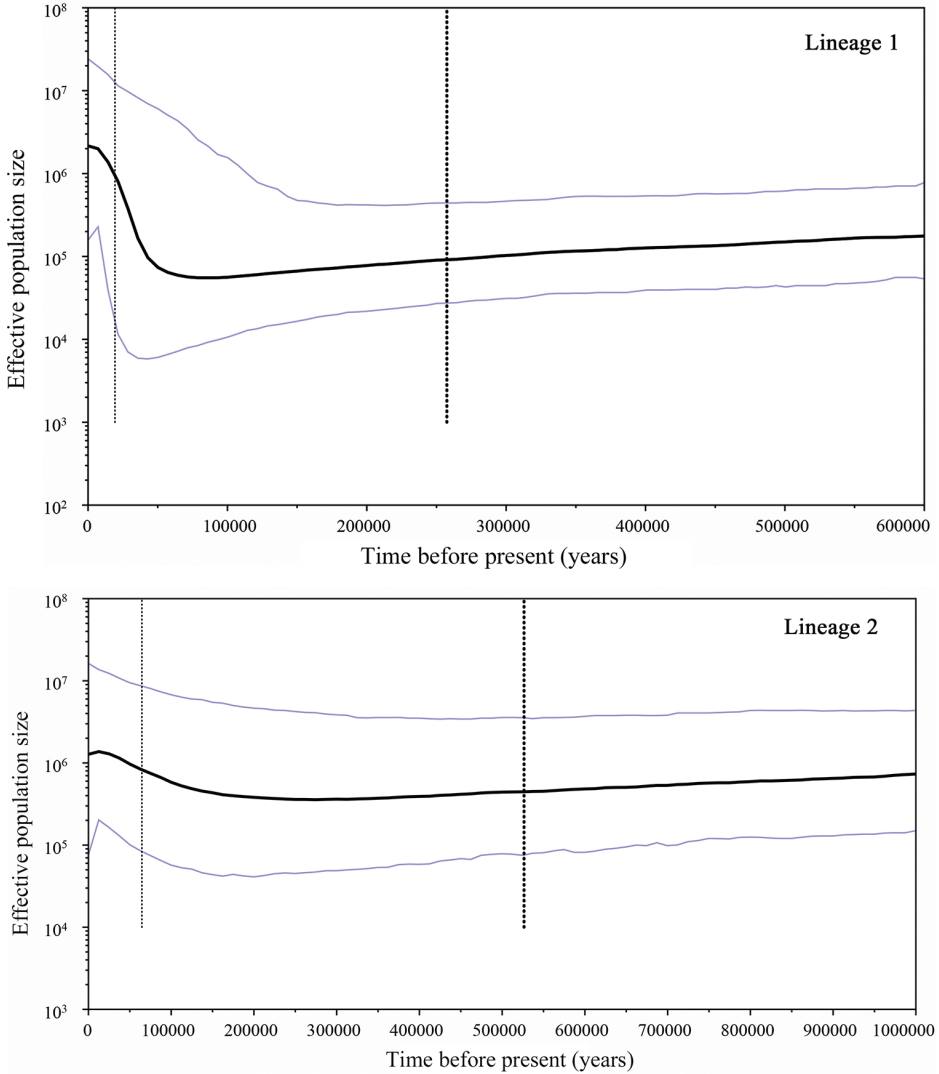


**Figure 7.** BSPs showing  $N_f T$  ( $N_f$  = effective population size;  $T$  = generation time) changes over time for *P. minor* based on *Cytb* sequences. The upper and lower limits of the blue line represent the 95% confidence intervals of highest posterior densities (HPD) analysis. The solid black line represents median estimates of  $N_f T$ .

## Discussion

Genetic diversity is the basis of both species and ecological diversity, while species and genetic diversity are both the basis of ecosystem diversity. Studies on the genetic diversity of species have attracted increasing attention from domestic and international researchers. The genetic diversity of a species directly affects its adaptation to the environment: the higher its level of diversity, the greater its potential for evolution and

the stronger its adaptation to environmental changes, whereas the opposite implies the possibility of its deterioration or extinction (Rosel et al. 1995).

Compared to the levels of intraspecific genetic diversity of Cytb gene sequences in *Trachidermus fasciatus* ( $h = 0.97 \pm 0.011$ ) (Gao et al. 2013), *P. argenteus* ( $h = 0.775 \pm 0.041$ ) (Zhao et al. 2011a), *Anguilla mossambica* ( $0.691 \pm 0.043$ ) (Frankowski et al. 2020) and other fishes, the genetic diversity of Chinese and Malaysian *P. minor* was at a moderate level. From a historical evolutionary perspective, large population sizes, environmental heterogeneity and life-history traits that favor rapid population increases are the main reasons for maintaining high haplotype diversity in natural populations of marine fishes. *Pampus minor* is widely distributed in the mid-southern East China Sea, South China Sea, and the coastal regions of Southeast Asian countries, indicating that large population sizes may account for the relatively high levels of haplotype diversity observed in this study. However, little is known about these life-history traits for *P. minor*, and further study is needed to examine this correlation. In any case, the *P. minor* populations had moderate haplotype diversity and low nucleotide diversity. Fish populations with this type of diversity pattern may have experienced historical expansion events, and a population bottleneck followed by rapid population growth and accumulation of mutations (Grant and Bowen 1998).

Stepien (1999) suggests that the stable number of shelf fish over the long term and a large effective population are the causes of its high haplotype diversity. Although pomfret fishery resources have declined due to overfishing (Jin et al. 2005), the larger amount of fishery resources and the number of effective populations of *P. minor* compared to other economic fishes have helped maintain its moderate level of genetic diversity. In addition, *P. minor* is a widely distributed species and has a wide dietary preference. Its spawning grounds exhibit different characteristics according to the different marine regions in which it is distributed, and its habitat conditions are heterogeneous (Wu et al. 2012). These life-history traits and the environmental heterogeneity of *P. minor* can promote rapid population growth, implying that the natural selection pressure faced by the population is relatively small, which may have led to the increased accumulation of genetic mutations and a rich genetic diversity.

The genetic diversity distribution of a species is not only affected by past historical events, but also by current evolutionary forces (e.g., migration). The discontinuity of habitats and the instability of population changes can result in differentiation between species populations (Stepien 1999). Both the NJ tree and unrooted MST showed two divergent lineages of *P. minor*. AMOVA also showed that the genetic differentiation primarily originated within populations. The time of divergence of the two lineages was approximately 300 Kya, and the different glacial refugia during Pleistocene low sea levels may have caused the divergence of the two lineages. Many previous studies have shown that Pleistocene glaciations are important factors in the genetic differentiation of many marine organisms (Liu et al. 2007; Shen et al. 2011; Zhao et al. 2011a, b; Wu et al. 2012; Gao et al. 2013).

In the Late Quaternary, the global climate experienced a series of glacial-interglacial cycles. In the last 800 Kya, climate fluctuations mainly occurred at intervals of

-100 Kya (Lambeck et al. 2002). The fourth glacial period ended at about 420 Kya (Petit et al. 1999), which coincided with the time of divergence for the two lineages of *P. minor*. With the arrival of the fourth glacial period, the sea level fell by about 120–140 m, and *P. minor* populations may have become isolated in the South China Sea refugium. After the glacial period, as sea levels rose, *P. minor* populations in the refugium expanded toward the coasts of China and Malaysia. The NJ tree and haplotype network tree show that Hap\_1 was the only shared haplotype between the Chinese and Malaysian populations, and accounted for a relatively large number of individuals. This indicated that it was the ancestral haplotype, thus further demonstrating that the *P. minor* populations originated from the same refugium.

The protein encoded by the mitochondrial *Cytb* gene acts as a subunit in complex V of the oxidative phosphorylation pathway (Saraste 1999). Studies have shown that non-synonymous mutations in the mitochondrial *Cytb* gene can affect the metabolism- and energy-related selective evolution of animals (Mishmar et al. 2003; da Fonseca et al. 2008; Xu et al. 2017). In marine fishes, different dimensions of natural selection between populations may be related to temperature adaptation and aerobic exercise associated with individual size (Bélanger-Deschênes et al. 2013; Jacobsen et al. 2016; Zhang et al. 2016). These results have also been validated in studies of *Sebastiscus marmoratus* (Xu et al. 2017). Currently, *P. minor* has a wide thermal amplitude. After undergoing population expansion, Chinese and Malaysian *P. minor* populations were able to adapt to the habitats of different marine regions and withstand different natural selection pressures. With the passing of time, many new mutations appeared, and abundant haplotype diversity accumulated to form a unique haplotype. Lineage 2 was composed entirely of the haplotype of the Malaysian population, and in lineage 1, only KS appeared in the ancestral haplotype Hap\_1, while all other haplotypes were from the Chinese populations. In other words, except for the ancestral haplotype, the remaining haplotypes of the Chinese and Malaysian *P. minor* populations have produced substantial differentiation, each accounting for their unique haplotypes. However, from the current perspective, there was still insufficient time for ample nucleotide variation to be produced.  $F_{ST}$  results also showed that significant genetic differentiation had occurred between the Chinese and Malaysian *P. minor* populations, further validating their respective accumulation of genetic variation to adapt to their living environments. Due to Malaysia's low latitude, high water temperature and greater number of habitats, as well as the effect of the monsoon systems, which cause the ocean currents to bring an abundance of plankton as a richer source of food, there is reduced pressure on the Malaysian *P. minor* population, allowing for the accumulation of more genetic variation, which in turn results in higher genetic diversity.

An interesting result was found in the Xiamen population, which showed significant differentiation from other populations, indicating that the breeding patterns of *P. minor* are complex. A second confirmation was performed on the sample sources and the results of the data analysis to eliminate the possible effects of these factors. Studies have reported that when *P. minor* was first discovered, the northern boundary of its

distribution range was in the Xiamen marine region, and its geographical distribution range was in the waters south of the Taiwan Strait (Liu and Li 1998). Xiamen is in the northern boundary of the *P. minor* population distribution range; that is, it is a marginal population. In studies of adaptive evolution, the marginal populations of species are more sensitive to environmental changes, exhibit more pronounced population differentiation, and genetic polymorphic sites associated with adaptive evolution are more readily detected (Bridle and Vines 2007). These phenomena have been confirmed in the Xiamen population, and this result, to some extent, also strongly supports the analysis of population genetic patterns and population evolution for marginal effects at a specific spatiotemporal scale of a single species. Xiamen Island is a semi-enclosed island surrounded by the mainland. Freshwater flows from the southeastern part of the Jiulong River and the outside are blocked by Jinmen Island, resulting in complex and variable hydrological environmental factors (Jing et al. 2011). This may also be the cause of *P. minor* differentiation in Xiamen.

Based on these results, we speculate that the time during which *P. minor* expanded from the refugium to occupy the coastal areas of China and Malaysia was relatively short. With the passage of time, the Chinese and Malaysian *P. minor* populations accumulated sufficient genetic variation to diverge completely. Similar results have been detected in the genetic structure of Chinese pomfret with similar distributions. The results of this study on the population genetics of *P. minor* are consistent with the proposed mesoscale boundary units suggested for the management of the region by Ablan et al. (2002). The Chinese coastal population should be classified as a north-central group (encompassing northwestern Taiwan, northern Vietnam, and the northwestern Philippines), and the Malaysian population should be classified as a southwestern group (comprising southern Vietnam and the eastern coast of mainland Malaysia). Unfortunately, the genetic diversity of *P. minor* in coastal China is lower than that of the Malaysian population, which is directly related to the high fishing pressure in China's offshore waters. Therefore, in order to safeguard fishery resources, emphasis should be placed on the protection of *P. minor* resources, fishing in coastal *P. minor* spawning grounds should be prohibited, and bottom trawling, gillnet and set net operations should be strictly prohibited. If these measures are taken seriously and implemented, *P. minor* resources will gradually recover, and the tragedy of resource decline of traditional commercial fishes in China, such as the large yellow croaker (*Larimichthys crocea*), small yellow croaker (*Larimichthys polyactis*), and hairtail (*Trichiurus haumela*), will be avoided.

## Conclusion

Genetic signature of *P. minor* in China and Malaysia coastal waters were evaluated. The results showed that all *P. minor* had moderate haplotype diversity and two divergent lineages. The phylogenetic structure of *P. minor* corresponded imperfectly with geographical location at the Cytb gene level, but significant divergence between Chinese and Malaysian populations was detected. To get precise phylogeographic structure, more

sensitive DNA markers such as SLAF, RAD and WGS will be employed and reveal the adaptive evolution mechanism of this species. Lower haplotype diversity is detected in China, which further indicated that Chinese fishery resources are facing greater fishing pressure and more focus is needed on fishery protection and management.

## Acknowledgements

The present study could not have been performed without assistance from Drs Binbin Shan, Xiang Zhang, Wentao Niu and Yan Li during the collection of *P. minor* specimens. The research was funded by the National Key Research and Development Program of China (2018YFC1406302), the National Programme on Global Change and Air-Sea Interaction (GASI-02-SCS-YDsum/spr/aut), the Bilateral Cooperation of Maritime Affairs (2200207), the Scientific Research Foundation of TIO, MNR (2019017, 2019018) and the University of Malaya, Research University Grant (TU001-2018). The authors declare no conflicts of interest including the implementation of research experiments and writing this manuscript.

## References

- Ablan MCA, McManus JW, Chen CA, Shao KT, Bell J, Cabanban AS, Tuan VS, Arthana IW (2002) Meso-scale transboundary units for the management of coral reefs in the South China Sea Area. *NAGA, World Fish Center Quarterly* 25: 4–9. [http://www.worldfish-center.org/Naga/Naga25-3&4/pdf/NAGA\\_25no3n4\\_features\\_a.pdf](http://www.worldfish-center.org/Naga/Naga25-3&4/pdf/NAGA_25no3n4_features_a.pdf)
- Aris-Brosou S, Excoffier L (1996) The impact of population expansion and mutation rate heterogeneity on DNA sequence polymorphism. *Molecular Biology and Evolution* 13: 494–504. <https://doi.org/10.1093/oxfordjournals.molbev.a025610>
- Avise JC (1998) The history and purview of phylogeography: a personal reflection. *Molecular Ecology* 7: 371–379. <https://doi.org/10.1046/j.1365-294x.1998.00391.x>
- Avise JC, Neigel JE, Arnold J (1984) Demographic influences on mitochondrial DNA lineage survivorship in animal populations. *Journal of Molecular Evolution*. 20: 99–105. <https://doi.org/10.1007/BF02257369>
- Bélanger-Deschênes S, Couture P, Campbell PGC, Bernatchez L (2013) Evolutionary change driven by metal exposure as revealed by coding SNP genome scan in wild yellow perch (*Percia flavescens*). *Ecotoxicology* 22(5): 938–957. <https://doi.org/10.1007/s10646-013-1083-8>
- Bridle JR, Vines TH (2007) Limits to evolution at range margins: when and why does adaptation fail? *Trends in Ecology and Evolution* 22: 140–147. <https://doi.org/10.1016/j.tree.2006.11.002>
- Butchart SHM, Walpole M, Collen B, Van Strien A, Scharlemann JPW, Almond REA, Bailie JEM, Bomhard B, Brown C, Bruno J, Carpenter KE, Carr GM, Chanson J, Chenery AM, Csirke J, Davidson NC, Dentener F, Foster M, Galli A, Galloway JN, Genovesi P, Gregory RD, Hockings M, Kapos V, Lamarque J-F, Leverington F, Loh J, McGeoch MA,

- McRae L, Minasyan A, Morcillo MH, Oldfield TEE, Pauly D, Quader S, Revenga C, Sauer JR, Skolnik B, Spear D, Stanwell-Smith D, Stuart SN, Symes A, Tierney M, Tyrrell TD, Vié J-C, Watson R (2010) Global biodiversity: indicators of recent declines. *Science* 328: 1164–1168. <https://doi.org/10.1126/science.1187512>
- Cui ZX, Liu Y, Liu J, Luan WS (2010) Molecular identification of *Pampus* fishes (*Perciformes*, *Stromateidae*). *Ichthyological Research* 57: 32–39. <https://doi.org/10.1007/s10228-009-0119-9>
- Da Fonseca RR, Johnson WE, O'Brien SJ, Ramos MJ, Antunes A (2008) The adaptive evolution of the mammalian mitochondrial genome. *BMC Genomics* 9: 1–119. <https://doi.org/10.1186/1471-2164-9-119>
- Drummond AJ, Suchard MA, Xie D, Rambaut A (2012) Bayesian phylogenetics with BEAUti and the BEAST 1.7. *Molecular Biology and Evolution* 29(8): 1969–1973. <https://doi.org/10.1093/molbev/mss075>
- Ellegren H (2014) Genome sequencing and population genomics in non-model organisms. *Trends in Ecology and Evolution* 29: 51–63. <https://doi.org/10.1016/j.tree.2013.09.008>
- Excoffier L, Laval G, Schneider S (2005) Arlequin (version 3.0): an integrated software package for population genetics data analysis. *Evolutionary Bioinformatics* 1: 47–50. <https://doi.org/10.1177/117693430500100003>
- Funk WC, McKay JK, Hohenlohe PA, Allendorf FW (2012) Harnessing genomics for delineating conservation units. *Trends in Ecology and Evolution* 27: 489–496. <https://doi.org/10.1016/j.tree.2012.05.012>
- Frankowski J, Lübke K, Coke M, Weyl OLF (2020) Genetic variability and demographic history of *Anguilla mossambica* (Peters, 1852) from continental Africa and Madagascar. *Journal of Fish Biology* 96(5): 1251–1259. <https://doi.org/10.1111/jfb.14220>
- Gao TX, Bi XX, Zhao LL, Li CJ (2013) Population genetic structure of roughskin sculpin *Trachidermus fasciatus* based on the mitochondrial Cytb sequence. *Acta Hydrobiologica Sinica* 37:199–207. [in Chinese with English abstract]
- Grant WAS, Bowen BW (1998) Shallow population histories in deep evolutionary lineages of marine fishes: Insights from sardines and anchovies and lessons for conservation. *Journal of Heredity* 89: 415–426. <https://doi.org/10.1093/jhered/89.5.415>
- Guo EM, Liu Y, Liu J, Cui ZX (2010) DNA barcoding discriminates *Pampus minor* (Liu et al. 1998) from *Pampus* species. *Chinese Journal of Oceanology and Limnology* 28: 1266–1274. <https://doi.org/10.1007/s00343-010-9917-1>
- Inoue JG, Miya M, Tsukamoto K, Nishida M (2001) A mitogenomic perspective on the basal teleostean phylogeny: resolving higher-level relationships with longer DNA sequences. *Molecular Phylogenetics and Evolution* 20: 275–285. <https://doi.org/10.1006/mpev.2001.0970>
- Jacobsen MW, Da Fonseca RR, Bernatchez L, Hansen MM (2016) Comparative analysis of complete mitochondrial genomes suggests that relaxed purifying selection is driving high non-synonymous evolutionary rate of the NADH2 gene in whitefish (*Coregonus* spp.). *Molecular Phylogenetics and Evolution* 95: 161–170. <https://doi.org/10.1016/j.ympev.2015.11.008>
- Jin XS, Zhao XY, Meng TX, Cui Y (2005) *Biology Resource and Environment in the Bohai Sea and Yellow Sea*. Scientific Press, Beijing. [in Chinese]

- Jing CS, Zhu XM, Bao XW, Song DH (2011) Three dimensional tidal current numerical simulation based on FVCOM in and around Xiamen Bay. *Journal of Applied of Oceanography* 30: 103–113. [in Chinese with English abstract]
- Lambeck K, Esat T, Potter E (2002) Links between climate and sea levels for the past three million years. *Nature* 419: 199–206. <https://doi.org/10.1038/nature01089>
- Li Y, Zhou YD, Li PF, Gao TX, Lin LS (2019a) Species identification and cryptic diversity in *Pampus* species as inferred from morphological and molecular characteristics. *Marine Biodiversity* 49: 2521–2534. <https://doi.org/10.1007/s12526-019-00976-6>
- Li Y, Zhang LY, Loh KH, Feng J, Zheng XQ, Song PQ, Lin LS (2019b) Genetic diversity comparison of *Pampus minor* between Chinese and Malaysian populations inferred from mtDNA Cytb. *Pakistan Journal of Zoology* 51: 149–157. <https://doi.org/10.17582/journal.pjz/2019.51.1.149.157>
- Librado P, Rozas J (2009) DnaSP v5: a software for comprehensive analysis of DNA polymorphism data. *Bioinformatics* 25: 1451–1452. <https://doi.org/10.1093/bioinformatics/btp187>
- Liu J, Li CS (1998) A new pomfret species, *Pampus minor* sp. nov. (Stromateidae) from Chinese waters. *Chinese Journal of Oceanology and Limnology* 16: 280–285. <https://doi.org/10.1007/BF02848735>
- Liu JX, Gao TX, Wu SF, Zhang YP (2007) Pleistocene isolation in the Northwestern Pacific marginal seas and limited dispersal in a marine fish, *Chelon haematocheilus* (Temminck & Schlegel, 1845). *Molecular Ecology* 16: 275–288. <https://doi.org/10.1111/j.1365-294X.2006.03140.x>
- Mishmar D, Ruiz-Pesini E, Golik P, Macaulay V, Clark AG, Hosseini S, Brandon M, Easley K, Chen E, Brown MD, Sukernik RI, Olckers A, Wallace DC (2003) Natural selection shaped regional mtDNA variation in humans. *Proceedings of the National Academy of Sciences* 100: 171–176. <https://doi.org/10.1073/pnas.0136972100>
- Ohdachi S, Masuda R, Abe H, Adachi J, Dokuchaev NE, Haukisalmi V, Yoshida MC (1997) Phylogeny of Eurasian soricine shrews (Insectivora, Mammalia) inferred from the mitochondrial Cytochrome *b* gene sequences. *Zoological Science* 14: 527–532. <https://doi.org/10.2108/zsj.14.527>
- Petit JR, Jouzel J, Raynaud D, Barkov NI, Barnola JM, Basile I, Bender M, Chappellaz J, Davis M, Delaygue G, Delmotte M, Kotlyakov VM, Legrand M, Lipenkov VY, Lorius C, Pépin L, Ritz C, Saltzman E, Stievenard M (1999) Climate and atmospheric history of the past 420,000 years from the Vostok ice core, Antarctica. *Nature* 399: 429–436. <https://doi.org/10.1038/20859>
- Tamura K, Peterson D, Peterson N, Stecher G, Nei M, Kumar S (2011) MEGA5: molecular evolutionary genetics analysis using maximum likelihood, evolutionary distance, and maximum parsimony methods. *Molecular Biology and Evolution* 28: 2731–2739. <https://doi.org/10.1093/molbev/msr121>
- Rogers AR, Harpending H (1992) Population growth makes waves in the distribution of pairwise genetic differences. *Molecular Biology and Evolution* 9: 552–569. <https://doi.org/10.1093/oxfordjournals.molbev.a040727>
- Rosel PE, Haygood MG, Perrin WF (1995) Phylogenetic relationships among the true porpoises (Cetacea: Phocoenidae). *Molecular Phylogenetics and Evolution* 4: 463–474. <https://doi.org/10.1006/mpev.1995.1043>

- Saraste M (1999) Oxidative phosphorylation at the fin de siecle. *Science* 283: 1488–1493. <https://doi.org/10.1126/science.283.5407.1488>
- Shen KN, Jamandre BW, Hsu CC, Tzeng WN, Durand JD (2011) Plio-Pleistocene sea level and temperature fluctuations in the northwestern Pacific promoted speciation in the globally-distributed flathead mullet *Mugil cephalus*. *BMC Evolutionary Biology* 11: 1–83. <https://doi.org/10.1186/1471-2148-11-83>
- Stepien CA (1999) Phylogeographical structure of the Dover sole *Microstomus pacificus*: the larval retention hypothesis and genetic divergence along the deep continental slope of the Northeastern Pacific Ocean. *Molecular Ecology* 8: 923–939. <https://doi.org/10.1046/j.1365-294x.1999.00643.x>
- Sun P, Tang BJ (2018) Low mtDNA variation and shallow population structure of the Chinese pomfret *Pampus chinensis* along the China coast. *Journal of Fish Biology* 92: 214–228. <https://doi.org/10.1111/jfb.13515>
- Wang P (1999) Response of Western Pacific marginal seas to glacial cycles: paleoceanographic and sedimentological features. *Marine Geology* 156: 5–39. [https://doi.org/10.1016/S0025-3227\(98\)00172-8](https://doi.org/10.1016/S0025-3227(98)00172-8)
- Wright S (1965) The interpretation of population structure by F-statistics with special regard to systems of mating. *Evolution* 19: 395–420. <https://doi.org/10.1111/j.1558-5646.1965.tb01731.x>
- Wu RX, Liang XH, Zhuang ZM, Liu SF (2012) Mitochondrial COI sequence variation of silver pomfret (*Pampus argenteus*) from Chinese coastal waters. *Acta Zootaxonomic Sinica* 37: 480–488. [in Chinese with English abstract]
- Xu SY, Sun DR, Song N, Han ZQ, Gao TX, Shui BN (2017) Local adaptation shapes pattern of mitochondrial population structure in *Sebastiscus marmoratus*. *Environmental Biology of Fishes* 100: 763–774. <https://doi.org/10.1007/s10641-017-0602-5>
- Zhang BD, Xue DX, Wang J, Li YL, Liu BJ, Liu JX (2016) Development and preliminary evaluation of a genomewide single nucleotide polymorphisms resource generated by RAD-seq for the small yellow croaker (*Larimichthys polyactis*). *Molecular Ecology Resources* 16: 755–768. <https://doi.org/10.1111/1755-0998.12476>
- Zhao F, Dong YH, Zhuang P, Zhang T, Zhang, LZ, Shi ZH (2011b) Genetic diversity of silver pomfret (*Pampus argenteus*) in the Southern Yellow and East China Seas. *Biochemical Systematics and Ecology* 39: 145–150. <https://doi.org/10.1016/j.bse.2011.02.002>
- Zhao F, Zhuang P, Zhang L, Shi ZH (2011a) Population genetic structure of *Pampus argenteus* in the Southern Yellow and East China Sea based on the mitochondrial Cytb sequence. *Acta Hydrobiologica Sinica* 35: 745–752. [in Chinese with English abstract]